

The Alberta Drug Administration Modeller (ADAM): a life-size, hands-on  
pharmacokinetics learning tool for our future healthcare professionals

by

Ines Zuna

A thesis submitted in partial fulfillment of the requirements for the degree  
of

Master of Science

Department of Pharmacology  
University of Alberta

© Ines Zuna, 2017

## ABSTRACT

The processes of absorption, distribution, metabolism, and elimination (ADME) determine a drug's pharmacokinetics (PK). Each of these processes is described with abstract modelling, and the relationships are characterised through equations and graphical analysis using both non-compartmental and compartmental methods. Patient physiology and environmental factors strongly influence these processes, affecting treatment outcomes and drug efficacy. As such, it is important for health professionals to use all patient and drug characteristics to relate desired pharmacological outcomes of the drug therapy with the appropriate route of administration, dose, and duration. Successful implementation of a dosing regimen depends not only on acknowledgement of factors, but on thorough understanding of drug PK, how the relationships relate, and how these factors affect the processes of ADME. Unfortunately, many health care students and health professionals are not adequately prepared to translate these concepts into the clinic, resulting in prescribing, dosing, and calculation errors; comprehension of mathematical modelling and current limitations in content delivery contribute significantly to this issue. Numerous instructors and institutions have attempted to implement curricula and learning techniques to circumvent the difficulty in learning, all with varying levels of success. In response to the lack of clinical context of teaching PK, we have developed a clinical application (Alberta Drug Administration Modeller; ADAM) aimed at enhancing student understanding of PK by providing a hands-on, patient-simulated learning experience.

ADAM is comprised of a series of peristaltic pumps, representing the contributions of different organs

to drug distribution and elimination kinetics, connected with Tygon tubing to mimic circulation. Drug (methylene blue dye) is administered to ADAM, and plasma and urine samples are collected over time; drug concentrations are determined spectrophotometrically and results graphed vs. time. The modeller mimics outcomes of 1- and 2-compartment distribution kinetics, IV injection and oral (PO) dosing, renal or hepatic failure, metabolic enzyme induction or inhibition, various adipose profiles, and applications to chronic dosing regimens including repeated IV/PO dosing with and without loading dose, and both intermittent and continuous IV infusion protocols. Data generated by the ADAM were analysed by hand using appropriate equations, and also entered into a PK modelling software package, PKSolver. Results showed consistency between the two analysis methods, validating the ADAM as a PK modelling tool. ADAM was introduced into a pharmacology undergraduate practical laboratory class and student performance was evaluated before and after lab modules. In line with an increase in students' self-reported understanding of PK concepts and calculation competence following the lab modules, PK test results also showed a significant improvement in student performance ( $p < 0.001$ ). Student attitudes were favourable, and the majority of students rated the ADAM as an effective educational learning tool for PK. Simple in design, ADAM successfully mimics human drug outputs while providing students with a hands-on learning opportunity and engagement with PK concepts and calculations. Highly quantitative, intuitive, and effective, ADAM translates the complexity of PK into a language health care students will understand.

## PREFACE

This thesis is an original work by me. The research project, of which this thesis is a part, received research ethics approval from the University of Alberta Human Research Ethics Board, Project Name "A Participative Model to Enhance Student Understanding of Drug Pharmacokinetics", No. Pro00056323, 05/13/15.

The apparatus was designed by Dr. Andy Holt, with design alteration suggestions made by myself. The ADAM was submitted and approved for a provisional patent entitled "Systems and Methods for Modelling Drug Pharmacokinetic Behaviour", No. 62/216,195, 09/09/15.

Parts of Chapter 2 and some data presented in Chapter 3 have been accepted for publication in the British Journal of Clinical Pharmacology in an article entitled: *ADAM, a hands-on patient simulator for teaching principles of drug disposition and compartmental pharmacokinetics*. doi:10.1111/bcp.13357. I was responsible for the data collection, analysis, and manuscript composition. Dr. Holt provided manuscript edits and was the supervisory author involved with concept formation and manuscript composition.

## ACKNOWLEDGEMENTS

It takes a village, and I am grateful to have had many forms of support over the years. Thank you to Dr. Andy Holt for allowing me to be a part of your laboratory – from the in-depth talks about scientific rationale and methods, to endless feedback (criticisms) about my grammar and writing, you've taught me never to accept less than my very best. I am very appreciative that you always took the time to listen, to find opportunities for me to explore my interests, and to push me to try things outside of my comfort zone. I leave the Holt lab with two lessons: that if there is a choice between taking the easy or the right path, the former should be avoided at all costs, and that "if it only needed to be done once, it would be called 'search', not 'research'."

Thank you to Julie Grandbois, who was an endless support during her time in the Holt lab, and who also always took the time to listen to my drawn-out presentations, and read and provide feedback for applications and abstracts – you were a fantastic personal and professional support. Thank you to my advisory committee, Dr. Glen Baker and Dr. Harley Kurata, for your encouragement and support at every meeting – this was an unconventional project, and I appreciated your openness and input. I would like to also thank Dr. Sandy Clanachan for "volunteering" to be my teaching mentor, providing me with endless feedback for my lectures, and creating a positive environment for my development as an instructor. Special thanks to Dancy and Jen for always having my back when it came to sorting out the logistics of grad school, and for being generous with your time when I needed some advice, or a friend to talk to. Thank you to Ray, for technical support, and for ensuring that I would be startled out of my skin at least once a day – it kept me on my toes. As well, thank you to each faculty member in the Department of Pharmacology – most of you taught me in undergrad at some point, and your collective influence is what inspired me to pursue graduate studies. Thank you to the funding agencies for the scholarship and lab support: Canadian Institutes of Health Research (CIHR) Masters Award, Faculty of Medicine and Dentistry Recruitment Scholarship, Queen Elizabeth II Masters Award, and the Teaching and Learning Enhancement Fund (TLEF).

I'd also like to thank my friends and family for their unwavering support. The community of people that supported me, listened to me, advised me, and encouraged me at every moment of doubt, frustration, or uncertainty is nothing short of amazing. Special thanks to my academic friends who went through similar obstacles and challenges – your camaraderie and friendship have been instrumental in helping me get to this point. Another huge thank you to my core group of friends - for all the board game nights, pub-crawls, trips, and outings – you've all kept me sane and provided me with endless laughter and memories. Cole, a "thank you" doesn't suffice the countless moments of unconditional support, coaching, and encouragement you've continuously given me, but I will say thank you, anyway. And finally, thank you to my parents, Ivica (Ivo) and Ljubica (Billie) Zuna. I quite literally would not have been able to pursue this degree without your personal, emotional, and financial support. Thank you for everything – I often reflect on who I would be if the two of you hadn't decided to pack up three suitcases and move to Canada. Your perseverance and strength over the years is an inspiration, and I am very proud to be your daughter. Thank you for always believing in me.

# LIST OF FIGURES

## CHAPTER 1: TEACHING AND LEARNING PHARMACOKINETICS

FIGURE 1.1 PLASMA CONCENTRATION TIME PROFILE. ....	3
FIGURE 1.2 CUMULATIVE AMOUNT OF DRUG IN URINE <i>VERSUS</i> TIME. ....	3
FIGURE 1.3 ZERO-ORDER ELIMINATION <i>VERSUS</i> FIRST-ORDER ELIMINATION KINETICS. ....	5
FIGURE 1.4 MICHAELIS MENTEN GRAPHICAL REPRESENTATION. ....	6
FIGURE 1.5 CHRONIC DOSING AND $C_{SS}$ . ....	8
FIGURE 1.6 LINEAR <i>VERSUS</i> NON-LINEAR PHARMACOKINETICS. ....	9
FIGURE 1.7 ACID AND BASE IONISATION. ....	11
FIGURE 1.8 COMPARISON OF AUC BETWEEN IV AND PO DOSING. ....	14
FIGURE 1.9 CHANGES IN $C_{MAX}$ , $T_{MAX}$ AND F. ....	18
FIGURE 1.10 ONE COMPARTMENT DISTRIBUTION MODEL. ....	31
FIGURE 1.11 ONE COMPARTMENT PLASMA-CONCENTRATION TIME PROFILE. ....	31
FIGURE 1.12 TWO COMPARTMENT DISTRIBUTION MODEL. ....	32
FIGURE 1.13 TWO COMPARTMENT PLASMA-CONCENTRATION TIME PROFILE. ....	33
FIGURE 1.14 METHOD OF RESIDUALS. ....	37
FIGURE 1.15 THE EFFECTS OF OBESITY ON LIPID-SOLUBLE DRUGS. ....	47
FIGURE 1.16 CLEARANCE DETERMINATION <i>VIA</i> BLOOD FLOW AND DRUG CONCENTRATION. ....	59
FIGURE 1.17 LOG DRUG AT INFINITY – DRUG IN URINE. ....	63
FIGURE 1. 18 COMPARTMENTAL CLEARANCE. ....	63
FIGURE 1.19 FIRST ORDER ELIMINATION HALF-LIFE. ....	65

## CHAPTER 2: DESIGN, METHODS, AND RESULTS FROM PRELIMINARY TESTING

FIGURE 2.1 SCHEMATIC OF THE ALBERTA DRUG ADMINISTRATION MODELLER (ADAM). ....	111
FIGURE 2.2 COMPARISONS FOR DRINKING WATER RESERVOIR VOLUME. ....	117
FIGURE 2.3 COMPARISONS FOR ON/OFF ELIMINATION PUMP SETTINGS. ....	120
FIGURE 2.4 COMPARISON OF HEART PUMP RATES AND INCLUSION/EXCLUSION OF THE 1 <sup>ST</sup> SAMPLE POINT. ....	124
FIGURE 2.5 CONSIDERATION TO TISSUE PUMP AND COMPARTMENT SETTINGS. ....	128

FIGURE 2.6 THE USE OF NEUTRAL RED AND OIL IN THE TISSUE COMPARTMENT.....	132
FIGURE 2.7 PUMP CALIBRATIONS.....	138

## CHAPTER 3: RESULTS

FIGURE 3.1. ONE-COMPARTMENT MODELLING OF IV AND PO DRUG-PLASMA CONCENTRATIONS UNDER VARIED ELIMINATION PUMP SETTINGS.....	141
FIGURE 3.2. COMPLEMENTARY ONE-COMPARTMENT MODELLING OF IV AND PO DRUG-URINE CONCENTRATIONS FOR DRUG-PLASMA DATA SHOWN IN FIGURE 3.1.....	145
FIGURE 3.3. ONE-COMPARTMENT MODELLING OF IV AND PO DRUG-PLASMA CONCENTRATIONS UNDER THE SAME VARIED ELIMINATION PUMP SETTINGS AS FIGURE 3.1.....	149
FIGURE 3.4. COMPLEMENTARY ONE-COMPARTMENT MODELLING OF IV AND PO DRUG-URINE CONCENTRATIONS FOR DRUG-PLASMA DATA SHOWN IN FIGURE 3.3.....	151
FIGURE 3.5. ONE-COMPARTMENT MODELLING OF IV AND PO DRUG-PLASMA AND -URINE CONCENTRATIONS TO ACHIEVE AN F OF 30% UNDER FAST AND SLOW ELIMINATION PUMP SETTINGS.....	154
FIGURE 3.6 ONE-COMPARTMENT MODELLING OF IV AND PO DRUG-PLASMA AND -URINE CONCENTRATIONS TO ACHIEVE AN F OF 30% UNDER FAST AND AN F OF 70% UNDER SLOW ELIMINATION PUMP SETTINGS.....	158
FIGURE 3.7. ONE-COMPARTMENT MODELLING OF DRUG-PLASMA CONCENTRATIONS FOLLOWING SINGLE IV DOSING, REPEATED IV DOSING, AND INTERMITTENT IV INFUSION.....	162
FIGURE 3.8. TWO-COMPARTMENT MODELLING OF IV DRUG-PLASMA CONCENTRATIONS UNDER VARIED ELIMINATION PUMP SETTINGS AND TISSUE COMPARTMENT VOLUMES.....	166
FIGURE 3.9. COMPLEMENTARY TWO-COMPARTMENT MODELLING OF IV DRUG-URINE CONCENTRATIONS FOR DRUG-PLASMA DATA SHOWN IN FIGURE 3.8.....	171
FIGURE 3.10. TWO-COMPARTMENT MODELLING OF IV AND PO DRUG-PLASMA CONCENTRATIONS UNDER VARIED TISSUE COMPARTMENT VOLUMES.....	174
FIGURE 3.11. COMPLEMENTARY TWO-COMPARTMENT IV AND PO DRUG-URINE CONCENTRATIONS FOR PLASMA DATA SHOWN IN FIGURE 3.10.....	176
FIGURE 3.12. MODELLING EFFECTS OF VARIED ORAL BIOAVAILABILITY PUMP RATES OR STOMACH VOLUMES ON TWO-COMPARTMENT PO DRUG-PLASMA CONCENTRATIONS.....	179
FIGURE 3.13. MODELLING EFFECTS OF VARIED TISSUE PUMP RATES ON TWO-COMPARTMENT IV DRUG-PLASMA CONCENTRATIONS.....	182

FIGURE 3.14. MODELLING EFFECTS OF VARIED TISSUE PUMP RATES AND TISSUE COMPARTMENT VOLUMES ON TWO-COMPARTMENT IV DRUG-PLASMA CONCENTRATIONS.....	185
FIGURE 3.15. MODELLING EFFECTS OF VARIED TISSUE COMPARTMENT VOLUMES ON TWO-COMPARTMENT IV DRUG-PLASMA CONCENTRATIONS. ....	188
FIGURE 3.16. MODELLING EFFECTS OF TISSUE COMPARTMENT VOLUME OF 1000 mL ON TWO-COMPARTMENT IV DRUG-PLASMA CONCENTRATIONS. ....	191
FIGURE 3.17. MODELLING EFFECTS OF TISSUE COMPARTMENT VOLUME OF 500 mL ON TWO-COMPARTMENT IV DRUG-PLASMA CONCENTRATIONS. ....	192
FIGURE 3.18. REPEATED OR CHRONIC DRUG ADMINISTRATION, WITH OR WITHOUT LOADING DOSE, BY IV AND PO ROUTES IN A TWO-COMPARTMENT CONFIGURATION. ....	197
FIGURE 3.19. DRUG-PLASMA CONCENTRATION TIME PROFILES FOLLOWING REPEATED PO DRUG ADMINISTRATION IN A TWO-COMPARTMENT CONFIGURATION USING TWO DIFFERENT DOSING INTERVALS: 15 MIN AND 10 MIN. ....	200
FIGURE 3.20. SCATTER PLOTS SHOWING UNDERGRADUATE STUDENT PERFORMANCE AND SELF-ASSESSMENT SCORES BEFORE AND AFTER COMPLETING TWO LABORATORY CLASSES WITH THE PK SIMULATOR. ....	203
FIGURE 3.21. SURVEY RESULTS SHOWING UNDERGRADUATE STUDENT RESPONSES TO QUESTIONS CONCERNING THE UNDERGRADUATE LABORATORY AND MODELLER RATED ON A SCALE OF 1 TO 5 (WHERE 1 CORRESPONDS TO <i>STRONGLY DISAGREE</i> AND 5 CORRESPONDS TO <i>STRONGLY AGREE</i> ).....	203
FIGURE 3.22. EXAMPLES OF REAL-TIME SPECTROPHOTOMETER OUTPUT, OBTAINED BY DIVERTING A SMALL PORTION OF SYSTEMIC CIRCULATION THROUGH A FLOW-THROUGH CUVETTE.....	205

# LIST OF TABLES

## CHAPTER 2: DESIGN, METHODS, AND RESULTS FROM PRELIMINARY TESTING

TABLE 2.1 EQUATIONS USED TO CALCULATE PK PARAMETERS FROM DATA GENERATED BY THE ADAM. ....	114
TABLE 2.2 PK PARAMETERS CALCULATED FOR CHANGES IN DRINKING WATER RESERVOIR VOLUME.....	118
TABLE 2.3 PK PARAMETERS CALCULATED FOR CHANGES BETWEEN ON/OFF ELIMINATION PUMP SETTINGS. ....	121
TABLE 2.4 PK PARAMETERS CALCULATED AT DIFFERENT HEART PUMP SETTINGS AND INCLUSION/EXCLUSION OF THE FIRST SAMPLE POINT. .....	125
TABLE 2.5 PK PARAMETERS CALCULATED FOR TISSUE PUMP AND COMPARTMENT SETTINGS. ....	129
TABLE 2.6 PK PARAMETERS CALCULATED WITH NEUTRAL RED AS DRUG AND OIL IN THE TISSUE COMPARTMENT. ....	133

## CHAPTER 3: RESULTS

TABLE 3.1 PK PARAMETERS CALCULATED FROM IV AND PO DRUG-PLASMA CONCENTRATIONS SHOWN IN FIGURE 3.1.....	142
TABLE 3.2 PK PARAMETERS CALCULATED FROM IV AND PO DRUG-URINE CONCENTRATIONS SHOWN IN FIGURE 3.2. ....	146
TABLE 3.3 PK PARAMETERS CALCULATED FROM IV AND PO DRUG-PLASMA CONCENTRATIONS SHOWN IN FIGURE 3.3.....	150
TABLE 3.4 PK PARAMETERS CALCULATED FROM IV AND PO DRUG-URINE CONCENTRATIONS SHOWN IN FIGURE 3.4.....	152
TABLE 3.5 PK PARAMETERS CALCULATED FROM IV AND PO DRUG-PLASMA CONCENTRATIONS SHOWN IN FIGURE 3.5 A AND B.....	155
TABLE 3.6 PK PARAMETERS CALCULATED FROM IV AND PO DRUG-URINE CONCENTRATIONS SHOWN IN FIGURE 3.5 C AND D. .	156
TABLE 3.7 PK PARAMETERS CALCULATED FROM IV AND PO DRUG-PLASMA CONCENTRATIONS SHOWN IN FIGURE 3.6 A AND B.....	159
TABLE 3.8 PK PARAMETERS CALCULATED FROM IV AND PO DRUG-URINE CONCENTRATIONS SHOWN IN FIGURE 3.6 C AND D. .	160
TABLE 3.9 PK PARAMETERS CALCULATED FROM ANALYSES OF IV DRUG-PLASMA CONCENTRATIONS FROM SINGLE, REPEATED, AND INTERMITTENT IV INFUSION EXPERIMENTS SHOWN IN FIGURE 3.7. ....	163
TABLE 3.10 PK PARAMETERS CALCULATED FROM IV DRUG-PLASMA CONCENTRATIONS SHOWN IN FIGURE 3.8.....	167
TABLE 3.11 PK PARAMETERS CALCULATED FROM IV DRUG-URINE CONCENTRATIONS SHOWN IN FIGURE 3.9. ....	172
TABLE 3.12 PK PARAMETERS CALCULATED FROM IV AND PO DRUG-PLASMA CONCENTRATIONS SHOWN IN FIGURE 3.10.....	175
TABLE 3.13 PK PARAMETERS CALCULATED FROM TWO-COMPARTMENT IV AND PO DRUG-URINE CONCENTRATIONS SHOWN IN FIGURE 3.11. ....	177
TABLE 3.14 PK PARAMETERS CALCULATED FROM PO DRUG-PLASMA CONCENTRATIONS SHOWN IN FIGURE 3.12. ....	180

TABLE 3.15 PK PARAMETERS CALCULATED FROM IV DRUG-PLASMA CONCENTRATIONS UNDER VARIED TISSUE PUMP RATES SHOWN IN FIGURE 3.13.....	183
TABLE 3.16 PK PARAMETERS CALCULATED FROM IV DRUG-PLASMA CONCENTRATIONS UNDER VARIED TISSUE PUMP RATES AND TISSUE COMPARTMENT VOLUMES SHOWN IN FIGURE 3.14. ....	186
TABLE 3.17 PK PARAMETERS CALCULATED FROM IV DRUG-PLASMA CONCENTRATIONS UNDER VARIED TISSUE COMPARTMENT VOLUMES SHOWN IN FIGURE 3.15. ....	189
TABLE 3.18 PK PARAMETERS CALCULATED FROM IV DRUG-PLASMA CONCENTRATIONS UNDER LARGER TISSUE COMPARTMENT VOLUMES SHOWN IN FIGURE 3.16 AND 3.17.....	193
TABLE 3.19 PK PARAMETERS CALCULATED FROM ANALYSES OF IV AND PO DRUG-PLASMA CONCENTRATIONS FROM SINGLE, AND REPEATED DOSING SHOWN IN FIGURE 3.18A, B, AND C. ....	198
TABLE 3.20 PK PARAMETERS CALCULATED FROM ANALYSES OF IV AND PO DRUG-PLASMA CONCENTRATIONS FROM REPEATED DOSING WITH LOADING DOSE, AND CONTINUOUS IV INFUSION EXPERIMENTS SHOWN IN FIGURE 3.18D, E, AND F. ....	199
TABLE 3.21 PK PARAMETERS CALCULATED FROM PO DRUG-PLASMA CONCENTRATIONS UNDER VARIED REPEATED PO DOSING REGIMENS SHOWN IN FIGURE 3.19. ....	201

## APPENDIX I

TABLE I.I PKSOLVER ANALYSIS OF ONE-COMPARTMENT IV DATA SHOWN IN FIGURE 3.6. ....	237
TABLE I.II PKSOLVER ANALYSIS OF TWO-COMPARTMENT IV DATA SHOWN IN FIGURE 3.8. ....	238
TABLE I.III PKSOLVER ANALYSIS OF TWO-COMPARTMENT IV DATA SHOWN IN FIGURE 3.13 WITH VARIED TISSUE PUMP RATES. ....	239
TABLE I.IV PKSOLVER ANALYSIS OF TWO-COMPARTMENT IV DATA SHOWN IN FIGURE 3.15 WITH VARIED TISSUE COMPARTMENT VOLUMES. ....	240

## LIST OF ABBREVIATIONS

**A:** intercept with log Y-axis of extrapolated distribution phase  
**AAG:**  $\alpha_1$ -acid glycoprotein  
**ADAM:** Alberta Drug Administration Modeller  
**ADEs:** adverse drug events  
**ADME:** Absorption, Distribution, Metabolism, Elimination  
**ANCOVA:** analysis of covariance  
**ARS:** audience response systems  
 **$\alpha$ :** first-order rate constant for distribution  
**AUC:** area under a concentration-time curve (time zero to infinity)  
**AUMC:** area under a time-concentration vs time curve (time zero to infinity)  
**AV<sub>D</sub>:** apparent volume of distribution  
**B:** intercept with log-Y axis of extrapolated elimination phase  
 **$\beta$ :** first-order rate constant for elimination  
**C<sub>A</sub>:** arterial concentration of the drug  
**C<sub>Av</sub>:** C<sub>SS</sub> in repeated dosing regimens  
**CBL:** case-based learning  
**CL:** clearance  
**CL<sub>int</sub>:** intrinsic clearance capacity of an organ  
**CL<sub>H</sub>:** hepatic clearance  
**CL<sub>R</sub>:** renal clearance  
**CL<sub>Organ</sub>:** clearance by eliminating organ  
**CL<sub>NR</sub>:** non-renal clearance  
**CL<sub>Total</sub>:** total body clearance  
**C<sub>max</sub>:** peak plasma concentration after a single (PO) drug dose or mean peak plasma concentration with repeated dosing at steady state  
**C<sub>min</sub>:** mean trough plasma concentration with repeated dosing at steady state  
**C<sub>u,p</sub>:** unbound drug plasma concentration  
**C<sub>p</sub>:** drug plasma concentration  
**C<sub>p, total</sub>:** total drug plasma concentration  
**C<sub>SS</sub>:** mean plasma concentration with repeated dosing at steady state  
**C<sub>t0</sub>:** concentration of drug in the plasma at t=0  
**C<sub>tn</sub>:** concentration of drug in the plasma at t=n  
**C<sub>u</sub>:** drug urine concentration  
**C<sub>v</sub>:** venous concentration of the drug  
**CPT:** clinical pharmacology and therapeutics  
**CYP:** Cytochrome P450 isoenzyme  
**CYP450:** Cytochrome P450

**Da:** Dalton  
**D<sub>∞</sub>:** drug in urine at time infinity  
**D:** dose  
**D<sub>B</sub>:** amount of drug in body  
**D<sub>U</sub>:** unchanged drug in urine  
**DDIs:** drug-drug interactions  
**ECV:** extracellular volume  
**ER:** extraction ratio  
**ER<sub>H</sub>:** hepatic extraction ratio  
**F:** oral bioavailability  
**F<sub>organ</sub>:** compound availability for eliminating organ  
**f<sub>b,p</sub>:** fraction drug bound in plasma  
**f<sub>u,p</sub>:** fraction drug unbound in plasma  
**F<sub>SS</sub>:** target fraction of C<sub>SS</sub>  
**FY1:** foundation year 1 doctors  
**GFR:** glomerular filtration rate  
**IM:** intramuscular (administration)  
**IV:** intravenous (administration)  
**HRMs:** high risk medications  
**k:** first order rate constant  
**k<sub>10</sub>:** first order rate constant for elimination of drug from central compartment only  
**k<sub>12</sub>:** first order rate constant for movement of drug from central to peripheral compartment  
**k<sub>21</sub>:** first order rate constant for movement of drug from peripheral to central compartment  
**k<sub>abs</sub>:** first order rate constant for absorption  
**k<sub>dist</sub>:** first order rate constant for distribution  
**k<sub>el</sub>:** first order rate constant for elimination  
**kg:** kilogram  
**K<sub>M</sub>:** Michaelis constant  
**LAL:** lecture-with-active learning  
**MAT:** mean absorbance time  
**MD:** maintenance dose  
**MDT:** mean dissolution time  
**MEC:** minimum effective concentration  
**MRT:** mean residence time  
**MRT<sub>IV</sub>:** mean residence time of IV administration  
**MRT<sub>NI</sub>:** mean residence time of non-IV administration  
**MTC:** maximum tolerated concentration  
**MW:** molecular weight  
**NSAIDs:** non-steroidal anti-inflammatory drugs  
**PBL:** problem-based learning

**PK:** pharmacokinetics  
**PO:** oral (administration)  
**PM:** poor metaboliser  
**PV:** plasma volume  
**Q:** blood flow  
**Q<sub>H</sub>:** hepatic blood flow  
**Q<sub>u</sub>:** urine flow  
**SC:** subcutaneous (administration)  
**TBL:** team-based learning  
**TBW:** total body water  
**t<sub>1/2</sub>:** half life  
**t<sub>1/2 dist</sub>:** distribution half life  
**t<sub>1/2 el</sub>:** elimination half life  
**t<sub>max</sub>:** time taken to reach C<sub>max</sub> after a single (PO) drug dose  
**τ:** dosing interval in repeated dosing regimen  
**T<sub>SS</sub>:** time to reach F<sub>SS</sub>  
**UM:** ultra-rapid metaboliser  
**V<sub>C</sub>:** volume of central compartment  
**V<sub>D</sub>:** volume of distribution  
**V<sub>D Area</sub>:** volume of distribution calculated by the area or beta method  
**V<sub>D SS</sub>:** volume of distribution calculated by the steady state method  
**V<sub>D Extrap</sub>:** volume of distribution calculated from the Y-intercept of the terminal elimination phase  
**V<sub>T</sub>:** volume of tissue compartment  
**V<sub>max</sub>:** maximal rate of enzyme or transporter activity

## TABLE OF CONTENTS

ABSTRACT .....	II
PREFACE .....	IV
ACKNOWLEDGEMENTS .....	V
LIST OF FIGURES .....	VI
LIST OF TABLES.....	IX
LIST OF ABBREVIATIONS.....	XI
<u>CHAPTER 1: TEACHING AND LEARNING PHARMACOKINETICS.....</u>	<u>1</u>
1.1 PHARMACOKINETIC BASIS OF THERAPEUTICS .....	1
1.1.1 INTRODUCTION .....	1
1.1.1.1 General Mathematical Principles.....	4
Rates of Reactions .....	4
Transporter and Enzyme Kinetics .....	5
Linear versus Nonlinear Pharmacokinetics .....	8
1.1.1.2 Physicochemical Properties of Drugs .....	9
The Cell Membrane.....	9
Passive Diffusion .....	10
Facilitated Diffusion.....	12
Carrier-Mediated Transport.....	12
1.1.2 ADME: ABSORPTION .....	13
1.1.2.1 Kinetic Definitions and Principles of Absorption.....	13
Bioavailability.....	13

First Pass Metabolism .....	15
Absorption Rate Constant .....	16
1.1.2.2 Physiological Aspects of Absorption .....	17
Routes of Administration .....	18
Intravenous Administration .....	19
Oral Administration.....	20
Formulation .....	21
Dissolution .....	22
Permeability.....	23
Ionisation .....	25
1.1.2.3 Patient Factors Affecting Absorption .....	26
Gastric Emptying .....	26
Diet .....	27
Age .....	28
Disease .....	29
1.1.3 ADME: DISTRIBUTION .....	30
1.1.3.1 Kinetic Definitions and Principles of Distribution .....	30
One Compartment Model.....	30
Two Compartment Model .....	32
Multi-Compartment Modelling.....	35
Volume Terms.....	38
Distribution Rate Constant .....	43
1.1.3.2 Physiological Aspects of Distribution .....	44
Plasma Protein Binding.....	44
Tissue Characteristics .....	46
1.1.3.3 Patient Factors Affecting Distribution .....	46
Obesity .....	46

Disease .....	48
Age .....	48
1.1.4 ADME: METABOLISM .....	49
Phase I Reactions .....	49
The Cytochrome P450 (CYP) System .....	50
Phase II Reactions .....	51
Kinetic Definitions and Principles of Metabolism .....	51
Metabolism Inhibition .....	52
Metabolism Induction .....	53
1.1.4.2 Patient Factors Affecting Metabolism .....	54
Genetics .....	54
Age .....	55
Disease .....	55
Diet .....	56
1.1.5 ADME: ELIMINATION .....	57
1.1.5.3 Kinetic Definitions and Principles of Elimination .....	57
Physiological Modelling .....	57
Hepatic Elimination .....	60
Renal Elimination .....	61
Compartmental Modelling .....	63
Elimination Rate Constant and Half-Life .....	64
1.1.5.2 Physiological Aspects of Elimination .....	67
Renal Elimination .....	67
Biliary Elimination .....	69
1.1.5.3 Patient Factors Affecting Elimination .....	69
Disease .....	69
Age .....	70

1.1.6 ANALYSIS AND APPLICATION OF PHARMACOKINETICS DATA .....	71
1.1.6.1 Compartmental Method.....	71
1.1.6.2 Non-compartmental Method .....	73
1.1.6.3 Chronic Dosing.....	78
Continuous Intravenous Infusions.....	79
Multiple Dosing Regimens .....	80
Loading Dose .....	83
<b>1.2 PRESCRIBING ERRORS .....</b>	<b>83</b>
1.2.1 DEFINITIONS, RISKS, AND IMPACTS .....	83
1.2.2 PREVALENCE AND CAUSES .....	85
<b>1.3 PHARMACOKINETICS IN THE CLASSROOM .....</b>	<b>90</b>
1.3.1 INADEQUATE TRAINING AND EDUCATION.....	90
1.3.2 PRACTICES AND INNOVATIONS FOR PK INSTRUCTION .....	94
1.3.2.1 Teaching in the Pharmacy Curriculum.....	94
Active Learning Techniques .....	95
Technology.....	97
Computer Simulations.....	98
The “Flipped” or “ Blended” Classroom .....	101
1.3.2.2 Teaching in the Medical Curriculum .....	102
Problem Based Learning (PBL) .....	103
Online Programs.....	105
Medical Apps.....	105
<b>1.4 THE ADAM AS A LEARNING TOOL.....</b>	<b>107</b>
<b><u>CHAPTER 2: DESIGN, METHODS, AND RESULTS OF PRELIMINARY TESTING .....</u></b>	<b><u>109</u></b>
<b>2.1 APPARATUS CONCEPT AND CONSTRUCTION.....</b>	<b>109</b>
<b>2.2 DRUG ADMINISTRATION.....</b>	<b>112</b>

<b>2.3 DESIGN AND ANALYSIS CHANGES, ADDITIONS, AND CONSIDERATIONS .....</b>	<b>114</b>
2.3.1 DRINKING WATER RESERVOIR VOLUME EFFECTS .....	115
2.3.2 ON VERSUS OFF SETTING OF PUMP G, I, AND J DURING DRUG ADMINISTRATION .	119
2.3.3 HEART PUMP RATE EFFECTS .....	123
2.3.4 EARLY SAMPLING POINT EFFECTS .....	125
2.3.5 DIALYSIS MEMBRANE .....	127
2.3.6 TISSUE PUMP AND COMPARTMENT SETTINGS.....	127
2.3.7 OIL IN THE TISSUE COMPARTMENT WITH PH CHANGES IN SYSTEM.....	129
2.3.8 MIMICKING ORAL BIOAVAILABILITY .....	134
2.3.9 PLATEAU CONSTRAINTS .....	134
2.3.10 USE OF $V_D$ EXTRAP IN CHRONIC DOSING .....	135
2.3.11 USE OF PK SOLVER FOR SYSTEM VALIDATION .....	135
<b>2.3 IN THE CLASSROOM.....</b>	<b>136</b>
<b>2.4 MATERIALS AND CALIBRATIONS.....</b>	<b>137</b>
<b><u>CHAPTER 3: RESULTS.....</u></b>	<b><u>140</u></b>
<b>3.1 ONE COMPARTMENT MODELLING .....</b>	<b>140</b>
ONE COMPARTMENT REPEATED DOSING .....	161
<b>3.2 TWO COMPARTMENT MODELLING.....</b>	<b>164</b>
TWO-COMPARTMENT CHRONIC DOSING.....	194
<b>3.3 STUDENT RESULTS.....</b>	<b>202</b>
<b>3.4 REAL TIME MONITORING .....</b>	<b>204</b>
<b><u>CHAPTER 4: DISCUSSION AND CONCLUSION .....</u></b>	<b><u>206</u></b>
<b>4.1 SUMMARY OF RESULTS .....</b>	<b>206</b>
<b>4.2 STRENGTHS, LIMITATIONS AND DESIGN ALTERATIONS.....</b>	<b>209</b>
<b>4.3 SIMILAR INNOVATIONS.....</b>	<b>214</b>
<b>4.4 FUTURE APPLICATIONS OF ADAM .....</b>	<b>219</b>

BIBLIOGRAPHY .....	222
APPENDIX I .....	237

# CHAPTER 1: TEACHING AND LEARNING PHARMACOKINETICS

## 1.1 PHARMACOKINETIC BASIS OF THERAPEUTICS

### 1.1.1 INTRODUCTION

Pharmacokinetics (PK) provides mathematical basis for the time course of a drug, and analysis quantifies the drug's absorption, distribution, metabolism, and elimination (ADME) (Dhillon & Kostrzewski, 2006). These four fundamental processes are distinct in function, but are often interrelated (Fan & de Lannoy, 2014). Absorption is the process affecting the rate and extent to which a drug reaches the systemic circulation; once in the circulation, distribution explains the transfer from the circulation into target and non-target tissues (Bauer, 2006). Eventually, metabolism converts the drug molecule into a metabolite primed for elimination, which results in the irreversible removal of the drug from the body (Bauer, 2006). Of the many parameters calculated, four are considered most useful for the application of PK in the clinic:

1. Clearance (CL; volume/time): a measure of the body's ability to eliminate a drug
2. Volume of Distribution (V; units of volume): the apparent volume or space containing the drug
3. Half-life ( $t_{1/2}$ ; units of time): the time it takes for a drug's concentration to decrease to 50% of its concentration
4. Bioavailability (F, unit-less, %): the fraction of a drug absorbed into the systemic circulation

With consideration to the 'pharmacokinetic basis of therapeutics', successful treatment is not exclusively comprised of simply choosing the proper drug (Greenblatt & Shader, 1985). Two or more drugs in a class may exert similar dose efficacy profiles, but the balance of favourable/unfavourable pharmacokinetic characteristics determines the drug of choice (Benet

& Zech, 1994). Clinicians must consider the proper dose, route of administration, frequency of administration, and patient factors that will achieve and maintain the drug's minimum effective concentration at the site of action for a specific period (Greenblatt & Shader, 1985). The applications of PK are quite comprehensive and include: bioavailability measurements, effects of physiological and pathological conditions on drug disposition and absorption, dosage adjustment in disease states, correlation of pharmacological responses with administered doses, evaluation for drug interactions, and using PK parameters to individualise dosing regimens (Jambhekar & Breen, 2009).

Most drugs are managed through standard procedure: the dose is based on unit per body mass ( $\text{mg kg}^{-1}$ ), and the dosage is adjusted based on the clinical response, known as the "titration to clinical effect" (Clarke, 2016). Some are assessed *via* their physiological outcomes, as obtained from laboratory measurements, such as statins and resulting blood lipid levels (Clarke, 2016). However, a small subset of drugs show a narrow therapeutic index or exhibit pharmacokinetics that are highly variable between individuals, requiring more extensive management through therapeutic drug monitoring (TDM) (Clarke, 2016; Dhillon & Kostrzewski, 2006). Though the application of PK may vary in terms of extent and frequency in the clinical context, developing a comprehensive knowledge base of this subject matter is necessary to ensure appropriate patient care in any situation and setting.

Ideally, the concentration of a drug is measured at its site of action: the target receptor (Dhillon & Kostrzewski, 2006). However, due to inaccessibility, drug concentrations are largely measured in plasma, though sometimes there is need for urine, cerebrospinal fluid or saliva sampling as well (Dhillon & Kostrzewski, 2006). The main considerations for the action of a drug (or its active metabolite) are its intensity and duration of action (Gibson & Skett, 2001). Plasma concentration-time profile visuals communicate these considerations, and are used to calculate and interpret PK parameters (Figure 1.1) (Jambhekar & Breen, 2009). These graphs convey a relationship between the blood and tissue levels, and as such, the biological activity exerted by the drug: its onset and duration of action, and whether its concentration remained within its therapeutic range (Wagner, 1961). Mathematical applications expand these visuals, and thorough analysis

can explain the extent to which the drug distributes into tissue, its rate-constants, bioavailability, and other parameters that are integral in understanding the drug's relationship with the body and its kinetics.

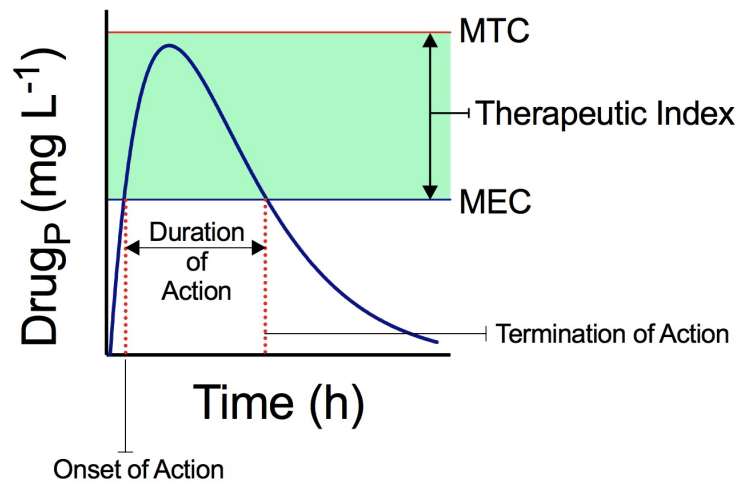


Figure 1.1 Plasma concentration time profile.

Drug is administered orally and drug concentrations are maintained within the therapeutic index until the levels fall below the MEC (minimum effective concentration). The drug levels do not exceed the MTC (maximum tolerated concentration).

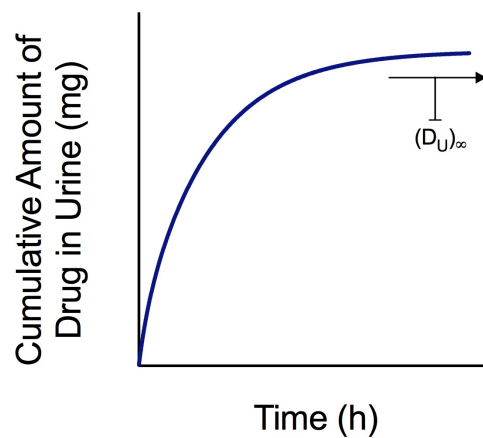


Figure 1.2 Cumulative amount of drug in urine *versus* time.

Drug is administered intravenously and accumulates in the urine over time until it reaches a plateau, representing Drug at time infinity ( $(D_U)_\infty$ ).

Non-invasive drug monitoring, such as urine sampling, is presented as a plot of cumulative amount of drug in urine *versus* time (Figure 1.2) Urine analysis can provide insight into a drug's elimination rate-constants, bioavailability, and other parameters without needing to consider mathematical or physiological models to the data (Jambhekar & Breen, 2009).

### 1.1.1.1 General Mathematical Principles

#### Rates of Reactions

The rates of the processes of ADME are each distinctive, and contribute to a drug's overall plasma-concentration profile. The rates, defined by the velocity at which they proceed, are categorised as either zero-order or first-order (Dhillon & Kostrzewski, 2006). In the case of zero-order reactions, the drug moves independently of the concentration of drug (Dhillon & Kostrzewski, 2006):

$$\frac{dA}{dt} = -k$$

(E. 1)

where  $k$  ( $\text{min}^{-1}$  or  $\text{h}^{-1}$ ) is the rate constant describing the elimination of the drug (Dhillon & Kostrzewski, 2006). The relationship is linear (Figure 1.3a), as the rate does not change at any point. A drug exhibiting this type of elimination would be subject to accumulation and potential overdose (Dhillon & Kostrzewski, 2006).

In contrast, a first-order rate reaction is dependent on drug concentration at the site, does not occur at a fixed rate, and varies continuously over time (Dhillon & Kostrzewski, 2006; Greenblatt & Shader, 1985). The first-order rate reaction for elimination is shown as:

$$\frac{dA}{dt} = -kA$$

(E. 2)

where  $k$  ( $\text{min}^{-1}$  or  $\text{h}^{-1}$ ) is the elimination rate constant of the drug and  $A$  ( $\text{mg L}^{-1}$ ) is the concentration of the drug at a specific time (Dhillon & Kostrzewski, 2006). Graphically, the

relationship is an exponential function (Figure 1.3b), and provides basis for determining the “half-life” value for the process (Greenblatt & Shader, 1985). Most drugs exhibit first order rate processes, and in the context of elimination, the elimination “half-life” will remain constant regardless of dose or plasma concentration (Greenblatt & Shader, 1985). However, a drug’s rate of reaction can shift to zero-order if there is saturation of the elimination or metabolic components (Dhillon & Kostrzewski, 2006).

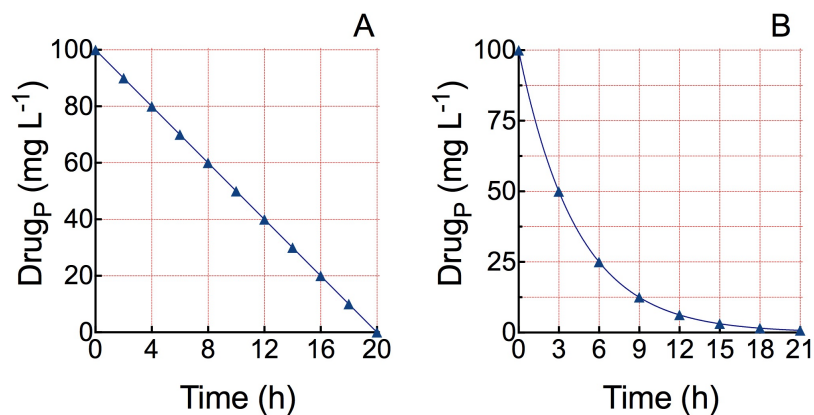


**Figure 1.3 Zero-order elimination *versus* first-order elimination kinetics.**

(A) Drug exhibiting zero-order elimination kinetics shows a linear relationship between the drug concentration of a drug and time. (B) Drug exhibiting first-order elimination kinetics displays an exponential decay relationship between drug concentration and time.

### Transporter and Enzyme Kinetics

Enzymes and transporters interact with drugs and influence their pharmacokinetics. Familiarity with principles and concepts of how drug concentrations relate to these components of pharmacokinetics is important. Enzymes interact with drugs to produce a drug-enzyme intermediate, which, when further processed, results in a metabolite eventually released from the enzyme (Mehvar, 2001). Transporters, in contrast, generally do not process the drug into a different molecule, but transport it into or out of a cell, depending on the compound (Giacomini & Sugiyama, 2011).

Enzymes and transporters are unique in their applications, and the intent in combining the following principles by which they are governed is a simplification, as both these protein families are subject to saturation, competition, and other processes that influence drug pharmacokinetics. The Michaelis-Menten equation provides a relation between substrate concentration to the activity of both enzymes and transporters at a rudimentary level (Giacomini & Sugiyama, 2011; Mehvar, 2001):

$$v = \frac{V_{\max}[S]}{K_m + [S]} \tag{E. 3}$$

where [S] is the substrate concentration,  $V_{\max}$  is the maximum transport or metabolic rate proportional to the density of transporters or enzymes (expressed as amount/time or concentration/time), and  $K_m$  is the Michaelis constant, representing the substrate concentration when the flux or metabolic rate is 50% of the  $V_{\max}$  (Giacomini & Sugiyama, 2011; Mehvar, 2001).

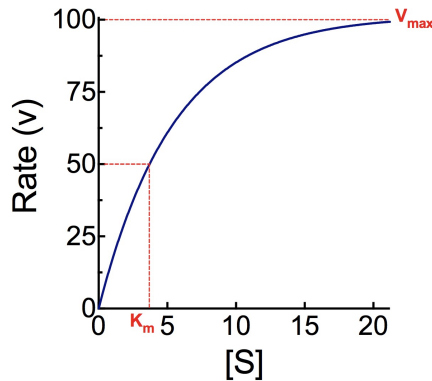


**Figure 1.4 Michaelis Menten Graphical Representation.**

Figure 1.4 illustrates the relationship between drug concentration and the rate of transport or metabolism as it relates to Michaelis-Menten kinetics. If the [S] of the drug  $\ll K_m$ , it is negligible in the denominator of Equation (E. 3):

$$v = \frac{V_{\max} \times [S]}{K_m + [S]} = \frac{V_{\max}}{K_m} \times [S]$$

$$v = \frac{V_{max}}{K_m} \times [S]$$

(E. 4)

The velocity of the reaction depends on  $V_{max}$  and  $K_m$ , which are known constants for the reaction, while the  $[S]$  is the concentration. The derivation reflects the relationship shown in Equation (E. 2), a first-order process (Mehvar, 2001). At this stage, increases in drug concentration will result in a proportional increase in the velocity of the reaction (Jambhekar & Breen, 2009). Eventually, the drug concentration increases to a point where Equation (E. 4) does not appropriately relate the parameters in the situation; Equation (E. 3) is most appropriate at this point. However, at extremely high  $[S]$ , the  $K_m$  in the denominator of Equation (E. 3) is negligible:

$$v = \frac{V_{max}[S]}{K_m + [S]} = \frac{V_{max} \times [S]}{[S]} = V_{max}$$

$$v = V_{max}$$

(E. 5)

Thus, when the drug concentration,  $[S] \gg K_m$ , the rate of transfer or metabolism is constant ( $V_{max}$ ), representing saturation of the process, and exhibiting a relationship resembling zero-order kinetics; Equation (E. 1) (Mehvar, 2001). An increase in the concentration of drug molecules will not change the rate of transport or metabolism of the compound (Jambhekar & Breen, 2009).

For most drugs, first-order rate reactions govern its ADME processes, and its PK parameters are not affected if different doses are administered, or if the drug is given through a different route of administration (Mehvar, 2001). However, there are a few clinically-used drugs that have one or more processes deviating from this norm, and as a result, the drug exhibits non-linear or dose-dependent kinetics (Greenblatt & Shader, 1985; Mehvar, 2001). Affected PK parameters may include clearance, volume of distribution, and half-life, which can drastically influence its efficacy and outcomes (Mehvar, 2001).

### Linear versus Nonlinear Pharmacokinetics

Figure 1.1 involves a single dose of drug achieving a therapeutic effect, but pharmaceuticals generally involves continuous or repeated dosing (Figure 1.5). Chronic dosing results in increasing plasma drug concentrations until the rate of elimination is in equilibrium with the rate of administration; the average amount of drug in the body reaches a constant value or **steady state ( $C_{SS}$ )** (Bauer, 2006). Achieving this steady state concentration is a therapeutic goal, and it requires consideration of PK parameters, patient factors, and correct application of PK equations. The relationship of  $C_{SS}$  with Dose provides insight into a drug's behaviour if a patient is administered repeated doses of a drug with subsequent monitoring of  $C_{SS}$  (Bauer, 2006). A proportionally increased or decreased  $C_{SS}$  to a respective increase or decrease in dose is indicative of linear pharmacokinetics, while a  $C_{SS}$  value that increases more than expected after an increased dose indicates that the processes of drug removal are saturated, and as such, the drug exhibits non-linear pharmacokinetics (Figure 1.6) (Bauer, 2006). While an appreciation for non-linear pharmacokinetics is important for understanding PK as it applies to patient care, this work will focus primarily on linear pharmacokinetics.

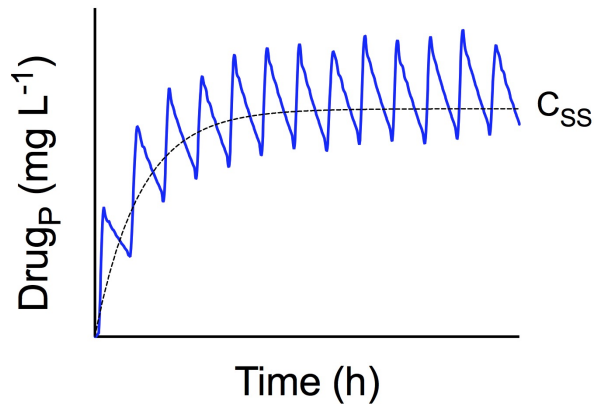


Figure 1.5 Chronic dosing and  $C_{SS}$ .

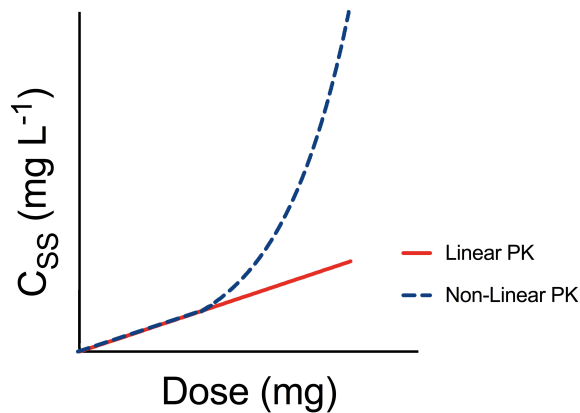


Figure 1.6 Linear *versus* non-linear pharmacokinetics.

### 1.1.1.2 Physicochemical Properties of Drugs

To access the general circulation and diffuse to target tissues, a drug must pass from its site of administration through or around one or more layers of cells (Shargel & Yu, 1999). Though a single layer of cells (e.g. arterial epithelium) may be the barrier to drug movement, the plasma membrane represents the common barrier for ADME (Buxton, Benet, Brunton, Chabner & Knollmann, 2011). Traversing the plasma membrane depends on the permeability of the compound, which is dependent on factors such as lipophilicity, molecular size, and charge (Fan & de Lannoy, 2014). Generally, a compound will have poor permeation if it has more than 5 H-bond donors, 10 H-bond acceptors, a molecular weight (MW) greater than 500 Daltons (Da), and/or a log partition ratio or coefficient (LogP) greater than 5 (Lipinski, Lombardo, Dominy & Feeney, 2001). As a note, the log partition relates to a compound's ability to diffuse through lipids, and the value is correlated with a drug's ability to partition between water and an organic solvent, such as octanol (Martinez & Amidon, 2002).

#### The Cell Membrane

The cell membrane is composed as a bilayer, with the polar head groups of the lipids located on the two membrane surfaces, and the hydrophobic "tails" in the interior, away from contact with water (Singer, 2004). Naturally, lipid-soluble drugs may have an easier time penetrating the

cell membrane in comparison to polar or charged molecules (Shargel & Yu, 1999). However, the lipid bilayer is intercalated by integral proteins or transmembrane proteins, which span the entire membrane (Singer, 2004). There are different types, and because most of these proteins are generally amphipathic, they act as channels and transporters, allowing ionic and hydrophilic compounds of varying size to be transported into the cell (Singer, 2004). Movement across the plasma membrane varies for different drugs due to regional differences in membrane polarity, hydrophobicity, and density (Martinez & Amidon, 2002).

### Passive Diffusion

Passive diffusion is characterised as molecules moving freely from areas of high concentration to regions of low concentration. The transfer is directly related to the LogP of the drug, possibly to the magnitude of an electrochemical gradient, and to the surface area of the membrane exposed to the drug (Buxton, Benet, Brunton, Chabner & Knollmann, 2011). The potential gradient ( $\Delta\mu$ ) is calculated by using the following equation:

$$\Delta\mu = zE_mF + RT\ln\left(\frac{C_i}{C_o}\right)$$

(E. 6)

where  $z$  is the charge valence of the solute,  $E_m$  is the membrane voltage (Volt),  $F$  is the Faraday constant,  $R$  is the gas constant,  $T$  is the absolute temperature (Kelvins),  $C_i$  is the concentration of solute inside, and  $C_o$  is the concentration outside the membrane (Giacomini & Sugiyama, 2011).

For most uncharged, and lipophilic molecules with molecular weights less than  $500 \text{ g mol}^{-1}$ , transcellular penetration is possible (Macheras, Karalis & Valsami, 2013). There are three processes contributing to simple diffusion across the cell membrane: partition from the aqueous to lipid phase, diffusion through the lipid bilayer, and partition into the aqueous phase on the other side (Giacomini & Sugiyama, 2011). For non-ionised compounds, the passive processes are described by Fick's Law of Diffusion:

$$J = -D \frac{dC}{dx}$$

(E. 7)

where J is the flux, D is the diffusion coefficient of the drug, C is its concentration, and x is the distance moved perpendicular to the surface of the membrane (Macheras, Karalis & Valsami, 2013). Drugs with characteristics of small size, charge, and hydrophilicity experience membrane passage *via* paracellular mechanisms or tight junctions (Macheras, Karalis & Valsami, 2013). All other drugs that do not enter through transcellular or para-cellular mechanisms may enter through influx transporters (Macheras, Karalis & Valsami, 2013). In addition, changes in pH influence the ionisation state of weak acids or bases, which affects drug transfer, as the ionised form does not partition as effectively as the non-ionised form (Buxton, Benet, Brunton, Chabner & Knollmann, 2011); (Fan & de Lannoy, 2014). The extent of ionisation of a weak acid or base depends on both the pK<sub>a</sub> of the drug and the pH of the medium it is dissolved in (Shargel & Yu, 1999). Figure 1.7 expands on the ionisation of weak acids and bases depending on their pK<sub>a</sub> and the pH of the solution.

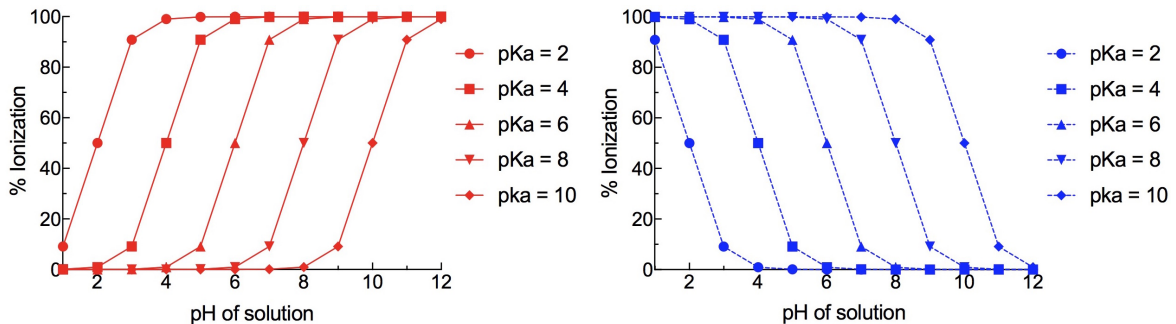


**Figure 1.7 Acid and Base Ionisation.**

Acid (red) and base (blue) ionisation % based on the compound's pK<sub>a</sub> and the pH of the solution. Adapted from a figure in Martinez and Amidon, 2002.

The Henderson and Hasselbalch equation describes these relationships (Buxton, Benet, Brunton, Chabner & Knollmann, 2011) as:

$$\log \frac{(\text{protonated form})}{(\text{unprotonated form})} = \text{pK}_a - \text{pH}$$

(E. 8)

### Facilitated Diffusion

This type of transport does not require energy input, and like passive diffusion, compounds move down their electrochemical potential gradient (Giacomini & Sugiyama, 2011). The key difference is that facilitated diffusion of compounds is mediated by transporters at the membrane (Giacomini & Sugiyama, 2011).

### Carrier-Mediated Transport

Though passive diffusion is the dominant process for most drugs, some depend on transport proteins, which shuttle the drug molecule from one side of the membrane to the other (Buxton, Benet, Brunton, Chabner & Knollmann, 2011; Shargel & Yu, 1999). Active transport is characterised by energy requirement, drug transport against a concentration gradient, saturability, selectivity, and competitive inhibition by co-transported compounds (Buxton, Benet, Brunton, Chabner & Knollmann, 2011; Shargel & Yu, 1999). The two types include **primary active transport**, where the transport is coupled with ATP hydrolysis, and **secondary active transport**, where the transport of one molecule is driven by the transport of another molecule moving down its concentration gradient (Giacomini & Sugiyama, 2011).

Two or more substrates can competitively interact and affect the flux of a principal compound (Giacomini & Sugiyama, 2011). **Competitive inhibition** involves competition for the same binding site on a transporter; the presence of the inhibitor substrate increases the apparent  $K_m$  value of the principal substrate (Giacomini & Sugiyama, 2011). **Non-competitive inhibition** involves an inhibitor exerting an allosteric effect on a transporter or enzyme, inhibiting the translocation of the principal compound (Giacomini & Sugiyama, 2011). Finally, **uncompetitive inhibition** involves an inhibitor which forms a complex with an intermediate complex of the principal substrate and transporter to inhibit the compound's translocation (Giacomini & Sugiyama, 2011).

## 1.1.2 ADME: ABSORPTION

Absorption is the movement of a drug from its site of administration into the central compartment, with every compound exhibiting its own unique absorption profile (Buxton, Benet, Brunton, Chabner & Knollmann, 2011); (Singer, 2004). The rate of absorption of a drug and/or the percentage of administered dose absorbed impacts the intensity and duration of the pharmacological response (Wagner, 1961). Changes in bioavailability and absorption rate depend on the anatomical site from which absorption takes place, as well as other physiological and pathological factors. Knowledge of how physiological factors directly influence drug absorption determines the dose, formulation, and even route of administration chosen for a compound (Buxton, Benet, Brunton, Chabner & Knollmann, 2011).

### 1.1.2.1 Kinetic Definitions and Principles of Absorption

#### **Bioavailability**

The bioavailability (F) of a drug administered through various routes is the fraction of unchanged drug which reaches the systemic circulation (Benet & Zia-Amirhosseini, 1995). Bioavailability is determined through analysis of data from concentration-time profile graphs. It describes the extent of absorption, but not the rate (Winter, 2010). Because an intravenous drug is administered directly into the systemic circulation, it is "100% bioavailable" ( $F=1$ ), and is the referenced standard when determining absolute bioavailability as the drug is administered directly into the systemic circulation (Benet & Zia-Amirhosseini, 1995; Jambhekar & Breen, 2009). Figure 1.8 demonstrates the plasma-concentration time profiles of the same dose of a drug administered parenterally and through an extravascular route. The area under the curve (AUC) is the calculated area under each concentration-time curve, calculated until time infinity.

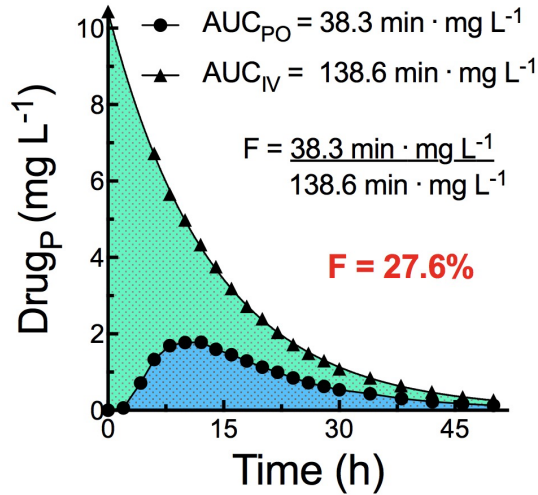


Figure 1.8 Comparison of AUC between IV and PO dosing.

Plasma-concentration time profile following administration of the same dose of a drug (1 mg) via an intravenous (IV) bolus and oral tablet (PO). AUC values were determined and used to calculate the oral bioavailability (F) of the oral tablet. The oral bioavailability, represented by a percentage, was calculated as 27.6%.

The fraction of an oral dose of drug available to the systemic circulation is calculated by comparing the ratio of the AUC following oral (PO) and intravenous (IV) dosing (Benet & Zia-Amirhosseini, 1995):

$$F = \frac{AUC_{0-\infty}^{PO}}{AUC_{0-\infty}^{IV}}$$

(E. 9)

A comparison of the cumulative amount of unchanged drug in the urine following PO and IV administration estimates bioavailability:

$$F = \frac{D_{urine,0-\infty}^{PO}}{D_{urine,0-\infty}^{IV}}$$

(E. 10)

where  $D^{PO}$  is the amount of cumulative unchanged compound excreted in the urine after oral administration, and  $D^{IV}$  is the amount of cumulative unchanged compound excreted in the urine after IV administration (Fan & de Lannoy, 2014). These calculations are appropriate when at least 20% of the dose is excreted in the urine after IV administration, and the fraction excreted does not vary (Fan & de Lannoy, 2014).

### **First Pass Metabolism**

An orally administered drug faces extensive GI factors which influence its ability to traverse plasma membranes, including chemical degradation in the stomach, metabolism by enzymes in the proximal small intestine and gut wall, as well as by bacteria in the distal intestine and colon (Gibaldi, 1984). Even if a drug successfully overcomes these obstacles, passes through cell membranes, and reaches the portal circulation, it may undergo extensive metabolism in the liver before reaching the systemic circulation (Winter, 2010). Early pharmacokinetic studies reported that AUC calculated for aspirin and lidocaine in dogs were considerably greater when the drug was administered into a peripheral vein as opposed to the portal vein (Boyes, Adams & Duce, 1970; Harris & Riegelman, 1969). The difference was attributed to the drug's initial exposure to the liver before reaching the sampled vascular sites, and termed the "first-pass" effect (Gibaldi, Boyes & Feldman, 1971). The liver is the most important site of pre-systemic metabolism, because of its unique anatomical location, high level of drug metabolising enzymes, and ability to rapidly metabolise many kinds of drug molecules (Gibaldi, 1984). The first-pass effect tremendously influences a drug's bioavailability (F), and has a major bearing upon drug dosing. The hepatic clearance ( $CL_H$ ) is calculated as:

$$CL_H = Q_H \times ER_H \tag{E. 11}$$

where  $Q_H$  is the hepatic blood flow, and  $ER_H$  is the hepatic extraction ratio (Gibaldi, 1984). The  $ER_H$  is the fraction of drug cleared by the liver while the remainder of the drug ( $1-ER_H$ ) reaches the systemic circulation (Gibaldi, 1984). Thus, to determine the AUC:

$$AUC_{0-\infty}^{PO} = \frac{f \times D(1 - ER_H)}{Q_H \times ER_H} \quad (\text{E. 12})$$

where  $f$  is the fraction of the Dose ( $D$ ) absorbed and subjected to the first-pass effect, and  $Q_H \times ER_H$  represents the  $CL_H$  (Gibaldi, 1984). Consideration of the relationship depicted in Equation (E. 9) results in:

$$\frac{AUC_{0-\infty}^{PO}}{AUC_{0-\infty}^{IV}} = \frac{f \times D(1 - ER_H)}{D_{IV}} \quad (\text{E. 13})$$

where  $f$  is the fraction of the Dose ( $D$ ) absorbed and subjected to the first-pass effect,  $ER_H$  is the hepatic extraction ratio, and  $D_{IV}$  is the intravenously administered dose and the reference amount. This relationship relates to oral bioavailability. If a drug exhibits an  $f$  of 1, and all drug reaches the portal circulation, then the drug's bioavailability is expressed as:

$$F = 1 - ER_H \quad (\text{E. 14})$$

The bioavailability of a drug depends on its hepatic extraction ratio, which will be discussed in greater detail in Section 1.1.5 ADME: Elimination. Drugs with low extraction ratios, such as warfarin, undergo little pre-systemic metabolism, translating into higher bioavailability. In contrast, propranolol, though well absorbed into the portal circulation, has an  $ER_H$  of ~0.7; ~30% of the initial dose reaches the systemic circulation (Gibaldi, 1984). Inter-individual variability in metabolism affects high extraction ratio drugs, and the extent of the first-pass effect can vary largely between individuals (Gibaldi, 1984).

### Absorption Rate Constant

The absorption rate constant ( $k_a$ ;  $hr^{-1}$  or  $min^{-1}$ ) describes the rate at which a drug undergoes absorption, eventually reaching its peak plasma concentration ( $C_{max}$ ) (Dhillon & Kostrzewski, 2006; Mahmood, 1998). The process is characterised by an absorption half-life ( $t_{1/2 \text{ abs}}$ )

independent of dose (Greenblatt & Shader, 1985). The  $k_a$  directly impacts the absorption half-life; short half-life values depict rapid absorption, while long half-lives indicate slower absorption and longer time to reach peak levels ( $t_{max}$ ) (Greenblatt & Shader, 1985). At  $C_{max}$ , the rate of drug absorption and drug removal (due to processes of distribution and elimination) reach an equilibrium (Greenblatt & Shader, 1985).

When rapid onset of drug effect is desired, such as with oral analgesics, anti-arrhythmic agents, or hypnotic agents, the absorption rate impacts drug efficacy in a major way (Greenblatt & Shader, 1985). In other cases, the  $k_a$  may not be as pertinent. The  $k_a$  is measured and calculated using a variety of analysis methods depending on the drug's distribution kinetics (Mahmood, 1998). Generally, the  $k_a$  value is deemed as a relatively "unstable" PK parameter; its outcome can vary considerably, even if, on two separate occasions, an individual ingests the same dose of a drug in identical conditions (Greenblatt & Shader, 1985). Thus, the calculation of this parameter has less statistical reliability than other rate constants (Greenblatt & Shader, 1985).

#### **1.1.2.2 Physiological Aspects of Absorption**

Absorption of oral drugs is influenced by numerous drug and patient factors, and thus the concentration-time profile for a single dose of drug varies both inter- and intra-individually. As the GI tract is a variable environment, it can impact a drug's properties, and the kinetic parameters associated with absorption. Clinically significant interactions are assessed in terms of absorption rate ( $k_a$ ) and extent (F), peak plasma drug concentrations ( $C_{max}$ ), time to  $C_{max}$  ( $t_{max}$ ) and AUC (Fleisher, Li, Zhou, Pao & Karim, 1999). Figure 1.9 demonstrates the various absorption profiles that can result from alterations to the absorption rate or bioavailability of a drug from various factors.

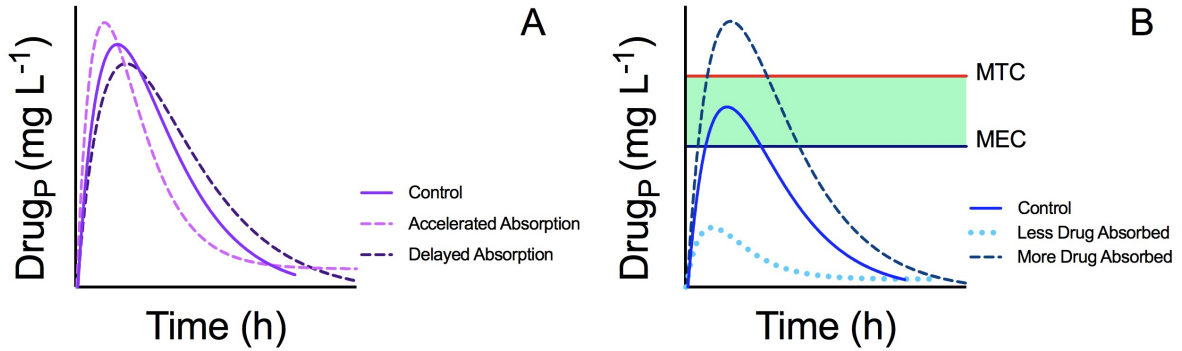


Figure 1.9 Changes in  $C_{max}$ ,  $t_{max}$ , and  $F$ .

Effect of absorption interaction on drug plasma-concentration time profiles of the same dose of an orally administered drug. (A) Accelerated and delayed absorption result in changes to the drug's  $C_{max}$  and  $t_{max}$ . (B) Decreased and increased amount of drug absorbed due to physiological or patient factors results in changes to the drug's  $C_{max}$ , AUC, therapeutic and toxicity potential. Adapted from a Figure by Fleisher *et al.*

### Routes of Administration

There are two categories describing routes of drug administration: intravascular (or parenteral) and extravascular (Jambhekar & Breen, 2009). Intravascular routes include intravenous and intra-arterial administration, lack an absorption phase resulting in almost immediate onset of action, and result in near 100% bioavailability and more predictable plasma concentrations (Jambhekar & Breen, 2009).

Extravascular routes of administration include: oral (PO; tablet, capsule, suspension), intramuscular (IM; solution and suspension), subcutaneous (SC; solution and suspension), sublingual or buccal (tablet), rectal (suppository or enema), transdermal (patch), or inhalation (inhaler) (Jambhekar & Breen, 2009). In contrast to intravascular routes, extravascular routes are characterised by an absorption phase, with onset of action influenced by factors such as formulation, route, and the physicochemical properties of the drug (Jambhekar & Breen, 2009). In addition, there is considerable variability in bioavailability, resulting in unpredictable plasma concentrations (Jambhekar & Breen, 2009).

The most frequently used injection routes in medication administration are IV, IM, and SC (Jin et al., 2015). Though some drugs are only administered *via* one injection route, others, such as epinephrine, have variable administration potential, and careful choice of route of administration is required, as each type of administration differs in absorption profile (Jin et al., 2015). To illustrate this point, an inappropriate route of administration (SC epinephrine rather than IM epinephrine in anaphylaxis treatment) resulted in a fatal adverse event at the Second Affiliated Hospital of Zhejiang University (SAHZU), People's Republic of China, due to delayed epinephrine absorption (Jin et al., 2015). This work will primarily focus on intravenous and oral administration.

### **Intravenous Administration**

Up to 80% of hospitalised patients receive intravenous therapy at some point during their stay (Waitt, Waitt & Pirmohamed, 2004). Intravenous routes allow for accurate control of drug levels, and for some compounds, it is the only route that allows the active form to reach its target site (Buxton, Benet, Brunton, Chabner & Knollmann, 2011; Waitt, Waitt & Pirmohamed, 2004). IV is practical in emergency situations, for unconscious or uncooperative patients, or if they are unable to swallow or absorb compounds due to illness (Buxton, Benet, Brunton, Chabner & Knollmann, 2011; Jambhekar & Breen, 2009; Li, Agweyu, English & Bejon, 2015). Drugs may be administered IV by bolus injection (small volume given rapidly) or by intravenous infusions (slower administration over a long period). (Buxton, Benet, Brunton, Chabner & Knollmann, 2011). IV administration is irreversible, and thus, precision in calculation of drug dose and administration of a compound is extremely critical (Jambhekar & Breen, 2009).

The IV route can rapidly yield high concentrations of drugs in the plasma, and though this is often the therapeutic goal, high concentrations of drug in the plasma increase the chance for overdose and risk to the patient (Buxton, Benet, Brunton, Chabner & Knollmann, 2011; Waitt, Waitt & Pirmohamed, 2004). For example, with IV bolus epinephrine, the frequencies of adverse cardiovascular issues and overdose are 10%, and 1.3%, respectively, in comparison with IM epinephrine (1.3% risk of cardiovascular issues and 0% overdose) (Campbell et al., 2015). IV

administration also requires skill on the part of the clinician and, if self-administering, of the patient, as well as expensive sterile agents, and vigilant maintenance of a sterile environment (Buxton, Benet, Brunton, Chabner & Knollmann, 2011). As well as complexities with administration, IV therapy may also result in harmful complications, including extravasation injury, thrombosis, and local and systemic infection (Li, Agweyu, English & Bejon, 2015).

Antibiotics are commonly and preferentially administered intravenously in high- and low-income countries, as the more rapidly achieved peak levels provide prompt treatment of rapidly progressing infections, such as severe sepsis or bacterial meningitis (Li, Agweyu, English & Bejon, 2015). However, the effectiveness of antibiotic therapy is more reliant on the period where there is maintenance of drug levels above the MEC (Vogelman, Gudmundsson, Leggett, Turnidge, Ebert & Craig, 1988; Waitt, Waitt & Pirmohamed, 2004). Larger doses of penicillin, it is reasoned, are more effective than smaller doses largely because of the greater length of time spent above the MEC (Wagner, 1961). Many oral antibiotics with sufficient bioavailability achieve concentrations above MEC, and in turn result in adequate concentrations in tissues; they express similar efficacy to the intravenous route (Li, Agweyu, English & Bejon, 2015). In addition, there is more ease with PO administration, reduced labour and administration costs, and generally, a reduced hospital stay for the patient (Waitt, Waitt & Pirmohamed, 2004). Thus, IV administration, though necessary in certain situations, is not always warranted as the best course of action if there are effective and safer alternatives.

### **Oral Administration**

PO administration is the most common route; it is economical and convenient for patients, resulting in high therapy compliance (Macheras, Karalis & Valsami, 2013). While the molecular structure of a compound influences its absorption, other factors, such as the drug's dosage form, dissolution, solubility, and permeability are also important (Amidon, Lennernas, Shah & Crison, 1995; Wagner, 1961). Dosage form encompasses a drug's chemical nature (whether or not it is formulated as a salt), physical state (amorphous or crystalline, solvated or non-solvated, polymorphic), particle size, and surface area of the drug in the dosage form (Wagner, 1961).

Orally administered drugs exist as solutions, suspensions, capsules, tablets, and coated tablets; the formulations affect the extent and rate of their absorption (Jambhekar & Breen, 2009).

### **Formulation**

The rate and/or extent of absorption of a drug can vary largely between different dosage forms and formulations (Jambhekar & Breen, 2009). As tablets must dissolve before they can be absorbed, the general (though not universal) guideline is that a solution or suspension form of the drug may exhibit faster absorption rates (Jambhekar & Breen, 2009). Many solutions, some suspensions containing drug in small particle sizes, and ordinary compressed tablets which rapidly disintegrate can, however, be characterised as “immediate-release dosage forms” (Jambhekar & Breen, 2009; Martinez & Amidon, 2002; Wagner, 1961). Generally, for these types of formulations, the absorption rate is controlled by the diffusion of drug molecules in GI fluids and/or through the cell membrane (Jambhekar & Breen, 2009; Martinez & Amidon, 2002; Wagner, 1961). Sustained-release or prolonged action dosage forms are also available; after a single dose, these formulations result in drug-plasma concentrations above the level required for therapeutic activity, but below the peak levels obtained with “immediate-release” or normal tablet drug versions (Wagner, 1961).

Sustained-release or extended-release preparations result in slow, uniform absorption of a drug for longer periods, reducing the frequency of administration and maintenance of therapeutic effect overnight, while also reducing the frequency and intensity of undesired effects (peaks extending above the MTC (maximum tolerated concentration)), and nontherapeutic levels (troughs lower than the MEC (minimum effective concentration)) (Buxton, Benet, Brunton, Chabner & Knollmann, 2011).

Sustained-release preparations are highly useful in treating disorders such as epilepsy, because patient adherence is vital in reducing rates of breakthrough or recurrent seizures (Pellock, Smith, Cloyd, Uthman & Wilder, 2004). Most immediate-release formulations of anti-epileptic drugs require frequent administration to maintain drug concentrations at therapeutic levels; despite frequent dosing, the formulations produce wide fluctuations in drug concentrations throughout

the day, causing intermittent side effects above the MTC, or increasing risk of seizures when below the MEC (Pellock, Smith, Cloyd, Uthman & Wilder, 2004). Extended-release formulations require less frequent administration than normal agents, and they minimise fluctuations in drug concentrations; these characteristics improve patient adherence to the therapies (Pellock, Smith, Cloyd, Uthman & Wilder, 2004). It was found in adult epilepsy patients that the incidence of CNS side effects decreased from 49% with immediate release Carbamazepine (CBZ) treatment to 20% following extended release CBZ treatment, with PK analysis showing reduced variability with the extended release CBZ (Miller, Krauss & Hamzeh, 2004).

### **Dissolution**

Unlike intravenous routes, it is impossible to control completely the rate at which a drug enters the bloodstream after oral administration (Wagner, 1961). Furthermore, when a drug is administered orally, there is a "lag time" between its ingestion and measurability in the systemic circulation (Greenblatt & Shader, 1985). Prior to undergoing absorption, a drug must exist in solution form; tablets or capsules must first dissolve in the gastrointestinal (GI) fluids (Jambhekar & Breen, 2009; Wagner, 1961). It was noted by Noyes and Whitney that the rate of dissolution of a drug is driven by a concentration gradient:

$$\frac{dx}{dt} = D(C_S - C_x)$$

(E. 15)

where D is a first-order dissolution rate constant,  $C_S$  is the solubility of the compound in the dissolution medium at the experiment temperature, and  $C_x$  is the concentration of solute in the bulk solution at time t (Noyes & Whitney, 1897). The equation, adapted for oral drug dissolution is (Martinez & Amidon, 2002):

$$\frac{dx}{dt} = \frac{D \times A}{V \times h} (C_S - C_x)$$

(E. 16)

where  $D$  is the diffusion coefficient,  $A$  is the surface area of the drug tablet,  $V$  is the volume of the dissolution medium,  $h$  is the thickness of the diffusion film adjacent to the dissolving surface,  $C_s$  is the saturation solubility of the compound, and  $C_x$  is the concentration of the solute (Martinez & Amidon, 2002).

If an orally absorbed drug is diffusion-controlled, the gastrointestinal content (dissolution medium) surrounding the solid drug particle is a saturated solution of the compound; the rate at which the drug molecules reach the bulk GI content depends on the drug's solubility (Wagner, 1961). Absolute particle size and particle size distribution as it relates to surface area also influences the rate of the dissolution of a drug (Wagner, 1961). The dissolution rate of a drug increases by: increasing the aqueous solubility of the compound (e.g. through temperature changes, pH changes, or converting the drug to a salt) or reducing the particle size, and therefore increasing the surface area (e.g. by grinding the tablet or using a wetting agent) (Fan & de Lannoy, 2014; Jambhekar & Breen, 2009; Martinez & Amidon, 2002).

### **Permeability**

Fick's law of diffusion when interpreted in terms of membrane permeability is:

$$J = P_w \times C_w$$

(E. 17)

where  $J$  is the drug flux,  $P_w$  is the permeability of the membrane and  $C_w$  is the drug concentration at the membrane (Amidon, Lennernas, Shah & Crison, 1995).  $P_w$  is considered as time- and position-dependent. Time-dependence factors include drug concentration (relating to carrier mediated transport), effects from other compounds in the formulation, changes in luminal contents, or the down/up-regulation of membrane transporters, while position-dependence factors are based on different morphologies and mucosal cells progressing through the intestine (Amidon, Lennernas, Shah & Crison, 1995). The complexity of these relationships influences drug development, and researchers have created quantitative models to mimic the flow, dissolution, and absorption processes occurring in the various sections of the

intestines to predict how a molecule will undergo absorption *in vivo* (Amidon, Lennernas, Shah & Crison, 1995).

While two drugs may have be similar in terms of their solubility, their permeability, and thus, bioavailability, may differ greatly; comparisons between delivery systems and dosage forms became an important aspect of drug design (Amidon, Lennernas, Shah & Crison, 1995). The Biopharmaceutics Classification System (BCS) is widely recognised as a reference guide for academia and industry, as it considers the three major factors that govern the rate and extent of absorption from immediate release solid oral forms: dissolution, solubility, and intestinal permeability (Shah & Amidon, 2014). By being aware of these characteristics of drug compounds, there is improved ability to predict how certain variables, like formulation, food, dosing regimen, and disease alter oral drug absorption (Martinez & Amidon, 2002). The four classifications (Amidon, Lennernas, Shah & Crison, 1995) are:

**Class I:** Highly soluble and highly permeable: drug is well absorbed and the rate limiting step is drug dissolution. Absorption rate is controlled by gastric emptying if there is rapid drug dissolution.

**Class II:** Poorly soluble but highly permeable: drug dissolution is the rate-limiting step and absorption is normally slower than Class I. The dissolution profile determines the concentration profile throughout the intestines. The absorption period is extended and variable due to the *in vivo* variables affecting the dissolution

**Class III:** Highly soluble but poorly permeable: drug's permeability is the rate-limiting step. Rate and extent of absorption is variable, but if dissolution is rapid, then absorption is variable and influenced by gastrointestinal transit, luminal contents, and membrane permeability, not dosage form factors

**Class IV:** Poorly soluble and poorly permeable: drug presents problems for effective oral delivery

For reference, the cut-off value for a highly soluble drug requires that its highest marketed dose (highest dose strength) is soluble in 250 mL of aqueous media over the entire pH range in the GI tract (pH 1.2-7.4) (Shah & Amidon, 2014). Permeability is defined as how effectively a drug is permeable to the human jejunal wall (Martinez & Amidon, 2002). The cut-off value for high permeability reflects an absorption greater than 90% in the media pH range of 1.2-7.4 (Shah & Amidon, 2014). Finally, at least 85% of a drug needs to dissolve within 30 minutes in a USP apparatus 1 or 2 at 100rpm or paddle method at 50 rpm in buffer of pH 1.2, 4.5, and 6.8 for it to be considered as rapidly dissolving (Shah & Amidon, 2014).

### **Ionisation**

Most drug absorption from the GI tract occurs by passive diffusion, and the permeability of a drug usually increases when it is non-ionised (Buxton, Benet, Brunton, Chabner & Knollmann, 2011). However, ionised drugs generally exhibit far greater aqueous solubility (Martinez & Amidon, 2002). The pH in the gastrointestinal tract ranges from 1-3.5 in the stomach, 5-7.4 in the duodenum, and ~8 in the lower ileum, and because drugs are exposed to such varying pH, these physiological influences affect their absorption and bioavailability (Wagner, 1961).

In consideration to the Henderson-Hasselbalch (Equation (E.8)), changes in a drug's environmental pH impact its ionisation and thus, its permeability and solubility. In the stomach, a weak acid such as salicylic acid will primarily exist in its non-ionised form; it is in an ideal conformation for permeability. However, in its non-ionised form, salicylic acid is less soluble in the extremely acidic gastrointestinal fluids. Only between 10-30% of the drug is absorbed in the stomach before reaching the intestines (Jambhekar & Breen, 2009).

Combined with reduced solubility, other points of consideration that affect salicylic acid's absorption (likely to a greater extent) are that the stomach is lined with a thick mucus layer, has a small surface area, and that the drug only resides in this environment for a short period (0.5-2h) before gastric emptying occurs (Buxton, Benet, Brunton, Chabner & Knollmann, 2011; Jambhekar & Breen, 2009). In contrast, in the upper intestine, the villi provide a surface area of approximately 200m<sup>2</sup> and the drug resides in the environment for much longer (Buxton, Benet,

Brunton, Chabner & Knollmann, 2011). However, there is a larger fraction of ionised salicylic acid molecules in this environment, affecting the permeability of the drug and extent of drug absorption (Buxton, Benet, Brunton, Chabner & Knollmann, 2011; Jambhekar & Breen, 2009).

### 1.1.2.3 Patient Factors Affecting Absorption

There are numerous complexities surrounding oral absorption, and many factors influence a drug's physicochemical properties as it transits through the GI tract: fasted/fed state, gastric emptying and intestinal transit, lumen contents (pH, enzymes, surfactants, lipids), drug absorption mechanisms, permeability, electrochemical gradients, effective absorbing surface area, degree of villous activity, degree of vascularity, the presence or absence of mucus, the presence or absence of complexing agents, temperature, hydrostatic and intraluminal pressure, enzymatic activity in the lumen, and the anatomical position and even relative activity of the patient (Amidon, Lennernas, Shah & Crison, 1995; Wagner, 2006).

#### Gastric Emptying

Some drugs, like erythromycin, are best absorbed when an individual is in a fasting state, while other drugs, like ticlopidine, have enhanced absorption in the presence of food (Shargel & Yu, 1999). In mammals, GI tract activity occurs in three phases which, in total, last 90 – 120 minutes, and move liquid and solid materials down the tract (Martinez & Amidon, 2002). If fluid volume increases, gastric emptying also increases, regardless of the current GI tract phase; a BCS Class I agent, which is highly soluble, may thus experience rapid absorption in this scenario if its absorption otherwise relies on gastric emptying to transport it into the intestines (Martinez & Amidon, 2002).

In some cases, PK study results can challenge currently accepted clinical practices. It is typically advised to take non-steroidal anti-inflammatory drugs (NSAIDs) with food or milk to reduce adverse GI effects (Moore, Derry, Wiffen & Straube, 2015). Recently, a systematic review found that fasting/fed state had no effect on the bioavailability of any NSAIDs as measured through  $AUC_{0-\infty}$ , but the ingestion of food delayed absorption for all drugs with a fasting  $t_{max}$  of <4 h,

increasing the  $t_{max}$  up to 250% (Moore, Derry, Wiffen & Straube, 2015). In addition, the presence of food reduced the  $C_{max}$  by ~50% for all drugs with a fasting  $t_{max}$  of <2h (Moore, Derry, Wiffen & Straube, 2015). Though ingestion of food does not influence NSAID bioavailability, the effects on  $t_{max}$  and  $C_{max}$  are substantial and may impact patient care, as there is increasing emphasis on the importance of early, high plasma drug concentrations for pain relief, especially for acute pain (Moore, Derry, Wiffen & Straube, 2015).

## Diet

The chemical makeup of ingested foods can also have significant effects: ingestion of dairy products with certain drugs reduces absorption due to calcium chelation, while ingestion of a heavy high fat meal can slow gastric emptying, and potentially the rate of absorption (Shargel & Yu, 1999). BCS Class II compounds experience increased absorption if certain foods influence their dissolution; high fat meals stimulate pancreatic and biliary secretions, increasing fluid volume, which promotes drug solubilisation and absorption, GI secretions and biliary solubilisation, enhancing drug dissolution and thus, its absorption (Carver, Fleisher, Zhou, Kaul, Kazanjian & Li, 1999; Martinez & Amidon, 2002).

Changes to gastric pH change the solubility of both weak acids and weak bases. For poorly water-soluble drugs, such as Class II compounds, changes in pH can dramatically affect dissolution (Abuhelwa, Foster & Upton, 2016). At gastric pH, weak bases exist in ionised form, and are highly water soluble in this environment (Carver, Fleisher, Zhou, Kaul, Kazanjian & Li, 1999). But, changes in the environment as a result of patient factors, can influence a drug's dissolution. For example, indinavir, a weak base, ( $pK_a$  values of 3.7 and 5.9) precipitates at higher gastric pH; taking the medication with food increases the gastric pH enough to affect absorption of the drug (Carver, Fleisher, Zhou, Kaul, Kazanjian & Li, 1999). Presumably, the increase in gastric pH upon food administration is due to the buffering effect of food exceeding the food-stimulated gastric acid secretions (Abuhelwa, Foster & Upton, 2016). In seven male HIV-infected subjects, comparisons of indinavir  $AUC_{0-\infty}$  were made between fasted state and after eating meals composed of protein, carbohydrate, and fat (Carver, Fleisher, Zhou, Kaul,

Kazanjian & Li, 1999). It was found that in comparison to fasted state  $AUC_{0-\infty}$ , protein, carbohydrate, and fat meal phases resulted in significantly decreased  $AUC_{0-\infty}$  by 68%, 45%, and 33% respectively (Carver, Fleisher, Zhou, Kaul, Kazanjian & Li, 1999). The protein meal exhibited the most dramatic reduction in all subjects tested, and as the gastric pH was elevated for 4-hours after the meal, it was inferred that this was a direct consequence of the effect of reduced drug dissolution (Carver, Fleisher, Zhou, Kaul, Kazanjian & Li, 1999).

Finally, nutrients in food can rapidly modulate intestinal P450 enzyme activity. Popular in discussion, grapefruit juice inhibits both P-glycoprotein (Pgp) and CYP3A4 in the intestines (Martinez & Amidon, 2002). Compounds transported or metabolised by these proteins, such as cyclosporine or estradiol, can experience enhanced bioavailability when administered with grapefruit juice (Martinez & Amidon, 2002).

### **Age**

Neonates and infants exhibit increased gastric pH and decreased gastric motility, and immature efflux transporters and/or intestinal metabolism in comparison to adults (some of these processes take up to 5 years to mature) (Anderson, 2010). These effects can decrease the bioavailability of weak acids, and reduce the clearance of drugs due to immature intestinal metabolism (Anderson, 2010).

Many age-absorption studies have neglected basic PK principles in study design, which largely contributed to incorrect conclusions about age-related changes in absorption (Mayersohn, 1994). Thus, the studies interpreting age effects on absorption offer varying conclusions; some, for instance, show reduced gastric emptying with increasing age, while others report no change for this factor (Mayersohn, 1994). However, general inferences about the reduction of metabolism with age are applied to reduced first-pass effects for high extraction drugs, which results in increased bioavailability (Mayersohn, 1994).

## Disease

Patient disease states play a factor in drug absorption and bioavailability, particularly when the disease affects a patient's intestinal blood flow, gastrointestinal motility, gastric emptying, gastric pH, intestinal pH, permeability of the gut wall, bile secretion, digestive enzyme secretion, and changes to the GI flora (Shargel & Yu, 1999).

Celiac patients are intolerant to gliadin, an alcohol-soluble fraction of gluten, present in wheat, barley, and rye; ingestion of gluten results in an inflammatory response which damages the mucosa and villi of the small bowel and leads to malabsorption and maldigestion (Wang & Hopper, 2014). While villous atrophy results in decreased surface area for drug absorption and may result in loss of CYP enzymes (resulting in a reduction of first-pass metabolism), celiacs also present with more alkaline pH in the small bowel, which can alter drug ionisation (Kitis et al., 1982; Lang et al., 1996; Wang & Hopper, 2014).

Parsons *et al.* compared the absorption of propranolol in patients with celiac disease to normal subjects. It was shown that computer-calculated  $AUC_{0-\infty}$  for propranolol in celiac subjects was double that of normal subjects, because of initially higher plasma concentration levels and a higher  $C_{max}$  (Parsons, Kaye, Raymond, Trounce & Turner, 1976). It was theorised that because orally administered propranolol experiences extensive first pass metabolism before entry into the circulation, the higher  $C_{max}$  and higher initial plasma concentrations in celiacs is a result of increased absorption rate (partly due to the more alkaline pH of the jejunum and the lipid-soluble nature of propranolol) (Parsons, Kaye, Raymond, Trounce & Turner, 1976). More rapid absorption of propranolol higher in the jejunum across the mucosa increases its concentration in the portal circulation, saturating first pass metabolism mechanisms, and allowing higher concentrations of drug to enter systemic circulation, resulting in higher initial plasma-concentration levels (Parsons, Kaye, Raymond, Trounce & Turner, 1976).

### 1.1.3 ADME: DISTRIBUTION

After absorption or administration into the bloodstream, a drug distributes into interstitial and intracellular fluids by the systemic circulation (Buxton, Benet, Brunton, Chabner & Knollmann, 2011). As well as being distributed to the target site, drug molecules are distributed to non-target sites, and can even cross the placenta and affect a developing fetus (Shargel & Yu, 1999). The movement of a drug between different “compartments” of the body (blood, adipose tissue, GI tract, liver, etc.) is complex and dynamic, and thus, the analysis of distribution requires abstract conceptualisation (Gibson & Skett, 2001). A variety of factors influence drug distribution, from the physicochemical properties of the drug to the physiological components of the body (Buxton, Benet, Brunton, Chabner & Knollmann, 2011; Fan & de Lannoy, 2014).

#### 1.1.3.1 Kinetic Definitions and Principles of Distribution

Pharmacokinetic modelling of a drug, specifically the process of distribution, consists of visualisations, mathematical relationships, and some data extraction. These models, though hypothetical, offer valid information about a drug’s behaviour in the body (Dhillon & Kostrzewski, 2006).

##### One Compartment Model

The most simplistic model depicts the body as a kinetically homogenous unit, where all body compartments are in rapid equilibrium with the central compartment (equated with the blood); The One Compartment Model (Figure 1.10) (Dhillon & Kostrzewski, 2006; Gibson & Skett, 2001). In this model, drug is injected directly into the central compartment, and instantaneously distributes, such that the drug concentration-time profile shows a monophasic response and  $\log C_t$  versus time graphs depict a linear relationship (Figure 1.11) (Dhillon & Kostrzewski, 2006; Gibson & Skett, 2001). The drug plasma concentration ( $C_t$ ) quantitatively reflects changes in the tissues, but does not represent the actual concentration in the tissues (Dhillon & Kostrzewski, 2006). Realistically, drug distribution is not instantaneous, and thus the semi-log plot of data as shown in Figure 1.11B slightly underrepresents the true  $C_{t0}$  of the drug (Gibson & Skett, 2001).

For most drugs, the one-compartment model is an idealised approach to analysis, and most likely does not describe the entire course of the systemic concentrations (Benet & Zia-Amirhosseini, 1995).

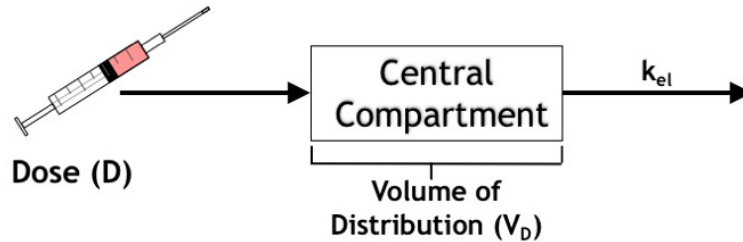


**Figure 1.10 One Compartment Distribution Model.**

Drug of a specific dose ( $D$ ) is administered into the central compartment, where there is instantaneous distribution throughout the entire volume. The body is a kinetically homogenous unit: drug enters and leaves all areas of the body with equal ease. The volume of distribution ( $V_D$ ) represents the volume into which the drug is distributed, and the elimination rate constant ( $k_{el}$ ) influences the rate at which the drug leaves the central compartment, or body.

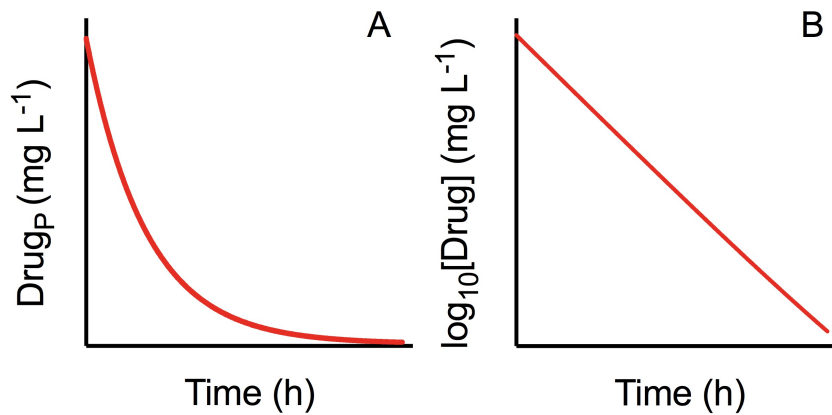


**Figure 1.11 One Compartment Plasma-Concentration Time Profile.**

The linear plot (A) displays a monophasic relationship. The semi-log plot (B) displays a linear relationship.

## Two Compartment Model

Physiologically, elimination occurs primarily from the blood or central compartment (*via* feces and/or urine), and it is well established that drugs do not distribute equally easily to all parts of the body (Gibson & Skett, 2001). Thus, the two-compartment model better illustrates a drug's distribution behaviour. As shown in Figure 1.12, the two-compartment model requires that, following drug administration into the central compartment ( $V_1$ ), drug also distributes into the peripheral compartment ( $V_2$ ) (Dhillon & Kostrzewski, 2006). Importantly, drug does not instantaneously distribute or equilibrate between the two compartments, and elimination only occurs from the central compartment (Gibson & Skett, 2001). The central compartment is generally equated to tissues that are highly perfused, such as the heart, lungs, kidneys, liver, and brain (Dhillon & Kostrzewski, 2006; Gibson & Skett, 2001), while the peripheral compartment is comprised of less well-perfused tissues like muscle, fat, and skin (Dhillon & Kostrzewski, 2006).

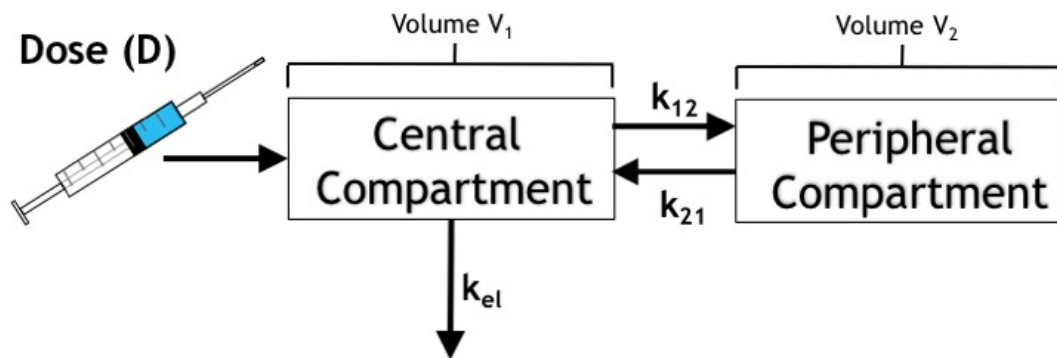


**Figure 1.12 Two Compartment Distribution Model.**

The central compartment is designated as its own separate volume ( $V_1$ ) from the peripheral compartment ( $V_2$ ). A specific dose of drug ( $D$ ) is administered into the central compartment, and the drug then distributes into and out of the peripheral compartment based on the value of the compartmental rate constants ( $k_{12}$  and  $k_{21}$ ) until an equilibrium is reached between the compartments; the distribution is not instantaneous. Drug can only be eliminated from the central compartment, and as more drug is eliminated, drug redistributes back from the peripheral compartment into the central compartment to maintain the equilibrium, until finally, all the drug is eliminated.

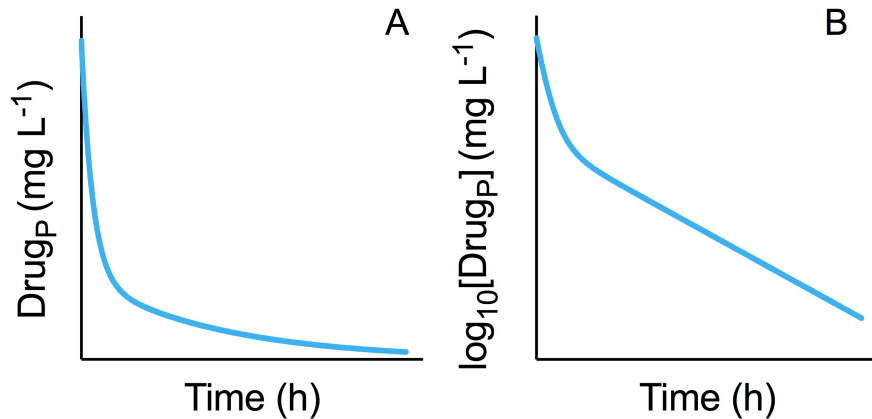


**Figure 1.13 Two Compartment Plasma-Concentration Time Profile.**

The linear plot (A) displays a biphasic relationship. The semi-log lot (B) displays two distinct slopes that contribute to the classic “hockey-stick” profile attributed to two-compartment kinetics. The steeper slope corresponds to the drug’s distribution into the peripheral compartment from the central compartment combined with its elimination from the central compartment. The shallow slope is attributed only to the drug’s elimination from the central compartment. The point at which the steeper curve shifts into the shallow curve is designated as the ‘equilibrium point’ and describes the moment wherein drug concentration in the central and peripheral compartments are in equilibrium with one another.

Figure 1.13 illustrates the linear and semi-logarithmic plots obtained from a two-compartment drug. The linear concentration-time profile (A) shows a biphasic curve fit, though it would be difficult to differentiate this plot from a monophasic curve as seen in Figure 1.11. The semi-log plot of the data (Figure 1.13B) however, displays two distinct slopes and processes occurring, showing the classic “hockey-stick” profile. The two distinct slopes correspond to the different processes occurring when a drug displays two compartment behaviour. The first (steeper) slope is primarily related to the distribution of the drug from the central to the peripheral compartment, though some of the elimination occurring from the central compartment also contributes to this rapid decline of blood drug concentrations (Gibson & Skett, 2001). The second (shallow) slope corresponds completely to the elimination of the drug from the central compartment (Gibson & Skett, 2001). The theoretical slope of the elimination phase can be implemented to calculate the drug’s  $k_{el}$  by using the equation:

$$\text{slope} = \frac{-k}{2.303}$$

(E. 18)

where slope is the slope calculated from the theoretical extrapolated line,  $k$  is the rate constant (elimination;  $\text{h}^{-1}$  or  $\text{min}^{-1}$ ). Though there will be further discussion of this concept as it relates to half-life and clearance, its origin can also be understood through distribution analysis.

The complexity of two-compartment modelling is apparent when considering the challenges in analysing the data. Unlike one-compartment modelling, the drug concentration in the central compartment is no longer related solely to drug elimination, but also to drug movement between it and the peripheral compartment (Gibson & Skett, 2001). The rate constants of  $k_{12}$ ,  $k_{21}$ , and  $k_{10}$  (see below) influence the drug's distribution and elimination rates, and consideration of these parameters contributes to the complexity of 2-compartment modelling (Gibson & Skett, 2001). In addition, the compartments offer conceptual understanding of the drug's distribution behaviour, and while they vaguely represent anatomical regions, the basis for explaining drug transfer is abstract (Gibson & Skett, 2001).

The rate constants, deemed "micro" rate constants, or inter-compartmental transfer rate constants, describe the transfer of drug from central to peripheral compartment ( $k_{12}$ ), from the peripheral to central compartment ( $k_{21}$ ), and the rate of elimination solely from the central compartment ( $k_{10}$ ) (Dhillon & Kostrzewski, 2006). In terms of the models, the variance in tissue drug concentration is reflected in the  $k_{12}/k_{21}$  ratio, which explains the rate of drug change in and out of the tissues (Shargel & Yu, 1999). If the rate "in" ( $k_{12} \times V_C$ ) is greater than the rate "out" ( $k_{21} \times V_T$ ), the plasma concentration declines while the tissue concentration increases (Shargel & Yu, 1999). These micro-constants cannot be determined directly, but rather estimated by a graphical method (Shargel & Yu, 1999).

The method of residuals (also called "feathering" or "peeling") is a compartmental approach for fitting a curve to the experimental data of a drug and separating the distribution and elimination phases to obtain more thorough analysis (Shargel & Yu, 1999).

Figure 1.14, based loosely on Fan & de Lannoy's review, details instructions for performing the method of residuals by hand for compartmental analysis (Fan & de Lannoy, 2014). Figure 3.14D shows the final analysis of each phase. A and B (labelled on the Y-axis) are the Y-intercept of the distribution phase, and the Y-intercept of the elimination phase, respectively (Fan & de Lannoy, 2014). Thus, the sum of A + B is equal to the  $C_{t0}$  (as shown in Figure 1.11B, in a one-compartment model,  $C_{t0}$  is obtained from the linear extrapolation the drug's elimination from the central compartment, as distribution is instantaneous and does not contribute to the drug's blood concentration profile). Each extrapolated line corresponds to a slope value, and as per Equation (E.18) allows for the calculation of both  $\alpha$  and  $\beta$ , the distribution and elimination rate constants, respectively. By obtaining these values through the graphical method, one can then calculate the micro-constants (Shargel & Yu, 1999):

$$k_{12} = \frac{AB(\beta - \alpha)^2}{(A + B)(A\beta + B\alpha)}$$

(E. 19)

$$k_{21} = \frac{A\beta + B\alpha}{(A + B)}$$

(E. 20)

$$k_{10} = \frac{\alpha\beta(A + B)}{A\beta + B\alpha}$$

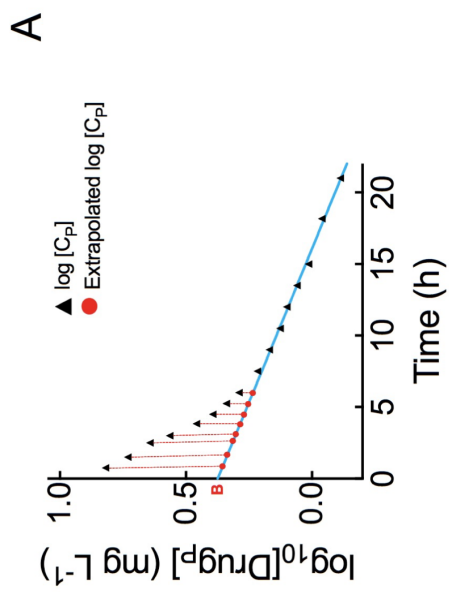
(E. 21)

where A ( $\text{mg L}^{-1}$ ) is the A-intercept from the distribution extrapolated line, B ( $\text{mg L}^{-1}$ ) is the B-intercept from the elimination extrapolated line,  $\alpha$  ( $\text{min}^{-1}$  or  $\text{h}^{-1}$ ) is the calculated distribution rate constant, and  $\beta$  ( $\text{min}^{-1}$  or  $\text{h}^{-1}$ ) is the calculated elimination rate constant.

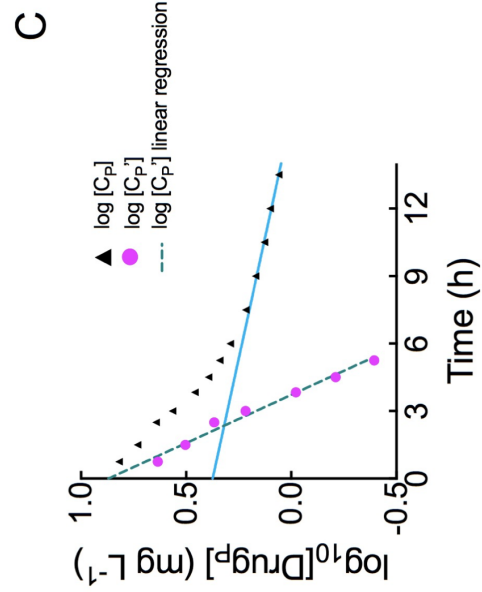
### Multi-Compartment Modelling

While two-compartment modelling breaks down drug distribution into a central and peripheral compartment, multi-compartment modelling includes more compartments for drug to distribute into. If samples are taken during the distribution phase(s) and elimination phase, most

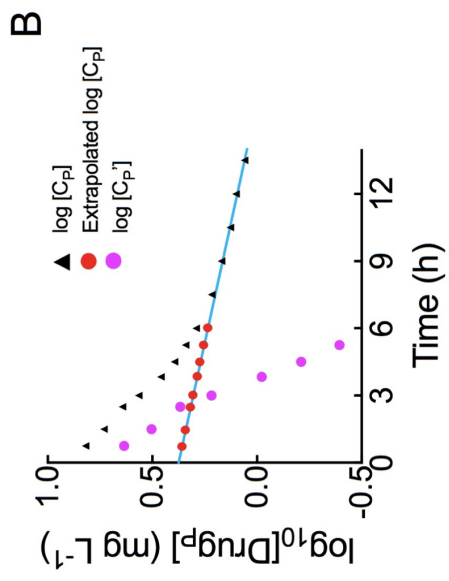
compounds exhibit multi-exponential declines in their plasma concentration time profiles as communicated on a semi-logarithmic plot (Fan & de Lannoy, 2014). In fact, there are three different types of 2-compartment models and 7 types of 3-compartment models, depending on the compartment responsible for elimination, which speaks to the level of complexity that drug distribution behaviours exhibit (Fan & de Lannoy, 2014).



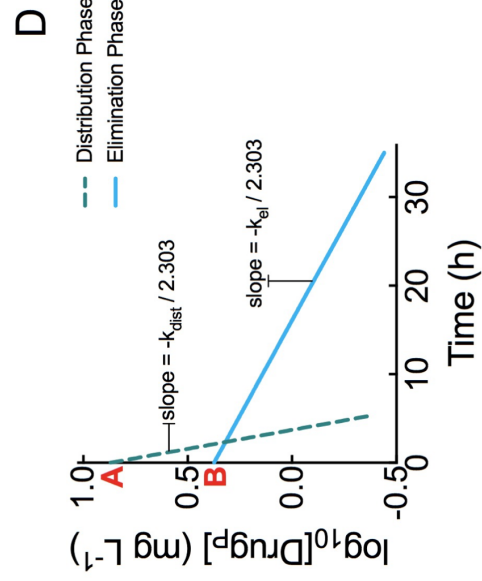
1. Each Measured Concentration correspond to an X (time)
2. Line Equation:  $y = mx + b$ ,  $y = -\text{slope} \times \text{time} + B$
3. Convert **Extrapolated log Y-values** into **Linear Y-values** ( $10^Y$ )



7. Fit log-Y values to a line and extrapolate to  $x=0$



5. Subtract **Linear Extrapolated Y-values** ( $10^Y$ ) from Measured Concentration Values
6. Convert Resulting Subtracted Values to **log-Y values** and plot on graph



- $k_{\text{dist}}$  or  $\alpha$ : distribution rate constant ( $\text{h}^{-1}$  or  $\text{min}^{-1}$ )  
 $k_{\text{el}}$  or  $\beta$ : elimination rate constant ( $\text{h}^{-1}$  or  $\text{min}^{-1}$ )

Figure 1.14 Method of Residuals

## Volume Terms

Volume terms in distribution are used in pharmacokinetics and biopharmaceutics for many purposes (Benet & Ronfeld, 1969). A volume constant can describe the actual size of a body region ( $V$ ), providing some physiological meaning to the value (Benet & Ronfeld, 1969). Total body water (TBW) occupies intracellular and extracellular spaces, making up about 63% (0.6L/kg) of body mass; a 70 kg individual would thus have about 42 L of TBW content (Armstrong, 2005; Benet & Zia-Amirhosseini, 1995). Further, extracellular volume (ECV), comprising of all the fluids outside of cells, such as the interstitial fluid and plasma water comprises 12 L (Benet & Zia-Amirhosseini, 1995). Of the ECV, the plasma volume (PV; liquid portion of blood), makes up about 3L, with the remaining attributed to the interstitial fluid. The complete blood volume in an average 70 kg human is 5.5 L (Benet & Zia-Amirhosseini, 1995).

It is difficult to equate calculated volumes of distribution ( $V_D$ ) with these actual body compartments. Conceptually, the calculated  $V_D$  may not entirely “fit” with actual assigned body volumes; a drug may only distribute within the blood plasma and have a  $V_D$  of ~4.5L, and if it permeates the TBW, the  $V_D$  may equal 60L, rather than 42L (Gibson & Skett, 2001). Conversely, a drug’s  $V_D$  may align with a physiological volume term, but its distribution profile may be entirely different; a drug with a  $V_D$  of 40L, for instance, may not be distributing into the TBW. However,  $V_D$  can still be conceptually useful, because it provides a quantitative estimate of the extent of a drug’s distribution outside of the central compartment (Greenblatt, 2014).

In some cases, the plasma concentration of the drug may be very low due to its sequestration into specific tissue, and with application of Equation (E. 22), the resulting  $V_D$  may seem larger than possible (in the realm of hundreds of litres) (Gibson & Skett, 2001). For example, digoxin, in a healthy volunteer, has a  $V_D$  of ~700 L; because of its lipid solubility, digoxin distributes predominantly into muscle and adipose tissue (Benet & Zia-Amirhosseini, 1995). Thus, a drug’s volume of distribution ( $V_D$ ) is a hypothetical value, and is also referred to as the **Apparent Volume of Distribution ( $AV_D$ )** (Benet & Zia-Amirhosseini, 1995; Dhillon & Kostrzewski, 2006). This pharmacokinetic parameter aims to relate the volume of body fluid required to dissolve the

drug if it were equally distributed throughout all portions of the body (Benet & Ronfeld, 1969; Benet & Zia-Amirhosseini, 1995; Dhillon & Kostrzewski, 2006).

Another use of volume terms is in reference to describing a volume or volume of distribution for a single compartment within a model, such as  $V_2$  (also referred to as  $V_T$ ; volume of tissue compartment) or  $V_1$  (also referred to as the  $V_C$ ; volume of central compartment) in Figure 1.12 (Benet & Ronfeld, 1969).

There are several types of Volumes of Distributions that, while offering no physiological meaning, describe certain aspects of a drug's distribution. Following IV bolus administration of a drug, there are three separate approaches by which volume of distribution may be calculated (Fan & de Lannoy, 2014). First, the central compartment volume ( $V_C$ ), the simplest of the terms, is calculated as:

$$V_C = \frac{D}{C_{t0}}$$

(E. 22)

where  $C_{t0}$  is the drug concentration at time 0 ( $\text{mg L}^{-1}$ ), and  $D$  is the administered drug dose (mg) (Fan & de Lannoy, 2014). This equation originates under the assumption that the drug administered into the circulation instantaneously distributes within the central compartment, which includes plasma, red blood cells, and rapidly distributing organs, prior to distributing into the tissue compartment (Fan & de Lannoy, 2014). The  $V_C$  value, thus, cannot be smaller than the volume of plasma in the body (Fan & de Lannoy, 2014). The  $V_C$ , as a PK parameter, is most useful for drugs that display one-compartment kinetics, as it provides an accurate  $C_{t0}$  without the influence of other factors on its distribution (Fan & de Lannoy, 2014). In a one-compartment model, the  $V_C$  value, as calculated in Equation (E. 22), is attributed as the drug's apparent volume of distribution ( $AV_D$ ). Similarly, in a two- or multi- compartment model, the volume of each tissue compartment is calculated by applying this equation (though, actual samples of these tissues would be required) (Shargel & Yu, 1999).

As discussed, most drugs display non-instantaneous distribution and slowly equilibrate into organs/tissues, resulting in bi- or multi- exponential profiles (as seen in Figure 1.13), and using volume terms can facilitate a more in-depth understanding of the drug's behaviour (Fan & de Lannoy, 2014). Of these, the two that are commonly used are: the volume of distribution during elimination phase ( $V_{D \text{ Area}}$  or  $V_{D \text{ Beta}}$ ) and the volume of distribution at steady-state ( $V_{D \text{ SS}}$ ) (Hanley, Abernethy & Greenblatt, 2010). The beta-phase volume of distribution ( $V_{D \text{ Beta}}$  or  $V_{D \text{ Area}}$ ) is valid at all points following distribution equilibrium, as it is determined by the ratio of Dose to the  $\beta$  calculated from the terminal phase of the semi-log plot (Benet & Zia-Amirhosseini, 1995; Hanley, Abernethy & Greenblatt, 2010):

$$V_{D \text{ Area}} = \frac{D}{k_{el} \times \text{AUC}} \tag{E. 23}$$

where  $k_{el}$  is the elimination rate phase ( $\beta$ ;  $\text{min}^{-1}$  or  $\text{h}^{-1}$ ),  $D$  is the dose of drug administered (mg), and  $\text{AUC}$  is the calculated area under the curve of the drug. Though earlier pharmacokinetic literature discussed  $V_{D \text{ Area}}$  as dependent on the total clearance, it is in fact mechanistically distinct from the PK parameter and independent of clearance (Greenblatt, 2014; Mehvar, 2006). More insight into the physiological changes affecting distribution will be discussed in the next section, 1.1.3.2. Overall, as the  $V_{D \text{ Area}}$  parameter is dependent on the  $\text{AUC}$  and terminal elimination phase, and these calculated parameters are less prone to dramatic shifts, the parameter is usually considered as "stable" (Greenblatt, 2014).

The volume of distribution at steady state, or  $V_{D \text{ SS}}$ , represents the volume in which a drug would appear to be distributed during steady state if the drug existed throughout that volume at the same concentration as that in the central compartment (measured fluid) (Benet & Zia-Amirhosseini, 1995).  $V_{D \text{ SS}}$  is calculated using the following equation (Greenblatt, Abernethy & Divoll, 1983):

$$V_{D \text{ SS}} = \frac{\text{Dose} \left( \frac{A}{\alpha^2} + \frac{B}{\beta^2} \right)}{\text{AUC}^2}$$

(E. 24)

where Dose is the amount of drug administered (mg), A is the A-intercept ( $\text{mg L}^{-1}$ ) obtained from the method of residuals, B is the B-intercept ( $\text{mg L}^{-1}$ ) obtained from elimination phase analysis,  $\alpha$  ( $\text{h}^{-1}$  or  $\text{min}^{-1}$ ) is the distribution rate constant and  $\beta$  ( $\text{h}^{-1}$  or  $\text{min}^{-1}$ ) is the elimination rate constant obtained from Equation (E. 18), and AUC is the calculated area under the curve value. Essentially,  $V_{D_{SS}}$  is a proportionality constant that determines drug distribution, and the value is most appropriate at steady-state during continuous intravenous infusion (Greenblatt, 2014). In this case, the rate of transfer from the central compartment to the tissue compartment is equal to the rate of transfer from the tissues to the central compartment, a state of equilibrium, or “steady state”:

$$k_{12} \times V_C = k_{21} \times V_T$$

(E. 25)

However, the  $V_{D_{SS}}$  provides limited useful information about a drug, as it is only valid at a single point in time: when the amount of drug in the tissue compartment is at its theoretical maximum, meaning that it will always underestimate the proportionality constant of  $V_{D_{Area}}$  (Benet & Ronfeld, 1969; Greenblatt, 2014; Greenblatt, Abernethy & Divoll, 1983). The term is also highly sensitive to changes in the initial distribution phase, which further reinforces that the  $V_{D_{SS}}$  is an “unstable parameter (Greenblatt, 2014; Hanley, Abernethy & Greenblatt, 2010).

Obtaining precise measurements for the initial phase of distribution is difficult for a variety of reasons (Greenblatt, Abernethy & Divoll, 1983). First, the assumption that there is instantaneous and homogenous distribution in the central compartment is not valid physiologically; the vascular circulation takes time to reach all central compartment tissues (Greenblatt, Abernethy & Divoll, 1983). Second, the sampling schedule can influence parameter estimates: small changes in the timing of the initial sample after dose, as well as number, frequency, and spacing of subsequent blood samples influence the concentration-time profile (Greenblatt, Abernethy & Divoll, 1983). If the sampling isn't appropriate, then, for instance, a two-compartment drug may complete its distribution prior to the first sample, resulting in an incorrect assumption that

one-compartment modelling explains the drug's behaviour. Finally, removing blood samples may take upwards of two minutes; while the post-distributional parameters are affected, the quantitation of the distribution parameters may result in similar half-life values to the time needed to obtain the samples (Greenblatt, Abernethy & Divoll, 1983). Because there are many factors influencing the distribution phase, the calculation of  $V_{D_{SS}}$  has a large possibility for inaccuracy (Greenblatt, Abernethy & Divoll, 1983).

With consideration to the equilibrium for  $V_{D_{SS}}$ , the distribution of a compound depends on binding to blood cells, plasma proteins, and tissue components (Fan & de Lannoy, 2014). As only unbound drug enters and leaves the plasma and tissue compartments, the  $V_{D_{SS}}$  is also expressed as:

$$V_{D_{SS}} = V_P + V_T \times \frac{f_{u,p}}{f_{u,t}}$$

**(E. 26)**

where  $V_P$  and  $V_T$  are the physiological volumes of plasma and tissue, respectively, and  $f_{u,p}$  and  $f_{u,t}$  are the fractions unbound in plasma and tissue, respectively (Benet & Zia-Amirhosseini, 1995; Fan & de Lannoy, 2014). Plasma protein binding may influence a drug's distribution behaviour, and will be discussed in the next section, 1.1.3.2.

An additional term calculated in approximating a drug's  $V_D$  is through the extrapolation of the elimination phase of the semi-logarithmic curve back to the zero-time intercept (Greenblatt & Shader, 1985). The extrapolated Y-intercept, otherwise known as B, is used in an adaptation of Equation (E. 22) (Greenblatt & Shader, 1985):

$$V_{D_{\text{Extrap}}} = \frac{\text{Dose}}{B}$$

**(E. 27)**

where Dose (mg) is the amount of drug initially administered, and B is the B-intercept. Intuitively, the approximation follows from the central compartment volume calculation, but

simplistically ignores the time required for the distribution phase (Greenblatt & Shader, 1985). As such, the B-intercept is widely underestimated, resulting in the  $V_{D \text{ Extrap}}$ , which is generally higher than both the  $V_{D \text{ Area}}$  and  $V_{D \text{ SS}}$  values.

### Distribution Rate Constant

Drug distribution is dependent on a drug's physicochemical properties as well as tissue characteristics, which will be discussed more in depth in the next section. A drug's distribution half-life ( $t_{1/2 \text{ dist}}$ ) is defined as the time required for 50% of drug to distribute into target tissues (Shargel & Yu, 1999). This parameter relies on the first order distribution rate constant, which is determined by Equation 21, as shown through the method of residuals, or the following equation:

$$k_{\text{dist}} = \frac{Q}{V \times R} \tag{E. 28}$$

where  $Q$  ( $\text{mL min}^{-1}$  or  $\text{L h}^{-1}$ ), is the blood flow to the organ  $V$  ( $\text{mL}$  or  $\text{L}$ ) is the volume of the organ, and  $R$  is the ratio of drug concentration in the organ tissue to the venous blood (Shargel & Yu, 1999). The ratio constant is determined experimentally from tissue samples, but because these are notoriously difficult to obtain, the partition coefficient ( $\text{CLogP}$ ; ratio of drug in oil phase to aqueous phase at equilibrium) is considered as an alternative (Shargel & Yu, 1999). Application of the  $k_{\text{dist}}$  value for the calculation of the  $t_{1/2 \text{ dist}}$  value is shown as (Shargel & Yu, 1999):

$$t_{1/2} = \frac{0.693}{k_{\text{dist}}} \tag{E. 29}$$

An increased  $Q$  value aims to decrease the distribution time, while an increased  $V$  has the potential to increase a drug's distribution  $t_{1/2}$  due to the longer time required to distribute within an organ (Shargel & Yu, 1999). If a drug's partition ratio for two separate tissues is similar, then the  $t_{1/2 \text{ dist}}$  would primarily depend on the  $V$  and  $Q$  (Shargel & Yu, 1999).

### 1.1.3.2 Physiological Aspects of Distribution

As discussed, a drug's properties influence whether it will traverse the lipid-bilayer cell membrane and thus, whether it is absorbed into the blood stream. Distribution follows similar principles, because once in the bloodstream, a drug must cross the membranes of cells into target tissues. One of the most important determinants of distribution is the drug's partition coefficient (Shargel & Yu, 1999). As such, a drug's lipid solubility is an important factor for determining how extensively it may distribute into tissues; lipid-soluble drugs diffuse more extensively than highly polar or water-soluble drugs (Shargel & Yu, 1999). Additionally, plasma proteins bind with drug molecules, and because only unbound drugs may enter a cell, the extent of binding has the potential to affect the distribution equilibrium to a high degree. As well, some drugs accumulate preferentially in tissues, as cellular components like proteins, phospholipids, and nuclear proteins bind reversibly to the compounds (Buxton, Benet, Brunton, Chabner & Knollmann, 2011).

#### Plasma Protein Binding

Currently, the discussion of plasma drug concentrations and volume of distribution values centre on the assumption that the entire amount of drug circulating in the systemic circulation diffuses into target tissues and exerts pharmacological activity (Greenblatt & Shader, 1985). For many drugs, this is not the case, as plasma proteins form bonds with drug molecules, preventing them from diffusing into tissues (Greenblatt & Shader, 1985). The drug-protein complexes are held together by weak, reversible bonds, and as such, the association and dissociation of these complexes is in equilibrium; the relative amount of bound and unbound drug in the plasma concentration is stable (Greenblatt & Shader, 1985). The equilibrium is expressed as a ratio:

$$f_{u,p} = \frac{C_{p,u}}{C_{p,total}}$$

(E. 30)

where  $f_{u,p}$  is the fraction drug unbound in the plasma,  $C_{p,u}$  is the unbound drug plasma concentration, and  $C_{p, total}$  is the total drug plasma concentration (Fan & de Lannoy, 2014;

Greenblatt & Shader, 1985). As a note, the  $C_{p,u}$  or the unbound drug plasma concentration is determined by the rate at which the drug reaches the systemic circulation, and by an organ's ability to remove or metabolise it (Greenblatt & Shader, 1985). In terms of the bound drug ( $f_{b,p}$ ), the fraction is expressed as:

$$f_{b,p} = 1 - f_{u,p}$$

**(E. 31)**

The value of both the  $f_{b,p}$  and the  $f_{u,p}$  ranges from 0.0 to 1.0. The key discriminant between the  $f_{u,p}$  and the  $C_{p,u}$  is that the fraction drug unbound in plasma ( $f_{u,p}$ ) is completely dependent on a drug's physicochemical properties and interaction with the plasma protein, while the  $C_{p,u}$  is influenced by the rate of drug entry into the body and its elimination as an unbound molecule (Greenblatt & Shader, 1985). The fraction drug unbound is influenced by the drug concentration, the affinity of binding sites for the drug, and the number of binding sites (Buxton, Benet, Brunton, Chabner & Knollmann, 2011). Thus, the  $f_{u,p}$  to  $f_{b,p}$  ratio generally remains constant over a range of concentrations, but at extremely high plasma concentrations of drug, the ratio may shift dramatically (Buxton, Benet, Brunton, Chabner & Knollmann, 2011; Greenblatt & Shader, 1985).

Some of the plasma proteins that bind a compound and/or its metabolites are albumin,  $\alpha_1$ -acid glycoprotein (AAG), lipoproteins, and  $\alpha$ -,  $\beta$ - and  $\gamma$ -globulins (Fan & de Lannoy, 2014). Albumin and AAG are responsible for the binding of most compounds, with albumin carrying acidic drugs, and AAG binding mostly basic drugs (Buxton, Benet, Brunton, Chabner & Knollmann, 2011; Fan & de Lannoy, 2014). Changes in binding protein concentrations influence the fraction drug unbound ratio, and impact a drug's distribution profile (Greenblatt & Shader, 1985). A highly plasma protein bound compound often exhibits a small volume of distribution, as it is largely contained within the circulation, whereas a compound extensively drawn into tissue components exhibits a  $V_D$  greater than the physiological volume of the body (Fan & de Lannoy, 2014). Clinically, drugs with extremely small  $f_{u,p}$  values (less than 0.1) are severely impacted by slight variations in this ratio (Greenblatt & Shader, 1985). As well, the plasma protein binding

must be considered when calculating such parameters as volume of distribution and clearance. However, as the  $f_{u,p}$  ratio increases, the binding becomes less important, and when the ratio is 0.25 or larger, protein binding is relatively negligible (Greenblatt & Shader, 1985).

### **Tissue Characteristics**

Distribution of a drug into the interstitial fluid, excluding organs like the brain, generally occurs rapidly, because the capillary endothelial membrane is highly permeable in nature (Buxton, Benet, Brunton, Chabner & Knollmann, 2011). However, tissues that are highly permeable to drugs are generally perfusion-limited, as the flow of blood determines the rate at which drug reaches the tissue (Shargel & Yu, 1999). For perfusion-limited drugs, drug distribution is rapid; up to 95% of the distribution possible in tissues that are well-perfused, like the liver, kidneys and adrenal glands occurs in less than 2 minutes (Buxton, Benet, Brunton, Chabner & Knollmann, 2011; Shargel & Yu, 1999). In contrast, the second phase of drug distribution, which involves a far larger fraction of body mass and generally includes the delivery of drug to poorly perfused organs such as the adipose tissue, may take up to 4 hours and more (Buxton, Benet, Brunton, Chabner & Knollmann, 2011; Shargel & Yu, 1999). Because of the relatively low blood flow to adipose tissue, fat is a stable reservoir for such compounds, and even if drug plasma concentrations are negligible, adipose tissue may contain a high concentration of the drug (Buxton, Benet, Brunton, Chabner & Knollmann, 2011).

#### **1.1.3.3 Patient Factors Affecting Distribution**

##### **Obesity**

Generally, drugs with extensive distribution into extravascular tissues have larger volumes of distribution (Hanley, Abernethy & Greenblatt, 2010). While physicochemical attributes of a drug, such as partition coefficient, largely influence this parameter, factors like obesity can also extensively alter a drug's volume of distribution, particularly for increasingly lipophilic substances (Blouin & Warren, 1999; Hanley, Abernethy & Greenblatt, 2010). Intuitively, an increased absolute amount and proportion of adipose tissue as seen in obese individuals translates into a larger reservoir, and thus increases the volume of distribution (Hanley,

Abernethy & Greenblatt, 2010). Figure 1.15, as adapted from Hanley *et al.* depicts this schematic by using two extreme examples: the behaviour of a drug highly bound to plasma proteins and one that is highly lipid soluble in lean versus obese individuals (Hanley, Abernethy & Greenblatt, 2010).

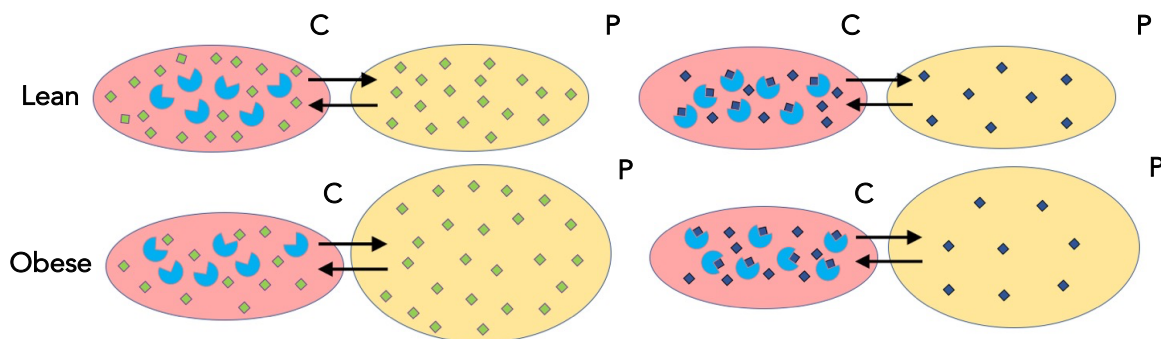


**Figure 1.15 The Effects of Obesity on Lipid-Soluble Drugs.**

Impact of obesity on the volume of distribution in a two-compartment model between a highly protein bound drug (◆) and highly lipophilic drug (◆) in lean (top) and an obese individual (bottom). The schematic represents the equilibrium between the central (C) and peripheral (P) compartments. For the highly protein bound drug (◆) administered at the same dose, the  $V_D$  is relatively the same between both obese and lean individuals as the drug does not distribute into excess adipose tissue, and thus, the “size” of P does not change. The highly lipophilic drug (◆) administered at the same dose to the lean and obese individuals, in contrast, distributes into the excess adipose tissue in the obese person. As such, the “size” of P changes, resulting in an increased volume of distribution.

A comparison of single-dosing of diazepam, a drug with a substantially high CLogP, showed that obese subjects (mean weight 92 kg) had significantly prolonged elimination half-lives in comparison to normal subjects (60 kg) (82 vs. 32 hours), accompanied with a substantial increase in volume of distribution (228 vs. 70 litres) (Abernethy, Greenblatt, Divoll & Shader, 1983). It was concluded that multi-dosing of diazepam would result in a prolonged period of residual drug effect in obese individuals in comparison to normal subjects (Abernethy, Greenblatt, Divoll & Shader, 1983). There are exceptions to obesity’s influence on drug distribution, as some drugs with high partition coefficients still display relatively consistent  $V_D$  values between obese and normal-weight individuals (Blouin & Warren, 1999).

## **Disease**

Disease states, such as liver cirrhosis, are associated with reduction in serum albumin concentration, leading to an increase in  $f_{u,p}$  of drugs with affinity for this plasma protein (Greenblatt & Shader, 1985). Conversely, some pathologies, like nephrotic syndrome, where there is accumulation of waste metabolites, affect the affinity of albumin for certain drugs through competition for binding sites, changing their distribution profile (Greenblatt & Shader, 1985; Klammt et al., 2012; Shargel & Yu, 1999).

In comparison to healthy volunteers, individuals with Crohn's disease, inflammatory arthritis, and chronic renal failure with superimposed inflammatory disease exhibited significantly greater plasma protein binding of propranolol and chlorpromazine (Piafsky, Borga, Odar-Cederlof, Johansson & Sjoqvist, 1978). This was directly correlated to a two-fold increase in AAG serum concentration (Gibaldi, 1984). Changes in drug binding resulting from disease produce significant alterations in the PK parameters of a drug (Gibaldi, 1984). Most directly, based on Equation (E. 26), there is an alteration to the volume of distribution parameter (Gibaldi, 1984).

## **Age**

When a constant dose of ethanol, a highly water-soluble compound, was administered to subjects ranging widely in age, elderly subjects displayed higher peaks of ethanol in their blood in comparison to younger subjects (Vestal, McGuire, Tobin, Andres, Norris & Mezey, 1977). This peak was accounted for by the observation that elderly patients typically have a smaller volume of TBW and decreased lean body mass in comparison to younger subjects (Gibaldi, 1984).

In terms of plasma protein binding, the general belief is that binding (usually of albumin) will decrease or stay relatively unchanged with increasing age (Mayersohn, 1994). In a study involving over 11,000 patients controlled for confounding factors, ranging in age from less than 40 to over 80 years, Greenblatt reported that after the age of 60, serum albumin concentrations decreased progressively with each decade of age (Greenblatt, 1979). Because diseases that affect distribution behaviours are prevalent in this population, the combination, in addition to

physiological changes associated with aging, warrants special care and consideration to the dosing and prescribing for these individuals (Mayersohn, 1994).

#### 1.1.4 ADME: METABOLISM

Though lipid solubility promotes drug passage through biological membranes and allows access to target tissues, it is not a desirable trait for drug elimination (Buxton, Benet, Brunton, Chabner & Knollmann, 2011). Most drugs are not eliminated unchanged from the body, rather, they must undergo transformation processes so they can be converted into a form suitable for elimination (Greenblatt & Shader, 1985). Many tissues in the body metabolise drugs, but the main organ responsible for most of the metabolism is the liver, and will be the focus of this section (Greenblatt & Shader, 1985). As discussed in the First Pass Effect section, the liver can extensively metabolise drugs prior to their entry into the systemic circulation, and thus, its role in these processes has a major impact on not only a drug's elimination, but also its bioavailability. Some drugs require more than one transformation to produce a derivative suitable for elimination, and some of these derivatives exert pharmacological activity, requiring more complex analysis of a drug's PK (Greenblatt & Shader, 1985). Drug metabolism or biotransformation reactions are generally classified into two phases: Phase I and Phase II.

##### Phase I Reactions

Phase I reactions introduce or expose a functional group on the original drug (Buxton, Benet, Brunton, Chabner & Knollmann, 2011). These reactions typically involve oxidations, reductions, and hydrolysis (Greenblatt & Shader, 1985). The enzymes involved in phase I reactions include most prominently the CYP enzymes, as well as Flavin-Containing Monooxygenases (FMOs), and hydrolytic enzymes such as epoxide hydrolase (Gonzalez, Coughtrie & Turkey, 2011). Phase I reactions generally result in loss of pharmacological activity, and yield intermediate products that are efficiently converted into highly polar, water-soluble metabolites (Buxton, Benet, Brunton, Chabner & Knollmann, 2011; Gonzalez, Coughtrie & Turkey, 2011; Greenblatt & Shader, 1985). Some drugs are transformed into metabolites that also exert pharmacological activity. Other drugs are administered as **prodrugs**, which are pharmacologically inactive, but

after undergoing Phase I biotransformation, are converted into active metabolites (Buxton, Benet, Brunton, Chabner & Knollmann, 2011).

### **The Cytochrome P450 (CYP) System**

The CYPs are a superfamily of enzymes which contain a heme protein within the polypeptide chain, and which are found on the membranes of the endoplasmic reticulum (Gonzalez, Coughtrie & Turkey, 2011; Sweeney & Bromilow, 2006). This enzyme system carries out phase I oxidation reactions by using  $O_2$  and the  $H^+$  from the cofactor, nicotinamide adenine dinucleotide phosphate (NADPH), to produce the oxidised substrate along with a molecule of water as a by-product (Gonzalez, Coughtrie & Turkey, 2011). Nomenclature for the CYP isoenzymes is three-tiered: the numerical and capital letter designates the amino acid sequence, while the final number indicates the individual enzyme (Sweeney & Bromilow, 2006). In humans, there are 43 subfamilies and 57 individual enzymes each coded by an individual gene (Sweeney & Bromilow, 2006). Of these individual enzymes, the CYPs that fall into families 1-3 are primarily involved in drug metabolism (Gonzalez, Coughtrie & Turkey, 2011). The major isoenzymes involved in metabolism are CYP1A2, CYP2C9, CYP2C19, CYP2D6, CYP2E1 and CYP3A4 (Pilgrim, Gerostamoulos & Drummer, 2011).

The CYPs are capable of metabolising diverse molecules because of the existence of these multiple forms of the enzyme (Gonzalez, Coughtrie & Turkey, 2011). In addition, unlike other enzymes which carry out very specific reactions, a single CYP has the capacity to metabolise many structurally-distinct drugs (Gonzalez, Coughtrie & Turkey, 2011). A single compound is potentially metabolised by multiple CYPs, at differing rates, and at different positions on the molecule; this extensive overlap is largely a result of the large and fluid binding sites within these enzymes (Gonzalez, Coughtrie & Turkey, 2011). The lack of specificity contributes a risk for adverse drug events, namely through drug-drug interactions (DDIs). In addition to drug-drug interactions, genetic variation, ethnicity, hormone levels, and diet are also capable of invoking variability in the expression and activity of these enzymes, and as such, influence the

metabolism, elimination, and plasma levels of a drug (Pilgrim, Gerostamoulos & Drummer, 2011).

### **Phase II Reactions**

While some drugs are converted into polar, water-soluble compounds after Phase I, most must undergo Phase II reactions, deemed the “final” biotransformation (Greenblatt & Shader, 1985). Phase II reactions are catalysed by conjugating enzymes, which create covalent linkages between the functional group revealed or added onto the parent compound and a respective conjugated molecule, such as a glucuronic acid, sulfate, glutathione, amino acid, methyl, or acetyl derivative (Buxton, Benet, Brunton, Chabner & Knollmann, 2011). Addition of these molecules result in drug metabolites that may exhibit altered pharmacological activity and/or a more polar confirmation which primes the compound for elimination.

### **Kinetic Definitions and Principles of Metabolism**

Enzyme activity is modulated *via* induction or inhibition by substrates, and in the context of DDIs, the consequences of these interactions range from a compound’s loss of efficacy to adverse effects associated with elevated levels of co-administered compounds (Orr et al., 2012). DDIs involving CYP activity are frequent, and in some cases, so severe that some drugs have been withdrawn from clinical practice (Orr et al., 2012).

Though the Michaelis-Menten model is used as the foundation for enzyme kinetics, some enzymes exhibit greater kinetic complexity and as such, Equation (E. 3) may not be appropriate or suitable. Though the CYP enzymes were initially believed to be monomers with a single catalytic site, current understanding of the enzymes suggests a higher degree of complexity (Shou, Dai, Cui, Korzekwa, Baillie & Rushmore, 2001). CYP3A4 accommodates relatively large substrates, and some studies have shown that multiple small or intermediate-sized molecules coexist in its active site (Shou, Dai, Cui, Korzekwa, Baillie & Rushmore, 2001). An active site accommodating two substrates simultaneously, with each influencing the oxidation of the other, would not follow simple Michaelis-Menten inhibition kinetics, and as such, appreciation for this

complexity is important when considering CYP metabolism (Shou, Dai, Cui, Korzekwa, Baillie & Rushmore, 2001). This work will not focus on the kinetics of metabolism, but there is value in discussing the mechanisms affecting metabolism as it relates to pharmacokinetics outcomes.

### **Metabolism Inhibition**

The basis of using the Michaelis-Menten model to explain enzyme kinetics is that the enzyme has one binding site for substrates (Figure 1.4; Equation E.3), and that reaction velocity,  $v$ , has a hyperbolic relationship with the substrate concentration (Sweeney & Bromilow, 2006). Thus, Michaelis-Menten inhibition involves two or more substrates competing for the same binding site where the “inhibitor” blocks the metabolism of the principal compound by one of several potential mechanisms (Sweeney & Bromilow, 2006). Inhibition of enzyme activity is normally categorised as reversible (competitive or non-competitive) or irreversible (Orr et al., 2012).

While reversible inhibition involves an interaction where the “inhibitor” shifts the principal compound’s  $K_m$  and/or affects its rate or access for metabolism, irreversible inhibition may involve reactive metabolites and results in destruction of the enzyme in question (Orr et al., 2012). Regardless of the principal substrate’s concentration or presence, the enzyme is catalytically inactive and therefore unable to metabolise the compound. Only *de novo* synthesis of the enzyme replenishes activity. Irreversible inhibition, of which mechanism-based inactivation (MBI) is the most commonly-occurring process, presents a great safety concern, because of increased potential for PK interactions after multiple dosing and sustained periods of these interactions even after initial removal of the inhibitor (Orr et al., 2012).

Interactions with nefazodone highlight the consequences of irreversible inhibition. The drug, a non-tricyclic antidepressant, is associated with increasing plasma concentrations and increasing AUC of a diverse number of CYP3A4 substrates when co-administered in humans (Orr et al., 2012). In a case study where nefazodone was co-administered with simvastatin (a relatively safe and effective hyperlipidemia medication), the patient, within 10 days, was diagnosed with rhabdomyolysis and experienced liver and kidney dysfunction (Skrabal, Stading & Monaghan, 2003). The nefazodone, through irreversible inhibition of the 3A4 enzyme, increased simvastatin

plasma levels, thereby creating the potential for toxic effects associated with the medication (Skrabal, Stading & Monaghan, 2003).

### **Metabolism Induction**

Conventionally, enzyme induction is the *de novo* creation of new enzyme protein because of increased transcription of its corresponding gene (Sweeney & Bromilow, 2006). In drug metabolism, induction is characterised as the increase in the amount and/or activity of an enzyme in response to exposure to an “inducer” (Sweeney & Bromilow, 2006). Many drugs are known to induce their own metabolism, or that of another drug (Gibson & Skett, 2001). Measurable parameters indicating potential induction include increased drug clearance, and decreased drug half-life, among others (Gibson & Skett, 2001).

In a small study involving 6 healthy volunteers, the PK parameters of cyclosporine were studied in the presence and absence of another drug, rifampin, a known inducer of cyclosporine metabolism (Hebert, Roberts, Prueksaritanont & Benet, 1992). Clinically, cyclosporine acts as an immunosuppressive agent in transplant patients to prevent rejection, but long-term immunosuppression predisposes patients to infections such as *Mycobacterium tuberculosis*, for which a conventional treatment combination includes rifampin (Hebert, Roberts, Prueksaritanont & Benet, 1992). Statistically significant decreases in plasma cyclosporine AUC and bioavailability, and increases in its clearance were observed with rifampin co-administration (Hebert, Roberts, Prueksaritanont & Benet, 1992). It was concluded that the induction of the CYP enzymes responsible for cyclosporine metabolism (in the intestines and in the liver) caused the observed changes in the PK parameters (Hebert, Roberts, Prueksaritanont & Benet, 1992). Thus, the co-administration of these drugs, despite the clinical need, would threaten patient outcomes in terms of transplant rejection.

The greatest risk of clinically significant DDIs centres upon the process of metabolism, whereby the “inducer” or “inhibitor” alters a substrate’s PK parameters, such as bioavailability and systemic clearance (Kamel & Harriman, 2013). Thus, the use of multiple drugs in patients is a major factor affecting metabolism. In 2014, in Canada alone, approximately 11% of 45-64 year-

olds and 30% of seniors aged 65-79 were taking at least five different medications concurrently; clearly, understanding the basis for DDIs should be a priority within healthcare (Rotermann, Sanmartin, Hennessy & Arthur, 2014).

#### **1.1.4.2 Patient Factors Affecting Metabolism**

##### **Genetics**

Variations in drug metabolism exist between human subjects, and discrete genetic sub-populations have been studied and identified (Gibson & Skett, 2001). Studies have shown that identical twins resemble each other very closely in terms of metabolism whereas fraternal twins show variations similar to those observed in the general population, revealing how prominent the genetic link is for drug metabolism (Gibson & Skett, 2001). In terms of the CYP enzymes, for example, CYP2D6 displays the most comprehensively understood example of variation in drug metabolism, as it possesses more than 80 documented allelic variants (Pilgrim, Gerostamoulos & Drummer, 2011). The activity in this enzyme ranges from complete deficiency (poor metabolisers; PM), where specific genes mandate the production of inactive or little enzyme, to ultrarapid (UM) metabolism, where the gene is duplicated or multi-duplicated, resulting in the ultra-rapid phenotype (Pilgrim, Gerostamoulos & Drummer, 2011). The presence of these types of genetic variations in an individual can cause significant increases or decreases in a drug's AUC, bioavailability, and clearance, affecting the outcome and increasing the risk of potentially negative side effects, or even death.

The death of a nine-year old child found to have elevated levels of fluoxetine and its primary metabolite in his blood and tissues raised suspicion of a homicide by his adoptive parents (Stipp, 2000). Genetic testing, however, cleared their names, after it was found that the child possessed a genetic variant of the CYP2D6 PM genotype, which caused the levels of the prescribed medication to increase to a point exceeding any previously reported cases of fluoxetine overdose (Stipp, 2000). Though tragic, cases such as these have provided traction to the field of pharmacogenetics, as an understanding of a patient's metabolic capacity can facilitate safe and effective therapeutics.

## Age

The young, particularly the newborn, and elderly are more susceptible to drug action (Gibson & Skett, 2001). While many factors, such as a decline in organ function, decrease metabolic capacity in the elderly, the increased sensitivity in neonates is largely connected to their low (and at times unmeasurable) drug-metabolising capacity (Gibson & Skett, 2001). A study involving caffeine therapy revealed that in comparison to a half-life of 4 hours in adults, the half-life of the substrate in newborns was 4 days (Gibaldi, 1984; Gibson & Skett, 2001). In addition, adults eliminated less than 2% of a caffeine dose unchanged in the urine, while the unmetabolised caffeine accounted for more than 85% of urinary excretion in the newborn (Aldridge, Aranda & Neims, 1979). This stark difference was a result of slow urinary excretion in the infant, and little to no metabolism of the caffeine. With increasing age, a subsequent decrease in caffeine half-life to 4 hours by the age of 8 months was observed (Aldridge, Aranda & Neims, 1979). Thus, an understanding of the effects of age on processes of drug pharmacokinetics allows clinicians to exhibit caution when administering therapies for vulnerable populations, such as newborns and the elderly.

Interestingly, older infants and children metabolise certain drugs more rapidly than adults; the rates reach a maximum somewhere between 6 months and 12 years of age and then decline after that point (Gibaldi, 1984). Specific CYP isoenzymes, such as CYP1A2, CYP2C9, and CYP3A4 have higher enzymatic activity in children *versus* adults, and as such, higher weight-corrected doses are required for drugs eliminated solely by these enzymes (Anderson, 2010).

## Disease

Many of the major effects on PK are observed with diseases affecting the liver; as the liver is major site for drug biotransformation, this is hardly surprising (Gibson & Skett, 2001). However, non-hepatic diseases, such as hyperthyroidism, diabetes, adrenal insufficiency, and thyroid or adrenal tumors, can also affect metabolism (Gibson & Skett, 2001). In patients with cirrhosis, the metabolism of several drugs is affected, likely because of decreased enzyme activity, altered

hepatic blood flow, and hypalbuminaemia (leading to changes in plasma protein binding); the effect on metabolism varies depending on the drug (Gibson & Skett, 2001).

## **Diet**

Acute ethanol exposure decreases drug metabolism for drugs metabolised by both phase I and phase II – the resulting interaction exhibits longer half-lives for these co-administered substrates (Gibson & Skett, 2001). It is hypothesised that the inhibition of phase I metabolism is partly due to ethanol binding to CYP2E1 in a competitive manner, alteration to the NADP<sup>+</sup>/NADPH ratio, and disruption of the lipid environment of the cells (Gibson & Skett, 2001).

The ingestion of cruciferous vegetables have also been shown to induce CYP enzymes, particularly CYP1A2 (Schein, 1997). A study was conducted in ten healthy human volunteers exploring the effects of a brussels sprouts and cabbage-containing diet on the metabolism of antipyrine and phenacetin (both of which are metabolised by CYP1A2) (Pantuck et al., 1979; Schein, 1997). Despite considerable intra-individual variability in drug response, there were some consistent findings on the effects of cruciferous vegetables on drug metabolism (Pantuck et al., 1979). In comparison to results while ingesting a control diet, volunteers eating a diet consisting of cruciferous vegetables had a 13% reduction in mean plasma half-lives of antipyrine and an 11% increase in metabolic clearance rate. In addition, when eating the brussels sprouts and cabbage-containing diet, volunteer data showed that mean-plasma concentrations of phenacetin were markedly decreased 34-67% at various time points, while the ratio of the plasma concentration of conjugated to unconjugated N-acetyl-p-aminophenol were increased 40-50%, suggesting a stimulation of phenacetin metabolism in the GI tract and/or during its first pass through the liver (Conney, 1982; Pantuck et al., 1979). When participants were again fed the control diet for several days, the metabolic clearance rates for antipyrine and ratios for phenacetin returned towards the control values (Pantuck et al., 1979).

### 1.1.5 ADME: ELIMINATION

Drug elimination encompasses the removal of drug from the body by all routes of elimination, including excretion and biotransformation (Shargel & Yu, 1999). The kidneys play a principal role in excretion of intact drug into urine, though other pathways for drug excretion, such as through bile, sweat, saliva, and the lungs, are possible (Gibaldi, 1984; Shargel & Yu, 1999). Biotransformation includes metabolism of drugs usually carried out in the liver, the major site, though other tissues also contribute (Gibaldi, 1984; Shargel & Yu, 1999). Elimination of a drug is closely linked to its clearance (CL), which, by means of these various organs of elimination, is additive (Benet & Zia-Amirhosseini, 1995). The clearance value, along with the volume of distribution, influences a drug's half-life ( $t_{1/2}$ ), a parameter which plays a vital role in designing dosing regimens (Benet & Zia-Amirhosseini, 1995). These parameters are widely influenced by patient factors, such as disease and age, and understanding these relationships provides insight into drug disposition. There are several ways to determine elimination parameters; conceptual modelling and physiological measurements can provide insight into this process

#### 1.1.5.3 Kinetic Definitions and Principles of Elimination

##### Physiological Modelling

The physiological modelling approach to clearance links the process to blood flow and to each organ's elimination ability, allowing for a more defined understanding of the impact of drug-drug interactions or disease states on clearance (Fan & de Lannoy, 2014; Shargel & Yu, 1999). An organ's clearance reflects the ability of the organ to remove the drug from blood (Fan & de Lannoy, 2014). Total systemic clearance is additive and calculated by (Benet & Zia-Amirhosseini, 1995; Dhillon & Kostrzewski, 2006):

$$CL_{\text{Total}} = CL_{\text{Renal}} + CL_{\text{Hepatic}} + CL_{\text{Lungs}} + CL_{\text{Gut}} + \dots CL_{\text{Other}}$$

(E. 32)

When a drug passes through an organ, it is possible to determine the organ's elimination contribution by considering changes in concentration of drug in the blood based on the rate of presentation and rate of exit (Benet & Zia-Amirhosseini, 1995):

$$\text{rate of presentation} = Q \times C_A$$

$$\text{rate of exit} = Q \times C_V$$

$$\text{rate of elimination} = Q \times C_A - Q \times C_V = (C_A - C_V)$$

(E. 33)

where  $Q$  is the blood flow,  $C_A$  is the arterial concentration of the drug, and  $C_V$  is the venous concentration of the drug. The difference between the rate of presentation and rate of exit determines the organ's elimination rate (Benet & Zia-Amirhosseini, 1995). In addition, the presented information allows for calculation of the extraction ratio (ER) of the organ by comparing the ratio of the presentation and exit concentrations (Benet & Zia-Amirhosseini, 1995; Shargel & Yu, 1999):

$$ER = \frac{(C_A - C_V)}{C_A}$$

(E. 34)

If no drug emerges into the venous blood after entering the organ, the extraction ratio is 1.0, which is the maximum possible value, whereas if  $C_V = C_A$ , the ER is 0 (Benet & Zia-Amirhosseini, 1995). By convention, drugs with an ER of 0.7 or greater are considered high extraction ratio drugs, while drugs with an ER of 0.3 or less are low extraction ratio drugs (Benet & Zia-Amirhosseini, 1995). As a note, because the ER ranges between 0 and 1, the organ clearance cannot exceed the blood flow rate perfusing the organ (Fan & de Lannoy, 2014). The availability of a compound after it passes through the eliminating organ can be expressed as  $F_{\text{organ}}$ , and calculated as (Fan & de Lannoy, 2014):

$$F_{\text{organ}} = 1 - ER$$

(E. 35)

The product of organ blood flow and extraction ratio of an organ describe the rate of when a certain amount of blood is cleared of a drug and is expressed as then the organ's clearance is expressed as (Benet & Zia-Amirhosseini, 1995; Shargel & Yu, 1999):

$$CL_{\text{Organ}} = ER \times Q$$

(E. 36)

Figure 1.16, as adapted from Shargel *et al.* and Benet *et al* illustrates organ relationships to clearance. To note, while the plasma measurements often require invasive techniques, urinary drug excretion is readily amenable to clearance measurements and calculations (Shargel & Yu, 1999).

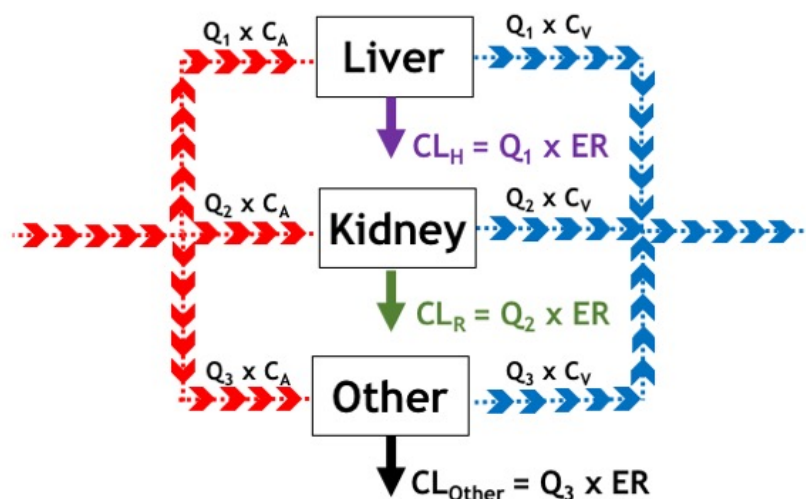


Figure 1.16 Clearance Determination via Blood Flow and Drug Concentration.

Drug concentrations can change after the blood containing the drug is perfused through an organ such as the liver or kidney. This change in drug concentration reflects the organ's extraction ratio (ER), which contributes to the calculation of an organ's clearance.

## Hepatic Elimination

Among the many eliminating organs, the liver has the highest metabolic capability (Benet & Zia-Amirhosseini, 1995). Plasma protein binding, as mentioned in Section 1.1.3.2, not only influences a drug's distribution behaviour, but impacts a drug's clearance. The  $f_{u,p}$  ratio is implemented into the calculation of an organ's clearance by using the well-stirred model, the most straightforward model for organ elimination and applied specifically for hepatic elimination (Benet & Zia-Amirhosseini, 1995):

$$CL_H = Q \times \frac{f_{u,p} \times CL_{int}}{Q + f_{u,p} \times CL_{int}} \quad (\text{E. 37})$$

where  $Q$  represents the blood flow to an organ,  $f_{u,p}$  represents the fraction unbound in plasma, and  $CL_{int}$  represents the organ's intrinsic ability to clear unbound drug if there are no limitations presented from flow or binding (Benet & Zia-Amirhosseini, 1995).

Organ clearance is equal to the product of the organ blood flow and extraction ratio of the organ, and as such, the  $ER_H$  is expressed as (Benet & Zia-Amirhosseini, 1995):

$$ER_H = \frac{f_{u,p} \times CL_{int}}{Q + f_{u,p} \times CL_{int}} \quad (\text{E. 38})$$

The relationships between these values offer important insight into how extraction ratios influence the clearance of a compound in healthy individuals. Based on the Clearance Equation (E. 37), if the  $CL_{int}$  of a drug is greater than 70% of the blood flow ( $Q$ ) to the liver ( $Q_H \ll f_{u,p} \times CL_{int}$ ), then the drug will experience high hepatic clearance (Benet & Zia-Amirhosseini, 1995; Fan & de Lannoy, 2014). The influence of a relatively large  $CL_{int}$  deems the  $Q$  in the denominator as virtually negligible, and the equation simplifies to:

$$CL_H = Q \times \frac{f_{u,p} \times CL_{int}}{Q + f_{u,p} \times CL_{int}} = Q \times 1 = Q$$

$$CL_H = Q$$

(E. 39)

Thus, changes in  $f_{u,p}$  or  $CL_{int}$ , will not influence the organ's clearance greatly, and the drug's elimination is highly dependent on blood flow. The drug, in general, will experience high first-pass elimination (if administered orally) and low oral bioavailability (Fan & de Lannoy, 2014). If the  $Q$  is altered in any way, a high extraction ratio drug's AUC and elimination half-life is markedly affected (Fan & de Lannoy, 2014).

If the  $CL_{int}$  is lower than 30% of the  $Q$  to the liver ( $Q_H \gg f_{u,p} \times CL_{int}$ ), the drug will experience low hepatic clearance, and changes in  $Q$  will not affect this value (Benet & Zia-Amirhosseini, 1995; Fan & de Lannoy, 2014). However, changes in  $f_{u,p}$  and  $CL_{int}$  will significantly affect the  $CL_H$ , as a relatively small  $CL_{int}$  value in the denominator is negligible, resulting the following relationship:

$$CL_H = Q \times \frac{f_{u,p} \times CL_{int}}{Q + f_{u,p} \times CL_{int}} = \frac{Q(f_{u,p} \times CL_{int})}{Q} = (f_{u,p} \times CL_{int})$$

$$CL_H = f_{u,p} \times CL_{int}$$

(E. 40)

Thus, any change in  $CL_{int}$  or  $f_{u,p}$  can proportionally influence the hepatic clearance of the drug, because with regard to low extraction ratio drugs, the activity of enzymes and transporters in the organ influence its elimination from that organ (Fan & de Lannoy, 2014). The bioavailability of the drug would thus be heavily influenced by changes in the  $CL_{int}$  or  $f_{u,p}$ ; an increased ratio of fraction unbound drug in the plasma or increased activity of the enzymes and transporters in the liver would increase the  $CL_H$  and thereby reduce the drug's bioavailability.

### Renal Elimination

In general, Equation 35 is adapted as:

$$CL_{Total} = CL_R + CL_{NR}$$

(E. 41)

where  $CL_{NR}$  is denoted as all clearance occurring through non-renal organs (assumed primarily to be hepatic clearance ( $CL_H$ )). For any drug cleared through the kidney, the rate of drug passing through kidney (via the three processes of filtration, reabsorption, and/or active secretion explained in a later section) equals the rate of drug excreted in the urine:

$$CL_R \times C_p = Q_u \times C_u$$

(E. 42)

where  $CL_R$  is the renal clearance,  $C_p$  is drug plasma concentration,  $Q_u$  is the rate of urine flow, and  $C_u$  is drug urine concentration (Shargel & Yu, 1999). In some cases, the  $CL_R$  for a drug is equal to the glomerular filtration rate (GFR), but usually, other processes occurring in the kidney contribute to the renal clearance (Shargel & Yu, 1999). Generally, the renal clearance can be related to the three processes occurring in the kidney to the plasma drug concentration as :

$$CL_R = \frac{\text{Filtration rate} + \text{secretion rate} - \text{reabsorption rate}}{C_p}$$

(E. 43)

There are numerous ways to use urinary data to calculate drug elimination parameters, and each has its own merits and downfalls. One strategy involves analysing urinary excretion data by the sigma-minus method (or the amount of drug remaining to be excreted method) (Shargel & Yu, 1999). Data may be analysed in this way when a significant amount of unchanged drug is excreted in the urine, when there is frequent sampling, and when the assay technique is specific for the unchanged drug and not its metabolites (Shargel & Yu, 1999). When almost all the drug is excreted (by convention, within 7 half-lives), the cumulative drug curve approaches an asymptote, representing drug at time infinity ( $(D_u)_\infty$ ) (see Figure 1.2) (Shargel & Yu, 1999). This approach requires accuracy in determining the  $(D_u)_\infty$  value, and as such, urine collection must be done until urinary drug excretion is virtually complete (Shargel & Yu, 1999).

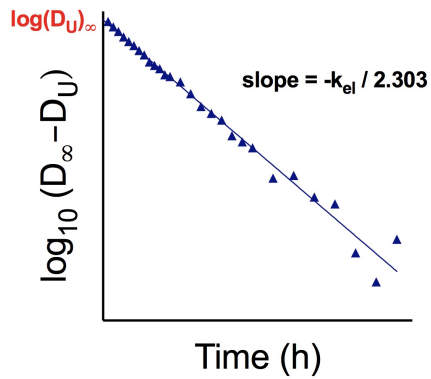


Figure 1.17 Log Drug at Infinity – Drug in Urine

The  $(D_U)_\infty$  value determined from the asymptote in the cumulative drug curve is the value for which all other  $D_U$  samples are subtracted from to determine the amount of drug remaining to be excreted. Figure 1.17 shows the expected semi-logarithmic plot of the data, and the slope of the line fitting the data allows for calculation of the  $k_{el}$  value for the drug.

### Compartmental Modelling

One of the simplest methods of determining clearance conceptualises the body as a space containing a specific volume of body fluid (an apparent volume of distribution) (Shargel & Yu, 1999). One compartment distribution modelling has been discussed, and Figure 1.18, adapted from Shargel *et al.* displays this model as it applies to elimination.

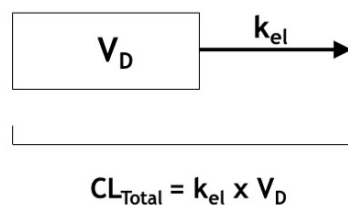


Figure 1.18 Compartmental Clearance

Essentially, clearance is defined as a fixed volume of fluid cleared of drug over a unit of time, and expressed as:

$$CL_{\text{Total}} = V_D \times k_{\text{el}} \quad (\text{E. 44})$$

where  $V_D$  represents the apparent volume of drug distribution (L or mL), and  $k_{\text{el}}$  is the elimination rate constant ( $\text{min}^{-1}$  or  $\text{h}^{-1}$ ) (Fan & de Lannoy, 2014). The concept of one-compartment modelling implies a defined model of drug behaviour wherein there is instantaneous distribution within the system, and the plasma concentrations reflect a parallel decline in tissue concentration (Fan & de Lannoy, 2014; Shargel & Yu, 1999). These assumptions are not always appropriate and as such should be considered with care.

The relationship depicted in Equation (E.44) is seemingly simple – if two of these parameters are known, the third is easily estimated (Mehvar, 2004). However, the simplicity of the relationship may result in erroneous conclusions if the physiological relationships are not adequately considered (Mehvar, 2004). Physiologically, clearance depends on parameters such as hepatic blood flow, degree of protein binding, and the intrinsic clearance of an organ, and if these values are altered because of drug-drug interactions or disease states, the clearance of the drug will change (Mehvar, 2004). Similarly, drug distribution is affected by its own independent factors, such as the physicochemical properties of the drug, disease states, tissue perfusion, and plasma and tissue binding (Mehvar, 2004; Shargel & Yu, 1999). Though both CL and  $V_D$  can change simultaneously, they do so independently of one another, though each exerts influence on the  $k_{\text{el}}$  parameter.

### **Elimination Rate Constant and Half-Life**

The elimination rate constant ( $k_{\text{el}}$ ;  $\text{min}^{-1}$  or  $\text{h}^{-1}$ ) describes the elimination of the drug from the body, which is generally a first-order reaction (Fan & de Lannoy, 2014; Shargel & Yu, 1999). It is determined from the slope of the terminal phase as shown in

Figure 1.14d and Equation (E. 18). This value is crucial for the calculation of the half-life, the time required for the amount of compound in the body to decrease by 50% (Fan & de Lannoy, 2014). For first-order rate reactions, the  $t_{1/2}$  is a constant (Figure 1.19), and its relationship to the elimination rate constant is related as (Fan & de Lannoy, 2014):

$$t_{1/2} = \frac{0.693}{k_{el}}$$

(E. 45)

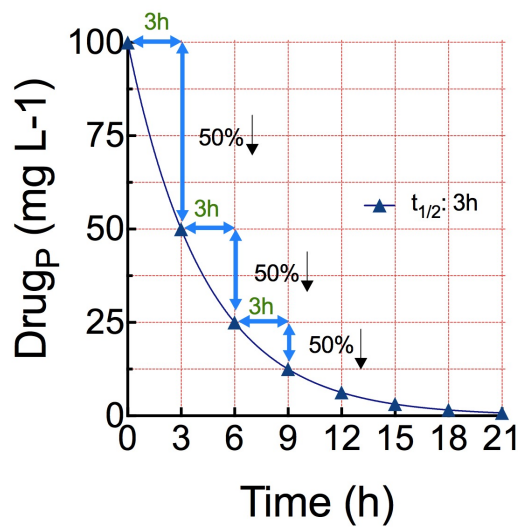


Figure 1.19 First Order Elimination Half-Life

The half-life, as such, is directly affected by changes associated with Equation (E. 44), and the physiological parameters of  $V_D$  and  $CL$  as it is inversely related to the  $k_{el}$ . By combining Equations (E. 44) and (E. 45),  $t_{1/2}$  is expressed as (Shargel & Yu, 1999):

$$t_{1/2} = \frac{0.693 \times V_D}{CL}$$

(E. 46)

Thus, an increase in the CL intuitively reflects a reduction in the half-life as drug is cleared more rapidly, while an increase in the  $V_D$  extends the half-life as drug distributes more extensively into the tissues (Mehvar, 2004).

The  $CL_{Total}$  of an antibiotic administered to a patient is calculated by Equation (E.44). Subsequent treatment, which includes administering fluids for patient hydration increases the  $V_D$  of the drug, affecting the  $k_{el}$  value, and thus, affecting the half-life (Mehvar, 2004). If the half-life is not adjusted appropriately, to determine the new  $CL_{Total}$  with altered  $V_D$ , then the  $CL_{Total}$  will be overestimated, resulting in toxicity; predicting changes using Equation (E. 44) without understanding the physiology of how these changes affect one another, can seriously affect treatment (Mehvar, 2004).

Predictably, a change in the  $V_D$  will result in a proportional increase (or decrease) in the drug's half-life, as illustrated by Equation (E. 46). However, there are always exceptions to consider, and without a proper understanding of the physiological relationships, the above equation can continue to perpetuate incorrect assumptions about the relationship between clearance and volume of distribution (Shargel & Yu, 1999). A drug highly bound to plasma proteins generally exhibits a low  $V_D$ , but can also exhibit an extremely long half-life. Only the fraction of unbound drug in plasma diffuses to organs responsible for clearance (Greenblatt & Shader, 1985). Restrictive drug clearance due to significant plasma protein binding for some compounds may result in  $CL_{Total}$  values lower than expected, and with reference to Equation (E. 46), may result in an extremely long half-life (Shargel & Yu, 1999).

Comparatively, a drug with a high volume of distribution and long-elimination half-life can still exhibit a relatively fast clearance rate (Shargel & Yu, 1999). The  $V_D$  may be so large, that the time required for drug distribution to occur contributes to the drug's duration in the body in a major way, and though the  $CL_{Total}$  can comparatively be quite high, the total  $V_D$  value is so much higher that it translates into a longer elimination half-life (Shargel & Yu, 1999). Thus, having a thorough understanding of the physiological relationships regarding distribution and

elimination can prevent the incorrect assumptions that occur when considering drug behaviour purely through the mathematical approach.

### 1.1.5.2 Physiological Aspects of Elimination

#### Renal Elimination

The kidneys are involved in eliminating almost every drug or drug metabolite to some degree; renal clearance is a major route of elimination (Gibaldi, 1984; Shargel & Yu, 1999). Generally, drugs which are non-volatile, water-soluble, and have low MW will undergo renal excretion; lipid soluble drugs usually undergo metabolism before they can be eliminated via the kidneys (Shargel & Yu, 1999). The process of renal excretion is complex and involves several components: glomerular filtration, active tubular secretion, passive reabsorption, and to a small extent, renal metabolism, all of which occur in different parts of the nephron (Gibaldi, 1984).

As a drug reaches the kidneys via the circulation, the hydrostatic pressure within the capillaries forces it to enter the glomerular filtrate; at this point, drug only traverses the cell membrane if it is unbound, small, and non-ionised (Shargel & Yu, 1999). As such, if the proportion of unbound drug in plasma increases, the glomerular filtration of the drug will increase proportionally, and for some drugs, increase its clearance (Shargel & Yu, 1999). The glomerular filtration rate (GFR) for an individual is measured by noting the renal clearance of drugs such as creatinine, which are only eliminated via this filtration process; an average individual has a GFR of  $\sim 130 \text{ mL min}^{-1}$  (Gibaldi, 1984).

Tubular secretion is an active transport process whereby drugs diffuse against concentration gradients from capillaries to the renal tubule; even if a drug is bound to plasma proteins, it will experience rapid dissociation from the complex due to the local concentration gradients generated by the rapid transport (Gibaldi, 1984). The process occurs in the proximal tubules of the nephron and relies on carrier-mediated transport, which is capacity limited; as such, each drug has its own maximum rate of transport (Fan & de Lannoy, 2014; Gibaldi 1984; Shargel & Yu, 1999). Specifically, weak acids and weak bases are known to use these transport systems,

and, interestingly, competitive inhibition of their respective transporters are sometimes used therapeutically to prolong the half-lives of these drugs (Gibaldi, 1984).

After drugs undergo glomerular filtration or secretion, they may undergo tubular reabsorption in the distal tubules; the process can be active, but it is usually passive (Fan & de Lannoy, 2014; Gibaldi, 1984; Shargel & Yu, 1999). In this case, lipid-soluble drugs are favoured for transport through the membranes and are thus reabsorbed quite efficiently while compounds that are poorly lipid soluble or ionised are poorly reabsorbed (Gibaldi, 1984).

The reabsorption of compounds that are weak acids or bases relies on the pH of the fluid in the renal tubule as well as the drug's  $pK_a$ ; a non-ionised drug is more lipid soluble, has greater membrane permeability, and thus will be reabsorbed to a greater degree (Shargel & Yu, 1999). In reference to Figure 1.7, and the Henderson Hasslebalch equation shown in Equation (E.8), a drug's  $pK_a$  is constant, and the pH of its environment can significantly change, impacting its degree of ionisation (Shargel & Yu, 1999). Normal urinary pH varies from 4.5-8.0 (the average pH is 6.3), depending on factors of diet, drug intake, and disease state (Shargel & Yu, 1999). Infusion of intravenous fluids containing sodium bicarbonate produce alkaline urine, while fluids containing ammonium chloride produce acidic urine (Gibaldi, 1984; Shargel & Yu, 1999).

Generally, acidification of the urine stimulates reabsorption of weak acids, as a smaller proportion of these drugs are ionised (Figure 1.7) (Gibaldi, 1984). In contrast, a weak base experiences increased clearance in the acidic tubule fluid as a larger proportion is ionised and undergoes less reabsorption; an alkaline pH would promote its reabsorption back into the body (Gibaldi, 1984).

The contributions of the mentioned processes to renal clearance are expressed as:

$$CL_R = [f_{u,p} \times (GFR + CL_{R,sec})] \times [1 - F_R] + CL_{R,m}$$

(E. 47)

where GFR is the glomerular filtration rate,  $CL_{R,sec}$  is tubular secretion clearance,  $F_R$  is the fraction of filtered and secreted compound reabsorbed, and  $CL_{R,m}$  is the renal metabolic clearance (Fan & de Lannoy, 2014). As mentioned, for many drugs, renal metabolism is negligible.

### **Biliary Elimination**

If a drug is taken up by hepatocytes, it undergoes metabolism and/or biliary excretion, though biliary excretion is not a major route of elimination (Fan & de Lannoy, 2014). Generally, compounds with a MW greater than 500 Da are excreted in this manner (Fan & de Lannoy, 2014). While some drugs secreted by the hepatocytes are excreted in the feces, others are reabsorbed in the small intestines by a process referred to as enterohepatic recirculation (Gibaldi, 1984). The enterohepatic recirculation of a drug results in multiple peaks in the drug-plasma concentration profile, as well as prolongation of the half-life (Fan & de Lannoy, 2014). The cycle of biotransformation, renal, and biliary excretion may be continuously repeated until a drug is finally eliminated (Gibaldi, 1984).

### **1.1.5.3 Patient Factors Affecting Elimination**

#### **Disease**

Renal disease, liver disease, and any dysfunction of an eliminating organ has the potential to affect half-life, and therapeutic efficacy of a drug. Further, the complex interplay between ADME processes, such as plasma binding and clearance, profoundly impacts a drug's PK parameters. Glomerulonephritis commonly affects individuals with autoimmune diseases, and results in increased urinary protein excretion, hypoalbuminemia, and reduced kidney function (Joy, 2012). Chronic proteinuria has the potential to alter various independent PK parameters, including the  $C_{max}$ ,  $C_{SS}$ ,  $T_{max}$ ,  $k_{el}$ ,  $t_{1/2}$ ,  $V_D$ , and the AUC of a drug (Joy, 2012). Rosiglitazone, an oral peroxisome proliferator-activated receptor- $\gamma$  (PPAR- $\gamma$ ) agonist, was administered to 11 patients between the ages of 4-28 years with confirmed focal segmental glomerulosclerosis (FSGS) (Joy et al., 2009). The data were compared to a previously published rosiglitazone PK study conducted in healthy controls, and patients with stage 2 and stage 4/5 chronic kidney disease (CKD). It was found that the FSGS patients had increased CL/F (apparent oral clearance)

and decreased AUC compared to healthy subjects and patients at all stages of CKD (Joy et al., 2009). The factor responsible was the reduction in serum albumin associated with proteinuria, as rosiglitazone is highly (99%) bound to this protein; the effect resulted in an increased unbound fraction and thus enhanced clearance of the drug (Joy, 2012; Joy et al., 2009). The results of the study supported the clinical rationale that raising the dose of rosiglitazone in patients with FSGS moderately (4 mg/m<sup>2</sup>) will increase AUC and therapeutic efficacy without compromising patient safety (Joy et al., 2009).

### **Age**

As is the case with metabolism, pediatric and elderly patients deviate from the norm with respect to elimination processes. Though the ratio of kidney weight to total body weight in the newborn is double that of the adult, the organ is not completely functional at that point of development; the GFR in neonates is 30-40% of that in adults (Gibaldi, 1984). By 6 months, the GFR increases steadily, but tubular secretion lags the development of the GFR; usually, by 1 year of age, renal function is fully matured (Anderson, 2010). Thus, weight-normalised doses of drugs excreted unchanged in the kidneys must be adjusted for neonates and infants (Anderson, 2010).

The influence of aging on renal function has been thoroughly studied, and the consensus is that renal function declines with age; it was demonstrated that the GFR in men 80 to 90 years of age was approximately half of the GFR in men 20-30 years of age (Davies & Shock, 1950; Mayersohn, 1994). Expected decreases in drug elimination in the elderly would be reasonable assumptions because of renal function decline (Gibaldi, 1984). Intravenous administration of the same dose of digoxin in 5 men (aged 73-81) versus 9 men (aged 20-33) resulted in significantly higher (almost two-fold) drug-plasma concentrations in the elderly men (Ewy, Kapadia, Yao, Lullin & Marcus, 1969). In addition, the blood half-life of digoxin in elderly subjects was prolonged to 73 h versus 51 h in the younger subjects; as the kidneys are the major route of excretion for digoxin, reduced renal function was thought to be the cause (Ewy, Kapadia, Yao, Lullin &

Marcus, 1969). The elderly individuals were not free of disease, but none had evidence of heart failure or a history of renal disease.

### **1.1.6 ANALYSIS AND APPLICATION OF PHARMACOKINETICS DATA**

The estimation of PK parameters from plasma concentration-time profiles is accomplished with non-compartmental or compartmental approaches (Fan & de Lannoy, 2014). Though the compartmental method was historically entrenched as the 'standard method', non-compartmental methods developed and evolved as both alternatives and adjuncts to the compartmental models (Gillespie, 1991). Each approach carries its own set of advantages and disadvantages, and usually, the chosen method depends on what is required from the analysis, as both are relevant for clinical PK applications (Gabrielsson & Weiner, 2012; Gillespie, 1991).

In general, PK parameters are obtained from single dose drug studies, analysed using compartmental (or non-compartmental) approaches, and the PK parameters are applied into equations that predict the appropriate, dose, frequency, or rate of administration of drug required to achieve the optimal  $C_{SS}$  and maintain drug-plasma concentrations within the therapeutic window (Shargel & Yu, 1999). In the clinic, the drug's PK as well as various patient factors should be considered in designing the dosing regimen.

#### **1.1.6.1 Compartmental Method**

The compartmental method represents the body as a system of one or more compartments that usually have no physiological or anatomical meaning (Fan & de Lannoy, 2014). The approach relies on nonlinear regression analysis to fit an exponential equation to the data, while rate constants are used to describe the transfer of molecules between compartments (Fan & de Lannoy, 2014). The compartmental approach has been highlighted throughout this work in terms of the method of residuals, distribution, and elimination processes. Some final considerations with respect to the compartmental method are examined below, as they are relevant for the data presented in the Results section.

The plasma-concentration time profile of a one-compartment drug administered through IV is a visual expression of:

$$C(t) = C_{t0}e^{-kt}$$

**(E. 48)**

where  $V$  (L) is the volume of distribution,  $k$  ( $\text{min}^{-1}$  or  $\text{h}^{-1}$ ) is the first-order elimination constant, and the  $C_{t0}$  ( $\text{mg L}^{-1}$ ) is the drug concentration at time ( $t=0$ ) (Fan & de Lannoy, 2014). The resulting drug-plasma concentration time profile of Equation (E.48) is a single-phase exponential decay.

Drug-plasma concentration time profiles exhibiting multi-compartmental behaviour, such as two-compartment distribution kinetics, following IV administration, are expressed as a bi-exponential phase decay:

$$C(t) = Ae^{-\alpha t} + Be^{-\beta t}$$

**(E. 49)**

where  $A$ ,  $B$ ,  $\alpha$ , and  $\beta$  are the intercepts and values obtained either through Method of Residuals (Figure 1.14) or non-linear regression analysis done by computer software (Fan & de Lannoy, 2014). Drugs exhibiting more complicated distribution behaviours, may result in tri-exponential phase decline profiles, and addition of another component (ie.  $Ce^{-\gamma t}$ ) may indicate two distribution phases, or one distribution phase with two different elimination phases (Fan & de Lannoy, 2014).

The compartmental approach has a reputation for being descriptive, but the level of intricacy possible with compartmental methods can provide realistic modelling (Gabrielsson & Weiner, 2012). However, a limitation with this type of modelling is that data are fitted to a specific equation based on assumptions about the drug's behaviour. Logarithmic plots of data can reveal drug distribution characteristics – e.g. if the plot of data is linear, then the drug is assumed to exhibit one-compartment kinetic behaviour and Equation (E. 48) is implemented for further analysis (Fan & de Lannoy, 2014). However, data collection can introduce inaccuracies - as

discussed for  $V_{DSS}$ , sampling schedules may exclude vital data points, thereby causing incorrect assumptions about a drug's behaviour, influencing the resulting analysis.

### 1.1.6.2 Non-compartmental Method

The non-compartmental method is also termed 'model-independent' or 'system analysis', permitting the inclusion of methods such as disposition decomposition analysis (Gillespie, 1991). Because this method identifies or assumes relatively few properties of the system, it is readily automated (Fan & de Lannoy, 2014; Gabrielsson & Weiner, 2012). Rooted in the statistical moment theory, the non-compartmental method allows for PK data interpretation without the use of a specific compartment model (Jambhekar & Breen, 2009).

Statistical moment theory describes the movement of individual drug molecules through a body compartment as governed by probability, and the resident time of a drug molecule in the body regarded as a random statistical variable (Jambhekar & Breen, 2009). Essentially, the time course of plasma concentration following a single dose of drug is regarded as a statistical distribution curve (Yamaoka, Nakagawa & Uno, 1978). Applying the statistical moment theory, a function of time,  $f(t)$  has a series of statistical moments described as:

$$\int_0^{\infty} t^m f(t) dt$$

(E. 50)

where the exponent,  $m$ , is the moment being considered. In PK, generally two statistical moments are considered: when  $m = 0$ ,  $m = 1$ , as higher moments are prone to unacceptable level of computational error (Gabrielsson & Weiner, 2012; Jambhekar & Breen, 2009). Here, the zeroth and first moment of the drug concentration time curve are defined respectively as (Mayer & Brazzell, 1988):

$$\int_0^{\infty} t^0 f(t) dt = \int_0^{\infty} f(t) dt = AUC_0^{\infty}$$

(E. 51)

$$\int_0^{\infty} t^1 f(t) dt = \int_0^{\infty} t \times f(t) dt = AUMC$$

(E. 52)

Calculations of the 0<sup>th</sup> moment, or  $AUC_{0-\infty}$  (units: mg·min/L) involves the application of the trapezoidal rule for measurements of the area under the drug concentration *versus* time curve (Gabrielsson & Weiner, 2012). The trapezoidal rule divides the area under the curve into segments between each observed data point (in the shape of a trapezoid) (Jambhekar & Breen, 2009). Each area segment is summed and added to the area of the final segment to time infinity (Jambhekar & Breen, 2009):

$$\int_0^{\infty} f(t) dt = AUC_0^{\infty} = \sum \frac{C_{n-1} + C_n}{2} \times (t_n - t_{n-1}) + \frac{C_{tn}}{k}$$

(E. 53)

The value for  $C_{tn}$  is either the last measured concentration or values predicted from linear regression analysis (Fan & de Lannoy, 2014). The extrapolated segment to time infinity should be as small as possible in comparison to the total area; as a rule, the value should not exceed 15% of  $AUC_{0-\infty}$  (Fan & de Lannoy, 2014; Gabrielsson & Weiner, 2012). If the extrapolated segment of this profile is a substantial portion of the total area, large errors in the calculation may result (Mayer & Brazzell, 1988).

The  $AUC_{0-\infty}$  is one of the most basic parameters necessary for PK data analysis, even when an explicit compartmental analysis is applicable (Jambhekar & Breen, 2009; Mayer & Brazzell, 1988). For example, the value of  $AUC_{0-\infty}$  is divided by the IV administered dose (units: mg) to calculate a drug's total body clearance,  $CL_{Total}$  (units: mL/min or mL/min/kg):

$$CL_{Total} = \frac{Dose^{IV}}{AUC_{0-\infty}^{IV}}$$

(E. 54)

For drugs administered through extravascular routes, the equation is adapted as:

$$\frac{CL_{Total}}{F} = \frac{Dose}{AUC_{0-\infty}}$$

(E. 55)

where the Dose and AUC, in this case are values obtained from the specific route of administration, and the F may or may not be known (Fan & de Lannoy, 2014). (Equations (E. 54) and (E. 55) are mirrored in Equations (E. 12) and (E. 13) for First Pass Effect.)

The first moment of the plasma concentration time profile, AUMC, is also estimated by the trapezoidal approximation, but it examines the area under the curve of the product of time and concentration versus time (units: mg·min<sup>2</sup>/L) (Fan & de Lannoy, 2014; Mayer & Brazzell, 1988). Like AUC<sub>0-∞</sub>, AUMC<sub>0-∞</sub> is equal to the sum of each trapezoidal segment, and requires extrapolation from the last point to infinity with the equation described as:

$$AUMC_{C_{tn}-\infty} = \frac{C_{tn} \times t}{k} + \frac{C_{tn}}{k^2}$$

(E. 56)

AUMC, unlike AUC<sub>0-∞</sub>, is not widely applied for describing pharmacokinetic behaviour (Jambhekar & Breen, 2009). However, the ratio of the AUMC to AUC for any drug calculates mean residence time (MRT):

$$MRT = \frac{AUC_{0-\infty}}{AUMC_{0-\infty}}$$

(E. 57)

When a dose of drug is administered, some of the drug molecules are eliminated, while others still reside in the body (Jambhekar & Breen, 2009; Yamaoka, Nakagawa & Uno, 1978). Thus, only the overall properties of a large mass of drug molecules are observable (Yamaoka, Nakagawa & Uno, 1978). The MRT, therefore, is interpreted as the average time for a mass of intact drug molecules to travel through the body, or the time required to eliminate 63.2% of an intravenous dose (Mayer & Brazzell, 1988; Yamaoka, Nakagawa & Uno, 1978). In fact, it may be possible to determine urinary excretion data by monitoring the time required for 63.2% of the

drug to be excreted unchanged (Gibaldi, 1984). The concept of MRT (units: min) is likened to the concept of half-life, and is inversely related to the elimination rate constant (units: min<sup>-1</sup>) for a one-compartment model with an intravenous bolus injection as:

$$\text{MRT} = \frac{1}{k}$$

**(E. 58)**

Though Equation (E. 58) specifically applies to instantaneous, parenteral modes of drug administration (IV administration for a single compartment), data from non-instantaneous modes of drug administration can use MRT to describe drug behaviour (Mayer & Brazzell, 1988). A multi-compartment drug with complex function related to distribution and elimination is expressed in terms of MRT as:

$$\text{MRT} = \frac{1}{k'}$$

**(E. 59)**

where  $k'$  is equal to the ratio of  $CL_{\text{Total}}$  to  $V_{D\text{ SS}}$  (Gibaldi, 1984). In addition, MAT (mean absorption time) describes the time for a drug molecule to remain unabsorbed, and is calculated from:

$$\text{MAT} = \text{MRT}_{\text{NI}} - \text{MRT}_{\text{IV}}$$

**(E. 60)**

where  $\text{MRT}_{\text{IV}}$  is the MRT following intravenous administration and  $\text{MRT}_{\text{NI}}$  is the MRT following a non-instantaneous (extravascular) administration (Mayer & Brazzell, 1988). If absorption is a first-order process, then the MAT is communicated as:

$$\text{MAT} = \frac{1}{k_{\text{abs}}}$$

**(E. 61)**

Thus, the  $k_{\text{abs}}$  is calculated as the inverse of MAT, while the absorption  $t_{1/2}$  is calculated as  $0.693 \times \text{MAT}$  (Gibaldi, 1984). To note, a zero-order absorption process is communicated as:

$$\text{MAT} = \frac{T}{2}$$

(E. 62)

where T is the time for absorption or input to complete (Gibaldi, 1984). The same principle is applied to the mean dissolution time (MDT) of a solid dosage form through comparing the MAT between it and the drug in solution form (Mayer & Brazzell, 1988). Comparisons such as these are useful for different drug formulations and determining their absorption characteristics (Gibaldi, 1984).

Estimation of the  $V_{D\text{SS}}$  after IV administration through moment analysis is also possible:

$$V_{D\text{SS}} = \text{CL}_{\text{Total}} \times \text{MRT}_{\text{IV}}$$

(E. 63)

or

$$V_{D\text{SS}} = \frac{\text{Dose} \times \text{AUMC}}{\text{AUC}^2}$$

(E. 64)

The volume parameter in this case, is the proportionality constant between the dose of drug in the body and plasma concentrations at steady state (Fan & de Lannoy, 2014; Mayer & Brazzell, 1988).

There are limitations to analysing PK data with this theory. The relationships described above become more complex when a two-compartment model is necessary to fit the data, and it must be assumed that elimination occurs only from the central compartment (Mayer & Brazzell, 1988). In addition, sufficient plasma concentration data must be collected to construct appropriate curves, especially data from the absorption and elimination phases (Mayer & Brazzell, 1988). Errors when calculating AUC and AUMC are possible, leading to incorrect calculation of other parameters (Mayer & Brazzell, 1988). Absorption characteristics are difficult to determine statistically, and as such, absorption data from statistical moment theory analysis may not always be accurate (Mayer & Brazzell, 1988). Despite these limitations, the statistical moment theory

still has prominent relevance for understanding drug PK through the non-compartmental approach.

### 1.1.6.3 Chronic Dosing

A single dose of drug may rapidly produce a desired therapeutic effect, but if maintenance of this effect is desired, a single dose is not sufficient (Rowland & Tozer, 1986). Normally, drugs are prescribed to be taken at a fixed dose, and fixed time interval, or they are administered at a constant rate, either through IV administration, or a constant-rate release device placed at a variety of body sites (Rowland & Tozer, 1986).

The aim of chronic drug dosing is to achieve a steady state concentration ( $C_{SS}$ ), where the input rate is equal to the output rate, and normally associated with stabilisation of a patient on a given course of therapy (Gibaldi, 1984; Rowland & Tozer, 1986). For multiple dosing regimens, the  $C_{SS}$  is also expressed as the  $C_{Av}$ , though it is not the arithmetic mean of the  $C_{max}$  and  $C_{min}$ , because plasma concentrations decline exponentially (Shargel & Yu, 1999). Rather, the  $C_{Av}$  is obtained by dividing the AUC for a dosing period by the dosing interval,  $\tau$ , at steady state ( $C_{Av}$  cannot be measured directly) (Shargel & Yu, 1999). In contrast, for intravenous infusions, where drug reaches a plateau, the  $C_{SS}$  is measured and determined directly (Shargel & Yu, 1999).

By convention, the time required for a drug to reach steady state is dependent on its half-life; it takes one half-life to reach 50% of the  $C_{SS}$ , two half-lives to reach 75%, three half-lives to reach 87.5%, and by five half-lives, the levels are therapeutically considered to be close to the target  $C_{SS}$  (fraction=1;  $F_{SS}$ ), although true steady state-conditions after multiple dosing or intravenous infusion would occur at time infinity (Mehvar, 2008; Winter, 2010).

It is widely accepted that the time to reach a fraction of steady-state ( $F_{SS}$ ) that is close to, but not equal to 1 ( $T_{SS}$ ) in multiple dosing regimens is dependent on only the drug half-life and independent of the dosage interval (Rowland & Tozer, 1986; Shargel & Yu, 1999). However, Mehvar challenged this assumption with modelling; a hypothetical drug ( $t_{1/2} = 10$  hours) was administered at 1000, 500, and 250 mg via intravenous bolus every 24, 12, or 6 hours,

respectively (Mehvar, 2008). The data revealed that the  $\tau$  influenced the  $T_{SS}$  parameter, as the  $\tau$  of 24 hours achieved an  $F_{SS}$  of 0.96 at 24 hours ( $2.4 t_{1/2}$ ), while the same  $F_{SS}$  (0.96) was first achieved at 36 hours and 42 hours for the 12- or 6-hour regimens, respectively (Mehvar, 2008). Though longer dosing intervals potentially result in shorter  $T_{SS}$  values (and potentially increased patient compliance), the caveat is that they are associated with higher fluctuations in plasma levels (Mehvar, 2008). Regardless, consideration of the  $\tau$  as well as the  $t_{1/2}$  for dosing regimen design is useful for not only intravenous bolus, but also intermittent intravenous infusions or multiple oral dosing, as consideration of only the  $t_{1/2}$  may result in overestimation of the  $T_{SS}$ , causing unnecessary delays in the adjustment of dosage regimens (Mehvar, 2008).

### Continuous Intravenous Infusions

When the intent of therapy is to maintain a drug's plasma concentration or amount in the body for a long period, an intravenous infusion is used (Rowland & Tozer, 1986). The rate of change of the drug in the body is governed by the difference between the rate of drug infusion and elimination (Rowland & Tozer, 1986). When the infusion starts, the amount of drug in the body is zero, but through continuous administration, the drug concentration eventually reaches the  $C_{SS}$ , or plateau, remaining stable if the infusion is maintained (Rowland & Tozer, 1986). Because the drug is given constantly, it is a zero-order input process, and the drug reaches the systemic circulation immediately (Shargel & Yu, 1999). In one-compartment modelling, the change in the amount of drug in the body at any time is the rate of input minus the rate of output:

$$\frac{dD_B}{dt} = R - k_{el}D_B \tag{E. 65}$$

where  $R$  is the infusion rate,  $k_{el}$  is the drug elimination rate constant, and the  $D_B$  is the amount of drug in the body (Shargel & Yu, 1999). The plasma concentration of drug is calculated as:

$$C_p = \frac{R}{V_D \times k_{el}} (1 - e^{-kt}) \tag{E. 66}$$

where  $V_D$  is the volume of distribution (L),  $k_{el}$  ( $\text{min}^{-1}$  or  $\text{h}^{-1}$ ) is the elimination rate constant, and  $R$  is the infusion rate (zero-order). Drug elimination still occurs in a first-order reaction rate, and as such, the drug concentration declines in a mono-phasic manner. Regardless of when the infusion rate is stopped (before or during steady state), the slope of the elimination curve will remain the same (Shargel & Yu, 1999).

As infusion of a drug continues,  $t$  increases in Equation (E. 66), and at infinite time (at  $C_{SS}$ ),  $e^{-k_{el}t}$  approaches zero, reducing the equation to:

$$C_p = \frac{R}{V_D \times k_{el}} (1 - e^{-k_{el}t}) = \frac{R}{V_D \times k_{el}} \times 1$$

$$C_{SS} = \frac{R}{V_D \times k_{el}} = \frac{R}{CL_{Total}}$$

(E. 67)

The  $T_{SS}$  depends on the elimination rate constant of the drug, and if the input rate is greater than output (likely with saturation of metabolism), then plasma drug concentration will continue to increase without a plateau; a potentially dangerous situation (Shargel & Yu, 1999). In most cases, the rate of elimination is concentration dependent, and as such, the time to reach  $C_{SS}$  is directly related to elimination half-life (Shargel & Yu, 1999). To note, increasing infusion rate does not reduce the  $T_{SS}$ , but results in an increase in  $C_{SS}$  while  $T_{SS}$  remains the same (Shargel & Yu, 1999).

### Multiple Dosing Regimens

Multiple dosing regimens include several routes and types of administration, including **intravenous injections/bolus**, **intermittent intravenous infusion**, and **oral administration** (Shargel & Yu, 1999). Intermittent IV Infusion consists of short, successive infusions of drug, accompanied by ongoing elimination (Shargel & Yu, 1999). Though the drug may not reach steady state, the rationale for intermittent IV infusion is to reduce transiently high drug concentrations and risk of side effects, which are more common with IV bolus dosing (Shargel & Yu, 1999).

If a drug is administered at a fixed dose and fixed-dosage interval, the amount of drug in the body will increase and eventually plateau, usually at a mean level higher than the  $C_{max}$  achieved after the first dose (Shargel & Yu, 1999). The plasma levels of drugs are maintained within limits to achieve maximal effectiveness without excessive fluctuation or drug accumulation (Shargel & Yu, 1999). As fluctuation is dependent on absorption rate, administration of drug via intravenous bolus results in the greatest fluctuations as this route of administration lacks an appreciable absorption phase (Rowland & Tozer, 1986). Large fluctuations between the  $C_{max}$  and  $C_{min}$  are not ideal for drugs with narrow therapeutic indexes, and as such, a strategy to reduce fluctuations is to employ greater frequency of administration with smaller doses (Rowland & Tozer, 1986; Shargel & Yu, 1999).

Designing dosing regimens for drugs intended for chronic use is largely dependent on two factors: the size of the drug dose, and the frequency of drug administration ( $\tau$ ) (Shargel & Yu, 1999). The  $C_{Av}$  is used most often in dosage calculations, as it does not fluctuate as dramatically as  $C_{max}$  or  $C_{min}$  (Shargel & Yu, 1999). For drugs with a wide therapeutic index, changing a dose and proportionally changing its frequency will maintain  $C_{Av}$  levels without risking potentially sub-therapeutic or toxic levels (Shargel & Yu, 1999). However, even slight changes to the dosing regimen for a drug with a narrow therapeutic index may affect the  $C_{max}$  and  $C_{min}$  sufficiently to pose risk to the patient (Shargel & Yu, 1999). For repeated intravenous injections, the dosing time interval is determined by:

$$\frac{C_{max}}{C_{min}} = \frac{1}{e^{-kt}}$$

(E. 68)

A longer dosing time interval should be offset by administering a larger dose, while a smaller dose would offset shorter time intervals. The PK parameters of the drug determine the appropriate dosing interval; once an appropriate dosing interval is selected, the dose of drug is calculated accordingly.

In multi-oral dosing (and for any route of administration, including repeated intravenous injections), the simplest approach in developing dosing regimens, or predicting the  $C_{SS}$  (or  $C_{Av}$ ) from a dosing regimen is:

$$C_{SS} = \frac{F \times D}{V_D \times k_{el} \times \tau} \quad (\text{E. 69})$$

where  $F$  is the bioavailability,  $D$  (mg) is the dose administered in each successive cycle (maintenance dose, MD; mg),  $V_D$  is the calculated volume of distribution (L),  $k_{el}$  is the elimination rate constant ( $\text{min}^{-1}$ ), and  $\tau$  is the time interval (min or h) (Shargel & Yu, 1999). Predictably, the  $C_{SS}$  will be higher for drugs possessing a small  $V_D$  or longer elimination half-lives than their counterparts administered at the same dose and with similar bioavailability (Shargel & Yu, 1999). The value of clearance is determined by  $V_D \times k_{el}$ , and Equation (E. 70) is rearranged as:

$$C_{SS} = \frac{F \times D}{CL_{Total} \times \tau} \quad (\text{E. 70})$$

A decrease in  $CL_{Total}$ , evidently, would result in an increase in the  $C_{SS}$  (Shargel & Yu, 1999). To determine drug concentration after one or more intermittent IV infusions, Equation (E. 66) is adapted as:

$$C_p = \frac{D}{t_{inf} \times V_D \times k_{el}} (1 - e^{-kt}) \quad (\text{E. 71})$$

where  $D/t_{inf} = R$  (rate of infusion), where  $D$  is the size of infusion dose and  $t_{inf}$  is the infusion period (Shargel & Yu, 1999). When the infusion stops, the drug concentration post-intermittent infusion is determined through first-order equations:

$$C_p = C_{Stop} e^{-kt} \quad (\text{E. 72})$$

where  $C_{\text{stop}}$  is the concentration when the infusion stopped, and  $t$  is the time elapsed since the infusion was stopped (Shargel & Yu, 1999).

### **Loading Dose**

In some cases, it is therapeutically desirable to establish the required plasma levels as early as possible, at which point, a loading dose is administered (Rowland & Tozer, 1986). This initial dose rapidly achieves the therapeutic response, while subsequent doses maintain the response by replacing drug lost during the dosing interval (Rowland, Benet & Graham, 1973). The loading dose is calculated by:

$$\text{Loading Dose} = \frac{V_D \times C_{SS}}{F}$$

**(E. 73)**

where  $V_D$  is the volume of distribution (L),  $C_{SS}$  is the desired plasma level ( $\text{mg L}^{-1}$ ), and  $F$  is the bioavailability (Winter, 2010). The calculation is implemented for rapid achievement of a drug administered through many routes of administration, including continuous intravenous infusion (Shargel & Yu, 1999).

Evidently, changes in PK parameters, such as a drug's half-life or volume of distribution are influenced by a variety of physiological and patient factors. The changes associated with pathologies, genetics, and environmental factors profoundly impact the design of dosing regimens and therapeutics. Understanding the intricacies of these complex relationships is a priority.

## **1.2 PRESCRIBING ERRORS**

### **1.2.1 DEFINITIONS, RISKS, AND IMPACTS**

Prescribing is a process: a diagnosis is accurately made, a therapeutic goal is established, a drug which is appropriate for the pathophysiology of the disease is selected, the drug's benefit-harm components are considered, the drug's PK parameters are considered, patient factors are

considered, the drug's dose, route, frequency and duration is considered, a dosing regimen is created, and finally, the decision, including its benefits, adverse events, and monitoring are communicated to the patient (Aronson, Henderson, Webb & Rawlins, 2006; Ross & Maxwell, 2012). The process requires an extremely thorough understanding of the pathophysiology of the problem, and the characteristics of the drug, including its pharmacokinetic properties (Aronson, Henderson, Webb & Rawlins, 2006). The task of prescribing is formidable, and unfortunately, the practice is becoming increasingly difficult; drugs are more pharmacologically complex, the population is aging, and polypharmacy is steadily increasing (Aronson, Henderson, Webb & Rawlins, 2006).

Drugs are the most commonly used clinical intervention, yet errors involving prescribing, dispensing, and administration are common (Ashcroft et al., 2015). Prescribing errors, the most frequent subtype of medication errors, affect 2% of patient days, 7% of medication orders, and remarkably, 50% of hospital admissions (Lewis, Dornan, Taylor, Tully, Wass & Ashcroft, 2009). The percentage of prescribing errors ranges from 29-56% of medication errors in adults, while these values are found to be higher in children (68-75%) (Alanazi, Tully & Lewis, 2016). Generally, the causes of prescribing errors are categorised as prescribing mistakes (knowledge-based and rule-based mistakes), or slips and lapses (Alanazi, Tully & Lewis, 2016). However, in the literature, there is considerable variation in classifying prescribing errors, and the definitions range from: if both the doctor and pharmacist agree on the error, if the error caused harm to the patient, if the prescription was inappropriate to the patient, or if the drug dose, dosage form, quantity, route, concentration, and/or rate of administration was incorrect (Lewis, Dornan, Taylor, Tully, Wass & Ashcroft, 2009). In addition, some studies are process-based, meaning that they do not measure harm, as the error is detected prior to any harm being caused, while outcome-based studies measure actual patient harm by reporting adverse drug events (ADEs) (Lewis, Dornan, Taylor, Tully, Wass & Ashcroft, 2009). As such, there is a wide range of the prevalence of prescribing errors, which causes some difficulty in interpreting the data conclusively.

Adverse drug events can result from prescribing errors, and various reports demonstrate the costly and devastating impacts of these events. In 1997, in the US, it was estimated that in one large tertiary care hospital, the annual costs attributed to preventable ADEs was \$2.8 million; if extrapolation of these results is appropriate, that would equate to approximately \$2 billion for the nation as a whole (Bates et al., 1997; Institute of Medicine (US), 2000). Such errors increase the cost of patient care due to increasing length of stay in the hospital and increases in pharmacy and laboratory costs (Bates et al., 1997; Classen, Pestotnik, Evans, Lloyd & Burke, 1997). They are also an opportunity cost; more money, is spent on repeat diagnostic testing, insurance costs and inflated co-payments (Institute of Medicine (US), 2000). The most alarming element of ADEs is not the cost, however, but that they are associated with an almost 2-fold increase in patient mortality (Classen, Pestotnik, Evans, Lloyd & Burke, 1997). As well, they are associated with a loss of trust and diminished satisfaction in the system by patients, and loss of morale and frustration for the health care providers; costs to which a dollar value can not be assigned (Institute of Medicine (US), 2000).

Many government agencies developed prescribing guidelines, and other bodies have responded by creating computerised reminders to reduce inappropriate prescribing for physicians (Aronson, 2006). Yet, the main concern is that guidelines are ineffective unless they are accompanied by either education, or financial incentives, while computerised programs contribute to “alert fatigue” and have not been shown to be hugely effective in reducing inappropriate prescribing (Aronson, 2006). In fact, the theme clear from the evidence collected from these strategies is that improving prescribing relies on enhancing education of health care providers (Aronson, 2006).

### **1.2.2 PREVALENCE AND CAUSES**

People err, and half of all prescription errors are preventable, though there are numerous root causes – from the working environment, and miscommunications, to a prescriber’s inadequate training, management, and knowledge of pharmacotherapy (Dean, Schachter, Vincent & Barber, 2002a; Keijsers, Segers, de Wildt, Brouwers, Keijsers & Jansen, 2015; Lesar, Lomaestro

& Pohl, 1997). Regardless of cause, errors likely go unrecognised by prescribers primarily because of the lack of knowledge required to recognise an order as inappropriate or capable of harming a patient (Lesar, Lomaestro & Pohl, 1997). Fundamental knowledge deficits typically underlie the more immediate causes of human error, especially when hospitals conduct internal quality investigations as to “why” an error occurred (Lehmann, 2011).

In a large prospective study in 20 National Health Trust hospitals over 7-day periods in the UK, prescribing errors occurred in 8.8% of newly prescribed medication orders (Ashcroft et al., 2015). Interestingly, doctors at all stages made prescribing errors, but foundation year 1 (FY1) and FY2 doctors were more than twice as likely to make prescribing errors in comparison to more senior personnel (Ashcroft et al., 2015). Over half of the errors found in the study were significant or had the potential to cause patient harm, with 7.3% of these errors rated as potentially life threatening; of these, the errors were more likely to occur during a patient’s hospital stay, and when patients were prescribed drugs to be administered parenterally (Ashcroft et al., 2015). In addition to environmental conditions, one of the main observations was that FY1 doctors lacked contextual knowledge and had difficulty framing the clinical problems (Ashcroft et al., 2015).

Lesar and colleagues conducted some of the earlier studies on physicians' prescribing errors, noting that in one year at a New York state teaching hospital, there were 905 prescription errors detected and averted from a total of 289411 medication orders, of which 58% had the potential to cause an adverse event (Lesar, Briceland, Delcours, Parmalee, Masta-Gornic & Pohl, 1990). First-year residents had higher error rates (4.25 per 1000 orders), and interestingly, the greatest error rates occurred between 12pm and 3:59 pm (Lesar, Briceland, Delcours, Parmalee, Masta-Gornic & Pohl, 1990). Lesar also published a 9-year study (1987-1995) based at the same hospital, noting 11,186 medication-prescribing errors, with a significant increase in error rates per medication order written, per hospital admission, and per patient-days provided in the later years (Lesar, Lomaestro & Pohl, 1997). Of these, dosing errors (overdoses and under-doses) constituted 56.1%, and inappropriate dosage forms made up 11.2% and demonstrated the greatest and most consistent increase in rates over the years (from 3.6% of errors in 1987 to 12% in 1993) (Lesar, Lomaestro & Pohl, 1997). There was a clear correlation between the

increase in dosage form errors and the rapid proliferation of sustained release dosage forms of cardiovascular agents after 1987 (Lesar, Lomaestro & Pohl, 1997).

Sustained release formulations improve an agent's bioavailability, patient compliance, or other features (Lesar, 2002). However, the availability of multiple dosage formulations, lack of prescribers' appreciation for the features and uses of these preparations, and the high potential for adverse events if the agents are used inappropriately, create conditions that can seriously injure patients (Lesar, 2002). Further study by Lesar *et al.* found that in a 16-month period between 1999 and 2000, the most common types of errors detected in the hospital were failures to specify controlled release formulations (69.7% of errors) (Lesar, 2002). In addition, they noted many different types of dosage form prescribing errors, including instances where controlled delivery formulations were prescribed at the wrong frequency, prescribers were unaware of bioavailability differences between formulations, or the route of administration was not appropriate for the drug formulation (Lesar, 2002). Evidently, lack of knowledge concerning many of the concepts associated with PK are contributing to prescribing errors and outcomes.

Dean *et al.* conducted a study in a UK teaching hospital over a 4-week period, where, of 36200 medication orders, 1.5% were identified as prescription errors, with 0.4% recorded as potentially serious (Dean, Schachter, Vincent & Barber, 2002b). Most of the errors occurred because of the wrong choice of dose (54%), and over a third were written by junior house officers (Dean, Schachter, Vincent & Barber, 2002b). Dean *et al.* conducted an additional study in the same year to explore the root causes of errors through more in-depth study approaches: interviewing prescribers within 96 h of their error (Dean, Schachter, Vincent & Barber, 2002a). Though there were many error-producing conditions, a surprising conclusion was that doctors would correctly prescribe the drug's name, but failed to adequately note the details of dose, form, frequency, route, duration, etc., leaving the responsibility to someone else (Dean, Schachter, Vincent & Barber, 2002a). In line with his previous study where over 50% of prescription errors were a result of inappropriate dosing, it can be inferred that dosing of drugs is not explicitly taught in medical school, but rather "acquired" during employment (Dean, Schachter, Vincent & Barber, 2002a). A direct quote:

“We get told about the drugs, the side effects, we learn, um, we don’t use the brand names, um, we use the original, proper names, and we learn a lot about side effects. We don’t learn about doses at medical school, how much to give, what frequency to give it at, that’s not taught, it’s something you pick up really in your first few weeks as a house officer” (Dean, Schachter, Vincent & Barber, 2002a).

Winterstein *et al.* reported similar themes in cause of error for a 12-week period in 2002 in a major university-affiliated tertiary care hospital which highlighted both outcome and process-based errors. Of 6000 patients admitted during the study, 240 medication errors were detected (a rate of 4%) (Winterstein, Johns, Rosenberg, Hatton, Gonzalez-Rothi & Kanjanarat, 2004). Of these errors, 95 manifested and caused patient harm, while 51 were averted (the other 94 did not manifest, though they were administered) (Winterstein, Johns, Rosenberg, Hatton, Gonzalez-Rothi & Kanjanarat, 2004). Of all 240 errors reported, overdoses were most frequent, at 29.2%, followed by under-doses at 19.6% (Winterstein, Johns, Rosenberg, Hatton, Gonzalez-Rothi & Kanjanarat, 2004). Of the 95 manifested errors, dosage errors were the principal type of drug-related problem, as 57% occurred because no, too little, or an ineffective drug was prescribed (Winterstein, Johns, Rosenberg, Hatton, Gonzalez-Rothi & Kanjanarat, 2004). Errors initiated at the prescribing step were most often attributable to knowledge deficits in dosing (38.3%), failure to consider lab test values (18.3%), knowledge deficits in drug selection (12.6%), and performance deficits (10.8%) (Winterstein, Johns, Rosenberg, Hatton, Gonzalez-Rothi & Kanjanarat, 2004).

A decade later, in eight Scottish hospitals, data on prescribing errors were collected over a 14-month period, and interviews were conducted with 40 FY1 and FY2 doctors about 100 specific errors 96 h after the prescription was written (Ross *et al.*, 2013). While the work and team environment were noted as the causes, the most frequent individual factor was lack of personal knowledge and experience, with patient complexity as the most frequently stated patient factor (Ross *et al.*, 2013).

A systematic review was conducted on the prevalence of prescribing errors in high risk medications (HRMs), which include drugs in the class of anticoagulants, injectable sedatives, opiates, insulin, antibiotics, chemotherapy, antipsychotics, and infusion fluids (Alanazi, Tully & Lewis, 2016). The general assumption was that HRMs would have a lower rate of error occurrence due to medication safety organisations and increased awareness of the risks, in addition to increased caution due to clinician's knowledge of the catastrophic consequences (Alanazi, Tully & Lewis, 2016). The main results illustrated that medication errors ranged from 0.24 to 89.6 errors per 100 orders of HRMs, though the cause was not immediately determined. In more than half of the studies evaluated (5/9), errors involving opioids were identified (Alanazi, Tully & Lewis, 2016).

Death from opioids, including hydromorphone through parenteral administration, is a result of errors in drug dosing, frequency, DDIs, and inattention to patient factors that predispose to drug toxicity (Lehmann, 2011). Lehmann, upon discussing five patient deaths due to opioid overdoses, notes that "had the fundamental principles of clinical pharmacology been properly understood, it is likely that these therapeutic misadventures would have been averted." Indeed, the clinical case studies reflect on clinicians' and prescribers' lack of understanding of the drugs' characteristics, misunderstanding of the dosing frequency, knowledge deficits concerning drug accumulation and dose, and failure to appreciate drug-drug interaction potential (Lehmann, 2011).

The knowledge deficit theme in prescribing errors spans decades, and borders, and evidently relates to the common lack of PK understanding within healthcare curricula throughout the world. Thus, more comprehensive pharmacology and therapeutics education is necessary for health care providers to appropriately consider the role, therapeutic value, and potential risks of the drugs they administer on a regular basis (Lesar, 2002).

## 1.3 PHARMACOKINETICS IN THE CLASSROOM

### 1.3.1 INADEQUATE TRAINING AND EDUCATION

From as early as the 1960s, it was noted that medical students and hospital staff are not adequately trained in the principles of pharmacology and therapeutics (Brater & Nierenberg, 1988). Despite numerous pharmacological societies raising concerns about these deficiencies, the Association for Medical School Pharmacology (AMSP) in the 1980s still found that most institutions had a deficiency in pharmacology education (only 14% of medical schools offered a course in clinical pharmacology) (Brater & Nierenberg, 1988). Almost forty years later, the profession is dealing with the same concerns – in a position paper “A Dangerous Lack of Pharmacology Education in Medical and Nursing Schools”, Peter Wiernik discussed his findings after reaching out to 50 medical schools in the US concerning pharmacology education (Wiernik, 2015). Of 39 respondents, 35 revealed there was a decrease in formal pharmacology training over recent years, as pressures to make the preclinical curriculum more “clinical” had disregarded basic pharmacological principles relevant to therapeutics (Wiernik, 2015). In fact, BBC News reported that in the UK, since the early 1990s, the reduction in clinical pharmacology and therapeutics teaching in the undergraduate medical curricula has contributed to a 500% increase in patient deaths due to adverse drug events (news article: <http://news.bbc.co.uk/2/hi/health/5192372.stm>).

A thorough PK knowledge base is vital for understanding drug toxicities and adverse reactions to drugs, and the subject matter is applicable to a diverse student population, including graduate, allied health-related sciences, dental, and medical students (Swanson, Piscik & Swanson, 2014). However, most health care students learn generalised PK knowledge without proper context, which hinders their ability to identify and handle complex medical treatments, make qualified judgments, and effectively communicate them to patients (Aronsson et al., 2015). The fundamentals of PK and therapeutics are too important for individuals to learn “on the job”, and providing sufficient background in the subject matter should be a priority (Wiernik,

2015). While each subset of healthcare personnel may have a different role and skillset within patient care, there are requirements for each specialty to master relevant aspects of drug treatments (Aronsson et al., 2015). In addition, the healthcare team must collaborate and complement one another's knowledge base to provide optimal care (Keijsers et al., 2014).

Traditionally, PK is taught following a didactic, lecture-based teaching format, in which the instructor defines, controls and directs the classroom (Schneider, Munro & Krishnan, 2014). In this format, students are not encouraged to develop the skills to gather, analyse or synthesise information, which can affect their ability to evaluate the logic of questions and problems (Schneider, Munro & Krishnan, 2014). Usually, students are presented with a bewildering array of equations, terms, and graphs in didactic lectures, and while practice problems are provided, the conceptual understanding of the relationships may not be clear when taught through just this one mode of instruction (Bolger, 1995). As PK is associated with mathematical relationships, a lack of immediate application can fail to provide students with the relevance of the information received, hindering their overall understanding of the subject matter (Schneider, Munro & Krishnan, 2014). Furthermore, the numerous and oftentimes tedious mathematics calculations may hinder the student from understanding the relationships between PK parameters – one that is clear is the often-misunderstood relationship between volume of distribution and clearance (Li, Wong & Chan, 1995; Mehvar, 2006).

Because each health profession contributes differently to patient care, it is expected that the extent of training of different student populations, such as pharmacy or medical students, will be different. For instance, at the University of Utrecht, in the Netherlands, pharmacy students attend 197 hours of mandatory pharmacology and pharmacotherapy training while medical students only have 35 mandatory hours of training (Keijsers et al., 2014). To test knowledge deficits between the two cohorts, Keijsers *et al.* distributed a validated test on basic and applied pharmacotherapy to the medical and pharmacy students, with results showing pharmacy students outperforming medical students on basic pharmacology knowledge (with a 9% lead on pharmacokinetics questions), while medical students outperformed pharmacy students on prescription writing (Keijsers et al., 2014). Interestingly, both cohorts performed similarly on

questions regarding applied pharmacology, suggesting that there is overlap in knowledge understanding for the two cohorts (Keijzers et al., 2014).

At two universities in Sweden, twelve students in their final semester of medical school, nursing school, and the specialist nursing program were encouraged to solve and discuss clinical cases involving pharmacodynamics and pharmacokinetics concepts (Aronsson et al., 2015). Results indicated that while the students could define the concepts, they could not engage in depth or apply concepts correctly to a clinical context – pharmacokinetics was especially difficult (Aronsson et al., 2015). A direct quote:

*“Half-life? Well, that’s tricky. I don’t know if I remember exactly what sort of stuff that is, ‘cause I failed that topic on the exam last time...” (Aronsson et al., 2015).*

Despite the small sample size, the qualitative aspect of the data illustrates that applied knowledge of pharmacology or PK is not necessary for people to complete the training for a profession responsible for drug administration successfully. More tragically, the formal education of health care professionals concerning the properties, availability, and appropriate administration of medications is clearly inadequate, leading to errors that compromise patient safety (Lesar, 2002).

Tobaiqy et al. issued a questionnaire to 90 FY1 doctors in the Grampian health region, in Scotland, on their clinical pharmacology and therapeutics (CPT) training. Of the 64 that replied, 77% had received undergraduate training in CPT, but only 8% rated their knowledge as “good” – 30% rated it as poor or very poor, while the remainder deemed it as “average’ (Tobaiqy, McLay & Ross, 2007). When asked to rate their confidence in prescribing to special patient groups, 58% of respondents felt confident with the elderly (Tobaiqy, McLay & Ross, 2007). Unfortunately, for other special groups, the numbers were not as promising: 81%, 75%, 73%, and 73% did not feel confident prescribing to pregnant women, children, patients with renal diseases, and patients with liver diseases, respectively (Tobaiqy, McLay & Ross, 2007). In addition, almost 75% of respondents said that their undergraduate teaching on drug

metabolism and clearance was insufficient to build their confidence in prescribing to these groups of patients (Tobaiqy, McLay & Ross, 2007). Generally, respondents felt that practical tutorial-based teaching in CPT using scenarios and real-life examples would improve their prescribing abilities, and that more extensive undergraduate training was required in pharmacokinetics, therapeutic drug monitoring, drug-drug interactions, and patients with special requirements (Tobaiqy, McLay & Ross, 2007).

Currently, the only validated pharmacology and pharmacotherapy education tool is the 6-step method of the World Health Organisation (WHO-6-step), which aims to improve the thinking process associated with prescribing (Keijsers, Segers, de Wildt, Brouwers, Keijsers & Jansen, 2015). Keijsers *et al.* implemented the WHO-6-step method into their medical school curriculum (for both Bachelor and Masters students) as an integrated, longitudinal learning program in pharmacology and pharmacotherapy to increase the patient context of education (Keijsers, Segers, de Wildt, Brouwers, Keijsers & Jansen, 2015). Through formative standardised assessment, they gauged student improvements in the following domains: basic pharmacology, applied pharmacology, and pharmacotherapy skills. Overall, it was shown that in comparison to earlier cohorts who did not receive the intervention, the WHO-6-step learning program was effective in improving pharmacology knowledge and pharmacotherapy skills for both Bachelor and Master medical students (Keijsers, Segers, de Wildt, Brouwers, Keijsers & Jansen, 2015). However, the intervention failed to inspire recognition of the importance of the subject matter, or to further students' interest in the area. In addition, Masters students who experienced the WHO-6-step intervention performed better than their non-intervention counterparts despite similar hours of instruction. In contrast, Bachelor students who underwent the WHO-6-step intervention had a 4-fold increase in instruction hours vs their non-intervention counterparts, and thus their improved performance may be a result of the increased instruction time (Keijsers, Segers, de Wildt, Brouwers, Keijsers & Jansen, 2015). Regardless, other strategies need to be adopted in order to provide quality education to future health care professionals. Pharmacological knowledge, specifically an in-depth understanding of pharmacokinetics and

pharmacodynamics, will promote long-term health, safety, ethics, and health economics (Aronsson et al., 2015).

## **1.3.2 PRACTICES AND INNOVATIONS FOR PK INSTRUCTION**

### **1.3.2.1 Teaching in the Pharmacy Curriculum**

Pharmacokinetics is an essential component of the pharmacy curriculum as it relates the drug concentration *versus* time relationship to the drug dose, and its relationship to efficacy and potential toxicity (Brocks, 2015). In application, this understanding allows for establishing dosing rates and intervals, designing individualised dosing regimens, recovering patient-specific parameters, and applying PK concepts in lieu of, or using mathematical calculations (Brocks, 2015; Persky, 2012). Teaching PK requires balancing the physiological variables affecting drug movement and the mathematical relationships which dictate this. Overemphasis on the mathematics may deter students from recognising the physiological considerations and their importance in clinical drug use, while under-emphasis may fail to develop students who are adept in using the tools of PK to successfully implement dosing regimens (Brocks, 2015).

Pharmacy students must acquire sufficient knowledge and skill in PK to make appropriate drug dosing decisions in the community or hospital setting (Persky, Stegall-Zanation & Dupuis, 2007). As such, the classroom must provide an experience that allows them to develop problem-solving and critical thinking related to PK principles (Persky, Stegall-Zanation & Dupuis, 2007). Unfortunately, many students do not enjoy PK coursework, either due to the mathematics involved, or to an inability to connect the physiological concepts to their education (Persky & Pollack, 2009). It is not surprising, then, that multiple reports have noted that pharmacy students (and even practicing pharmacists) often find it difficult to apply PK concepts learned in the classroom to patient care (Brackett & Reuning, 1999; Brocks, 2015; Edginton & Holbrook, 2010; Persky & Pollack, 2009).

Learning encompasses both “retention” – the ability to use information for a period after learning, and “transfer” – the ability to use information in a slightly different context than the

original learning (Persky & Dupuis, 2014). Thus, Brackett *et al.* suggest that the limitation in learning PK is a lack of clinical context in the classroom, with students failing to develop the ability to solve problems in a bidirectional fashion: working back from an observed adverse event to the relevant PK principles to solve the problem, and working from the principles to reason out a dosing regimen (Brackett & Reuning, 1999).

Reports have supported the idea that students must participate in meaningful activities during class time to ensure they are not just passively receiving information (Lucas, Testman, Hoyland, Kimble & Euler, 2013). The term “active learning” represents a shift in the teaching paradigm, as activities throughout a lecture stimulate higher-order thinking in students, and motivates them to take responsibility for their education (Lucas, Testman, Hoyland, Kimble & Euler, 2013). The following will discuss innovative pharmacy curriculum approaches to teaching PK, including the use of active learning techniques, technology, computer simulations, and flipped classrooms. The variety of approaches brings attention to the fact that there is a real need for improving how PK concepts are taught, not only to our future pharmacists, but to other health care professionals.

### **Active Learning Techniques**

Didactic lecturing has been around since universities were founded over 900 years ago, and it continues to be the predominant mode of instruction for all subjects, including PK (Freeman *et al.*, 2014). Lectures have a purpose; the instructor, through this mode, can transmit new information, explain or clarify concepts, organise and even challenge ideas, model problem solving, and motivate students (Steinert & Snell, 1999). However, there are emerging theories challenging this traditional, “instructor-focused”, “teaching-by-telling” approach, as attention-span studies have shown a significant reduction in attention to traditional lectures after 20-30 minutes of instruction, and other studies show that students only recall about 25% of the material presented in a lecture three hours after the end of the lecture (Collins, 2008; Collins, 2007; Freeman *et al.*, 2014). To alleviate these issues, instructors are changing their teaching style to incorporate “active learning”, defined as “any instructional method that engages

students in the learning process” (Swanson, Piscik & Swanson, 2014). Essentially, active learning encompasses various methodologies: engaging lectures with short periods of breaks, small group activities, peer instruction, and formative assessments (Miller, McNear & Metz, 2013).

A recent meta-analysis compared the results of 225 studies that documented student performance in traditional science, technology, engineering, and mathematics (STEM) courses with courses that incorporated some type of active learning technique: it was shown, that on average, student performance increased by just under half a standard deviation with some active learning compared with just lecturing, and that on average, students in traditional courses were 1.5 times more likely to fail than students in courses with active learning (Freeman et al., 2014). In a physiology course for DMD students, engaging lectures lead to statistically significant higher averages on unit exams compared to traditional didactic lectures (8.6% higher), and even translated into longer retention of information as evidenced by higher scores on comprehensive final exams (22.9% higher in engaging lectures vs. traditional) (Miller, McNear & Metz, 2013).

Notably, instructors at the University of North Carolina at Chapel Hill have taken great efforts to expand their teaching strategies to include active learning in two courses: Foundational Pharmacokinetics and Applied Pharmacokinetics for their PharmD cohorts. First, the instructors implemented several games that served to provide an overall semester review, applications of PK in the community setting, and the development of critical thinking skills (Persky, Stegall-Zanation & Dupuis, 2007). While student exam scores did not significantly change in the Foundations course, instructors did note performance improvements of this cohort in the Applied PK course (Persky, Stegall-Zanation & Dupuis, 2007). The majority of students felt the games were effective as supplements to lectures (Persky, Stegall-Zanation & Dupuis, 2007). Additional innovations included the concept of the “jigsaw strategy” to teach renal concepts, where each student in a group learns about a particular part of a case study on their own and then communicates the concepts to their group members as the “expert” (Persky & Pollack, 2009). While the students were able to learn the concepts to the same degree as historical cohorts, the time commitment resulted in less favourable attitudes about the innovation (Persky

& Pollack, 2009). Other innovations included team-based learning (TBL) for patient cases where students met in small groups with a preceptor, solved cases and discussed any discrepancies with the whole class (Persky, 2012). Overall, the observation was that students obtained greater mastery of content as evidenced through exam scores, and could develop stronger critical thinking and communication skills through the activity (Persky, 2012). Similarly, the introduction of case-based learning for small group discussion also translated into enhanced learning of the application of PK in a clinical context (Dupuis & Persky, 2008). By incorporating a variety of different activities and gauging student performance and attitude, this group has demonstrated how active learning, particularly for PK, can benefit learners, improve their experience with the subject matter, and create more competent health professionals.

### **Technology**

Increasingly, computers and multimedia are used not only to enable students to visualise PK scenarios through simulations, but to interact with problem-solving exercises, and perform real-time calculations (Munar, Singh, Belle, Brackett & Earle, 2006). Munar *et al.* describes the implementation of workshops where PharmD students use commercially available computer programs to construct their own PK models in order to solve patient cases and achieve learning objectives. Assessments showed that the computer implementation caused a significantly higher performance on examinations (84.3% vs. 88.7% mean) (Munar, Singh, Belle, Brackett & Earle, 2006).

Other instructors have developed on-line module-orientated assignments using spreadsheet files to provide students with an unlimited numbers of PK practice problems with immediate feedback (Mehvar, 1999). Results indicated that students who used this innovation scored approximately 10% higher on the assignments, suggesting that multiple opportunities for practice and feedback allowed for more clear understanding of the concepts (Mehvar, 1999).

Audience response systems (ARS) are regularly used in the classroom for student engagement and informal assessment. Students respond to questions in lectures with wireless keypads such as iClickers, or even wireless devices such as their own computers, the facilitator receives the

results via a base station and software on their computer, and the results are almost immediately tabulated and shown for class discussion (Collins, 2008). ARS creates an engaging environment, as students can provide anonymous responses and gain instant feedback on their performance, and studies using ARS have shown increased student participation, attendance, and learning (Collins, 2008; Gauci, Dantas, Williams & Kemm, 2009).

A cloud-based ARS, Lecture Tools, was implemented into a graduate level PK course and student feedback revealed that overall, the innovation enhanced attentiveness, engagement, and participation but did not significantly change assessment outcomes in comparison to cohorts that did not use the innovation (Swanson, Piscik & Swanson, 2014). While the software package provided versatility in the types of questions asked, a large drawback was the amount of time required for collection of responses (Swanson, Piscik & Swanson, 2014).

In general, responses obtained through ARS questions can communicate potential confusions, misconceptions and knowledge deficits, which can shift the direction of a lecture and allow for more productive teaching (Collins, 2008). However, the limitations of using such technology includes the inconvenience of transporting equipment, technical difficulties, the expense, the reduction in lecture content, and instructor familiarity with software (Collins, 2007). Most importantly, implementing ARS requires time and effort on the instructor's part to design appropriate questions which require higher levels of reasoning and integration; as PK involves theory and application, the breadth of the questions may therefore not be as extensive if there are time constraints for presentation of the lecture (Collins, 2008). While ARS have clear value in the education environment, their application for the teaching of PK requires careful consideration and design, and should not be the sole teaching enhancement used for this subject.

### **Computer Simulations**

The many advantages of using computer simulations for teaching include: (i) visualisation of dynamic processes, (ii) increased student engagement by allowing control of a simulated world, (iii) an opportunity to explore concepts that might otherwise be impractical due to cost, safety,

or time constraints, and (iv) the simulation highlights the relevant and integral components of the educational objectives (Sullivan, 1988). Pharmacokinetics simulations provide opportunities for students to evaluate 'what-if' scenarios by examining how changes in dosage regimens and/or physiological parameters affect the shape of a drug's concentration *versus* time curve (Mehvar, 2012). The graphs provide a visualisation of the interplay between the different PK parameters, and provide students with the visual flexibility in terms of evaluating how changes in PK parameters affect the disposition of a drug (Hedaya, 1998; Robbins, Wedlund & Williams, 1989). Supplementing traditional instruction in PK with software programs provides an additional mechanism for developing problem solving skills and strategic thinking in students (Difazio & Shargel, 1989). In addition, PK computer simulations extend beyond the classroom, as Wurster and Shrewsbury describe a simulator that clinicians can use prior to patient drug administration – one which simulates optimum therapeutics by identifying regimens which would produce sub or supra-therapeutic blood concentrations of the drug (Wurster & Shrewsbury, 1981).

Early developments of PK computer simulations used spreadsheet programs to simulate PK data, and as computer technology advanced, it became more widespread to use commercially available programs. MicroPharm-K (MP-K) was developed specifically for analysing experimental data and PK modelling, and with capability for non-linear fitting, the authors stated that the program could be used for educational purposes, though implementation with students has currently not been reported (Urien, 1995). Some software programs specifically explore acute and chronic one-compartment kinetics (Difazio & Shargel, 1989; Robbins, Wedlund & Williams, 1989), while others also analyse 2- or 3-compartment kinetics (Li, Wong & Chan, 1995; Sullivan, 1988).

In the early versions of PK computer simulations, the main disadvantages were that students' comfort and know-how with the technology was limited, and extra time needed to be spent on simply learning how to use the software (Sullivan, 1992). In addition, several of the early simulation packages were hampered by lack of flexibility or only had limited simulation options (Li, Wong & Chan, 1995).

Of the more complex simulations, Cyber Patient™ is a multimedia PK simulation software package that describes one and two compartment PK models following single or multiple doses from IV or oral routes of administration (Bolger, 1995). Students are encouraged to take on the role of the health care professional with primary care responsibility for a virtual patient receiving medication (Bolger, 1995). They follow the simulation, take “data points”, and analyse the resulting concentration versus time graphs throughout different clinical case studies. The intervention resulted in an increase in problem-solving and critical thinking for students, and almost the entire class felt that the problems in the case studies helped to reinforce the lectures and discussions (Bolger, 1995). More simplistic simulations also allow for students to find value in engaging with these programs for their learning. LeBlanc *et al.* introduced a pharmacokinetic simulation software package into a course of 100 students, and the setup consisted of a graphical window of concentration versus time, a table of the PK parameters modified, and a feedback and dialog window for engagement (Leblanc & Aiache, 1994). Overall, 72% of the students surveyed found the approach preferential to the traditional lecture approach.

Recently, an Excel-based simulation program has been developed at the University of Alberta to assist in the teaching of basic PK to undergraduate students – the program is called uSIMPk (Brocks, 2015). With a range of modules, uSIMPk allows students to alter PK parameters by using slide bars and to observe the result of these changes through a visual representation of the drug’s concentration-time profile. By incorporating the program in class, the instructor was able to record student predictions of what they thought would happen if parameter  $x$  increased/decreased, which in turn stimulated discussion and provided more in-depth understanding of these relationships (Brocks, 2015). Survey results showed that of the students who participated, there was strong agreement that the use of uSIMPk helped students understand the relationship between PK parameter changes and changes in concentration vs. time graphs ( $81 \pm 21\%$ ), and that the program was used effectively in class ( $78 \pm 23\%$ ) (Brocks, 2015).

The use of computer simulations shows promise for enhancing student performance, as Mehvar demonstrated that by encouraging his students to use an online module for 10 minutes in class,

their assessment score increased by 21% in comparison to their pre-test score (Mehvar, 2012). A large portion of students indicated that after participating in the educational intervention, the use of online simulations was an effective learning tool and should be continued (Mehvar, 2012).

Hedaya demonstrated a similar trend, as students showed a significant increase in performance in their post-test assessment in comparison to their pretest assessment ( $8.9 \pm 1.16$  vs  $5.4 \pm 3.13$  out of ten) after using an online PK simulation package for an unlimited amount of time (Hedaya, 1998). Developed by Authorware® software, the 24 computer-based interactive modules each covered one PK topic, included a self-instructional lesson, simulation exercise, and self-assessment (Hedaya & Collins, 1999). The general consensus amongst the students who participated in a feedback survey was that the innovation made it easier for them to visualise and understand the basic PK concepts, and to appreciate the clinical significance of these concepts (Hedaya & Collins, 1999)

### **The “Flipped” or “Blended” Classroom**

Flipping the classroom involves re-arranging face-to-face contact time with students by directing them to view pre-recorded material in their own time and using class time for varying active engagement techniques (Schneider, Munro & Krishnan, 2014). In comparison to traditional lectures, blended courses are cited to result in higher satisfaction levels among faculty and students, increased access and flexibility in time, place, and pace of learning, and better learning outcomes for students (Edginton & Holbrook, 2010).

Schneider *et al.* made use of class time by having students work through a worksheet containing short answer (SA) and multiple choice (MC) questions on recorded content, apply them to case scenarios, and then discuss the results with other students. These scenarios allowed students to apply their knowledge to calculate dosing for patients with different medical conditions, and calculate drug parameters like elimination rate constants, clearance, and volume of distribution (Schneider, Munro & Krishnan, 2014). In contrast to the previous cohort that only received didactic lectures, the students' in the flipped classroom overall felt more favourably about the

course and the content, though there was markedly very little difference on performance in major assessments between the two groups (Schneider, Munro & Krishnan, 2014).

Persky and Dupuis observed pharmacy student performance over an eight-year period in the “flipped” model in a foundational PK and clinical PK course, which shifted from the lecture-with-active learning (LAL) format to strategies encompassing team-based learning (TBL) and case-based learning (CBL) (Persky & Dupuis, 2014). Though these changes resulted in higher performances in comparison to the LAL format, the student evaluations/attitudes decreased (Persky & Dupuis, 2014). Other groups found students in their blended learning course valued the face-to-face interaction with instructors as it allowed them to gain feedback and better understand PK concepts (Edginton & Holbrook, 2010).

### **1.3.2.2 Teaching in the Medical Curriculum**

Currently, preparation for prescribing is the major challenge facing undergraduate medical education (Ross & Maxwell, 2012). Concerning trends affecting the quality of prescribing and knowledge of pharmacology include more rapid throughput of patients, increased drug developments in novel areas, increased complexity and use of medical care, increased specialisation, increased polypharmacy, aging and sick populations that are vulnerable, and finally, patient demands for specific drugs or use of alternate therapies (Flockhart, Usdin Yasuda, Pezzullo & Knollmann, 2002; Maxwell, Walley & Ferner, 2002). New medical graduates need to be optimally prepared with a sound understanding of the principles of clinical pharmacology, therapeutics, and appreciation of uncertainty and good judgment (Ross & Maxwell, 2012). In the US, all residency and fellowship programs for physician trainees approved by the Accreditation Council of Graduate Medical Education (ACGME) are required to organise their training programs around six broad educational competencies (Lewis & Nierenberg, 2007). In the context of clinical pharmacology, these competencies range from providing excellent patient care through selecting optimal and appropriate therapies, to applying medical knowledge by estimating a patient’s GFR and successfully modifying a dosing schedule for patients with renal failure (Lewis & Nierenberg, 2007).

Ross and Maxwell, in the *British Journal of Clinical Pharmacology*, highlight a list of learning outcomes for medical graduates after five years of undergraduate study, specifically for clinical pharmacology and drug classes. The listed PK competencies range from concepts such as explaining the fundamental differences between various routes of drug administration, defining volume of distribution, explaining how drug metabolism creates potential for DDIs, to describing a typical concentration-time curve for a drug with first-order kinetics, and how patient factors alter pharmacokinetic handling of drugs (Ross & Maxwell, 2012). These concepts (and many others) are discussed in the first part of this work, and as such, the subject matter is vital for proper and appropriate patient care. Yet, opinion pieces, such as the one by Wiernik are still currently circulated, suggesting disconnects between the classroom and the clinic (Wiernik, 2015).

Woodman *et al.* describe recent changes in medical education made in Australia, which echo changes also made in medical education globally. Specifically, problem-based learning (PBL) is a large component of the curriculum, and basic science disciplines are integrated horizontally into study of the major body systems for more clinical training early in the program (Keijsers, Leendertse, Faber, Brouwers, de Wildt & Jansen, 2015; Woodman, Dodds, Frauman & Mosepele, 2004). The overarching question is: how is PK competence successfully integrated into these training programs? There are a variety of educational innovations for PK and basic pharmacology, which were expanded in the pharmacy section, and the following will briefly highlight additional strategies in medicine.

### **Problem Based Learning (PBL)**

PBL is delivered through a variety of formats between schools, but the basic premise is that tutorial groups with a non-specialist tutor (basic scientist or a clinician) are presented with detailed case studies, including patient history and laboratory results (Woodman, Dodds, Frauman & Mosepele, 2004). Each student researches a learning issue, and in the second week, they reconvene to answer and “solve” the clinical issue, usually through a therapeutic approach (Woodman, Dodds, Frauman & Mosepele, 2004). The use of PBL allows discussion of drug

action in a clinical context, and the hope is that students will have greater motivation to understand concepts related to pharmacology (Michel, Bischoff, Zu Heringdorf, Neumann & Jakobs, 2002).

The usefulness of PBL in relation to lecture-based learning is a hotly debated topic, as there is variation in its delivery between schools, and there is concern that teaching pharmacological concepts through this approach may not be ideal. The findings of Woodman *et al.* suggest that there are challenges in writing cases focusing on PK, when the curriculum is systems-based, and the focus of PBL is physiology and pathology rather than drug action (Woodman, Dodds, Frauman & Mosepele, 2004). After implementation of a case-study meant to provoke discussion about the ADME of a drug, there was feedback that medical students wanted more emphasis on the clinical condition, rather than drug behaviour (Woodman, Dodds, Frauman & Mosepele, 2004).

At the University of Essen, differences in pharmacological learning between student cohorts in PBL *versus* lecture-based learning were observed. Students in PBL rated their course as a positive experience and rated it higher in regards to increased knowledge and interest of pharmacology *versus* students in lecture-based formats (Michel, Bischoff, Zu Heringdorf, Neumann & Jakobs, 2002). Student performance on standardised testing in pharmacology showed that the PBL group performed slightly better, but not overwhelmingly better than lecture-based students ( $523 \pm 76$  points vs  $500 \pm 91$  points).

Lubawy and colleagues reported positive results after implementing PBL into their curriculum: in comparison to a lecture-based cohort, the case-based method cohort scored significantly higher on the course's cumulative test; mean scores were 84.6% *versus* 67.5%, respectively (Lubawy & Brandt, 2002). In addition, students commented that they felt motivated to learn because they saw the relevance of the subject in practice, and its application to patient counselling and disease state management (Lubawy & Brandt, 2002). Thus, variations in the delivery of this innovation impacts student learning and development of competence. Developing physicians well-versed in the PK of drug action is achievable through this mode of

learning, but the caveat is that the outcome depends on other aspects of the teaching environment and priorities.

### **Online Programs**

In response to growing concerns about inadequate training, Maxwell and colleagues developed a drug formulary, eDrug, in order to provide students with an accessible resource and virtual learning environment for understanding drug action (Maxwell, McQueen & Ellaway, 2006). The program was implemented for 5 years during lectures, providing useful information about specific drugs, and with medical students encouraged to use it (Maxwell, McQueen & Ellaway, 2006). As such, student responses on questionnaires concerning the innovation were positive, with many believing that the program successfully integrated material from different courses (Maxwell, McQueen & Ellaway, 2006). eDrug Calc, as an extension of eDrug, was developed to provide students with calculation questions concerning drug dosing and skills (McQueen, Begg & Maxwell, 2010). Designed as a formative self-assessment tool, eDrugCalc tests were implemented at various points of students' medical education; of the people who completed the assessments, there was a significantly higher mean score in test 6 compared to test 1 (16.6/20 versus 12.6/20) (McQueen, Begg & Maxwell, 2010). Students also reported feeling more confident with drug dosing calculation, and overall felt the innovation was an effective learning tool (McQueen, Begg & Maxwell, 2010). Though there were confounding issues, like lack of control to non-innovation groups, and uncertainty with regard to what aspect of the program improved performance, it was nevertheless found to be a cost-effective and minimally disruptive innovation that provided value for the cohort (McQueen, Begg & Maxwell, 2010).

### **Medical Apps**

More than 85% of clinicians own smartphones, and approximately 50% use applications in clinical practice (Franko & Tirrell, 2012). Medical apps can prove to be very efficient and convenient in the medical setting; they are smaller, more accessible, more portable, and offer faster access at the point of care (Haffey, Brady & Maxwell, 2013). They can also update quickly in response to new developments or changes in clinical guidelines (Haffey, Brady & Maxwell,

2013). Thus, harnessing such a tool and providing relevant information for prescribing is obvious.

In a pediatric department in Northern Ireland, participants (28 doctors and 7 medical students) were recruited to participate in two hypothetical clinical scenarios involving hypotensive children with meningococcal septicaemia (Flannigan & McAloon, 2011). Participants were divided into two groups: one using the British National Formulary for Children (BNFC) reference, while others used the PICU calculator on an iPhone (Flannigan & McAloon, 2011). Participants were asked to calculate appropriate dopamine and adrenaline infusions within 10 minutes, and provide their self-assessed confidence in the result. All participants using the smartphone app correctly prescribed the infusions while only 28.6% of the BNFC group achieved the same outcome. In addition, the smartphone calculation was 376% quicker than the BNFC, with the group reporting more confidence in the prescription, irrespective of clinical experience (Flannigan & McAloon, 2011). While this example clearly outlines the advantages of technology, the main caveat is that the quality of every medical app in use may not be sufficiently high.

Haffey & Brady explored the use of opioid switching apps, as it reflects a need within the medical community; the patient deaths reported by Lehmann, in fact, were associated with complications concerning opioid switching. Opioid switching is usually required if the current opioid causes adverse effects or is ineffective in pain control, or contributes to a DDI (Haffey, Brady & Maxwell, 2013). In addition, changes in patient status, or the need for a different route of administration, can also contribute to the need for a change in drug (Haffey, Brady & Maxwell, 2013). Equianalgesic tables, though rather dated, are routinely used to aid in opioid conversion, but the advent of medical apps has created a potential new strategy (Haffey, Brady & Maxwell, 2013). Though the authors identified 23 apps associated with opioid switching, 12 had no stated medical professional involvement. More concerning, however, is that only 11 apps provided references for their opioid conversions in the form of journal articles and pain management textbooks. Unfortunately, overall, the calculated dosages were highly variable, with statistically significant differences in conversion outputs for hydromorphone with and without stated medical involvement (Haffey, Brady & Maxwell, 2013).

In fact, a recent systematic review searching for all apps which outline core prescribing competencies like prescribing drugs, IV infusions, and pharmacology resulted in 306 identified apps (Haffey, Brady & Maxwell, 2014). One hundred and four of these were identified as directly supporting prescribing, including drug dosing calculations, IV drip or dilution calculations, drug dosing conversions, DDI checkers, and drug formularies. Interestingly, 33% of the identified apps did not show evidence of medical or professional involvement, while 18% had disclaimers assuming no liability for patient harm through app use. There is clear benefit to the use of apps in educating clinical personnel and in enhancing their ability to adjust dose based on patient-specific factors (Haffey, Brady & Maxwell, 2014). However, to use medical apps effectively and assess the validity of the resulting information that they generate, medical trainees require knowledge and skills in basic pharmacology and PK. Generation of critical thinking and application as it applies to therapeutics begins in the medical school curriculum, and as such, there must be greater emphasis on these competencies.

#### **1.4 THE ADAM AS A LEARNING TOOL**

The scope of this work entails the kinetic and physiological complexities concerning pharmacokinetics and its application to clinical settings. The complexities contribute to knowledge deficits and lack of confidence in healthcare personnel, as demonstrated through prescribing errors resulting in adverse drug events, drug-drug interactions, and patient harm. The recognition of these deficits has spurred numerous societies, universities, and individual instructors to innovate and develop more robust, comprehensive, and engaging strategies for the delivery and learning of pharmacokinetics.

Despite the many innovations, ranging from complex computer programming to enhanced lectures, there continues to be a lack of clinical-like context within the scope of pharmacokinetics teaching. What happens when a patient is administered a drug? To where does the drug distribute? What impacts half-life? How does repeated dosing impact drug accumulation? How does renal failure impact drug behaviour? The concepts continue to be abstract in undergraduate science, medical, pharmacy, and nursing training. Arguably the best

way to understand the scope and impact of drug administration is through administering a dose to a patient (or animal) and monitoring and analysing the drug levels. However, these historical approaches are discouraged and often precluded by progressing ethical standards. A report in *Pharmacology Matters*, an online publication of the British Pharmacological Society, which described a novel pharmacokinetics teaching tool where methylene blue dye was transferred between two beakers by a peristaltic pump to mimic clearance, inspired this work. This thesis will highlight development and testing of the Alberta Drug Administration Modeller (ADAM); the objectives of this study were:

- 1.) To design the apparatus, including additions, changes, and improvements.
- 2.) To validate the apparatus in modelling complex pharmacokinetic relationships and applications.
- 3.) To incorporate the modeller into an undergraduate laboratory course.
- 4.) To identify strengths, limitations, and potential additional features for the ADAM.
- 5.) To envision future applications of ADAM in health care curricula.

## CHAPTER 2: DESIGN, METHODS, AND RESULTS OF PRELIMINARY TESTING

### 2.1 APPARATUS CONCEPT AND CONSTRUCTION

The apparatus is composed of six peristaltic pumps connected with Tygon tubing, through which water, representing the plasma, is circulated (Figure 2.1). The HEART pump (D) circulates the water within the main circuit, which represents the central compartment. The LIVER pump (G) and KIDNEY 1 pump (J) control hepatic and renal clearance, respectively. Each pump drains water (containing methylene blue) from the central compartment into hepatic waste (P), equivalent to drug and/or metabolites in faeces plus metabolites in urine, or into a urine beaker (O), equivalent to unchanged drug eliminated in urine. To maintain urine flow at a relatively constant rate, the volume of fluid pumped from the circulation into the urine beaker *per minute* by the KIDNEY 1 pump is supplemented with water supplied through the KIDNEY 2 pump (I), such that the combined outputs from both pumps is held constant. This allows renal clearance to be increased or decreased without changing the rate of urine production. The ORAL BIOAVAILABILITY pump (H) moves water containing orally-administered drug from the stomach (C), an air-tight vessel, into hepatic waste (P) to mimic incomplete absorption and/or first-pass metabolism.

The fluid volume lost from the circulation through the combined action of pumps G, H and J is replaced by drinking water (A), which is drawn into the air-tight stomach in response to fluid draining from the stomach. An air-tight tissue compartment bottle (N) can be introduced by opening two diversion taps (K and L), allowing drug to be circulated both through the main circuit and, in parallel, through the tissue compartment, under the control of the TISSUE pump (M). Varying the volume of the tissue compartment bottle, or varying the speed of the TISSUE pump, alters the rate and extent of drug distribution.

Immediately upstream of the IV injection port, 3-way taps allow a portion of the flow to be redirected through a glass flow-through cuvette (Q) before returning to the systemic circulation,

via another medium-flow peristaltic pump. Drug concentration can thus be monitored in real time by continuous monitoring of absorbance, without the need for collection of blood samples. The absorbance at 664 nm of fluid passing through the flow-through cuvette at  $7 \text{ mL min}^{-1}$  was measured in a Cary 60 spectrophotometer; this instrument may be operated with the sample chamber lid open, facilitating use of the flow-through cuvette.

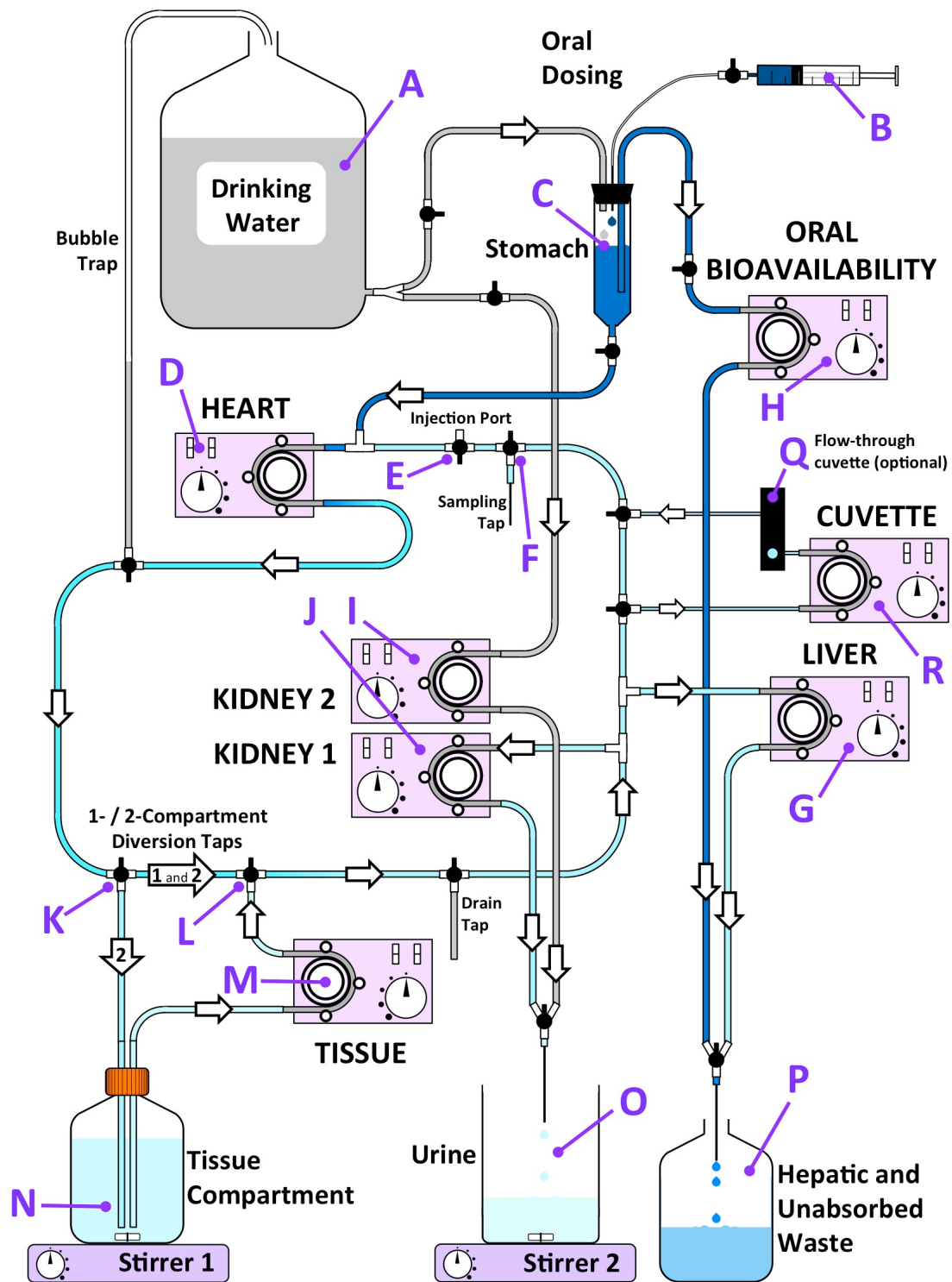


Figure 2.1 Schematic of the Alberta Drug Administration Modeller (ADAM).

## 2.2 DRUG ADMINISTRATION

Drug can be administered into the system orally, from a syringe (B) into an airtight 50 ml conical centrifuge tube representing the stomach (C). When drug was administered by this route, a further 2 mL of water were injected to flush the entire dose of methylene blue from the cannula into the stomach. By changing the volume of liquid initially present in the stomach vessel, it is possible to change the absorption rate constant ( $k_{abs}$ ) for the drug, as well as both the peak concentration of drug in plasma ( $C_{max}$ ) and the time required to reach  $C_{max}$  ( $t_{max}$ ). The degree to which these parameters can be modified can be expanded by increasing the volume of the stomach vessel. Adjusting the ORAL BIOAVAILABILITY pump (H) varies the proportion of the initial dose of drug that reaches the systemic circulation. Drug then passes from the stomach into the circulation as fluid moves from the stomach to replace that lost to hepatic and renal waste.

Drug can also be administered intravenously from a syringe *via* an injection port (E) comprised of a 3-way tap with a luer fitting. When drug was administered by this route, the injection was administered slowly over a period of 30-45 seconds, to allow complete mixing of drug throughout the central compartment to occur as quickly as possible. On entering the systemic circulation, an intravenous bolus dose of drug typically completes around five circuits of the plasma compartment before mixing of drug with water representing blood is complete. As soon as drug is present in the main circuit, it can undergo elimination *via* the liver and kidney pumps, with kinetics that model elimination from a one-compartment system. However, by opening up the diversion taps (K and L) to include the TISSUE pump (M) and Tissue compartment (N), it is possible to mimic two-compartment distribution and elimination behaviour.

At selected time points, samples (< 1 ml) are collected into microfuge tubes *via* the sampling port (F), or from the urine container (O). Absorbance values for these samples are measured in a spectrophotometer or microplate reader at 664 nm and, after "blank" subtraction, are then converted to concentrations (molar absorption coefficient 70,130  $M^{-1}cm^{-1}$ ).

Concentration data are plotted *versus* time on linear or semi-logarithmic axes using GraphPad Prism (versions 6.0f or 7.0a), and data are fitted to appropriate equations to determine a variety of PK constants. One-compartment IV modelling plasma data are fitted to a single-phase decay equation, while two-compartment IV modelling plasma data are fitted to a two-phase decay equation. When the experiment consists of PO dosing, no attempt is made to fit plasma data points to an equation. Semi-logarithmic data (for the terminal phase of both IV and PO dosing, and the distribution phase in 2-compartment dosing), are fitted to a non-linear regression straight line (when comparing parameters statistically), or to a linear regression line, with GraphPad Prism.

When urine samples are collected, the cumulative urine volume is also measured at each time point so that the cumulative amount of drug eliminated in the urine may be determined; data are corrected to account for the urine removed for absorbance measurements. Urine data for PO dosing and two-compartment modelling are not fitted to an equation; rather, the points are simply connected. The plateau (i.e. the mean of the last three points measured) on the cumulative amount of urine *versus* time plot is considered as  $D_{U\infty}$ , and the sigma minus method is used to generate a semi-logarithmic plot of the data for determination of  $k_{el}$ . The semi-logarithmic plot data are fitted to a non-linear regression straight line with weighting set as  $1/X^2$ . The weighting was implemented to account for the large margin of error occurring with very small absorbance values resulting from later time points where most of the drug has been cleared from the system. Table 2.1 illustrates the equations used throughout the study to calculate PK parameters from the data, and to predict dosing regimens.

(1) $V_D = \frac{\text{Dose}}{C_{t0}}$	(8) $t_{1/2} = \frac{0.693}{k}$	(14) $\frac{C_{\text{max at steady state}}}{C_{\text{min at steady state}}} = \frac{1}{e^{-k_{el}t}}$
(2) $CL_{\text{Total}} = k_{el} \times V_D$	(9) $CL_R = \left(\frac{\text{Plateau}}{\text{Dose}}\right) \times CL_{\text{Total}}$	(15) $k_{12} = \frac{AB(\beta - \alpha)^2}{(A + B)(A\beta + B\alpha)}$
(3) $CL_{\text{Total}} = \frac{\text{Dose} (\times F)}{AUC_{t_{n-1}}^{t_n}}$	(10) $V_{D\text{ SS}} = \frac{\left(\text{Dose} \times \left(\frac{A}{\alpha^2} + \frac{B}{\beta^2}\right)\right)}{AUC^2}$	(16) $k_{21} = \frac{(A\beta + B\alpha)}{A + B}$
(4) $AUC_{t_{n-1}}^{t_n} = \frac{C_{t0}}{k_{el}}$	(11) $V_{D\text{ Area}} = \frac{\text{Dose}}{(AUC \times \beta)}$	(17) $k_{10} = \frac{\alpha \beta (A + B)}{(A\beta + B\alpha)}$
(5) $AUC = \sum AUC_{t_{n-1}}^{t_n} + \frac{C_{tn}}{k_{el}}$	(12) $V_{D\text{ Extrapolation}} = \frac{\text{Dose}}{B}$	(18) $\text{Oral Dose Rate} = \frac{\text{IV Dose Rate}}{F}$
(6) $F = \frac{AUC_{PO}}{AUC_{IV}}$	(13) $C_{SS} = \frac{\text{Maintenance Dose Rate}}{V_D \times k_{el}}$	(19) $\text{Loading Dose} = C_{SS} \times V_D$
(7) $-k = \text{slope} \times 2.303$		

Table 2.1 Equations used to calculate PK parameters from data generated by the ADAM.

## 2.3 DESIGN AND ANALYSIS CHANGES, ADDITIONS, AND CONSIDERATIONS

Extensive tests were conducted on the apparatus to determine the optimal configurations that would accurately mimic one or two-compartment PK behaviour and would provide the most accurate data for analysis purposes. With consideration to the system design, tests were conducted to determine the influence of a variety of factors on system performance, and thus on the PK parameters of the drug. The following tests were conducted:

- 2.3.1 The effects of drinking water reservoir (A) volume on the system
- 2.3.2 The effects of the timing of ON setting of pumps G, I, and J for drug administration in a one-compartment configuration
- 2.3.3 The effects of changing the rate of the HEART pump (D) in a one compartment configuration

- 2.3.4 The effects of including or omitting early sampling points on the resulting equation fits in a one compartment configuration
- 2.3.5 The use of a dialysis membrane to model two compartment behaviour
- 2.3.6 The effect of TISSUE pump (M) rate and tissue compartment (N) volume on the distribution behaviour in two compartment configurations
- 2.3.7 The effect of using oil in the tissue compartment bottle (N), and changing the pH of the system to modify solubility and spectral characteristics of a different drug
- 2.3.8 The addition of an ORAL BIOAVAILABILITY PUMP (H) to mimic First Pass Metabolism

Other considerations in analysis were explored to ensure accurate portrayal and proper analysis of the data points. Analysis considerations included:

- 2.3.9 Plateau constraints for biphasic decay fit
- 2.3.10 Urine analysis in PO dosing and 2-compartment configuration
- 2.3.11 Use of PK Solver for Data Validation

### **2.3.1 DRINKING WATER RESERVOIR VOLUME EFFECTS**

Because the drinking water reservoir replaces water lost to hepatic and renal clearance by a gravity-feed system, it was important to determine the effect of manometric pressure at different reservoir volumes on PK parameters. With all other parameters set constant, two experiments were conducted with the drinking water reservoir initially containing 4 L or 2.5L of water. In both cases, the water reservoir was not refilled for the duration of the experiments. Figure 2.2A displays the biphasic decay fit of the data, while Figure 2.1B shows the non-linear regression analysis based on the terminal phase of the experiment (both experiments were

analysed from  $t=5.5$  min). PK analysis was performed on both sets of experiments, as shown in Table 2.2. Most notably, the distribution and elimination half-life values were prolonged in the experiment with a 2.5 L water reservoir ( $t_{1/2 \text{ dist}}$ : 0.6 min vs. 1.0 min, and  $t_{1/2 \text{ elim}}$ : 8.4 min vs 10.5 min). The change in half-life was also accompanied by slight increases in  $V_{D \text{ Extrap}}$  and AUC, with a decrease in  $CL_{\text{Total}}$  with the 2.5 L reservoir volume.

Statistical analysis was performed using GraphPad Prism software. The statistical analysis was an extra-sum-of-squares-F test to compare the two exponential phase decay fits generated by the 2.5 and 4 L reservoir volumes. The parameters of A, B,  $k_{el}$ , and  $k_{\text{dist}}$  were compared between the reservoir volumes of 4 L and 2.5 L revealing statistically significant differences for the A ( $P<0.001$ ), B ( $P=0.001$ ),  $k_{el}$  ( $P=0.0003$ ), and  $k_{\text{dist}}$  ( $P<0.001$ ) parameters. As most of these parameters are involved, in some way, in the calculation of other PK parameters, the change in water reservoir volume can affect these calculated parameters. Though the calculated slope of the terminal phase obtained in the two of experiments are very similar when compared by eye, they were determined as statistically different: comparisons between the slopes using Graph Pad Prism software statistical methods equivalent to analysis of covariance (ANCOVA) revealed the two slopes in Figure 2.2 to be statistically different ( $P<0.0001$ ). The change in the calculated PK parameters, along with the statistically significant change in slope for nonlinear regression analysis thus indicate that larger volumes in the drinking water reservoir affect the pressure in the system, resulting in slightly shorter distribution and elimination half-lives, lower AUC values, and increased clearance.

All experiments in ONE and TWO compartment configurations were conducted with an initial water reservoir volume of approximately 4 L, and the reservoir was regularly topped up to 4 L, to ensure consistency between experiments.

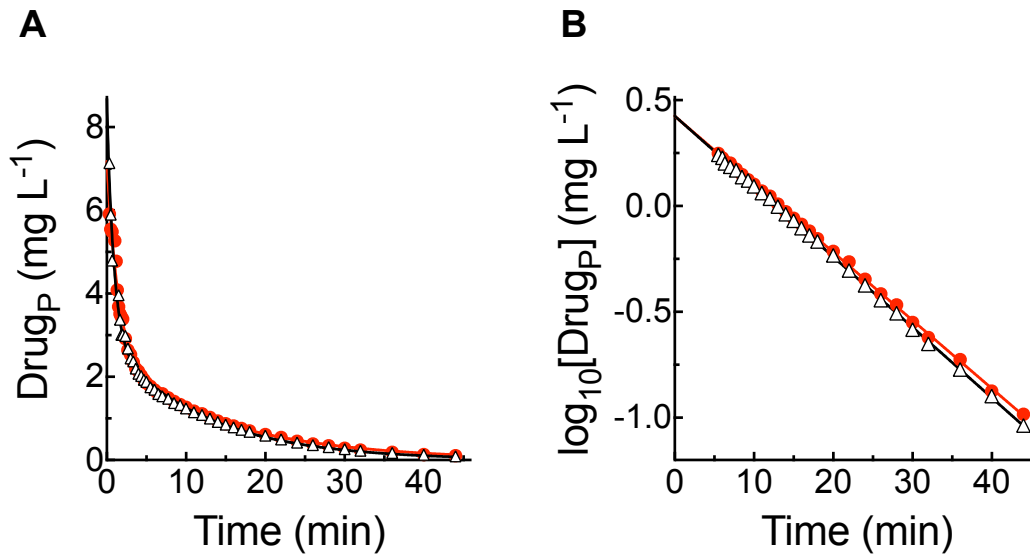


**Figure 2.2 Comparisons for drinking water reservoir volume.**

Calculated PK parameters are shown in Table 2.2. HEART pump: 132 mL min<sup>-1</sup>, LIVER pump: 14 mL min<sup>-1</sup>, TISSUE pump: 26 mL min<sup>-1</sup>, TISSUE compartment volume: 100 mL, KIDNEY 1 pump: 3 mL min<sup>-1</sup>, KIDNEY 2 pump: 4 mL min<sup>-1</sup>. **(A)** Plasma data of single IV dose (0.96) mg administered into the modeller with a two-compartment configuration and fitted to a two-phase exponential decay equation when the drinking water reservoir volume was 4L (Δ) or 2.5 L (●). **(B)** The terminal phase of data in (A) plotted on a semi-logarithmic y-axis. The calculated slope values were significantly different based on methods equivalent to ANCOVA ( $P < 0.0001$ ), suggesting that drinking water reservoir volume can affect subsequent PK parameters and calculations.

Figure 2.2 Plasma Analysis			
Tissue Pump Setting		26 mL min <sup>-1</sup>	
Kidney 1 Setting; Kidney 2 Setting		3 mL min <sup>-1</sup> ; 4 mL min <sup>-1</sup>	
Liver Pump Setting		14 mL min <sup>-1</sup>	
Tissue Compartment Volume		100 mL	
Drug Dose: 0.96 mg		4 L Water Reservoir Volume	2.5 L Water Reservoir Volume
PK Parameter	Equation/Method Used	△	●
<b>C<sub>10</sub> (A + B)</b>	Two-Phase Exponential Decay Fit	8.68 mg L <sup>-1</sup>	7.18 mg L <sup>-1</sup>
<b>k<sub>dist</sub></b>	Two-Phase Exponential Decay Fit	1.16 min <sup>-1</sup>	0.667 min <sup>-1</sup>
<b>t<sub>1/2 dist</sub></b>	Two-Phase Exponential Decay Fit	0.60 min	1.0 min
<b>k<sub>el</sub></b>	Two-Phase Exponential Decay Fit	0.0827 min <sup>-1</sup>	0.0662 min <sup>-1</sup>
<b>t<sub>1/2 el</sub></b>	Two-Phase Exponential Decay Fit	8.4 min	10.5 min
<b>AUC<sub>0-∞</sub></b>	AUC <sub>0-∞</sub> = AUC + C <sub>10</sub> /k	40.6 min · mg L <sup>-1</sup>	42.0 min · mg L <sup>-1</sup>
<b>V<sub>D Extrap</sub></b>	V <sub>D Extrap</sub> = Dose / B	359 mL	364 mL
<b>CL<sub>Total</sub></b>	CL <sub>Total</sub> = Dose / AUC <sub>0-∞</sub>	23.6 mL min <sup>-1</sup>	22.8 mL min <sup>-1</sup>
<b>r<sup>2</sup></b>	Two-Phase Exponential Decay Fit	0.9913	0.9929
<b>P value, A</b>	Extra-sum-of-squares F test	<0.0001	
<b>P value, B</b>	Extra-sum-of-squares F test	<0.0001	
<b>P value, k<sub>dist</sub></b>	Extra-sum-of-squares F test	<0.0001	
<b>P value, k<sub>el</sub></b>	Extra-sum-of-squares F test	0.0003	
<b>Y-intercept</b>	Nonlinear Regression Line	0.4248	0.4255
<b>B</b>	10 <sup>Y-intercept</sup>	2.65 mg L <sup>-1</sup>	2.66 mg L <sup>-1</sup>
<b>slope</b>	Nonlinear Regression Line	-0.0322	-0.0333
<b>β</b>	β = -slope x 2.303	0.074 min <sup>-1</sup>	0.077 min <sup>-1</sup>
<b>t<sub>1/2 el</sub></b>	t <sub>1/2 el</sub> = 0.693 / β	9.4 min	9.0 min
<b>r<sup>2</sup></b>	Nonlinear Regression Line	0.9990	0.9994
<b>P value, slope</b>	Analysis of covariance (ANCOVA)	<0.0001	

Table 2.2 PK parameters calculated for changes in drinking water reservoir volume.

PK parameters calculated from drug-plasma concentrations obtained in Figure 2.2.

### 2.3.2 ON VERSUS OFF SETTING OF PUMP G, I, AND J DURING DRUG ADMINISTRATION

The premise of one-compartment distribution is based on an assumption of instantaneous distribution of drug within the central compartment. Though the one compartment approach is an idealised approach to PK analysis, in the modeller, one-compartment distribution is mimicked quite successfully due to the small volume within the central compartment (~100 mL) and the high flow rate of the HEART pump (generally set to 132 mL min<sup>-1</sup>); drug distribution (mixing within the central compartment) is complete within approximately 5 circuits through the central compartment (usually within 3 minutes of administration). When a dose of drug is administered into the apparatus with all pumps turned on and all taps opened, elimination and distribution (if mimicking two-compartment distribution) commence immediately (it is physiologically accurate).

A strategy to result in more “complete” distribution earlier in data collection was assessed. A dose of drug was administered when only the HEART pump (D) was turned on, with the two-compartment diversion taps (K and L) configured to stop drug from distributing into the tissue compartment, and as such, allow circulation only within the central compartment. Once the drug was considered as completely distributed (within 5 circuits; ~3 minutes), then the LIVER pump (G), KIDNEY 1 and KIDNEY 2 pumps (I and J) were turned on, and sampling began. Figure 2.3 displays two separate experiments, with IV drug administration of the same dose of drug (0.96 mg) when all pumps were on and elimination was occurring concurrently with administration (Figure 2.3A and C), and another where the pumps were turned off, and on, as described above (Figure 2.3B and D). Table 2.3 discusses the PK parameters between each.

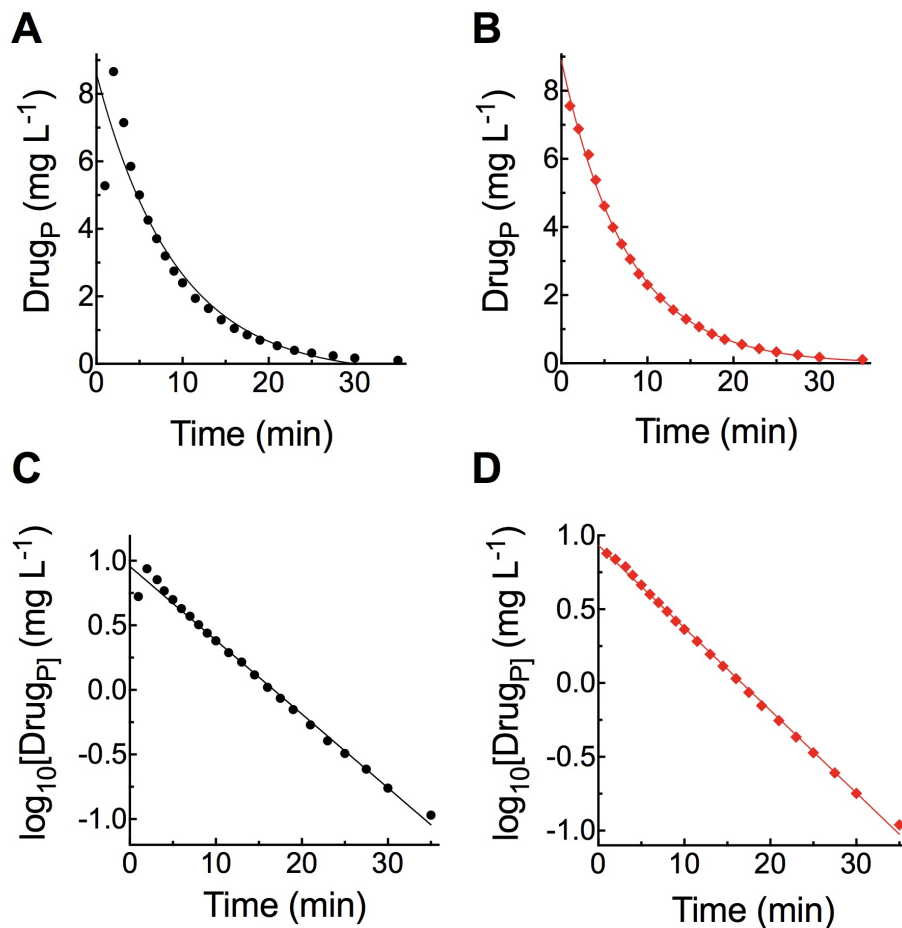


**Figure 2.3 Comparisons for ON/OFF elimination pump settings.**

Calculated PK parameters are shown in Table 2.3. HEART pump: 132 mL min<sup>-1</sup>, LIVER pump: 7 mL min<sup>-1</sup>, KIDNEY 1 pump: 3 mL min<sup>-1</sup>, KIDNEY 2 pump: 4 mL min<sup>-1</sup>. **(A)** Plasma data of a single IV dose (0.96) mg administered into the modeller in a one-compartment configuration and fitted to a single-phase exponential decay equation when the elimination pump settings were turned ON (●) during administration. **(B)** Plasma data of a single IV dose (0.96) mg administered into the modeller in a one-compartment configuration and fitted to a single-phase exponential decay equation when the elimination pump settings were turned OFF (◆) during administration. **(C)** The terminal phase of data in (A) plotted on a semi-logarithmic graph. **(D)** The terminal phase of data in (B) plotted on a logarithmic y-axis. The calculated slope values in (C) and (D) were not significantly different ( $P = 0.3584$ ), suggesting that drug administration when the elimination pumps are ON does not markedly affect drug distribution and subsequent PK parameter calculations in comparison to when the pumps are turned on *after* distribution has occurred.

Figure 2.3 Plasma Analysis			
Liver Pump Setting		7 mL min <sup>-1</sup>	
Kidney 1 Pump Setting		4 mL min <sup>-1</sup>	
Kidney 2 Pump Setting		3 mL min <sup>-1</sup>	
Drug Dose: 0.96 mg		Pumps ON at Start	Pumps OFF at Start
PK Parameter	Equation/Method Used	▲	◆
C <sub>t0</sub>	Single-Phase Exponential Decay Fit	8.60 mg L <sup>-1</sup>	8.90 mg L <sup>-1</sup>
k	Single-Phase Exponential Decay Fit	0.110 min <sup>-1</sup>	0.132 min <sup>-1</sup>
t <sub>1/2</sub>	Single-Phase Exponential Decay Fit	6.3 min	5.3 min
AUC <sub>0-∞</sub>	AUC <sub>0-∞</sub> = AUC + C <sub>tr</sub> /k	78.2 min · mg L <sup>-1</sup>	67.4 min · mg L <sup>-1</sup>
V <sub>D</sub>	V <sub>D</sub> = Dose / C <sub>t0</sub>	112 mL	108 mL
CL <sub>Total</sub>	CL <sub>Total</sub> = k <sub>el</sub> × V <sub>D</sub>	12.3 mL min <sup>-1</sup>	14.3 mL min <sup>-1</sup>
r <sup>2</sup>	Single-Phase Exponential Decay Fit	0.9142	0.9984
P value, C <sub>t0</sub>	Extra-sum-of-squares F test	0.5436	
P value, k <sub>el</sub>	Extra-sum-of-squares F test	0.1475	
Elimination Phase		—	—
Y-intercept	Nonlinear Regression Line	0.9563	0.9337
C <sub>t0</sub>	10 <sup>Y-intercept</sup>	9.04 mg L <sup>-1</sup>	8.58 mg L <sup>-1</sup>
slope	Nonlinear Regression Line	-0.0571	-0.0556
β	β = slope × 2.303	0.132 min <sup>-1</sup>	0.137 min <sup>-1</sup>
t <sub>1/2</sub>	t <sub>1/2</sub> = 0.693 / β	5.3 min	5.1 min
r <sup>2</sup>	Nonlinear Regression Line	0.9908	0.9987
P value, slope	Analysis of covariance (ANCOVA)	0.3584	

Table 2.3 PK parameters calculated for changes between ON/OFF elimination pump settings. PK parameters calculated from drug-plasma concentrations obtained in Figure 2.3.

Data analysis included the sample points taken at minute 1 for each condition. Overall, facilitating more equal distribution of the drug in the central compartment prior to turning on the elimination pumps and sampling resulted in data points that did not deviate from the single-phase exponential decay fit, contributing to an r<sup>2</sup> of 0.9987 versus 0.9908 when pumps were turned on during administration. Between the two experimental protocols, the C<sub>t0</sub> and V<sub>D</sub> were not substantially different. However, the t<sub>1/2</sub>, CL<sub>Total</sub>, and AUC were different between experiments, as the analysis from when the pumps were turned ON at administration revealed

slower drug elimination. The linear regression of the slopes calculated from each experiment differed slightly, and the GraphPad prism software equivalent ANCOVA statistical analysis revealed the P as 0.3584; the slopes comparing the two methods were not significantly different.

In addition, results of the extra-sum-of-squares F test generated by GraphPad prism software comparing the two single-phase decay fits of data obtained with pumps ON or OFF prior to drug administration did not show any statistical differences between the  $C_{t0}$  ( $P=0.5436$ ) and the  $k_{el}$  ( $P=0.1475$ ). Overall, the experiment revealed that while turning on the pumps once distribution within the central compartment was complete resulted in slightly-improved curve fitting, there was a lack of significant deviation of fitted parameters between the single-phase decay fits or semi-logarithmic plots if the pumps were turned on during drug administration. In addition to this, the lack of physiological relevance in keeping the pumps turned OFF for complete distribution, and the incompatibility with multi-dosing or infusion experiments negated further use of this modified approach.

All experiments in ONE and TWO compartment configurations had ALL appropriate pumps turned ON, and all diversion taps appropriately set *prior* to drug administration.

### 2.3.3 HEART PUMP RATE EFFECTS

Variations to the HEART pump rate on drug **distribution** was explored, where the same dose of drug (0.96 mg) was administered when the HEART pump was programmed at 132 mL min<sup>-1</sup> or 250 mL min<sup>-1</sup> with all other pumps held constant in a one-compartment configuration (Figure 2.4 and Table 2.4). It was reasoned that a faster heart rate would facilitate more rapid distribution for one-compartment settings, allowing earlier sampling for more accurate analysis. The first sampling data point (t=2 min) was included in the analysis of both experiments Figure 2.4A. In each case, inclusion of the first sampling point affected analysis and fit. GraphPad Prism software extra-sum-of-squares F tests were conducted on the two single-phase decay fits comparing the HEART pump at 132 mL min<sup>-1</sup> and 250 mL min<sup>-1</sup>, and resulted in statistically significant changes for the C<sub>t0</sub> (P value of 0.0002), but not the k<sub>el</sub> (P value of 0.0930).

As the C<sub>t0</sub> is used to generate the AUC and V<sub>D</sub> parameters, the significant difference in this value between the two conditions may influence calculation of the drug's PK parameters. Calculated V<sub>D</sub> values with the HEART pump at 132 mL min<sup>-1</sup> and 250 mL min<sup>-1</sup> are 127 mL and 88 mL, respectively (Table 2.4). This is a substantial difference, and as the central compartment volume is approximately 100 mL, the HEART pump at 250 mL min<sup>-1</sup> would potentially deliver more accuracy in calculating this parameter when the first sampling point is included.

However, GraphPad ANCOVA statistical analysis of the slopes of the semi-logarithmic plots of the data comparing the HEART pump at 132 and 250 mL min<sup>-1</sup> resulted in a P value of 0.0626; thus, PK parameters generated from the semi-logarithmic plot data may be more consistent between the two HEART pump conditions. Though the effects of the HEART pump rate reveal large discrepancies between calculated drug PK parameters like V<sub>D</sub>, the position of the early sampling point did not suggest instantaneous distribution with the faster HEART pump speed as predicted; thus, the use of the increased speed of the HEART pump may not facilitate use of early sampling time points.

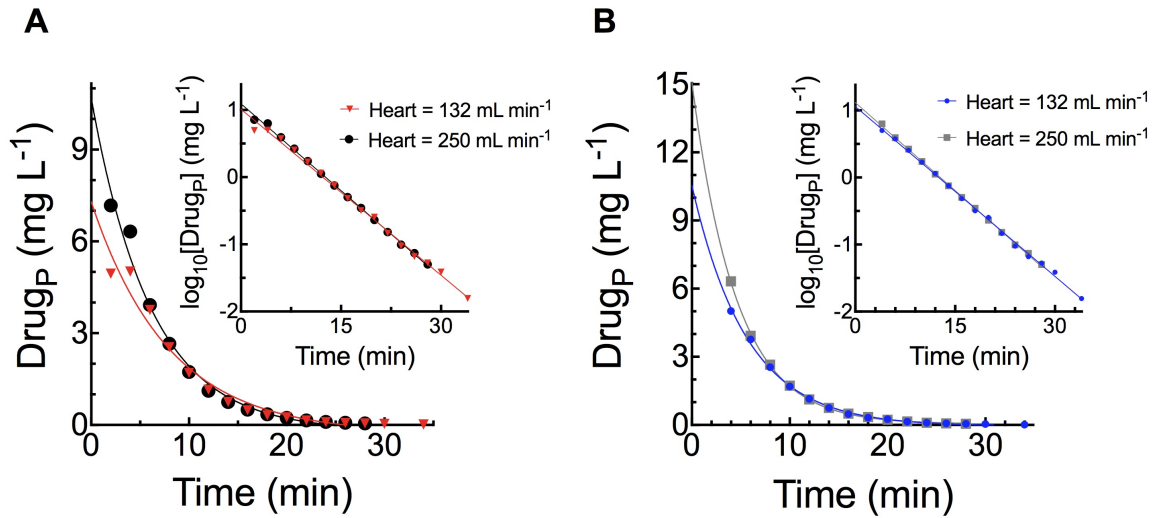


Figure 2.4 Comparison of HEART pump rates and inclusion/exclusion of the 1<sup>st</sup> sample point.

Calculated PK parameters are shown in Table 2.4. HEART pump: 132 mL min<sup>-1</sup> **or** 250 mL min<sup>-1</sup>, LIVER pump: 14 mL min<sup>-1</sup>, KIDNEY 1 pump: 3 mL min<sup>-1</sup>, KIDNEY 2 pump: 5 mL min<sup>-1</sup>. **(A)** Plasma data of single IV dose (0.96) mg administered into the modeller with a one-compartment configuration and fitted to a single-phase exponential decay equation when the HEART pump was set to 132 mL min<sup>-1</sup> (▼) or 250 mL min<sup>-1</sup> (●) with the first sample point included in the analysis. Inset graph: the terminal phase of data in (A) plotted on a logarithmic y-axis. **(B)** Plasma data of single IV dose (0.96) mg administered into the modeller with a one-compartment configuration and fitted to a single-phase exponential decay equation when the HEART pump was set to 132 mL min<sup>-1</sup> (●) or 250 mL min<sup>-1</sup> (■) with the first sample point excluded from the analysis. Inset graph: the terminal phase of data in (B) plotted on a logarithmic y-axis.

Figure 2.4 Plasma Analysis					
Liver Pump Setting		14 mL min <sup>-1</sup>			
Kidney 1 Pump Setting; Kidney 2 Pump Setting		3 mL min <sup>-1</sup> ; 5 mL min <sup>-1</sup>			
Heart Pump Setting		132 mL min <sup>-1</sup>	250 mL min <sup>-1</sup>	132 mL min <sup>-1</sup>	250 mL min <sup>-1</sup>
Drug Dose: 0.96 mg		Figure 2.4 A		Figure 2.4 B	
PK Parameter	Equation/Method Used	▼	●	●	■
C <sub>10</sub>	Single-Phase Exponential Decay Fit	7.58 mg L <sup>-1</sup>	10.88 mg L <sup>-1</sup>	10.6 mg L <sup>-1</sup>	15.1 mg L <sup>-1</sup>
k	Single-Phase Exponential Decay Fit	0.126 min <sup>-1</sup>	0.163 min <sup>-1</sup>	0.179 min <sup>-1</sup>	0.221 min <sup>-1</sup>
t <sub>1/2</sub>	Single-Phase Exponential Decay Fit	5.5 min	4.2 min	3.9 min	3.1 min
AUC <sub>0-∞</sub>	AUC <sub>0-∞</sub> = AUC + C <sub>10</sub> /k	60.2 min · mg L <sup>-1</sup>	66.7 min · mg L <sup>-1</sup>	59.2 min · mg L <sup>-1</sup>	68.1 min · mg L <sup>-1</sup>
V <sub>D</sub>	V <sub>D</sub> = Dose / C <sub>10</sub>	127 mL	88 mL	90.5 mL	64 mL
CL <sub>Total</sub>	CL <sub>Total</sub> = k <sub>el</sub> × V <sub>D</sub>	16.0 mL min <sup>-1</sup>	14.3 mL min <sup>-1</sup>	16.2 mL min <sup>-1</sup>	14.1 mL min <sup>-1</sup>
r <sup>2</sup>	Single-Phase Exponential Decay Fit	0.9675	0.9846	0.9978	0.9995
P value, C <sub>10</sub>	Extra-sum-of-squares F test	0.0002		<0.0001	
P value, k <sub>el</sub>	Extra-sum-of-squares F test	0.0930		<0.0001	
Elimination Phase		Figure 2.4 C		Figure 2.4 D	
PK Parameter	Equation/Method Used	▼	●	●	■
Y-intercept	Nonlinear Regression Line	1.011	1.092	1.058	1.117
C <sub>10</sub>	10 <sup>Y-intercept</sup>	10.3 mg L <sup>-1</sup>	12.4 mg L <sup>-1</sup>	11.6 mg L <sup>-1</sup>	13.1 mg L <sup>-1</sup>
slope	Nonlinear Regression Line	-0.0824	-0.0862	-0.08444	-0.08741
β	β = slope × 2.303	0.190 min <sup>-1</sup>	0.199 min <sup>-1</sup>	0.194 min <sup>-1</sup>	0.201 min <sup>-1</sup>
t <sub>1/2</sub>	t <sub>1/2</sub> = 0.693 / β	3.7 min	3.5 min	3.6 min	3.4 min
r <sup>2</sup>	Nonlinear Regression Line	0.9953	0.9985	0.9981	0.9992
P value, slope	Analysis of covariance (ANCOVA)	0.0626		0.0411	

Table 2.4 PK parameters calculated at different HEART pump settings and inclusion/exclusion of the first sample point.

PK parameters calculated from drug-plasma concentrations obtained in Figure 2.4.

### 2.3.4 EARLY SAMPLING POINT EFFECTS

Further analysis of the experiments excluded the first sampling point (up to and including t=2 minutes) for both HEART pump speeds to determine the effects of including or excluding the first few sampling points, and whether the HEART pump at 250 mL min<sup>-1</sup> facilitates better equation fits (Figure 2.4B). When the HEART pump was set to 132 mL min<sup>-1</sup>, exclusion of the first sampling point, which caused some deviation in these experiments, increased the r<sup>2</sup> value from 0.9675 to 0.9978. GraphPad Prism extra-sum-of-squares F tests of the two single-phase decay fits between the HEART pump at 132 mL min<sup>-1</sup> with and without inclusion of the first sampling point resulted in statistically significant changes for the C<sub>10</sub> (P value of 0.0019), and

the  $k_{el}$  (P value of 0.017). There is a clear difference in calculated  $V_D$  in experiments with the HEART pump set at  $132 \text{ mL min}^{-1}$  with and without the first sample point ( $127 \text{ mL}$  versus  $90.5 \text{ mL}$ ), with the latter representing a more realistic parameter for the one-compartment setting in the system.

Similarly, there were statistically significant changes for the single-phase decay fits between data obtained with the HEART pump at  $250 \text{ mL min}^{-1}$  with and without inclusion of the first sampling point also; the  $C_{t0}$  (P value of 0.0018), and the  $k_{el}$  (P value of 0.012) were significantly affected by the exclusion of the first sample point. The calculated  $V_D$  decreased, along with the  $CL_{Total}$  and half-life, which was consistent with the changes seen in the HEART at  $132 \text{ mL min}^{-1}$ .

Though the  $r^2$  value increased for the HEART pump at  $250 \text{ mL min}^{-1}$  versus  $132 \text{ mL min}^{-1}$  under either analysis condition, suggesting a marginally better overall fit with the faster HEART pump rate, it is unclear whether the increased rate of the HEART pump, and the resulting increase in pressure within the system, could have increased clearance mediated by the liver and kidney pumps (these were only calibrated with the HEART pump set at  $132 \text{ mL min}^{-1}$ ). The HEART pump rate of  $250 \text{ mL min}^{-1}$  did not appear to cause an appreciable change in distribution than a rate of  $132 \text{ mL min}^{-1}$  in the system, as shown by Figure 2.4A. While the equation fits were slightly improved with the HEART pump at  $250 \text{ mL min}^{-1}$ , the use of the HEART pump at  $132 \text{ mL min}^{-1}$  with the exclusion of the first few sample points (if required) generates reasonable equation fits, translating into reasonable calculations for the drug's PK parameters.

HEART pump setting was  $132 \text{ mL min}^{-1}$  for ALL experiments (1- and 2- compartment).

All data analyses in the ONE compartment configuration were done with points obtained no earlier than 2 minutes after drug administration.

Early sampling points (2-4 minutes) that were clearly outliers were excluded from the general data fit.

### 2.3.5 DIALYSIS MEMBRANE

Prior to inclusion of the TISSUE pump and tissue compartment in the apparatus, the use of a dialysis membrane to mimic two-compartment drug distribution was explored. A circuit parallel to the central compartment contained a length of dialysis membrane immersed in a container of water. The dialysis membrane had a high molecular weight cut-off (1,000 kDa), and the assumption was that methylene blue would move rapidly across the membrane between the circulation and the container of water, mimicking the distribution of drug into tissues. Unfortunately, diffusion of drug out of the dialysis membrane into the water was extremely slow; diffusion was much slower than the simultaneous elimination of drug from the central compartment via LIVER and KIDNEY 1 pumps, and the resulting concentration *versus* time profile resembled one-compartment kinetics. Subsequently, the introduction of the TISSUE pump and air-tight tissue compartment allowed for more flexibility in terms of perfusion rates and fluid volumes, and was used instead of the dialysis membrane.

### 2.3.6 TISSUE PUMP AND COMPARTMENT SETTINGS

Consideration of the sampling schedule, tissue compartment volume, and TISSUE pump rate is important for two-compartment distribution kinetics. A TISSUE pump flow rate that is too rapid, combined with a tissue compartment volume that is too low, may not achieve the desired modelling of two-compartment distribution behaviour. In addition, if the first plasma sample is not collected soon enough, then there is also a possibility that the distribution phase may not be apparent, as all samples could be collected after distribution has already occurred. Figure 2.5 emphasises these limitations. Though the apparatus was theoretically set to a “Two-Compartment” configuration, the results in Figure 2.5C, shown on a semi-logarithmic plot, reveal a linear relationship, reminiscent of 1-compartment distribution kinetics. Indeed, the analysis of Table 2.5 compares a single-exponential decay fit to a bi-phasic exponential decay fit. Interestingly, elimination parameters,  $C_{t0}$ , and even the  $r^2$  values are identical between the two analyses. Attempts by the bi-phasic exponential decay regression to calculate  $k_{dist}$  and  $t_{1/2 dist}$  values from the data were clearly inappropriate. The conclusions drawn from this

experiment set the limits of the apparatus in terms of TISSUE pump rate and compartment volume, and revealed the importance of sampling frequently (every ~20 seconds) within the first five minutes when using a two-compartment configuration.

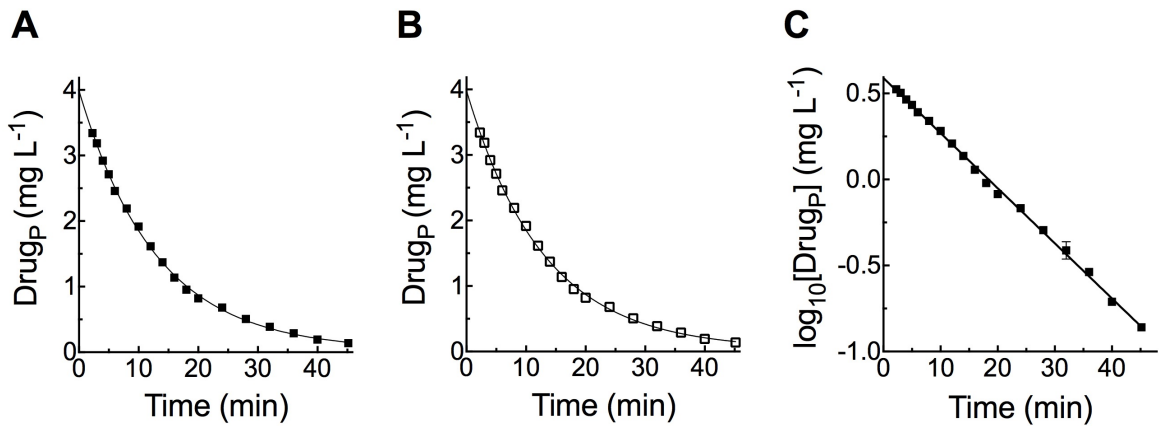


**Figure 2.5 Consideration to TISSUE pump and Compartment Settings.**

Calculated PK parameters are shown in Table 2.5. HEART pump: 132 mL min<sup>-1</sup>, LIVER pump: 7 mL min<sup>-1</sup>, TISSUE pump: 44 mL min<sup>-1</sup>, TISSUE compartment volume: 70 mL, KIDNEY 1 pump: 3 mL min<sup>-1</sup>, KIDNEY 2 pump: 4 mL min<sup>-1</sup>. **(A)** Plasma data following a single IV dose (0.96) mg administered into the modeller in a two-compartment configuration and fitted to a two-phase exponential decay equation (■) **(B)** Same data shown in (A) fitted to a one-phase exponential decay equation (□). **(C)** Data shown in (A) and (B) on a logarithmic y-axis and fitted to a linear regression line.

Figure 2.5 Plasma Analysis			
Liver Pump Setting		14 mL min <sup>-1</sup>	
Kidney 1 Pump Setting; Kidney 2 Pump Setting		3 mL min <sup>-1</sup> ; 4 mL min <sup>-1</sup>	
Tissue Pump Setting; Tissue Compartment Volume		44 mL min <sup>-1</sup> ; 70 mL	
Drug Dose: 0.96 mg		Acute Intravenous Administration	
PK Parameter	Equation/Method Used	Figure 2.5A <input checked="" type="checkbox"/>	Figure 2.5B <input type="checkbox"/>
C <sub>10</sub>	<input checked="" type="checkbox"/> Two-Phase Exponential Decay Fit	3.99 mg L <sup>-1</sup>	
	<input type="checkbox"/> One-Phase Exponential Decay Fit	3.99 mg L <sup>-1</sup>	
k <sub>dist</sub>	<input checked="" type="checkbox"/> Two-Phase Exponential Decay Fit	0.00929 min <sup>-1</sup>	
t <sub>1/2 dist</sub>	<input type="checkbox"/> Two-Phase Exponential Decay Fit	74.7 min	
k <sub>el</sub>	<input checked="" type="checkbox"/> Two-Phase Exponential Decay Fit	0.0779 min <sup>-1</sup>	
	<input type="checkbox"/> One-Phase Exponential Decay Fit	0.0776 min <sup>-1</sup>	
t <sub>1/2 el</sub>	<input checked="" type="checkbox"/> Two-Phase Exponential Decay Fit	8.9 min	
	<input type="checkbox"/> One-Phase Exponential Decay Fit	8.9 min	
AUC <sub>0-∞</sub>	AUC <sub>0-∞</sub> = AUC + C <sub>tn</sub> / k	53.0 min · mg L <sup>-1</sup>	
V <sub>D</sub>	V <sub>D</sub> = Dose / C <sub>10</sub>	241 mL	
CL <sub>Total</sub>	CL <sub>Total</sub> = Dose / AUC	18.1 mL min <sup>-1</sup>	
r <sup>2</sup>	<input checked="" type="checkbox"/> Two-Phase Exponential Decay Fit	0.9987	
	<input type="checkbox"/> One-Phase Exponential Decay Fit	0.9987	
Elimination Phase			
Y-intercept	Linear-Regression Line	0.590	
B	10 <sup>Y-intercept</sup>	3.89 mg L <sup>-1</sup>	
slope	Linear-Regression Line	-0.0320	
β	β = slope x 2.303	0.074 min <sup>-1</sup>	
t <sub>1/2 el</sub>	t <sub>1/2 el</sub> = 0.693 / β	9.4 min	
r <sup>2</sup>	Linear-Regression Line	0.9984	

Table 2.5 PK parameters calculated for TISSUE pump and compartment settings.

PK parameters calculated from drug-plasma concentrations shown in Figure 2.5.

### 2.3.7 OIL IN THE TISSUE COMPARTMENT WITH PH CHANGES IN SYSTEM

Generally, lipid-soluble molecules move freely into the fat deposits of the body, while charged compounds are not lipid-soluble. Weak acids and weak bases are influenced by the pH of their

environment, which controls the extent of the ionisation of the molecules and the charge. Notably, infusion therapy of certain buffers is sometimes used to influence the pH of blood or urine to invoke movement of drug from tissues into the blood and then into the urine for elimination.

To mimic more complexity and provide further visualisation to students on the concept of drug partitioning into and out of tissues, ~50 mL of regular cooking oil was introduced into the tissue compartment containing 100 mL of water, and the lower water layer was stirred gently. Neutral Red ( $pK_A$  6.8) was used as the drug, as methylene blue, which is charged, does not partition into oil. To generate an uncharged species of Neutral Red, and facilitate partitioning into the oil, the pH of the system was adjusted accordingly. As the fluid within the system is unbuffered water, its pH was easily changed with the addition of NaOH into the drinking water reservoir and also with IV administration through the injection port (E). The NaOH was circulated within the system for ~30 minutes, and prior to the experiment, the pH of the tissue compartment was measured as 11.90; this is well above the drug's  $pK_A$  of 6.7. Prior to administration, neutral red was converted to its basic form with addition of a very small amount of NaOH. The drug was administered into the system, and sample points were collected.

The yellow colour apparent under basic conditions, indicative of non-ionised drug, had a calculated molar absorption coefficient of  $4,184 \text{ M}^{-1}\text{cm}^{-1}$ , while the acidic, ionised drug form had a molar absorption coefficient of  $31,310 \text{ M}^{-1}\text{cm}^{-1}$ . Indeed, when the samples were collected from the modeller, each sample showed a very faint yellow colour, which was almost indiscernible; there were concerns that due to the low molar absorbance coefficient, the plate reader would not be able to quantify small differences between samples, introducing increased error in the analysis. Thus,  $2 \mu\text{L}$  of 12M HCl was added to each sample (~1 mL) that was collected during the experiment, which shifted the equilibrium, resulting in the charged, red species. The acidic samples were read in the plate reader at 530nm, converted to concentrations, and the resulting data plots were analysed for PK parameters. Figure 2.6 displays the results of the neutral red and oil experiment, with Table 2.6 discussing the calculated PK parameters. Figure 2.6A displays the biphasic decay fit to the data, while Figure 2.6B displays the method of

residuals results of both distribution and elimination. Figure 2.6C and D were included to show the linear regression fits to the terminal and distribution phase, respectively.

The inclusion of the oil in the tissue compartment, and the data analysis of Neutral Red administration show that the sample points were more scattered in comparison to experiments conducted using methylene blue under the same experimental conditions. The conversion of uncharged species samples into the charged species for absorbance reading introduced error and probably contributed to the scattered plots.

The dose of neutral red administered was 7.2 mg; a significantly higher amount than was used when methylene blue was injected. The rationale for this experiment was that there would be significant partitioning of the drug into the oil, and as such, a larger amount of drug would provide a more dramatic visual. Given that the uncharged species of neutral red is a yellow colour, it was hoped that use of a large drug dose would allow the colour of the dye to be evident within the oil layer, providing a visual display of drug partitioning for students.

Unfortunately, the colour proved barely discernible in the oil, while the  $t_{1/2\text{ el}}$  and  $t_{1/2\text{ dist}}$  for neutral red were consistent with other experiments run under the same apparatus settings but without oil in the compartment and using methylene blue (0.96 mg) as the drug. It was possible that the neutral red did not partition into the oil to any great degree during the time course of the experiment. However, some differences in the  $k_{12}$  and  $k_{21}$  values were observed, as was a slight increase in  $V_{D\text{ Aarea}}$  as compared to experiments conducted with methylene blue without the oil in the compartment (461 mL versus 301 mL).

Thus, using Neutral Red for the experiment with oil in the tissue compartment did not meet the objectives of providing a dramatic visual of drug partitioning, as the colour of the drug and oil were too similar. In addition, while it is probable that some of the drug partitioned into the oil, the PK parameters did not indicate that drug partitioning occurred to any great degree within the time-frame of the experiment. Finally, adjusting the pH of the system and the drug throughout the experiment created extra time constraints in running the demonstration for

students. For all of these reasons, the use of this approach to create a visual demonstration of partitioning was not pursued.

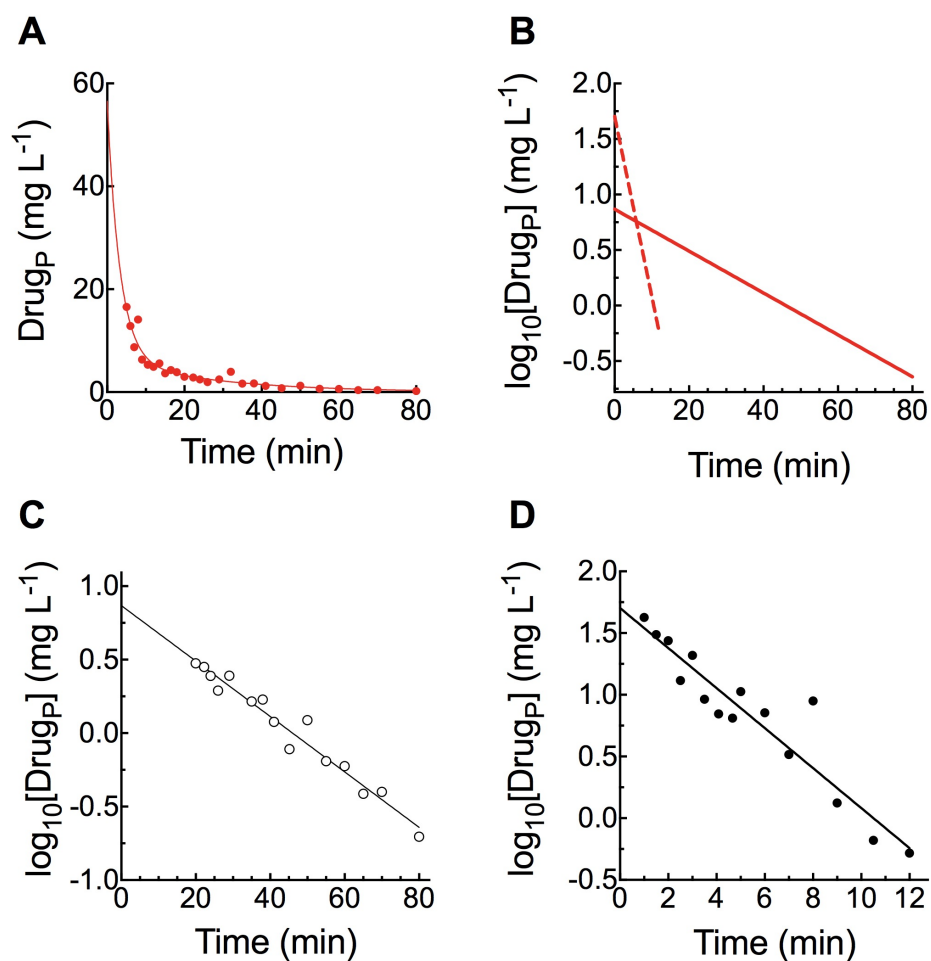


**Figure 2.6** The use of neutral red and oil in the tissue compartment.

Calculated PK parameters are shown in Table 2.5. HEART pump:  $132 \text{ mL min}^{-1}$ , LIVER pump:  $10 \text{ mL min}^{-1}$ , TISSUE pump:  $12 \text{ mL min}^{-1}$ , TISSUE compartment volume:  $100 \text{ mL water}$ ,  $50 \text{ mL oil}$ , KIDNEY 1 pump:  $3 \text{ mL min}^{-1}$ , KIDNEY 2 pump:  $4 \text{ mL min}^{-1}$ . **(A)** Plasma data of single IV dose ( $7.2 \text{ mg}$ ) neutral red administered into the modeller in a two-compartment configuration and fitted to a two-phase exponential decay equation ( $\bullet$ ) **(B)** Linear regression fits of data in (A) plotted on a logarithmic y-axis following curve-stripping to separate the distribution and elimination phases. **(C)** Terminal phase data (O) from (A) plotted on a logarithmic y-axis. **(D)** Distribution phase data ( $\bullet$ ) of (A) plotted on a logarithmic y-axis.

Figure 2.6 Plasma Analysis		
Tissue Pump Setting		12 mL min <sup>-1</sup>
Kidney 1 Pump Setting; Kidney 2 Pump Setting		3 mL min <sup>-1</sup> ; 4 mL min <sup>-1</sup>
Liver Pump Setting		10 mL min <sup>-1</sup>
Tissue Compartment Volume: Water		100 mL
Tissue Compartment Volume: Oil		50 mL
Neutral Red, Drug Dose: 7.2 mg		Acute Intravenous Administration
<b>PK Parameter</b>	<b>Equation/Method Used</b>	
<b>C<sub>t0</sub></b>	Two-Phase Exponential Decay Fit	56.5 mg L <sup>-1</sup>
<b>k<sub>dist</sub></b>	Two-Phase Exponential Decay Fit	0.306 min <sup>-1</sup>
<b>t<sub>1/2 dist</sub></b>	Two-Phase Exponential Decay Fit	2.3 min
<b>k<sub>el</sub></b>	Two-Phase Exponential Decay Fit	0.0373 min <sup>-1</sup>
<b>t<sub>1/2 el</sub></b>	Two-Phase Exponential Decay Fit	18.6 min
<b>AUC<sub>0-∞</sub></b>	$AUC_{0-∞} = AUC + C_{pn}/k$	359.9 min · mg L <sup>-1</sup>
<b>V<sub>D SS</sub></b>	$V_{D SS} = (Dose \times (A / \alpha^2 + B / \beta^2)) / AUC^2$	238 mL
<b>V<sub>D Area</sub></b>	$V_{D Area} = Dose / (AUC \times \beta)$	461 mL
<b>V<sub>D Extrap</sub></b>	$V_{D Extrap} = Dose / B\text{-intercept}$	977 mL
<b>CL<sub>Total</sub></b>	$CL_{Total} = Dose / AUC_{0-∞}$	20.0 mL min <sup>-1</sup>
<b>r<sup>2</sup></b>	Two-Phase Exponential Decay Fit	0.9209
<b>Elimination Phase</b>		
<b>Y-intercept</b>	Linear-Regression Line	0.8677
<b>B</b>	$10^{Y\text{-intercept}}$	7.37 mg L <sup>-1</sup>
<b>slope</b>	Linear-Regression Line	-0.01886
<b>β</b>	$\beta = \text{-slope} \times 2.303$	0.0434 min <sup>-1</sup>
<b>t<sub>1/2 el</sub></b>	$t_{1/2 el} = 0.693 / \beta$	16.0 min
<b>r<sup>2</sup></b>	Linear-Regression Line	0.9594
<b>Distribution Phase</b>		
<b>Y-intercept</b>	Linear-Regression Line	1.703
<b>A</b>	$10^{Y\text{-intercept}}$	50.5 mg L <sup>-1</sup>
<b>slope</b>	Linear-Regression Line	-0.1621
<b>α</b>	$\alpha = \text{-slope} \times 2.303$	0.373 min <sup>-1</sup>
<b>t<sub>1/2 dist</sub></b>	$t_{1/2 dist} = 0.693 / \alpha$	1.9 min
<b>r<sup>2</sup></b>	Linear-Regression Line	0.8886
<b>k<sub>12</sub></b>	$k_{12} = (AB \times (\beta - \alpha)^2) / ((A+B) \times (A\beta + Ba))$	0.141 min <sup>-1</sup>
<b>k<sub>21</sub></b>	$k_{21} = (A\beta + Ba) / (A + B)$	0.085 min <sup>-1</sup>
<b>k<sub>10</sub></b>	$k_{10} = (\alpha\beta \times (A + B)) / (A\beta + Ba)$	0.190 min <sup>-1</sup>

Table 2.6 PK parameters calculated with neutral red as drug and oil in the TISSUE compartment. PK parameters calculated from drug-plasma concentrations shown in Figure 2.6.

### 2.3.8 MIMICKING ORAL BIOAVAILABILITY

Initial designs of the apparatus did not include an ORAL BIOAVAILABILITY pump; the complete dose of drug entering the stomach compartment would reach systemic circulation. There was no barrier to “absorption” and the bioavailability for all orally administered drugs was 100%. Prior to the addition of the ORAL BIOAVAILABILITY pump, the dose of an orally administered drug was altered to reflect the predicted F as compared to the IV dose. Thus, if the IV dose was 1 mg, and the goal of PO dosing was 70% bioavailability, only 0.7mg of the drug would be administered, while all other factors (pump settings, etc.) would be held constant. Examples of both strategies are presented in this work, as the data are comparable, providing equally valid PK analyses. The ORAL BIOAVAILABILITY pump addition serves to add a more physiological approach to drug absorption, and provides a visual representation of the first pass effect.

Early testing of the apparatus also involved freezing a small volume of methylene blue solution, and administering the dose straight into the stomach compartment in the form of an ice cube. To reduce errors associated with drug loss in the form of residue in the ice cube tray and loss during transfer to the stomach, liquid solutions of the drug are now administered; only the results of PO solution administration are presented in this work.

### 2.3.9 PLATEAU CONSTRAINTS

One-compartment IV modelling data are fitted to a single phase decay equation, and because there are few variables to consider for this approach, analysis is generally straightforward, and PK parameters are calculated without issues of ambiguity. In contrast, two-compartment modelling is more complex because of the additional variables that the software must consider while fitting the data. To reduce ambiguity associated with dependent variables and a failure of the graphing software to calculate best-fit parameters, the plateau of two-compartment drug analysis was constrained to 0, and all PK parameters were then determined based on the fit provided. Without the plateau constraint, the software often provided an “ambiguous fit” due to the number of dependent variables. One further reason as to why constraining the plateau

increases success with two-compartment model fitting is that after most of the drug has been cleared from the system, the sample absorbance values are very small, and there may be a large relative degree of error in measuring absorbances at these later data points. Determination of the plateau by the regression software would thus be more difficult; use of a plateau constraint following subtraction of an appropriate blank value helps in this regard.

### **2.3.10 USE OF $V_{D \text{ EXTRAP}}$ IN CHRONIC DOSING**

The  $V_{D \text{ Extrap}}$  value, calculated by the equation  $V_{D \text{ Extrap}} = \text{Dose} / \text{B-intercept}$  in the two-compartment configuration, is significantly higher than the sum of the central and peripheral compartment volumes. The value overestimates the volume of the system, and is generally not the most appropriate to use for chronic dosing regimens (Winter, 2010).

However, extrapolating the B-intercept and subsequently using it for the estimation of " $V_D$ " is the method most commonly taught to undergraduate students; the approach mirrors the calculation of  $V_D$  in the one-compartment model. Because the approach was most familiar to students, the chronic dosing regimens shown in the results section were typically calculated using the  $V_{D \text{ Extrap}}$  value rather than using any of the other calculated volume terms. Generally, the  $V_{D \text{ Extrap}}$  value, though higher than other calculated volume terms, did not deviate excessively from them, and was appropriate for the context. Though some dosing regimens resulted in drug levels slightly above the target  $C_{SS}$ , generally, the use of the  $V_{D \text{ Extrap}}$  yielded suitable drug levels within the system.

### **2.3.11 USE OF PK SOLVER FOR SYSTEM VALIDATION**

The authenticity of data generated by the modeller was also assessed through use of a no-cost add-in program for Microsoft Excel, PKSolver (Zhang, Huo, Zhou & Xie, 2010); this analytical tool is similar to Phoenix WinNonlin, a PK modelling software package used by many pharmaceutical companies. Appendix I shows example data from the results section as analysed by PK solver.

## 2.3 IN THE CLASSROOM

The modeller was introduced into a third-year experimental course for undergraduate pharmacology students at the University of Alberta, in two consecutive practical classes. During the classes, students worked in small groups on a dedicated apparatus to obtain PK constants in their patient, and then used these values to design a chronic dosing regimen. During the initial class, students administered a single dose of methylene blue to their patient by the IV and PO routes and collected blood and urine samples at suitable intervals prior to analysing concentration-time profiles. Prior to the second class, students were asked to design two chronic dosing regimens (an IV infusion regimen and a repeated oral dosing regimen in which peak and trough concentrations were required not to exceed the upper and lower limits of a therapeutic window) based upon PK parameters calculated from data obtained in the initial class. Patients were then subjected to both chronic regimens; once again, students sampled blood and generated plasma concentration-time profiles to confirm that PK targets had been achieved.

Students who had previously been exposed to principles of PK for 10 hours in a second year lecture-based course were also divided into two similar groups based upon examination performance. Before the first practical class, students completed a 7-question multiple choice test involving PK calculations, with each group issued one of two different test versions. Students were permitted unlimited time to complete the test. Following the second practical class, students completed the version of the test that they had not previously answered. Students were also asked to complete a self-assessment of their confidence and competence working with PK concepts and calculations. Consent was obtained to use results from tests and self-assessments, as approved by the Human Ethics Research Board at the University of Alberta (Study ID Pro00056323).

## 2.4 MATERIALS AND CALIBRATIONS

All peristaltic pumps were purchased from VWR (Mississauga, Ontario) and were supplied with several different diameters of tubing that could be inserted between the rollers on the pump head to allow a wide range of flow rates; each pump has a FAST or SLOW setting calibration. Flow rates for FAST or SLOW settings for each pump are shown in Figure 2.7, with data fitted to a linear regression, and line equations shown in the legends. HEART pump (model 3389, medium-high flow; 4-600 mL min<sup>-1</sup>) was calibrated gravimetrically for flow rates between 120 and 250 mL min<sup>-1</sup> using 4.8 mm tubing diameter (Figure 2.7A). All other pump units were calibrated gravimetrically *in situ*, with the HEART pump circulating water at 132 mL min<sup>-1</sup>, since pressure generated by the heart pump within the main circuit could cause modest effects on fluid movement through other pump units.

The LIVER and ORAL BIOAVAILABILITY pumps (model 3386, medium flow; 0.4-85 mL min<sup>-1</sup>) were calibrated for flow rates between 2.4 and 7.7 mL min<sup>-1</sup> (tubing diameter 1.6 mm), and between 7.7 and 17 mL min<sup>-1</sup> (tubing diameter 2.4 mm), respectively (Figure 2.7B). The TISSUE pump (also model 3386) was calibrated for flow rates between 2.4 and 50 mL min<sup>-1</sup> (Figure 2.7B and C). KIDNEY pumps (model 3385, low flow; 0.03-8.2 mL min<sup>-1</sup>) were calibrated for flow rates between 2.5 and 5.0 mL min<sup>-1</sup> using tubing diameter of 4.8 mm (Figure 2.7D). KIDNEY pumps were run simultaneously to achieve a combined flow rate of around 8 mL min<sup>-1</sup>. In addition, another low flow pump, model 3385, was calibrated between 0.85 mL min<sup>-1</sup> and 1.2 mL min<sup>-1</sup> using tubing diameter of 2.4 mm (Figure 2.7E) for experiments involving continuous or intermittent IV infusion.

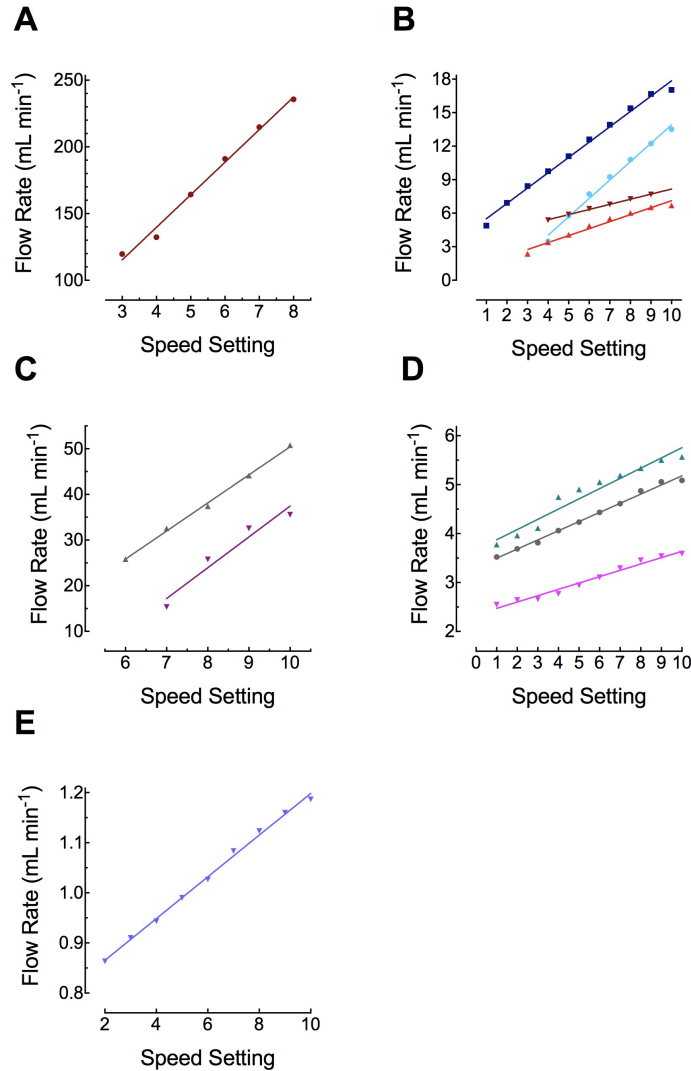


**Figure 2.7 Pump Calibrations.**

(A) Pump IV calibrations (●) used for HEART pump at FAST settings using 4.8 mm tubing diameter, resulting in flow rates of 120 – 250 mL min<sup>-1</sup> and fitted to a linear regression line. Equation:  $Y = 24.4X + 42.08$ . (B) Pump III calibrations with HEART pump at 132 mL min<sup>-1</sup> used for LIVER, TISSUE, and ORAL BIOAVAILABILITY pumps at FAST and SLOW settings using tubing diameter 2.4 mm and 1.6 mm. The flow rates varied between 3 – 18 mL min<sup>-1</sup>. 2.4 mm SLOW (●) ( $Y = 1.65X - 2.57$ ) and 2.4 mm FAST (■) ( $Y = 1.37X + 4.1$ ), 1.6 mm SLOW (▲) ( $Y = 0.63X + 0.87$ ) and 1.6 mm FAST (▼) ( $Y = 0.46X + 3.58$ ). (C) Pump III calibrations with HEART pump at 132 mL min<sup>-1</sup> used for LIVER, TISSUE, and ORAL BIOAVAILABILITY pump at FAST and SLOW settings using tubing diameter 4.8 mm. The flow rates varied from 15 – 50 mL min<sup>-1</sup>. SLOW (▼) ( $Y = 6.74X - 30$ ) and FAST (▲) ( $Y = 6.15X - 11.1$ ). (D) Pump II calibrations with HEART pump at 132 mL min<sup>-1</sup> used for KIDNEY 1 and KIDNEY 2 pumps at FAST and SLOW settings using tubing diameter 4.8 mm. The flow rates varied from 2.5 – 5 mL min<sup>-1</sup>. KIDNEY 1 SLOW (▼) ( $Y = 0.13X - 18.1$ ), KIDNEY 1 FAST (▲) ( $Y = 0.21X + 3.66$ ), KIDNEY 2 SLOW (●) ( $Y = 0.19X + 3.3$ ). (E) Pump II calibrations with HEART pump at 132 mL min<sup>-1</sup> used for IV INFUSION pump at FAST setting using tubing diameter 2.4 mm. The flow rates were between 0.85 and 1.2 mL min<sup>-1</sup>. IV INFUSION FAST (▼) ( $Y = 0.042X + 0.78$ ).

Drinking water drained into the circulatory system *via* the stomach from a 5000 mL Kimax Reservoir bottle (VWR). The tissue compartment was comprised of a 250 mL or 1000 mL storage/media bottle (VWR) with a screw cap equipped with two hose connectors and air-tight gasket, manufactured by Duran Group (Mainz, Germany) and purchased as a special order item from Fisher Scientific (Ottawa, Ontario). The stomach was manufactured from a 50 mL conical centrifuge tube (Eppendorf; Mississauga, Ontario), with a hole drilled through the base of the tube and a luer-to-tubing barb fitting inserted and cemented in place. The tube was sealed with a rubber stopper drilled to accommodate three stainless tubes (3/32" od), onto which short lengths of Tygon tubing (1/16" id) were attached to accommodate insertion of luer fittings or cannulae.

The circulatory system was comprised of Tygon tubing (1/4" id, 3/8" od), with a total volume for the main circuit of approximately 100 mL. Tubing was attached to other components of the apparatus through a variety of nylon luer fittings (Cole-Parmer, Montréal, Québec): 1-way stopcocks (catalogue 30600-00), 3-way stopcocks (30600-02), T-connectors 1/4" (40610-30), Y-connectors 1/4" (40726-45), female luer fittings 1/4" (45502-20), male luer lock rings 1/4" (45505-19), wide-bore luer adapters - male luer lock to 1/16" id (45505-31), male luer plugs (45505-56) and several items from a luer fittings kit (45511-00). Polyethylene tubing (1.19 mm id, 1.7 mm od; Becton Dickinson, Mississauga, Ontario) served to facilitate introduction of drug to the stomach from a syringe, to drain fluid from the system into hepatic or renal waste, to redirect a portion of the circulation *via* a flow-through cuvette, or as a conduit from the sampling tap.

Methylene blue was purchased from Sigma-Aldrich (Oakville, Ontario). Neutral Red was purchased from Sigma-Aldrich (Oakville, Ontario). Absorbance values of samples (300 µl) were read in polystyrene microplates (Greiner Bio-One; VWR), in a FlexStation 3 (Molecular Devices, Sunnyvale, California) with PathCheck activated. In some experiments, drug concentration was monitored continuously in a glass flow-through cuvette, in a Cary 60 UV-Visible spectrophotometer (Agilent Technologies, Mississauga, Ontario).

## CHAPTER 3: RESULTS

The following will illustrate the physiological conditions that the ADAM is capable of mimicking. The experiments include single dose IV and PO administration in one-compartment and two-compartment configurations. As noted, the ORAL BIOAVAILABILITY pump was added to the ADAM in the later stages of development of the apparatus, and as such, some of the data presented will include the earlier form of modelling oral bioavailability (i.e. administering a lower dose, compared with the IV dose). Chronic dosing experiments include multi-IV administration, multi-PO administration, continuous IV infusion, intermittent IV infusion, and dosing with a loading dose. This section illustrates the physiological complexity and clinical applications that the modeller can simulate. Data collected from students in the laboratory course will also be presented, including quiz results and questionnaire answers, illustrating that the apparatus has a positive impact on student learning and performance.

### 3.1 ONE COMPARTMENT MODELLING

Drug can be circulated throughout the main circuit, with diversion taps closed to isolate the tissue compartment, and facilitate one-compartment kinetics. In one-compartment kinetics, drug distribution is instantaneous or extremely rapid, and the ADAM models this in a straightforward manner.

Figure 3.1A shows results from experiments in a one-compartment configuration where an identical dose of drug (0.32 mg) was administered intravenously into the system with LIVER and KIDNEY 1 pumps altered between experiments to mimic inter-individual variability (the KIDNEY 2 pump was altered accordingly). The experiments were conducted with the LIVER pump set at 7 or 14 mL min<sup>-1</sup>, and the KIDNEY 1 pump set at 3 or 4 mL min<sup>-1</sup>, depicting increased or decreased clearance in the simplest configuration. The data were fitted to a single-phase exponential decay equation. Figure 3.1B is a semi-logarithmic plot of the data in Figure 3.1A, with the straight line demonstrating the one-compartment behaviour of the drug.

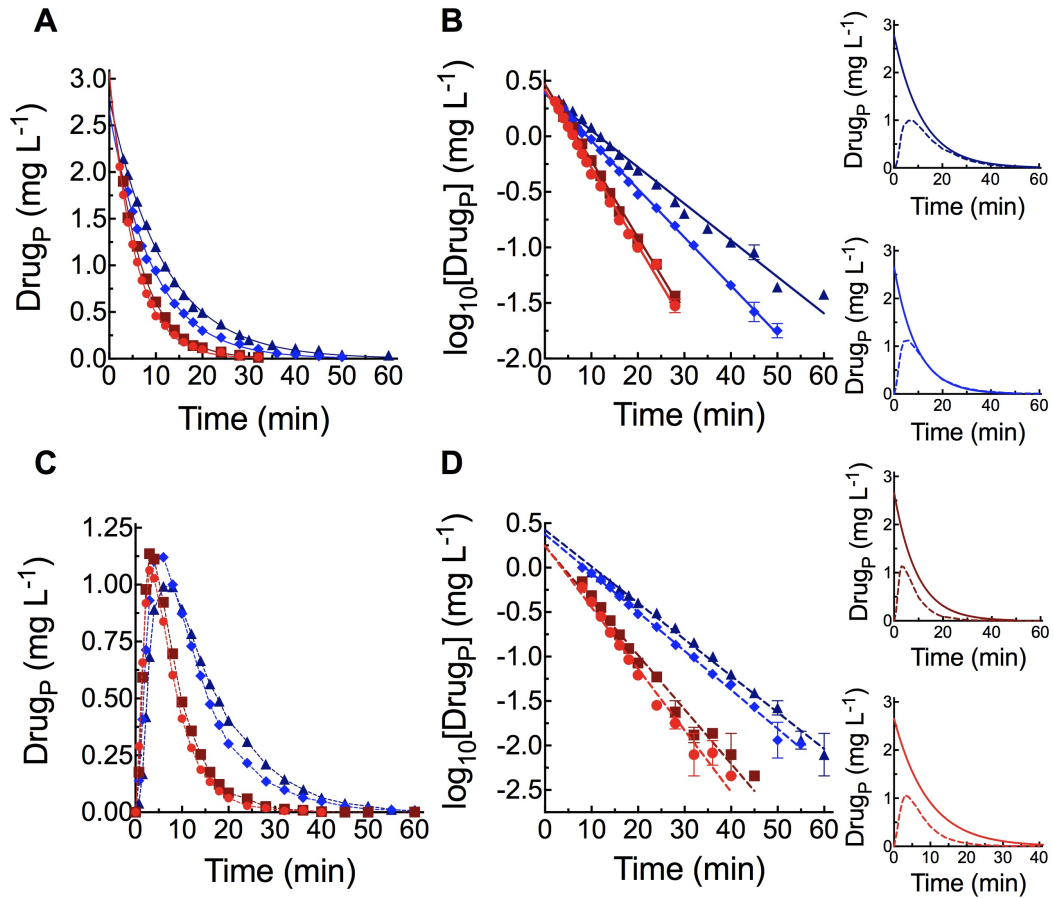


**Figure 3.1. One-compartment modelling of IV and PO drug-plasma concentrations under varied elimination pump settings.**

Calculated PK parameters are in Table 3.1. HEART pump setting:  $132 \text{ mL min}^{-1}$ . **(A)** Drug in plasma following IV administration ( $0.32 \text{ mg}$ ). Conditions were: LIVER pump  $7 \text{ mL min}^{-1}$  and KIDNEY 1 pump  $3 \text{ mL min}^{-1}$  ( $\blacktriangle$ ) or  $4 \text{ mL min}^{-1}$  ( $\blacklozenge$ ), and LIVER pump  $14 \text{ mL min}^{-1}$  and KIDNEY 1 pump  $3 \text{ mL min}^{-1}$  ( $\blacksquare$ ) or  $4 \text{ mL min}^{-1}$  ( $\bullet$ ). **(B)** Classic semi-logarithmic plot of IV elimination data from (A) **(C)** Drug in plasma following PO administration ( $0.22 \text{ mg}$ ). Conditions were: LIVER pump  $7 \text{ mL min}^{-1}$  and KIDNEY 1 pump  $3 \text{ mL min}^{-1}$  ( $\blacktriangle$ ) or  $4 \text{ mL min}^{-1}$  ( $\blacklozenge$ ), and LIVER pump  $14 \text{ mL min}^{-1}$  and KIDNEY 1 pump  $3 \text{ mL min}^{-1}$  ( $\blacksquare$ ) or  $4 \text{ mL min}^{-1}$  ( $\bullet$ ). **(D)** Classic semi-logarithmic plot of IV elimination data from (C) Each inset graph compares the corresponding PO data (dotted line) to the IV data (solid line) from experiments conducted under identical conditions (colours correspond to (A) and (B)).

Figure 3.1 Plasma Analysis					
Figure 3.1 A and B					
Liver Pump Setting		7 mL min <sup>-1</sup>		14 mL min <sup>-1</sup>	
Kidney 2 Pump Setting		5 mL min <sup>-1</sup>	3 mL min <sup>-1</sup>	5 mL min <sup>-1</sup>	3 mL min <sup>-1</sup>
Kidney 1 Pump Setting		3 mL min <sup>-1</sup>	4 mL min <sup>-1</sup>	3 mL min <sup>-1</sup>	4 mL min <sup>-1</sup>
Drug Dose: 0.32 mg		Acute Intravenous Administration			
PK Parameter	Equation/Method Used	▲	◆	■	●
C <sub>10</sub>	Single-Phase Exponential Decay Fit	2.79 mg L <sup>-1</sup>	2.66 mg L <sup>-1</sup>	3.03 mg L <sup>-1</sup>	3.07 mg L <sup>-1</sup>
k	Single-Phase Exponential Decay Fit	0.086 min <sup>-1</sup>	0.11 min <sup>-1</sup>	0.17 min <sup>-1</sup>	0.18 min <sup>-1</sup>
t <sub>1/2</sub>	Single-Phase Exponential Decay Fit	8.1 min	6.5 min	4.3 min	3.8 min
AUC <sub>0-∞</sub>	AUC <sub>0-∞</sub> = C <sub>10</sub> / k	32.4 min · mg L <sup>-1</sup>	24.2 min · mg L <sup>-1</sup>	17.8 min · mg L <sup>-1</sup>	16.2 min · mg L <sup>-1</sup>
V <sub>D</sub>	V <sub>D</sub> = Dose / C <sub>10</sub>	115 mL	120 mL	106 mL	104 mL
CL <sub>Total</sub>	CL <sub>Total</sub> = k x V <sub>D</sub>	9.9 mL min <sup>-1</sup>	13.2 mL min <sup>-1</sup>	17.9 mL min <sup>-1</sup>	19.8 mL min <sup>-1</sup>
r <sup>2</sup>	Single-Phase Exponential Decay Fit	0.9987	0.9978	0.9967	0.9986
Elimination Phase					
Y-intercept	Linear-Regression Line	0.3821	0.3962	0.470	0.420
C <sub>10</sub>	10 <sup>Y-intercept</sup>	2.41 mg L <sup>-1</sup>	2.49 mg L <sup>-1</sup>	2.95 mg L <sup>-1</sup>	2.63 mg L <sup>-1</sup>
slope	Linear-Regression Line	-0.0329	-0.0435	-0.0689	-0.0701
β	β = slope x 2.303	0.076 min <sup>-1</sup>	0.100 min <sup>-1</sup>	0.16 min <sup>-1</sup>	0.16 min <sup>-1</sup>
t <sub>1/2</sub>	t <sub>1/2</sub> = 0.693 / β	9.1 min	6.9 min	4.4 min	4.3 min
r <sup>2</sup>	Linear-Regression Line	0.9838	0.9947	0.9926	0.9905
Figure 3.1 C and D					
Drug Dose: 0.22 mg		Acute Oral Administration			
PK Parameter	Equation/Method Used	▲	◆	■	●
AUC <sub>0-∞</sub>	AUC <sub>0-∞</sub> = AUC + C <sub>10</sub> /k	18.2 min · mg L <sup>-1</sup>	17.3 min · mg L <sup>-1</sup>	10.7 min · mg L <sup>-1</sup>	9.4 min · mg L <sup>-1</sup>
F	F = (AUC <sub>PO</sub> / AUC <sub>IV</sub> ) x 100%	56.2%	71.9%	60.1%	58.0%
Elimination Phase					
Y-intercept	Linear-Regression Line	0.4242	0.3753	0.2385	0.2471
C <sub>10</sub>	10 <sup>Y-intercept</sup>	2.66 mg L <sup>-1</sup>	2.37 mg L <sup>-1</sup>	1.73 mg L <sup>-1</sup>	1.76 mg L <sup>-1</sup>
slope	Linear-Regression Line	-0.0410	-0.0437	-0.0611	-0.0692
β	β = slope x 2.303	0.094 min <sup>-1</sup>	0.10 min <sup>-1</sup>	0.14 min <sup>-1</sup>	0.16 min <sup>-1</sup>
t <sub>1/2</sub>	t <sub>1/2</sub> = 0.693 / β	7.3 min	6.9 min	4.9 min	4.3 min
r <sup>2</sup>	Linear-Regression Line	0.9807	0.9811	0.9642	0.9600

Table 3.1 PK parameters calculated from IV and PO drug-plasma concentrations shown in Figure 3.1.

Pharmacokinetic parameters calculated from one-compartment IV and PO dosing experiments after collecting plasma samples.

Figure 3.1C shows results from experiments where ~70% of the IV dose (0.22 mg) was administered orally for each different condition described above (this was prior to the addition of the ORAL BIOAVAILABILITY pump), with the aim of achieving 70% oral bioavailability with these experiments. However, setting the ORAL BIOAVAILABILITY pump to 0.43x the combined rates of the LIVER and KIDNEY 1 pumps, so that approximately 30% of the drug in the stomach would be transferred to the waste without ever reaching the systemic circulation, would provide equivalent results to these data. The PO data in Figure 3.1C were not fitted to an equation; rather, points were connected by straight lines. Figure 3.1D is a semi-logarithmic plot of the terminal phase of the data (PO dosing also exhibits an absorption phase that was excluded from the analysis). The inset graphs each depict visual comparisons of the IV and PO doses under identical conditions. Table 3.1 describes the analysis of the single-phase exponential decay fits, as well as the slopes from the linear regressions obtained through GraphPad software, with additional PK parameters obtained through calculations using Table 2.1 equations. The AUC values for each data set are calculated as shown in Table 3.1, and comparisons of the  $AUC_{PO}$  and  $AUC_{IV}$  allowed for oral bioavailability calculations, which ranged between 56 and 72%, which were reasonably close to the predicted 70% bioavailability.

The tubing of the main circuit representing the central compartment is approximately 100 mL in volume, and the  $V_D$  values calculated from IV dosing were within range of this value (between 104 and 120 mL). Theoretically, the  $V_D$  (or  $AV_D$ ) for one-compartment distribution represents the total volume into which a drug rapidly distributes, as drug is only administered and distributed within one homogenous compartment. Thus, if the calculated  $V_D$  of the drug is consistent with the volume of the central compartment in the apparatus, the results indicate that the ADAM successfully represents the relationship expected of one-compartment distribution kinetics.

By changing the LIVER or KIDNEY 1 pump rates, it was possible to model increased clearance in the system. During IV administration, when the LIVER pump was set at  $7 \text{ mL min}^{-1}$ , increasing the KIDNEY 1 pump resulted in a decreased half-life, decreased AUC, and increased  $CL_{Total}$ , as would be expected. When the LIVER pump was set to  $14 \text{ mL min}^{-1}$ , these PK values followed

the same trend as was seen with increased KIDNEY 1 pump settings. In addition, the doubling of the LIVER pump rate resulted in almost a two-fold decrease in half-life when compared between identical conditions, with decreases in AUC and  $CL_{Total}$ . Comparison of the semi-logarithmic plots between the IV and PO administration under each identical condition showed similarity in calculated slope values, calculated  $\beta$  values, and subsequent half-life values, indicating consistency in the settings.

In addition to plasma sampling, urinary data were collected for each experiment described in Figure 3.1, and the resulting data were graphed in Figure 3.2. The cumulative amount of drug in the urine following IV and PO administration is shown in Figure 3.2A, and Figure 3.2B, respectively. The data points are not fitted to an equation, but rather are connected with straight lines due to the complexity in urine data modelling, as described in Chapter 2. The plateau of the data in Figure 3.2A and B were determined by calculating the mean of the last three sample points, and is represented as the  $D_{\infty}$ . This value was used in the sigma minus beta method, which is represented in Figure 3.2C and Figure 3.2D for IV and PO administration, respectively. The urine data generated from the PO administration experiment (Figure 3.2B) showed some plateau deviation in comparison to the urine IV data. This could be attributed to the reduced dose circulating within the modeller, and the large margin of error associated with extremely small absorbance values at the later points.

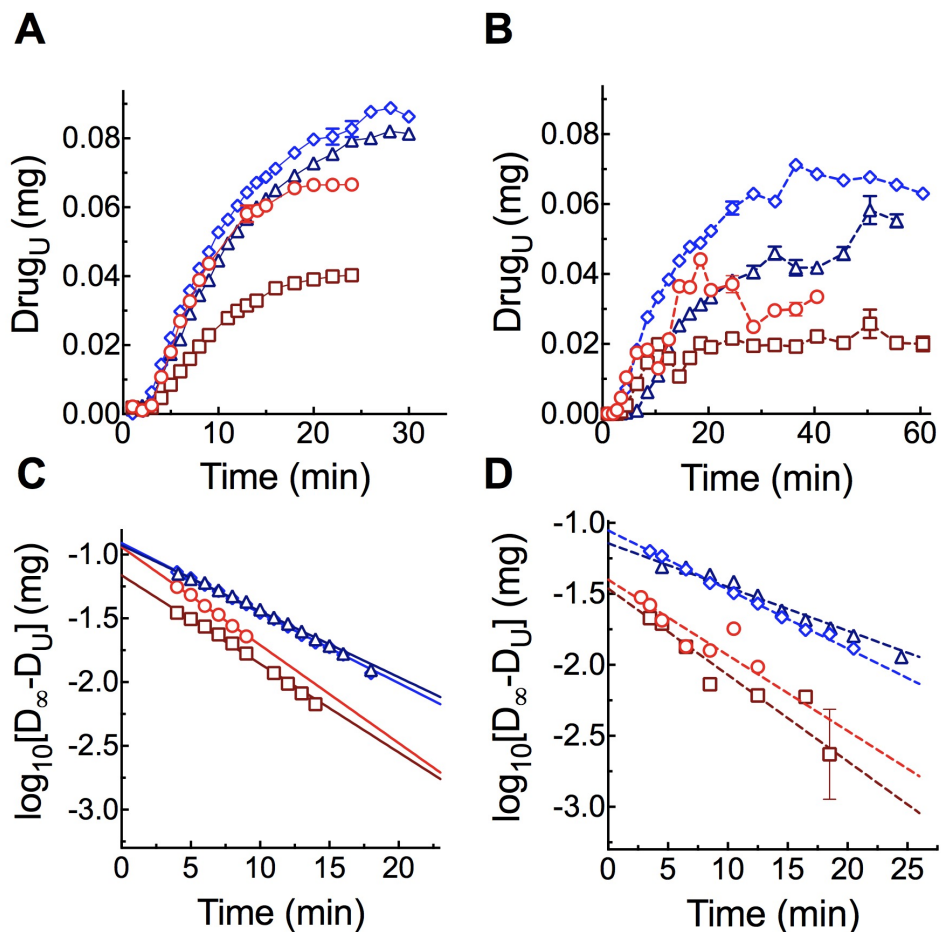


Figure 3.2. Complementary one-compartment modelling of IV and PO drug-urine concentrations for drug-plasma data shown in Figure 3.1.

Calculated parameters are shown in Table 3.2. HEART pump setting:  $132 \text{ mL min}^{-1}$ . **(A)** Cumulative drug in urine following IV administration (0.32 mg). Conditions were: LIVER pump  $7 \text{ mL min}^{-1}$  and KIDNEY 1 pump  $3 \text{ mL min}^{-1}$  ( $\Delta$ ) or  $4 \text{ mL min}^{-1}$  ( $\diamond$ ), and LIVER pump  $14 \text{ mL min}^{-1}$  and KIDNEY 1 pump  $3 \text{ mL min}^{-1}$  ( $\square$ ) or  $4 \text{ mL min}^{-1}$  ( $\circ$ ). **(B)** Cumulative drug in urine following PO administration (0.22 mg). Conditions were: LIVER pump  $7 \text{ mL min}^{-1}$  and KIDNEY 1 pump  $3 \text{ mL min}^{-1}$  ( $\Delta$ ) or  $4 \text{ mL min}^{-1}$  ( $\diamond$ ), and LIVER pump  $14 \text{ mL min}^{-1}$  and KIDNEY 1 pump  $3 \text{ mL min}^{-1}$  ( $\square$ ) or  $4 \text{ mL min}^{-1}$  ( $\circ$ ). **(C)** Analysis of IV data from (A) by the sigma-minus method. **(D)** Analysis of PO data from (B) by the sigma-minus method.

Figure 3.2 Urine Analysis					
Figure 3.2 A and C					
Liver Setting		7 mL min <sup>-1</sup>		14 mL min <sup>-1</sup>	
Kidney 1 Setting		3 mL min <sup>-1</sup>	4 mL min <sup>-1</sup>	3 mL min <sup>-1</sup>	4 mL min <sup>-1</sup>
Drug Dose: 0.32 mg		Acute Intravenous Administration			
PK Parameter	Equation/Method Used				
plateau (D <sub>∞</sub> )	Average of last three data points	0.0817 mg	0.0876 mg	0.0397 mg	0.0665 mg
slope	(D <sub>∞</sub> -D <sub>U</sub> ) non-linear regression line	-0.0517	-0.0550	-0.0694	-0.0768
β	β = slope x 2.303	0.12 min <sup>-1</sup>	0.13 min <sup>-1</sup>	0.16 min <sup>-1</sup>	0.18 min <sup>-1</sup>
t <sub>1/2</sub>	t <sub>1/2</sub> = 0.693 / β	5.8 min	5.5 min	4.3 min	3.9 min
CL <sub>R</sub>	CL <sub>R</sub> = (Plateau / Total Dose) x CL <sub>Total</sub>	2.5 mL min <sup>-1</sup>	3.6 mL min <sup>-1</sup>	2.2 mL min <sup>-1</sup>	4.1 mL min <sup>-1</sup>
CL <sub>H</sub>	CL <sub>H</sub> = CL <sub>Total</sub> - CL <sub>R</sub>	7.4 mL min <sup>-1</sup>	9.6 mL min <sup>-1</sup>	15.7 mL min <sup>-1</sup>	15.7 mL min <sup>-1</sup>
r <sup>2</sup>	(D <sub>∞</sub> -D <sub>U</sub> ) non-linear regression line	0.9920	0.9943	0.9851	0.9952
Figure 3.2 B and D					
Drug Dose: 0.22 mg		Acute Oral Administration			
PK Parameter	Equation/Method Used				
plateau (D <sub>∞</sub> )	Average of last three data points	0.049 mg	0.065 mg	0.022 mg	0.031mg
slope	(D <sub>∞</sub> -D <sub>U</sub> ) non-linear regression line	-0.0308	-0.0416	-0.0608	-0.0532
β	k = slope x 2.303	0.071 min <sup>-1</sup>	0.096 min <sup>-1</sup>	0.14 min <sup>-1</sup>	0.12 min <sup>-1</sup>
t <sub>1/2</sub>	t <sub>1/2</sub> = 0.693 / β	9.8 min	7.2 min	4.9 min	5.7 min
r <sup>2</sup>	(D <sub>∞</sub> -D <sub>U</sub> ) non-linear regression line	0.9496	0.9954	0.8771	0.808

Table 3.2 PK paramters calculated from IV and PO drug-urine concentrations shown in Figure 3.2.

Pharmacokinetic parameters calculated from one-compartment IV and PO dosing experiments after collecting urine samples.

Generally, urine data are rather variable in patients, and yet the data generated in Figure 3.2 offer reasonably accurate PK values. The  $t_{1/2}$  values generated from the slopes of the lines in Figure 3.2C and D were within range of the plasma values, though there were some deviations. For example, in the first condition (LIVER pump  $7 \text{ mL min}^{-1}$  and KIDNEY pump  $3 \text{ mL min}^{-1}$ ), the linear regression values generated from plasma analysis were 9.1 and 7.3 min for the IV and PO administration, respectively. In comparison, the linear regression generated from urine analysis resulted in  $t_{1/2}$  values of 5.8 and 9.8 min for the IV and PO administration, respectively. At faster elimination pump settings, such as LIVER pump  $14 \text{ mL min}^{-1}$  and KIDNEY 1 pump  $3 \text{ mL min}^{-1}$ , the plasma linear regression  $t_{1/2}$  values were 4.4 and 4.9 min for IV and PO administration, respectively. The complementary IV and PO urinary data showed linear regression  $t_{1/2}$  values of 4.3 and 4.9 min, respectively, yielding similar results to those obtained from plasma samples. Though there are some deviations in the urinary data generated by the modeller, urinary sampling is not the method of choice for determining drug half-life. Nevertheless, the data generated are reasonably consistent with the results obtained from plasma analysis.

Table 3.2 also shows the calculation of  $CL_R$  and  $CL_H$  values, which are determined by calculating the ratio of the plateau to the drug dose, and using the value to determine the fraction of drug eliminated by the KIDNEY 1 pump. The  $CL_R$  for each of the four experiments was calculated within range of that expected based on the KIDNEY 1 pump setting (the settings were either  $3 \text{ mL min}^{-1}$  or  $4 \text{ mL min}^{-1}$ ). The values ranged from  $2.2 \text{ mL min}^{-1}$  to  $2.5 \text{ mL min}^{-1}$ , and from  $3.6 \text{ mL min}^{-1}$  to  $4.1 \text{ mL min}^{-1}$  when the KIDNEY 1 pump was set to  $3 \text{ mL min}^{-1}$ , and  $4 \text{ mL min}^{-1}$ , respectively. The calculated  $CL_H$  value for all four experiments were also within range of that expected based on the LIVER pump setting during the experiments.

To further validate the results obtained in Figure 3.1 and Figure 3.2, a larger dose of drug (0.96 mg) was administered intravenously under the same four experimental conditions described. Figure 3.3A shows IV data fitted to a single-phase exponential decay equation, while Figure 3.3B shows a semi-logarithmic plot of the data in A. In this set of experiments, the PO dose was  $\sim 10\%$  of the IV dose (0.096 mg), and was administered in the same manner as done previously. To note, equivalent results would be achieved by setting the ORAL BIOAVAILABILITY pump to

9x the combined rates of the LIVER and KIDNEY 1 pumps. In much the same way as in Figure 3.1C, the PO data points in Figure 3.3C were connected by straight lines; Figure 3.3D shows the semi-logarithmic plot of the terminal phase. Table 3.3 describes the analysis of the single-phase exponential decay fits and linear regression lines, and confirms that the parameters associated with elimination were consistent with the parameters reported from Figure 3.1, though  $C_{t0}$  and AUC values changed in proportion to the increased dose. The  $V_D$ , regardless of change in  $CL_{Total}$  or dose, remained within the expected range, further confirming that the modeller mimics one-compartment behaviour.

Accompanying urine data for IV and PO administration are shown in Figure 3.4, with Table 3.4 providing all the calculated PK parameters. Once again, PO urine data demonstrated plateau variability, and this was attributed to the large margin of error associated with extremely low absorbance readings in the urine. However, the values generated from the sigma-minus method were still relatively consistent with the plasma IV and PO data.

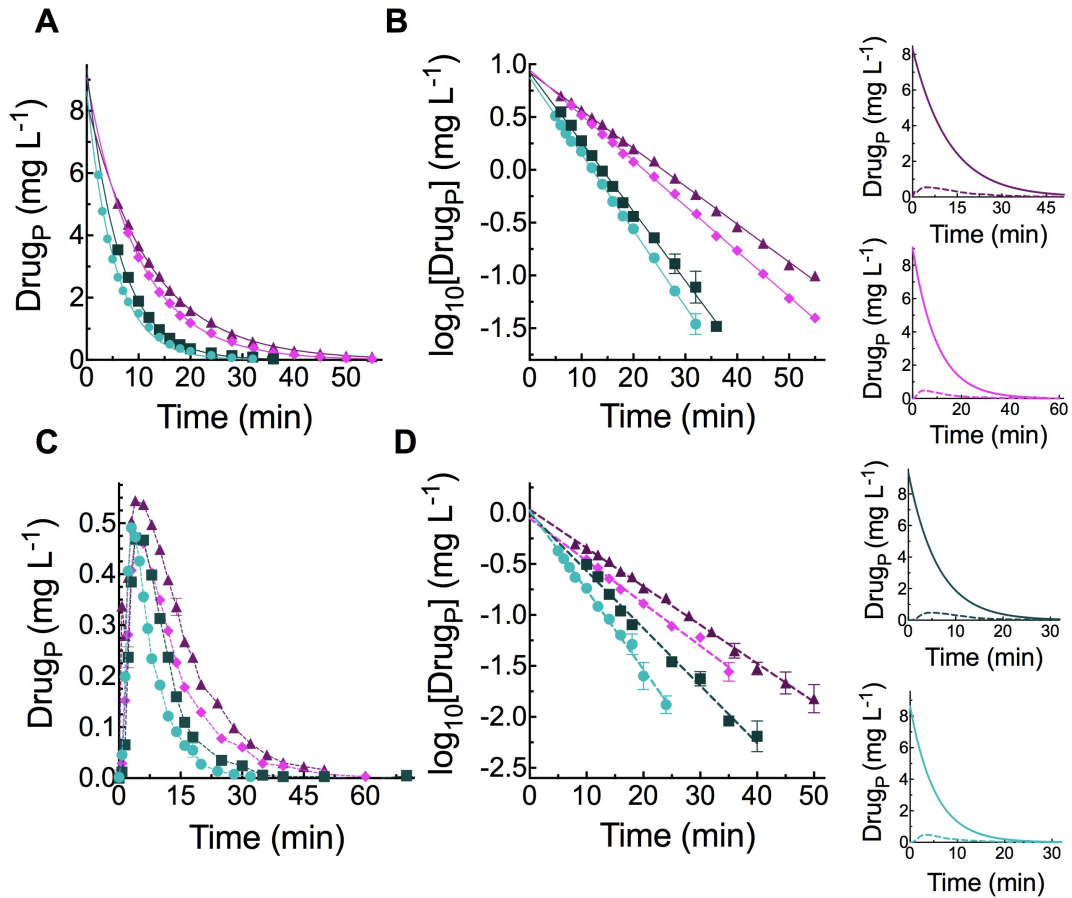


Figure 3.3. One-compartment modelling of IV and PO drug-plasma concentrations under the same varied elimination pump settings as Figure 3.1.

Calculated PK parameters are in Table 3.3. HEART pump setting:  $132 \text{ mL min}^{-1}$ . **(A)** Drug in plasma following IV administration ( $0.96 \text{ mg}$ ). Conditions were: LIVER pump  $7 \text{ mL min}^{-1}$  and KIDNEY 1 pump  $3 \text{ mL min}^{-1}$  ( $\blacktriangle$ ) or  $4 \text{ mL min}^{-1}$  ( $\blacklozenge$ ), and LIVER pump  $14 \text{ mL min}^{-1}$  and KIDNEY 1 pump  $3 \text{ mL min}^{-1}$  ( $\blacksquare$ ) or  $4 \text{ mL min}^{-1}$  ( $\bullet$ ). **(B)** Classic semi-logarithmic plot of IV elimination data from (A) **(C)** Drug in plasma following PO administration ( $0.096 \text{ mg}$ ). Conditions were: LIVER pump  $7 \text{ mL min}^{-1}$  and KIDNEY 1 pump  $3 \text{ mL min}^{-1}$  ( $\blacklozenge$ ) or  $4 \text{ mL min}^{-1}$  ( $\blacktriangle$ ), and LIVER pump  $14 \text{ mL min}^{-1}$  and KIDNEY 1 pump  $3 \text{ mL min}^{-1}$  ( $\blacksquare$ ) or  $4 \text{ mL min}^{-1}$  ( $\bullet$ ). **(D)** Classic semi-logarithmic plot of IV elimination data from (C) Each inset graph compares the corresponding PO data (dotted line) to the IV data (solid line) from experiments conducted under identical conditions (colours correspond to (A) and (B)).

Figure 3.3 Plasma Analysis					
Figure 3.3 A and B					
Liver Pump Setting		7 mL min <sup>-1</sup>		14 mL min <sup>-1</sup>	
Kidney 2 Pump Setting		5 mL min <sup>-1</sup>	3 mL min <sup>-1</sup>	5 mL min <sup>-1</sup>	3 mL min <sup>-1</sup>
Kidney 1 Pump Setting		3 mL min <sup>-1</sup>	4 mL min <sup>-1</sup>	3 mL min <sup>-1</sup>	4 mL min <sup>-1</sup>
Drug Dose: 0.96 mg		Acute Intravenous Administration			
PK Parameter	Equation/Method Used	▲	◆	■	●
<b>C<sub>10</sub></b>	Single-Phase Exponential Decay Fit	8.30 mg L <sup>-1</sup>	9.07 mg L <sup>-1</sup>	9.35 mg L <sup>-1</sup>	8.62 mg L <sup>-1</sup>
<b>k</b>	Single-Phase Exponential Decay Fit	0.082 min <sup>-1</sup>	0.10 min <sup>-1</sup>	0.16 min <sup>-1</sup>	0.19 min <sup>-1</sup>
<b>t<sub>1/2</sub></b>	Single-Phase Exponential Decay Fit	8.5 min	6.9 min	4.3 min	3.7 min
<b>AUC<sub>0-∞</sub></b>	$AUC_{0-∞} = C_{10} / k$	101.2 min · mg L <sup>-1</sup>	90.7 min · mg L <sup>-1</sup>	58.4 min · mg L <sup>-1</sup>	53.9 min · mg L <sup>-1</sup>
<b>V<sub>D</sub></b>	$V_D = \text{Dose} / C_{10}$	116 mL	106 mL	103 mL	111 mL
<b>CL<sub>Total</sub></b>	$CL_{Total} = k \times V_D$	9.5 mL min <sup>-1</sup>	10.6 mL min <sup>-1</sup>	16.4 mL min <sup>-1</sup>	17.8 mL min <sup>-1</sup>
<b>r<sup>2</sup></b>	Single-Phase Exponential Decay Fit	0.9994	0.9993	0.9986	0.9941
Elimination Phase					
<b>Y-intercept</b>	Linear-Regression Line	0.9222	0.9468	0.9203	0.8739
<b>C<sub>10</sub></b>	10 <sup>Y-intercept</sup>	8.36 mg L <sup>-1</sup>	8.85 mg L <sup>-1</sup>	8.32 mg L <sup>-1</sup>	7.48 mg L <sup>-1</sup>
<b>slope</b>	Linear-Regression Line	-0.0359	-0.0429	-0.0657	-0.0723
<b>β</b>	$\beta = \text{slope} \times 2.303$	0.083 min <sup>-1</sup>	0.099 min <sup>-1</sup>	0.15 min <sup>-1</sup>	0.17 min <sup>-1</sup>
<b>t<sub>1/2</sub></b>	$t_{1/2} = 0.693 / \beta$	8.4 min	7.0 min	4.6 min	4.2 min
<b>r<sup>2</sup></b>	Linear-Regression Line	0.9979	0.999	0.9812	0.995
Figure 3.3 C and D					
Drug Dose: 0.096 mg		Acute Oral Administration			
PK Parameter	Equation/Method Used	▲	◆	■	●
<b>AUC<sub>0-∞</sub></b>	$AUC_{0-∞} = AUC + C_{10}/k$	10.2 min · mg L <sup>-1</sup>	7.6 min · mg L <sup>-1</sup>	6.2 min · mg L <sup>-1</sup>	4.5 min · mg L <sup>-1</sup>
<b>F</b>	$F = (AUC_{PO} / AUC_{IV}) \times 100\%$	10.1%	8.4%	10.6%	9.9%
Elimination Phase					
<b>Y-intercept</b>	Linear-Regression Line	0.03412	-0.0516	-0.004547	0.2448
<b>C<sub>10</sub></b>	10 <sup>Y-intercept</sup>	1.08 mg L <sup>-1</sup>	0.89 mg L <sup>-1</sup>	0.99 mg L <sup>-1</sup>	1.76 mg L <sup>-1</sup>
<b>slope</b>	Linear-Regression Line	-0.0377	-0.0417	-0.0563	-0.0779
<b>β</b>	$k = \text{slope} \times 2.303$	0.087 min <sup>-1</sup>	0.096 min <sup>-1</sup>	0.13 min <sup>-1</sup>	0.18 min <sup>-1</sup>
<b>t<sub>1/2</sub></b>	$t_{1/2} = 0.693 / \beta$	8.0 min	7.2 min	5.3 min	3.9 min
<b>r<sup>2</sup></b>	Linear-Regression Line	0.9735	0.9672	0.9758	0.9624

Table 3.3 PK parameters calculated from IV and PO drug-plasma concentrations shown in Figure 3.3.

Pharmacokinetic parameters calculated from one-compartment IV and PO dosing experiments after collecting plasma samples.

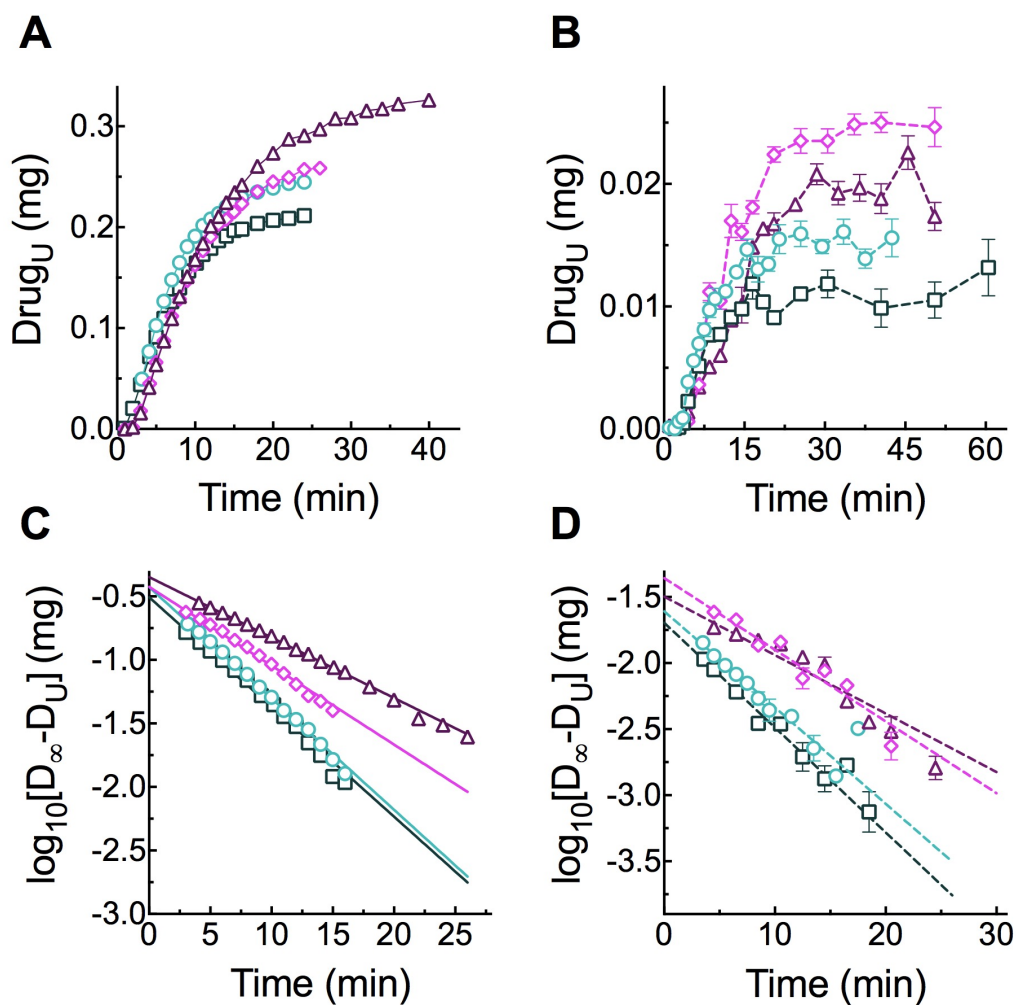


Figure 3.4. Complementary one-compartment modelling of IV and PO drug-urine concentrations for drug-plasma data shown in Figure 3.3.

Calculated parameters are shown in Table 3.4. HEART pump setting:  $132 \text{ mL min}^{-1}$ . **(A)** Cumulative drug in urine following IV administration (0.96 mg). Conditions were: LIVER pump  $7 \text{ mL min}^{-1}$  and KIDNEY 1 pump  $3 \text{ mL min}^{-1}$  ( $\Delta$ ) or  $4 \text{ mL min}^{-1}$  ( $\diamond$ ), and LIVER pump  $14 \text{ mL min}^{-1}$  and KIDNEY 1 pump  $3 \text{ mL min}^{-1}$  ( $\square$ ) or  $4 \text{ mL min}^{-1}$  ( $\circ$ ). **(B)** Cumulative drug in urine following PO administration (0.096 mg). Conditions were: LIVER pump  $7 \text{ mL min}^{-1}$  and KIDNEY 1 pump  $3 \text{ mL min}^{-1}$  ( $\Delta$ ) or  $4 \text{ mL min}^{-1}$  ( $\diamond$ ), and LIVER pump  $14 \text{ mL min}^{-1}$  and KIDNEY 1 pump  $3 \text{ mL min}^{-1}$  ( $\square$ ) or  $4 \text{ mL min}^{-1}$  ( $\circ$ ). **(C)** Analysis of IV data from (A) by the sigma-minus method. **(D)** Analysis of PO data from (B) by the sigma-minus method.

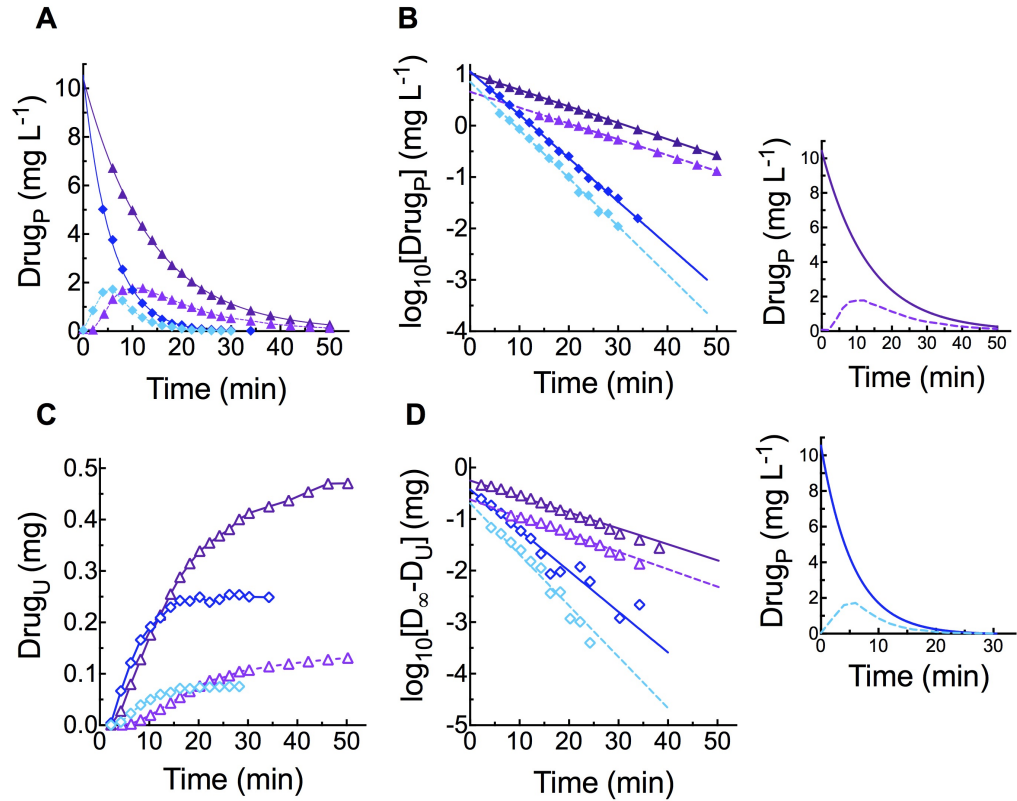
Figure 3.4 Urine Analysis					
Figure 3.4 A and C					
Liver Pump Setting		7 mL min <sup>-1</sup>		14 mL min <sup>-1</sup>	
Kidney 2 Pump Setting		5 mL min <sup>-1</sup>	3 mL min <sup>-1</sup>	5 mL min <sup>-1</sup>	3 mL min <sup>-1</sup>
Kidney 1 Pump Setting		3 mL min <sup>-1</sup>	4 mL min <sup>-1</sup>	3 mL min <sup>-1</sup>	4 mL min <sup>-1</sup>
Drug Dose: 0.96 mg		Acute Intravenous Administration			
PK Parameter	Equation/Method Used				
plateau (D <sub>∞</sub> )	Average of last three data points	0.322 mg	0.255 mg	0.209 mg	0.242 mg
slope	(D <sub>∞</sub> -D <sub>U</sub> ) non-linear regression line	-0.0476	-0.0630	-0.0864	-0.0876
β	β = slope x 2.303	0.110 min <sup>-1</sup>	0.145 min <sup>-1</sup>	0.199 min <sup>-1</sup>	0.202 min <sup>-1</sup>
t <sub>1/2</sub>	t <sub>1/2</sub> = 0.693 / β	6.3 min	4.8 min	3.5 min	3.4 min
CL <sub>R</sub>	CL <sub>R</sub> = (Plateau / Total Dose) x CL <sub>Total</sub>	3.2 mL min <sup>-1</sup>	2.8 mL min <sup>-1</sup>	3.6 mL min <sup>-1</sup>	4.5 mL min <sup>-1</sup>
CL <sub>H</sub>	CL <sub>H</sub> = CL <sub>Total</sub> - CL <sub>R</sub>	6.3 mL min <sup>-1</sup>	7.8 mL min <sup>-1</sup>	12.8 mL min <sup>-1</sup>	13.3 mL min <sup>-1</sup>
r <sup>2</sup>	(D <sub>∞</sub> -D <sub>U</sub> ) non-linear regression line	0.9959	0.9906	0.9908	0.9969
Figure 3.4 B and D					
Drug Dose: 0.096 mg		Acute Oral Administration			
PK Parameter	Equation/Method Used				
plateau (D <sub>∞</sub> )	Average of last three data points	0.0196 mg	0.0248 mg	0.0112 mg	0.0152 mg
slope	(D <sub>∞</sub> -D <sub>U</sub> ) non-linear regression line	-0.0443	-0.0543	-0.0794	-0.0729
β	β = slope x 2.303	0.102 min <sup>-1</sup>	0.125 min <sup>-1</sup>	0.183 min <sup>-1</sup>	0.168 min <sup>-1</sup>
t <sub>1/2</sub>	t <sub>1/2</sub> = 0.693 / β	6.8 min	5.5 min	3.8 min	4.1 min
r <sup>2</sup>	(D <sub>∞</sub> -D <sub>U</sub> ) non-linear regression line	0.8843	0.9075	0.9501	0.9209

Table 3.4 PK parameters calculated from IV and PO drug-urine concentrations shown in Figure 3.4.

Pharmacokinetic parameters calculated from one-compartment IV and PO dosing experiments after collecting urine samples.

Additional experiments were conducted in the one-compartment configuration, where drug was administered intravenously or orally under *fast* (LIVER pump 14 mL min<sup>-1</sup> and KIDNEY 1 pump 4 mL min<sup>-1</sup>) or *slow* (LIVER pump 3 mL min<sup>-1</sup> and KIDNEY 1 pump 3 mL min<sup>-1</sup>) elimination pump settings. Figure 3.5 displays plasma (A and B) and urine (C and D) data of IV (0.96mg) and PO (0.32) administration with a predicted F of 30%. The equivalent setting of the ORAL BIOAVAILABILITY pump to achieve similar PK parameter values would be 2.3x higher than the combined rates of the LIVER and KIDNEY 1 pumps; this would ensure that 70% of the drug does not reach the circulation.

Table 3.5 and Table 3.6 display plasma and urine results, respectively. Table 3.5 confirms that parameters such as C<sub>t0</sub> remained constant, while CL<sub>Total</sub>, AUC, and t<sub>1/2</sub> changed appropriately relative to the altered pump settings. To note, though the CL<sub>Total</sub> value between the *fast* and *slow* elimination configurations changed dramatically, the V<sub>D</sub> remained constant at ~ 90mL, reflecting the one-compartment behaviour of the drug. Although the V<sub>D</sub> did not change, the increased CL<sub>Total</sub> parameter under the *fast* elimination pump settings increased the half-life accordingly, further validating the relationship of Equation (E.44):  $CL_{Total} = V_D \times k_{el}$ . Table 3.6 displays the urinary analysis of the data, and the values generated for CL<sub>R</sub> and CL<sub>H</sub> were consistent with the predicted elimination settings.



**Figure 3.5.** One-compartment modelling of IV and PO drug-plasma and -urine concentrations to achieve an F of 30% under *fast* and *slow* elimination pump settings.

Calculated PK parameters are shown in Tables 3.5 and 3.6. HEART pump setting:  $132 \text{ mL min}^{-1}$ . **(A)** Drug in plasma following IV ( $\blacklozenge$ ) (0.96 mg) and PO ( $\blacklozenge$ ) (0.32 mg) administration under *fast* (LIVER pump  $14 \text{ mL min}^{-1}$  and KIDNEY 1 pump  $4 \text{ mL min}^{-1}$ ) elimination pump settings. IV ( $\blacktriangle$ ) (0.96 mg) and PO ( $\blacktriangle$ ) (0.32 mg) administration under *slow* (LIVER pump  $3 \text{ mL min}^{-1}$  and KIDNEY 1 pump  $3 \text{ mL min}^{-1}$ ) elimination pump settings. **(B)** Classic semi-logarithmic plot of IV and PO elimination data from (A) **(C)** Cumulative drug in urine following IV ( $\blacklozenge$ ) (0.96 mg) and PO ( $\blacklozenge$ ) (0.32 mg) administration under *fast* pump settings in (A), and cumulative drug in urine following IV ( $\blacktriangle$ ) (0.96 mg) and PO ( $\blacktriangle$ ) (0.32 mg) administration under *slow* pump settings in (A). **(D)** Analysis of IV and PO urinary data in (C) by the sigma-minus method. Each inset graph compares the corresponding PO data (dotted line) to the IV data (solid line) conducted under the *fast* (bottom inset) or *slow* (top inset) elimination conditions.

Figure 3.5 Plasma Analysis			
Figure 3.5 A and B			
Liver Pump Setting		3 mL min <sup>-1</sup>	14 mL min <sup>-1</sup>
Kidney 2 Pump Setting		5 mL min <sup>-1</sup>	4 mL min <sup>-1</sup>
Kidney 1 Pump Setting		3 mL min <sup>-1</sup>	4 mL min <sup>-1</sup>
Drug Dose: 0.96 mg		Acute Intravenous Administration	
PK Parameter	Equation/Method Used	▲	◆
C <sub>10</sub>	Single-Phase Exponential Decay Fit	10.43 mg L <sup>-1</sup>	10.6 mg L <sup>-1</sup>
k	Single-Phase Exponential Decay Fit	0.074 min <sup>-1</sup>	0.18 min <sup>-1</sup>
t <sub>1/2</sub>	Single-Phase Exponential Decay Fit	9.3 min	3.9 min
AUC <sub>0-∞</sub>	AUC <sub>0-∞</sub> = C <sub>10</sub> / k	140.9 min · mg L <sup>-1</sup>	58.9 min · mg L <sup>-1</sup>
V <sub>D</sub>	V <sub>D</sub> = Dose / C <sub>10</sub>	92 mL	91 mL
CL <sub>Total</sub>	CL <sub>Total</sub> = k x V <sub>D</sub>	6.8 mL min <sup>-1</sup>	16.4 mL min <sup>-1</sup>
r <sup>2</sup>	Single-Phase Exponential Decay Fit	0.9994	0.9978
Elimination Phase			
Y-intercept	Linear-Regression Line	1.015	1.058
C <sub>10</sub>	10 <sup>Y-intercept</sup>	10.35 mg L <sup>-1</sup>	11.42 mg L <sup>-1</sup>
slope	Linear-Regression Line	-0.0319	-0.0844
β	β = slope x 2.303	0.073 min <sup>-1</sup>	0.19 min <sup>-1</sup>
t <sub>1/2</sub>	t <sub>1/2</sub> = 0.693 / β	9.4 min	3.6 min
r <sup>2</sup>	Linear-Regression Line	0.9995	0.9981
Drug Dose: 0.32		Acute Oral Administration	
PK Parameter	Equation/Method Used	▲	◆
AUC <sub>0-∞</sub>	AUC <sub>0-∞</sub> = AUC + C <sub>10</sub> / k	40.2 min · mg L <sup>-1</sup>	15.8 min · mg L <sup>-1</sup>
F	F = (AUC <sub>PO</sub> / AUC <sub>IV</sub> ) x 100%	28.5%	26.8%
Elimination Phase			
Y-intercept	Linear-Regression Fit	0.6607	0.8559
C <sub>10</sub>	10 <sup>Y-intercept</sup>	4.58 mg L <sup>-1</sup>	7.18 mg L <sup>-1</sup>
slope	Linear-Regression Fit	-0.0308	-0.0937
β	β = slope x 2.303	0.071 min <sup>-1</sup>	0.22 min <sup>-1</sup>
t <sub>1/2</sub>	t <sub>1/2</sub> = 0.693 / β	9.8 min	3.2 min
r <sup>2</sup>	Linear-Regression Fit	0.9989	0.9981

Table 3.5 PK parameters calculated from IV and PO drug-plasma concentrations shown in Figure 3.5 A and B.

Pharmacokinetic parameters calculated from one-compartment IV and PO dosing experiments after collecting plasma samples.

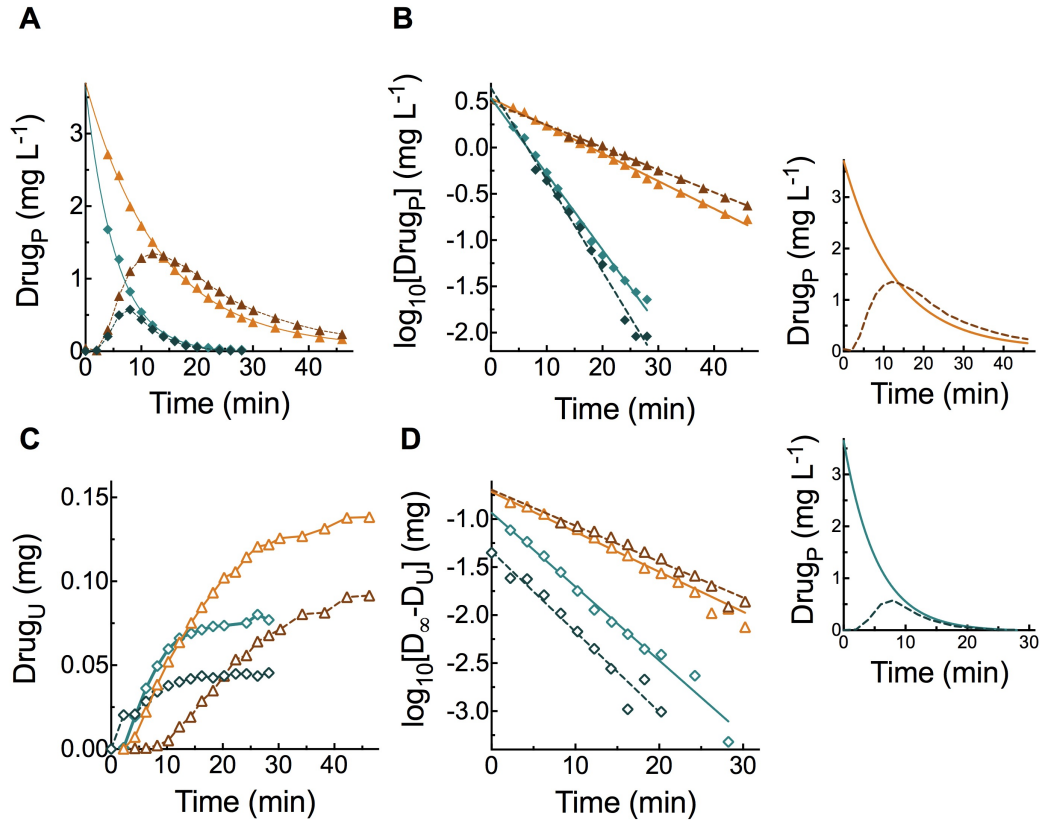
Figure 3.5 Urine Analysis			
Figure 3.5 C and D			
Liver Pump Setting		3 mL min <sup>-1</sup>	14 mL min <sup>-1</sup>
Kidney 2 Pump Setting		5 mL min <sup>-1</sup>	4 mL min <sup>-1</sup>
Kidney 1 Pump Setting		3 mL min <sup>-1</sup>	4 mL min <sup>-1</sup>
Drug Dose: 0.96 mg		Acute Intravenous Administration	
PK Parameter	Equation/Method Used		
plateau (D <sub>∞</sub> )	Average of last three data points	0.465 mg	0.251 mg
slope	(D <sub>∞</sub> -D <sub>U</sub> ) non-linear regression line	-0.0310	-0.0791
β	β = slope x 2.303	0.071 min <sup>-1</sup>	0.18 min <sup>-1</sup>
t <sub>1/2</sub>	t <sub>1/2</sub> = 0.693 / β	9.7 min	3.8 min
CL <sub>R</sub>	CL <sub>R</sub> = (Plateau / Total Dose) x CL <sub>Total</sub>	3.0 mL min <sup>-1</sup>	3.9 mL min <sup>-1</sup>
CL <sub>H</sub>	CL <sub>H</sub> = CL <sub>Total</sub> - CL <sub>R</sub>	3.8 mL min <sup>-1</sup>	12.5 mL min <sup>-1</sup>
r <sup>2</sup>	(D <sub>∞</sub> -D <sub>U</sub> ) non-linear regression line	0.9827	0.9743
Drug Dose: 0.32 mg		Acute Oral Administration	
PK Parameter	Equation/Method Used		
plateau (D <sub>∞</sub> )	Average of last three data points	0.128 mg	0.0752 mg
slope	(D <sub>∞</sub> -D <sub>U</sub> ) non-linear regression line	-0.0338	-0.0993
β	β = slope x 2.303	0.078 min <sup>-1</sup>	0.23 min <sup>-1</sup>
t <sub>1/2</sub>	t <sub>1/2</sub> = 0.693 / β	8.9 min	3.0 min
r <sup>2</sup>	(D <sub>∞</sub> -D <sub>U</sub> ) non-linear regression line	0.9836	0.9706

Table 3.6 PK parameters calculated from IV and PO drug-urine concentrations shown in Figure 3.5 C and D.

Pharmacokinetic parameters calculated from one-compartment IV and PO dosing experiments after collecting urine samples.

Figure 3.6 illustrates plasma (A and B) and urine (C and D) data under identical modeller settings using a different dose of drug administered intravenously (0.32 mg), and mimicking 70% and 30% F with 0.22 mg and 0.096 mg doses of drug administered orally (the ORAL BIOAVAILABILITY pump equivalent setting would be set to 0.43x and 2.3x the combined LIVER and KIDNEY 1 pump rates for 70% and 30% oral bioavailability, respectively). The plasma PK parameters shown in Table 3.7 mirror the parameters shown in Table 3.5, except for altered  $C_{t0}$  and AUC resulting from the reduced administered dose. Every other aspect of the analysis, including the single-phase exponential decay fits and linear regression line slopes were relatively consistent. The urinary analysis shown in Table 3.8 also closely matched the urinary analysis of Table 3.6, except for the plateau value, which was altered to reflect the dose. The observations between these sets of data further reinforced the modeller's capability of modelling one-compartment behaviour.

Figure 3.7A displays a single-phase exponential fit following IV administration, with calculated parameters shown in Table 3.9. Using the values obtained from the acute dosing experiment, chronic dosing parameters were calculated to achieve a steady state of  $6 \text{ mg L}^{-1}$  using repeated IV doses of drug (Figure 3.7B), and intermittent IV infusions (Figure 3.7C), while maintaining a peak:trough ratio of 2 (between  $8 \text{ mg L}^{-1}$  and  $4 \text{ mg L}^{-1}$ ), and 1.4 (between  $7 \text{ mg L}^{-1}$  and  $5 \text{ mg L}^{-1}$ ), respectively. Table 3.9 lists the equations used to obtain the chronic dosing regimen parameters. Results shown in Figure 3.7B and C confirm that within approximately 5-half lives, the  $C_{Av}$  (or  $C_{SS}$ ) achieved was  $5.62 \text{ mg L}^{-1}$  (93.7% of  $C_{SS}$ ) and  $5.69 \text{ mg L}^{-1}$  (94.8% of  $C_{SS}$ ) for the repeated IV and intermittent IV infusion experiments, respectively. The dosing also successfully maintained the drug plasma concentration within the therapeutic window, illustrating the ADAM's capabilities in mimicking clinical outcomes with both repeated IV dosing regimens and IV infusion dosing regimens in the one-compartment configuration.



**Figure 3.6** One-compartment modelling of IV and PO drug-plasma and -urine concentrations to achieve an F of 30% under *fast* and an F of 70% under *slow* elimination pump settings.

Calculated PK parameters are in Table 3.7 and 3.8. HEART pump setting:  $132 \text{ mL min}^{-1}$ . **(A)** Drug in plasma following IV ( $\blacklozenge$ ) (0.32 mg) and PO ( $\blacklozenge$ ) (0.096 mg) administration under *fast* (LIVER pump  $14 \text{ mL min}^{-1}$  and KIDNEY 1 pump  $4 \text{ mL min}^{-1}$ ) elimination pump settings. IV ( $\blacktriangle$ ) (0.32 mg) and PO ( $\blacktriangle$ ) (0.22 mg) administration under *slow* (LIVER pump  $3 \text{ mL min}^{-1}$  and KIDNEY 1 pump  $3 \text{ mL min}^{-1}$ ) elimination pump settings. **(B)** Classic semi-logarithmic plot of IV and PO elimination data from (A) **(C)** Cumulative drug in urine following IV ( $\blacktriangle$ ) (0.32 mg) and PO ( $\blacktriangle$ ) (0.096 mg) administration under *fast* pump settings in (A), and cumulative drug in urine following IV ( $\blacklozenge$ ) (0.32 mg) and PO ( $\blacklozenge$ ) (0.22 mg) administration under *slow* pump settings in (A). **(D)** Analysis of IV and PO urinary data in (C) by the sigma-minus method. Each inset graph compares the corresponding PO data (dotted line) to the IV data (solid line) conducted under the *fast* (bottom inset) or *slow* (top inset) elimination conditions.

Figure 3.6 Plasma Analysis			
Figure 3.6 A and B			
Liver Pump Setting		3 mL min <sup>-1</sup>	14 mL min <sup>-1</sup>
Kidney 2 Pump Setting		5 mL min <sup>-1</sup>	4 mL min <sup>-1</sup>
Kidney 1 Pump Setting		3 mL min <sup>-1</sup>	4 mL min <sup>-1</sup>
Drug Dose: 0.32 mg		Acute Intravenous Administration	
PK Parameter	Equation/Method Used	▲	◆
C <sub>10</sub>	Single-Phase Exponential Decay Fit	3.65 mg L <sup>-1</sup>	3.66 mg L <sup>-1</sup>
k	Single-Phase Exponential Decay Fit	0.076 min <sup>-1</sup>	0.19 min <sup>-1</sup>
t <sub>1/2</sub>	Single-Phase Exponential Decay Fit	9.1 min	3.7 min
AUC <sub>0-∞</sub>	AUC <sub>0-∞</sub> = C <sub>10</sub> / k	48.0 min · mg L <sup>-1</sup>	19.3 min · mg L <sup>-1</sup>
V <sub>D</sub>	V <sub>D</sub> = Dose / C <sub>10</sub>	88 mL	87.4 mL
CL <sub>Total</sub>	CL <sub>Total</sub> = k x V <sub>D</sub>	6.7 mL min <sup>-1</sup>	16.6 mL min <sup>-1</sup>
r <sup>2</sup>	Single-Phase Exponential Decay Fit	0.9991	0.9963
Elimination Phase			
Y-intercept	Linear-Regression Line	0.5332	0.5362
C <sub>10</sub>	10 <sup>Y-intercept</sup>	3.41 mg L <sup>-1</sup>	3.44 mg L <sup>-1</sup>
slope	Linear-Regression Line	-0.0298	-0.0820
β	β = slope x 2.303	0.069 min <sup>-1</sup>	0.19 min <sup>-1</sup>
t <sub>1/2</sub>	t <sub>1/2</sub> = 0.693 / β	10.1 min	3.7 min
r <sup>2</sup>	Linear-Regression Line	0.9961	0.9928
Acute Oral Administration		Drug Dose: 0.22	Drug Dose: 0.096
PK Parameter	Equation/Method Used	▲	◆
AUC <sub>0-∞</sub>	AUC <sub>0-∞</sub> = AUC + C <sub>10</sub> / k	32.3 min · mg L <sup>-1</sup>	5.4 min · mg L <sup>-1</sup>
F	F = (AUC <sub>PO</sub> / AUC <sub>IV</sub> ) x 100%	67.3%	28.0%
Elimination Phase			
Y-intercept	Linear-Regression Fit	0.4877	0.6462
C <sub>10</sub>	10 <sup>Y-intercept</sup>	3.07 mg L <sup>-1</sup>	4.42 mg L <sup>-1</sup>
slope	Linear-Regression Fit	-0.0243	-0.0992
β	k = slope x 2.303	0.056 min <sup>-1</sup>	0.23 min <sup>-1</sup>
t <sub>1/2</sub>	t <sub>1/2</sub> = 0.693 / β	12.4 min	3.0 min
r <sup>2</sup>	Linear-Regression Fit	0.9976	0.9857

Table 3.7 PK parameters calculated from IV and PO drug-plasma concentrations shown in Figure 3.6 A and B.

Pharmacokinetic parameters calculated from one-compartment IV and PO dosing experiments after collecting plasma samples.

Figure 3.6 Urine Analysis			
Figure 3.6 C and D			
Liver Pump Setting		3 mL min <sup>-1</sup>	14 mL min <sup>-1</sup>
Kidney 2 Pump Setting		5 mL min <sup>-1</sup>	4 mL min <sup>-1</sup>
Kidney 1 Pump Setting		3 mL min <sup>-1</sup>	4 mL min <sup>-1</sup>
Drug Dose: 0.32 mg		Acute Intravenous Administration	
PK Parameter	Equation/Method Used		
plateau (D <sub>∞</sub> )	Average of last three data points	0.136 mg	0.0775 mg
slope	(D <sub>∞</sub> -D <sub>U</sub> ) non-linear regression line	-0.0416	-0.0769
β	β = slope x 2.303	0.096 min <sup>-1</sup>	0.18 min <sup>-1</sup>
t <sub>1/2</sub>	t <sub>1/2</sub> = 0.693 / β	7.2 min	3.9 min
CL <sub>R</sub>	CL <sub>R</sub> = (Plateau / Total Dose) x CL <sub>Total</sub>	2.8 mL min <sup>-1</sup>	4.0 mL min <sup>-1</sup>
CL <sub>H</sub>	CL <sub>H</sub> = CL <sub>Total</sub> - CL <sub>R</sub>	3.9 mL min <sup>-1</sup>	12.6 mL min <sup>-1</sup>
r <sup>2</sup>	(D <sub>∞</sub> -D <sub>U</sub> ) non-linear regression line	0.9849	0.9926
Acute Oral Administration		Drug Dose: 0.22	Drug Dose: 0.096
PK Parameter	Equation/Method Used		
plateau (D <sub>∞</sub> )	Average of last three data points	0.0878 mg	0.0446 mg
slope	(D <sub>∞</sub> -D <sub>U</sub> ) non-linear regression line	-0.0374	-0.0835
β	β = slope x 2.303	0.086 min <sup>-1</sup>	0.19 min <sup>-1</sup>
t <sub>1/2</sub>	t <sub>1/2</sub> = 0.693 / β	8.0 min	3.6 min
r <sup>2</sup>	(D <sub>∞</sub> -D <sub>U</sub> ) non-linear regression line	0.9721	0.9569

Table 3.8 PK parameters calculated from IV and PO drug-urine concentrations shown in Figure 3.6 C and D.

Pharmacokinetic parameters calculated from one-compartment IV and PO dosing experiments after collecting urine samples.

## ONE COMPARTMENT REPEATED DOSING

Figure 3.7A displays a single-phase exponential fit following IV administration, with calculated parameters shown in Table 3.9. Using the values obtained from the acute dosing experiment, chronic dosing parameters were calculated to achieve a steady state of  $6 \text{ mg L}^{-1}$  using repeated IV doses of drug (Figure 3.7B), and intermittent IV infusions (Figure 3.7C), while maintaining a peak:trough ratio of 2 (between  $8 \text{ mg L}^{-1}$  and  $4 \text{ mg L}^{-1}$ ), and 1.4 (between  $7 \text{ mg L}^{-1}$  and  $5 \text{ mg L}^{-1}$ ), respectively. Table 3.9 lists the equations used to obtain the chronic dosing regimen parameters. Results shown in Figure 3.7B and C confirm that within approximately 5-half lives, the  $C_{Av}$  (or  $C_{SS}$ ) achieved was  $5.62 \text{ mg L}^{-1}$  (93.7% of  $C_{SS}$ ) and  $5.69 \text{ mg L}^{-1}$  (94.8% of  $C_{SS}$ ) for the repeated IV and intermittent IV infusion experiments, respectively. The dosing also successfully maintained the drug plasma concentration within the therapeutic window, illustrating the ADAM's capabilities in mimicking clinical outcomes with both repeated IV dosing regimens and IV infusion dosing regimens in the one-compartment configuration.

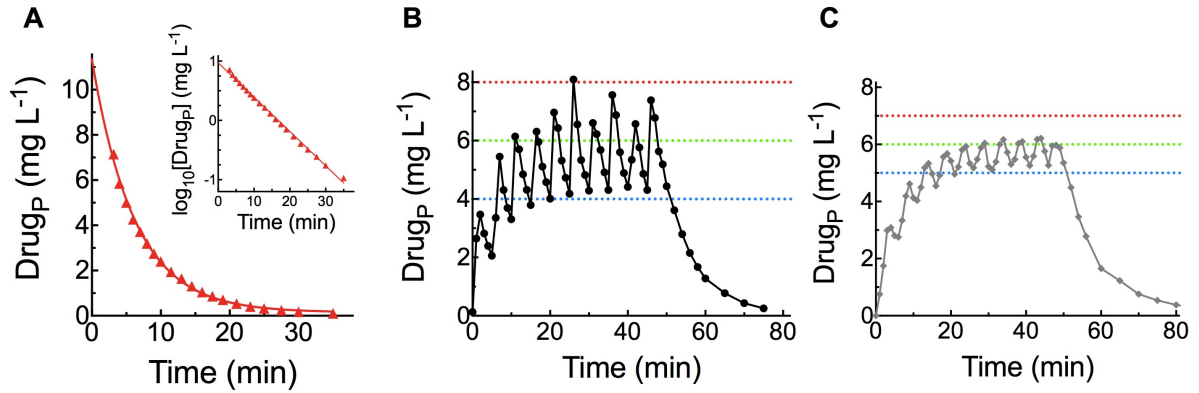


Figure 3.7. One-compartment modelling of drug-plasma concentrations following single IV dosing, repeated IV dosing, and intermittent IV infusion.

Single (A) (▲) and repeated (B) (●) IV dosing, and intermittent IV infusion (C) (◆) in a one-compartment configuration. Pump settings: HEART pump: 132 mL min<sup>-1</sup>, LIVER pump: 7 mL min<sup>-1</sup>, KIDNEY 1 pump: 4 mL min<sup>-1</sup>, KIDNEY 2 pump: 3 mL min<sup>-1</sup>. PK parameters (Table 3.9) were based on results from the single dose experiment shown in (A) and were used to calculate repeated dosing and intermittent IV infusion regimens that would maintain a  $C_{SS}$  of 6 mg L<sup>-1</sup> (- - -) and between a MEC (- - -) and MTC (- - -). (B) Drug concentrations were maintained between 4 and 8 mg L<sup>-1</sup> and the calculated  $C_{AV}$  was 5.62 mg L<sup>-1</sup>. (C) Drug concentrations were maintained between 5 and 7 mg L<sup>-1</sup> and the calculated  $C_{AV}$  was 5.69 mg L<sup>-1</sup>.

Figure 3.7 Plasma Analysis		
Figure 3.7 A		
Liver Pump Setting		7 mL min <sup>-1</sup>
Kidney 1 Pump Setting		4 mL min <sup>-1</sup>
Kidney 2 Pump Setting		3 mL min <sup>-1</sup>
Drug Dose: 0.96 mg		Acute Intravenous Administration
PK Parameter	Equation/Method Used	▲
C <sub>10</sub>	Single-Phase Exponential Decay Fit	11.35 mg L <sup>-1</sup>
k	Single-Phase Exponential Decay Fit	0.15 min <sup>-1</sup>
t <sub>1/2</sub>	Single-Phase Exponential Decay Fit	4.3 min
V <sub>D</sub>	V <sub>D</sub> = Dose / C <sub>10</sub>	85 mL
CL <sub>Total</sub>	CL <sub>Total</sub> = k x V <sub>D</sub>	12.7 mL min <sup>-1</sup>
r <sup>2</sup>	Single-Phase Exponential Decay Fit	0.9976
Elimination Phase		
Y-intercept	Linear-Regression Line	0.972
C <sub>10</sub>	10 <sup>Y-intercept</sup>	9.38 mg L <sup>-1</sup>
slope	Linear-Regression Line	-0.05791
β	β = slope x 2.303	0.13 min <sup>-1</sup>
t <sub>1/2</sub>	t <sub>1/2</sub> = 0.693 / β	5.2 min
r <sup>2</sup>	Linear-Regression Line	0.9967
Figure 3.7 B		
Multi Intravenous Dosing		
PK Parameter	Equation/Method Used	▲
Maintenance Dose Rate	Maintenance Dose Rate = C <sub>SS</sub> x V <sub>D</sub> x k <sub>el</sub>	0.077 mg min <sup>-1</sup>
τ	C <sub>max</sub> / C <sub>min</sub> = 1 / e <sup>-kt</sup> ; 8 mg L <sup>-1</sup> , C <sub>min</sub> : 4 mg L <sup>-1</sup> = 4.62 min	5 min
Total Dose every 5 min	Total Dose = Maintenance Dose Rate (mg min <sup>-1</sup> ) x 5 (min)	0.39 mg
Achieved C <sub>Av</sub>	Average of AUCs of Dosing Interval at C <sub>SS</sub> / Dosing Time (5 min)	5.62 mg L <sup>-1</sup>
Figure 3.7 C		
Intermittent Intravenous Infusion		
PK Parameter	Equation/Method Used	◆
Maintenance Dose Rate	Maintenance Dose Rate = C <sub>SS</sub> x V <sub>D</sub> x k <sub>el</sub>	0.077 mg min <sup>-1</sup>
IV Protocol	C <sub>max</sub> / C <sub>min</sub> = 1 / e <sup>-kt</sup> ; 7 mg L <sup>-1</sup> , C <sub>min</sub> : 5 mg L <sup>-1</sup> = 2.24 min	Infusion: 3 min, Stop Infusion: 2 min
Total Dose every minute	Total Dose per Minute = (Maintenance Dose Rate) x 5 / 3	0.128 min <sup>-1</sup>
Total Dose every 3 min	Total Dose = Total Dose per Minute (mg min <sup>-1</sup> ) x 3 (min)	0.39 mg
Achieved C <sub>Av</sub>	AUC of Dosing Interval at C <sub>SS</sub> / Dosing Interval (5 min)	5.69 mg L <sup>-1</sup>

Table 3.9 PK parameters calculated from analyses of IV drug-plasma concentrations from single, repeated, and intermittent IV infusion experiments shown in Figure 3.7.

Pharmacokinetic parameters calculated from one-compartment acute and repeated IV dosing and intermittent IV infusion experiments after collecting plasma samples.

## 3.2 TWO COMPARTMENT MODELLING

Figure 3.8 shows linear and semi-logarithmic plots of plasma data obtained following a single IV dose of drug administered to the apparatus in a two-compartment configuration, with the TISSUE pump operating at  $26 \text{ mL min}^{-1}$ , at two different tissue compartment volumes, and with *slow* or *fast* elimination pump settings. The first column (Figure 3.8 A, D, G, J) displays linear plots of the data, while the second column (Figure 3.8 B, E, H, K) illustrates the corresponding classic “hockey stick” curve on semi-logarithmic plots, indicating successful two-compartment modelling. The third column (Figure 3.8 C, F, I, L) displays the curve-stripping results obtained from extrapolating the terminal phase to the Y-axis and using the method of residuals to separate and quantify the contribution of the distribution process to drug disappearance from the central compartment. The results and PK parameters calculated for the plasma analysis are shown in Table 3.10.

In Figure 3.8, the first two rows of data were obtained when the LIVER pump was set to  $7 \text{ mL min}^{-1}$  (*slow* pump settings), and the TISSUE compartment volume varied between 100 (1<sup>st</sup> row) or 200 mL (2<sup>nd</sup> row). The third and fourth row, by contrast, show data obtained when the LIVER pump was set to  $14 \text{ mL min}^{-1}$  (*fast* pump settings), with the TISSUE compartment volume varied between 100 (3<sup>rd</sup> row) and 200 mL (4<sup>th</sup> row). Increasing the TISSUE compartment volume under both elimination settings resulted in an extended  $t_{1/2 \text{ el}}$ ; these are expected outcomes for the conditions.

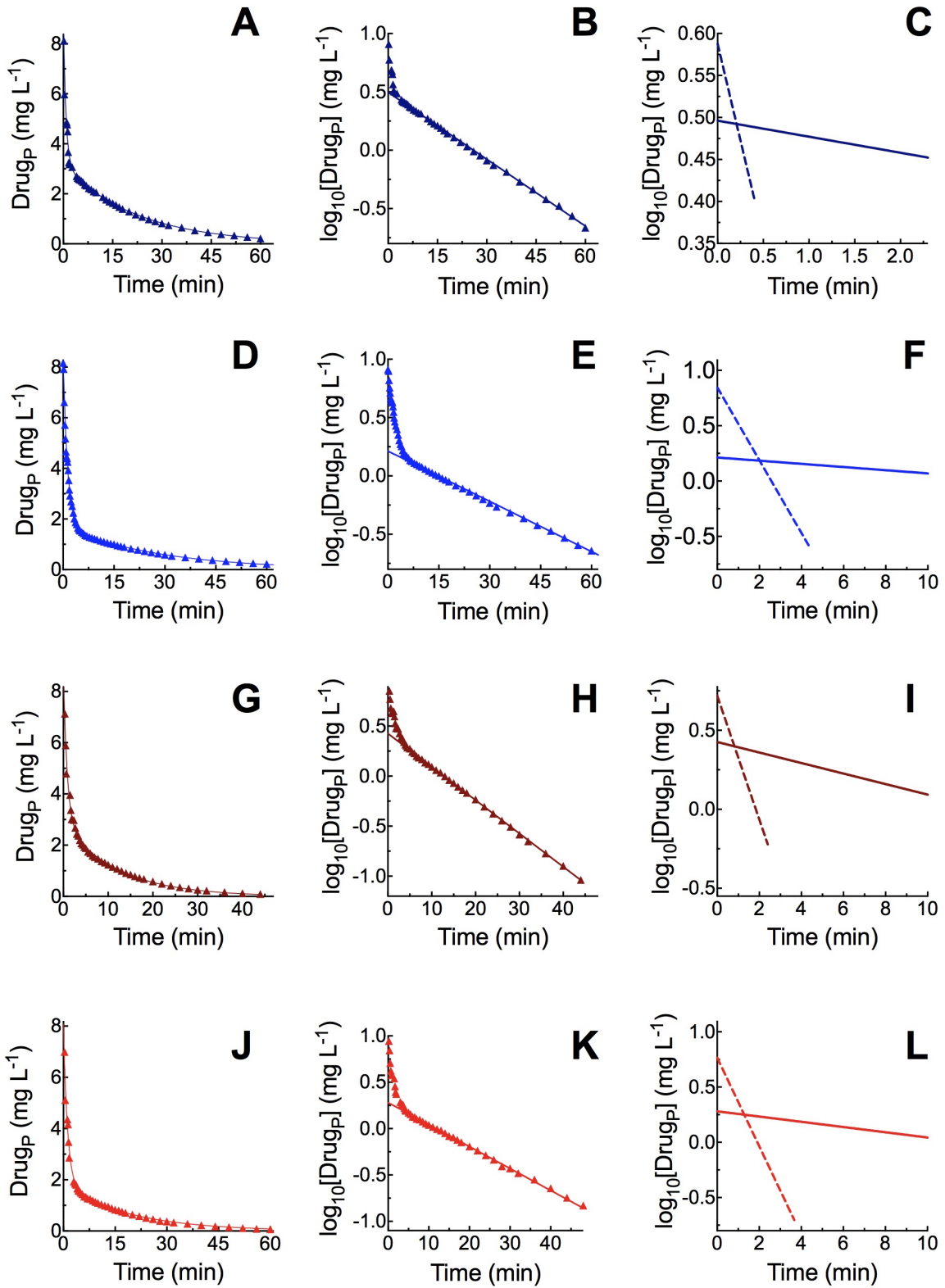


**Figure 3.8. Two-compartment modelling of IV drug-plasma concentrations under varied elimination pump settings and TISSUE compartment volumes.**

Calculated PK parameters are shown in Table 3.10. HEART pump setting:  $132 \text{ mL min}^{-1}$  and TISSUE pump setting:  $26 \text{ mL min}^{-1}$ . Each row displays plasma data fitted to a two-phase exponential decay equation (1<sup>st</sup> column), semi-logarithmic plots of the data showing the classic hockey-stick profile (2<sup>nd</sup> column), and the distribution and elimination phases plotted following curve-stripping by the method of residuals (3<sup>rd</sup> column). **Row 1 (A, B, C):** *slow* elimination settings, LIVER pump setting:  $7 \text{ mL min}^{-1}$ , TISSUE compartment volume: 100 mL (▲). **Row 2 (D, E, F):** *slow* elimination settings, LIVER pump setting:  $7 \text{ mL min}^{-1}$ , TISSUE compartment volume: 200 mL (▲). **Row 3 (G, H, I):** *fast* elimination settings, LIVER pump setting:  $14 \text{ mL min}^{-1}$ , TISSUE compartment volume: 100 mL (▲). **Row 4 (J, K, L):** *fast* elimination settings, LIVER pump setting:  $14 \text{ mL min}^{-1}$ , TISSUE compartment volume: 200 mL (▲).

Figure 3.8 Plasma Analysis					
Tissue Pump Setting		26 mL min <sup>-1</sup>			
Kidney 1 Setting; Kidney 2 Setting		3 mL min <sup>-1</sup> ; 4 mL min <sup>-1</sup>			
Liver Pump Setting		7 mL min <sup>-1</sup>		14 mL min <sup>-1</sup>	
Tissue Compartment Volume		100 mL	200 mL	100 mL	200 mL
Drug Dose: 0.96		Acute Intravenous Administration			
PK Parameter	Equation/Method Used	▲	▲	▲	▲
<b>C<sub>10</sub></b>	Two-Phase Exponential Decay Fit	8.67 mg L <sup>-1</sup>	8.17 mg L <sup>-1</sup>	8.68 mg L <sup>-1</sup>	8.08 mg L <sup>-1</sup>
<b>k<sub>dist</sub></b>	Two-Phase Exponential Decay Fit	1.22 min <sup>-1</sup>	0.77 min <sup>-1</sup>	1.16 min <sup>-1</sup>	0.84 min <sup>-1</sup>
<b>t<sub>1/2 dist</sub></b>	Two-Phase Exponential Decay Fit	0.60 min	0.90 min	0.60 min	0.84 min
<b>k<sub>el</sub></b>	Two-Phase Exponential Decay Fit	0.044 min <sup>-1</sup>	0.035 min <sup>-1</sup>	0.083 min <sup>-1</sup>	0.051 min <sup>-1</sup>
<b>t<sub>1/2 el</sub></b>	Two-Phase Exponential Decay Fit	15.5 min	19.6 min	8.4 min	13.5 min
<b>AUC<sub>0-∞</sub></b>	$AUC_{0-∞} = AUC + C_{in}/k$	75.7 min · mg L <sup>-1</sup>	57.8 min · mg L <sup>-1</sup>	40.6 min · mg L <sup>-1</sup>	41.9 min · mg L <sup>-1</sup>
<b>V<sub>D SS</sub></b>	$V_{D SS} = (Dose \times (A/\alpha^2 + B/\beta^2)) / AUC^2$	272 mL	433 mL	268 mL	355 mL
<b>V<sub>D Area</sub></b>	$V_{D Area} = Dose / (AUC \times \beta)$	288 mL	502 mL	308 mL	420 mL
<b>V<sub>D Extrap</sub></b>	$V_{D Extrap} = Dose / B$	306 mL	588 mL	360 mL	503 mL
<b>CL<sub>Total</sub></b>	$CL_{Total} = Dose / AUC_{0-∞}$	12.7 mL min <sup>-1</sup>	16.6 mL min <sup>-1</sup>	23.6 mL min <sup>-1</sup>	22.9 mL min <sup>-1</sup>
<b>r<sup>2</sup></b>	Two-Phase Exponential Decay Fit	0.9850	0.9939	0.9925	0.9857
<b>Elimination Phase</b>		—	—	—	—
<b>Y-intercept</b>	Linear Regression Line	0.4962	0.2129	0.4261	0.2804
<b>B</b>	$10^{Y\text{-intercept}}$	3.13 mg L <sup>-1</sup>	1.63 mg L <sup>-1</sup>	2.67 mg L <sup>-1</sup>	1.91 mg L <sup>-1</sup>
<b>slope</b>	Linear Regression Line	-0.0191	-0.0144	-0.0333	-0.0237
<b>β</b>	$\beta = slope \times 2.303$	0.044 min <sup>-1</sup>	0.033 min <sup>-1</sup>	0.077 min <sup>-1</sup>	0.055 min <sup>-1</sup>
<b>t<sub>1/2 el</sub></b>	$t_{1/2 el} = 0.693 / \beta$	15.8 min	21.0 min	9.0 min	12.7 min
<b>r<sup>2</sup></b>	Linear Regression Line	0.9991	0.9981	0.999	0.9977
<b>Distribution Phase</b>		.....	.....	.....	.....
<b>Y-intercept</b>	Linear Regression Line	0.5878	0.8463	0.7185	0.7663
<b>A</b>	$10^{Y\text{-intercept}}$	3.87 mg L <sup>-1</sup>	7.02 mg L <sup>-1</sup>	5.22 mg L <sup>-1</sup>	5.84 mg L <sup>-1</sup>
<b>slope</b>	Linear Regression Line	-0.460	-0.329	-0.392	-0.401
<b>α</b>	$\alpha = slope \times 2.303$	1.06 min <sup>-1</sup>	0.76 min <sup>-1</sup>	0.90 min <sup>-1</sup>	0.92 min <sup>-1</sup>
<b>t<sub>1/2 dist</sub></b>	$t_{1/2 dist} = 0.693 / \alpha$	0.65 min	0.91 min	0.77 min	0.75 min
<b>r<sup>2</sup></b>	Linear-Regression Fit	0.9208	0.9940	0.9453	0.9423
<b>k<sub>12</sub></b>	$k_{12} = (AB \times (\beta - \alpha)^2) / ((A+B) \times (A\beta + Ba))$	0.51 min <sup>-1</sup>	0.47 min <sup>-1</sup>	0.44 min <sup>-1</sup>	0.52 min <sup>-1</sup>
<b>k<sub>21</sub></b>	$k_{21} = (A\beta + Ba) / (A+B)$	0.50 min <sup>-1</sup>	0.17 min <sup>-1</sup>	0.36 min <sup>-1</sup>	0.27 min <sup>-1</sup>
<b>k<sub>10</sub></b>	$k_{10} = (\alpha\beta \times (A+B)) / (A\beta + Ba)$	0.094 min <sup>-1</sup>	0.15 min <sup>-1</sup>	0.19 min <sup>-1</sup>	0.19 min <sup>-1</sup>

Table 3.10 PK parameters calculated from IV drug-plasma concentrations shown in Figure 3.8.

Pharmacokinetic parameters calculated from plasma samples collected from two-compartment IV dosing experiments with varied elimination pump settings and tissue compartment volumes.

The  $CL_{Total}$  values were also appropriately altered in response to the changed LIVER pump setting. However, unlike the one-compartment configuration, the  $CL_{Total}$  in the two-compartment configuration was calculated by using non-compartmental analysis, which is directly influenced by the AUC value. The slightly lower AUC value for the *slow* elimination setting 200 mL experiment resulted in a  $CL_{Total}$  estimation of  $16.6 \text{ mL min}^{-1}$  in comparison to the  $12.7 \text{ mL min}^{-1}$  calculated when the TISSUE compartment was at 100 mL. Realistically, the  $CL_{Total}$  value should be maintained at  $\sim 10\text{-}12 \text{ mL min}^{-1}$  under *slow* elimination conditions, and the slight increase in  $CL_{Total}$  when the TISSUE compartment was increased was not expected. The  $C_{t0}$  values calculated from the two-phase exponential decay fit were comparable among the experiments, suggesting similar dose administration. Thus, the AUC discrepancy could result from absorbance reading error, or possibly slight alterations in the LIVER pump settings between the two experiments. However, the *slow* elimination experiments are still comparable, as the half-life values changed relative to the altered conditions, and the overall analysis still showed the relationship between distribution and elimination effectively. In contrast, the AUC values calculated under the *fast* elimination settings between both sets of TISSUE compartment volumes were almost identical, and the  $CL_{Total}$  values were also comparable.

The total volume of the system with the addition of the TISSUE compartment includes the  $\sim 40$  mL of extra tubing connecting the TISSUE compartment to the central compartment, as well as the volume indicated in the TISSUE compartment; the true volume of the system for the two TISSUE compartment conditions were  $\sim 240$  mL and  $\sim 340$  mL, respectively. Unlike one-compartment kinetics, two-compartment kinetics may often result in volume terms that vary considerably from the sum of the central and peripheral compartments. This is also seen in human patients, as the concentration of the drug in the TISSUE compartment is generally higher than in the central compartment due to drug sequestration in the tissues. Analysis of the data generates B-intercepts that are underestimated, contributing to large  $V_{D \text{ Extrap}}$  values. Thus,  $V_{D \text{ SS}}$  and  $V_{D \text{ Area}}$  are typically more representative of the actual volume in the apparatus; the  $V_{D \text{ SS}}$  is the value which provides the best estimate of actual volume of water in the modeller.

When the TISSUE compartment volume was increased, the volume terms between the *slow* and *fast* elimination sets of experiments increased accordingly. When the TISSUE compartment volume increased, the smallest of these terms, the  $V_{D_{SS}}$ , was altered from 272 mL to 433 mL and 268 mL to 355 mL between the *slow* and *fast* elimination settings, respectively. Between the *slow* and *fast* elimination settings, the  $V_{D_{Area}}$ , deemed as the most “stable” term, increased from 288 mL to 502 mL, and 308 mL to 420 mL, respectively. The  $V_{D_{Extrap}}$ , known to be overestimated because of the underestimation of the B-intercept in analysis, followed the same trend as the other volume terms in both sets of experiments. As a note, the volume terms were comparable under the same TISSUE compartment volume settings, despite changes in the elimination settings, which were adequately reflected in the changed half-life values. This relationship was important to elucidate as it notably reflects the *in vivo* relationship of clearance and volume of distribution.

Curve-stripping allowed for the calculation of slopes and intercepts for the lines associated with distribution and elimination processes, and subsequent calculations facilitated for the determination of their first order rate constants. Interestingly, the extrapolated B-intercepts in both sets of experiments decreased with increasing TISSUE compartment volumes; a higher peripheral volume resulted in more extensive drug distribution from the central compartment, resulting in decreased extrapolated Y-intercepts. The elimination rate constant,  $\beta$ , decreased with increasing TISSUE compartment volume, resulting in increased elimination half-lives. Between the *slow* and *fast* elimination settings, the  $\beta$  increased appropriately as per the increased clearance setting. The A-intercepts for the experiments were variable, with no discernible trend between sets of experiments, and the calculated distribution rate constant,  $\alpha$ , did not vary extensively. The extrapolated values obtained by the method of residuals allowed for calculation of the inter-compartmental micro-constants,  $k_{12}$ ,  $k_{21}$ , which are associated with drug transfer from the central compartment to the tissue compartment and from the tissue compartment to the central compartment, respectively, and  $k_{10}$ , associated with drug elimination from the central compartment. The  $k_{12}$  was consistent between the experiments, reflecting the constant TISSUE pump rate employed for all experiments. However, the  $k_{21}$  value

was decreased when the TISSUE compartment volume increased, reflecting the appropriate effect of increased distribution volume on a drug's proportional transfer back to the central compartment. Essentially, increased TISSUE compartment volume results in a reduced rate of transfer of drug back, regardless of TISSUE pump rate. The calculated  $k_{10}$ , the micro-constant for drug elimination from the central compartment (~100 mL), changed appropriately to the increased clearance rate. Under *fast* settings and both 100 mL and 200 mL TISSUE compartment conditions, the  $k_{10}$  was calculated as  $0.19 \text{ min}^{-1}$ ; as the LIVER pump rate was set to  $14 \text{ mL min}^{-1}$ , and the KIDNEY 1 pump rate was  $3 \text{ mL min}^{-1}$ , the correlation to the sum of the clearance rates was consistent.

Complementary urine data were also obtained for the experiments shown in Figure 3.8. In Figure 3.9, each row of data corresponds to the same row in Figure 3.8. Table 3.11 displays all calculated PK parameters from urine data. Figure 3.9A, C, E, and G represent cumulative drug in urine *versus* time, allowing estimation of the drug plateau or  $D_{\infty}$ . The  $D_{\infty}$  value was applied to the sigma-minus method, resulting in a semi-logarithmic plot of drug remaining to be excreted in the urine (Figure 3.9B, D, F, and H). The data from the central portion of the curve corresponding to the period following drug distribution were fitted to a straight line, and the slope of the line was used to calculate the elimination rate constant in each experiment. The values calculated from the urine data correspond reasonably well to their complementary plasma data, but the trends associated with TISSUE compartment changes are not as easily elucidated. Estimates for  $CL_R$  and  $CL_H$  were based on the plateau value, and the calculated  $CL_R$  values for all of the conditions reasonably coincide with the KIDNEY 1 pump setting of  $3 \text{ mL min}^{-1}$ . The  $CL_H$  value, particularly under the *slow* elimination pump settings and with a TISSUE compartment volume of 200 mL were dramatically higher than expected because of the high calculated  $CL_{\text{Total}}$  value; the other  $CL_H$  values coincided reasonably with the respective LIVER pump setting.

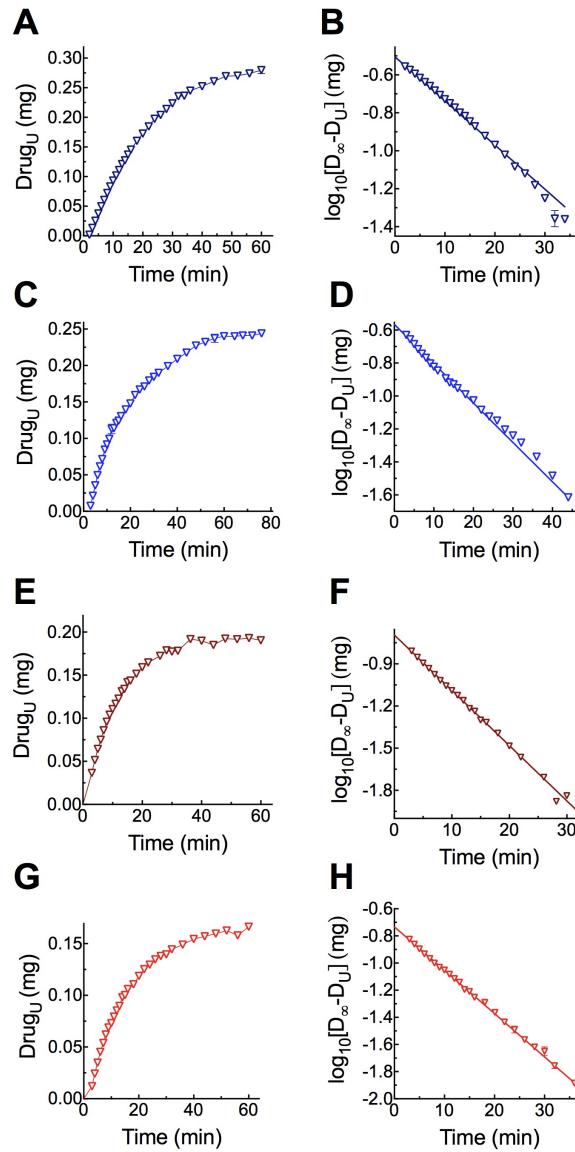


**Figure 3.9. Complementary two-compartment modelling of IV drug-urine concentrations for drug-plasma data shown in Figure 3.8.**

Calculated parameters are shown in Table 3.9. HEART pump setting:  $132 \text{ mL min}^{-1}$  and TISSUE pump setting:  $26 \text{ mL min}^{-1}$ . Each row displays urinary data connected with straight lines to show cumulative drug in urine (1<sup>st</sup> column), and analysis of the data by the sigma-minus method followed by nonlinear regression analysis (2<sup>nd</sup> column). **Row 1 (A, B):** slow elimination settings, LIVER pump setting:  $7 \text{ mL min}^{-1}$ , TISSUE compartment volume: 100 mL ( $\nabla$ ). **Row 2 (C, D):** slow elimination settings, LIVER pump setting:  $7 \text{ mL min}^{-1}$ , TISSUE compartment volume: 200 mL ( $\nabla$ ). **Row 3 (E, F):** fast elimination settings, LIVER pump setting:  $14 \text{ mL min}^{-1}$ , TISSUE compartment volume: 100 mL ( $\nabla$ ). **Row 4 (G,H):** fast elimination settings, LIVER pump setting:  $14 \text{ mL min}^{-1}$ , TISSUE compartment volume: 200 mL ( $\nabla$ ).

Figure 3.9 Urine Analysis					
Tissue Pump Setting		26 mL min <sup>-1</sup>			
Kidney 1 Setting; Kidney 2 Setting		3 mL min <sup>-1</sup> ; 4 mL min <sup>-1</sup>			
Liver Pump Setting		7 mL min <sup>-1</sup>		14 mL min <sup>-1</sup>	
Tissue Compartment Volume		100 mL	200 mL	100 mL	200 mL
Drug Dose: 0.96		Acute Intravenous Administration			
PK Parameter	Equation/Method Used	▽	▽	▽	▽
plateau (D <sub>∞</sub> )	Average of last three data points	0.275 mg	0.242 mg	0.192 mg	0.162 mg
slope	(D <sub>∞</sub> -D <sub>U</sub> ) non-linear regression line	-0.0233	-0.0239	-0.0394	-0.0319
k	k = slope x 2.303	0.054 min <sup>-1</sup>	0.0550 min <sup>-1</sup>	0.091 min <sup>-1</sup>	0.074 min <sup>-1</sup>
t <sub>1/2</sub>	t <sub>1/2</sub> = 0.693 / k	12.9 min	12.6 min	7.6 min	9.4 min
CL <sub>R</sub>	CL <sub>R</sub> = ( Plateau / Total Dose) x CL <sub>Total</sub>	3.6 mL min <sup>-1</sup>	4.2 mL min <sup>-1</sup>	4.7 mL min <sup>-1</sup>	3.9 mL min <sup>-1</sup>
CL <sub>H</sub>	CL <sub>H</sub> = CL <sub>Total</sub> - CL <sub>R</sub>	9.1 mL min <sup>-1</sup>	12.4 mL min <sup>-1</sup>	18.9 mL min <sup>-1</sup>	19.0 mL min <sup>-1</sup>
r <sup>2</sup>	(D <sub>∞</sub> -D <sub>U</sub> ) non-linear regression line	0.9934	0.9920	0.9974	0.9978

Table 3.11 PK parameters calculated from IV drug-urine concentrations shown in Figure 3.9.

Pharmacokinetic parameters calculated from urines samples collected from two-compartment IV dosing experiments with varied elimination pump settings and tissue compartment volumes.

In much the same manner as one-compartment modelling, comparisons between IV and PO dosing are possible when the apparatus is in the two-compartment configuration. Figure 3.10 illustrates plasma data from IV and PO dosing with a target F of 70%, with all pump settings consistent, but with varied TISSUE compartment volumes (100 and 200 mL). These experiments were also conducted prior to the addition of the ORAL BIOAVAILABILITY pump to the apparatus, and as such, the administered PO dose was ~70% of the IV dose (the equivalent ORAL BIOAVAILABILITY pump setting would be around 0.5 x the combined rates of the LIVER and KIDNEY 1 pumps (5 mL min<sup>-1</sup>)). As would be expected, the IV data showed increased  $t_{1/2\text{ elim}}$  values, and volume terms with increased TISSUE COMPARTMENT volume, similar  $k_{12}$  values (as the TISSUE pump rate was constant), and reduced  $k_{21}$ . The near identical  $CL_{\text{Total}}$  and  $k_{10}$  values between the two IV experiments reflected the consistency of the elimination pump settings.

The PO comparison values for the two different conditions of TISSUE compartment volumes of 100 mL (Figure 3.10A, B, C, and D) and 200 mL (Figure 3.10E, F, G, and H) resulted in F values of 78.6%, and 56.2%, respectively. These calculated values did not match the target F of 70% (though the deviation was not substantial), and the potential discrepancy might be accounted for, at least in part, by error in the volume of the PO dose administered. Despite the AUC discrepancy, the terminal phase extrapolation of the PO dosing showed  $t_{1/2}$  elimination values consistent with the complementary IV experiments, confirming that the parameter settings were reproducible between the experiments.

Finally, the TISSUE pump setting of 9 mL min<sup>-1</sup> is drastically reduced from the previous Figure 3.8, where the TISSUE pump was set to almost 3x that rate. Comparing the values generated in Table 3.10 with the values generated in Table 3.8, where the IV dose, elimination pump settings (LIVER pump: 7 mL min<sup>-1</sup>, and KIDNEY 1 pump: 3 mL min<sup>-1</sup>), and TISSUE COMPARTMENT volumes (100 and 200 mL) were identical, shows that the reduction in TISSUE pump rate prolongs the elimination half-life of the drug. This is a trend that is shown throughout the results section.

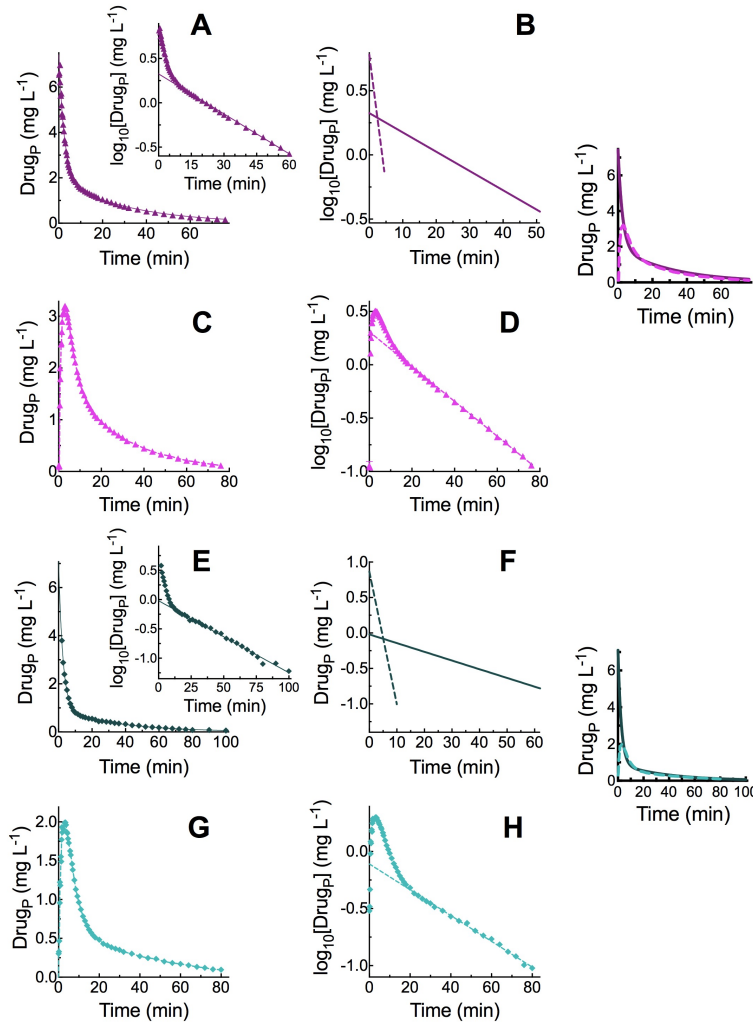


**Figure 3.10.** Two-compartment modelling of IV and PO drug-plasma concentrations under varied TISSUE compartment volumes.

Calculated PK parameters are shown in Table 3.12. HEART pump setting:  $132 \text{ mL min}^{-1}$ , TISSUE pump setting:  $9 \text{ mL min}^{-1}$ , LIVER pump setting:  $7 \text{ mL min}^{-1}$ . **Row 1 and 2:** IV and PO data comparison with TISSUE compartment volume set at 100 mL (including top inset graph, far right) **(A)** IV plasma data fitted to a two-phase exponential decay ( $\blacktriangle$ ) with inset graph showing the classic hockey stick distribution profile. **(B)** Distribution and elimination phase of data in (A) plotted on semi-logarithmic graph using the method of residuals. **(C)** Drug in plasma following PO administration (0.67 mg) ( $\blacktriangle$ ). **(D)** Elimination phase of data in (C) plotted on a semi-logarithmic graph. **Row 3 and 4:** IV and PO data comparison with TISSUE compartment volume set at 200 mL (including bottom inset graph, far right). **(E)** IV plasma data fitted to a two-phase exponential decay ( $\blacklozenge$ ) with inset graph showing the classic hockey stick distribution profile. **(F)** Distribution and elimination phase of data in (E) plotted on semi-logarithmic graph using the method of residuals. **(G)** Drug in plasma following PO administration (0.67 mg) ( $\blacklozenge$ ). **(H)** Elimination phase of data in (G) plotted on a semi-logarithmic graph.

Figure 3.10 Plasma Analysis			
Figure 3.10 A, B, E, and F			
Tissue Pump Setting		9 mL min <sup>-1</sup>	
Kidney 1 Pump Setting; Kidney 2 Pump Setting		3 mL min <sup>-1</sup> ; 4 mL min <sup>-1</sup>	
Liver Pump Setting		7 mL min <sup>-1</sup>	
Tissue Compartment Volume		100 mL	200 mL
Acute IV Administration		IV (0.96 mg)	IV (0.96 mg)
PK Parameter	Equation/Method Used	▲	◆
C <sub>10</sub>	Two-Phase Exponential Decay Fit	7.43 mg L <sup>-1</sup>	7.97 mg L <sup>-1</sup>
k <sub>dist</sub>	Two-Phase Exponential Decay Fit	0.39 min <sup>-1</sup>	0.37 min <sup>-1</sup>
t <sub>1/2 dist</sub>	Two-Phase Exponential Decay Fit	1.8 min	1.9 min
k <sub>el</sub>	Two-Phase Exponential Decay Fit	0.032 min <sup>-1</sup>	0.020 min <sup>-1</sup>
t <sub>1/2 el</sub>	Two-Phase Exponential Decay Fit	21.9 min	34.4 min
AUC <sub>0-∞</sub>	AUC <sub>0-∞</sub> = AUC + C <sub>m</sub> / k	74.2 min · mg L <sup>-1</sup>	71.2 min · mg L <sup>-1</sup>
V <sub>D SS</sub>	V <sub>D SS</sub> = (Dose x (A / α <sup>2</sup> + B / β <sup>2</sup> )) / AUC <sup>2</sup>	313 mL	482 mL
V <sub>D Area</sub>	V <sub>D Area</sub> = Dose / (AUC x β)	374 mL	646 mL
V <sub>D Extrap</sub>	V <sub>D Extrap</sub> = Dose / B	453 mL	881 mL
CL <sub>Total</sub>	CL <sub>Total</sub> = Dose / AUC <sub>0-∞</sub>	12.9 mL min <sup>-1</sup>	13.5 mL min <sup>-1</sup>
r <sup>2</sup>	Two-Phase Exponential Decay Fit	0.9947	0.9977
Elimination Phase			
Y-intercept	Linear Regression Line	0.3258	0.03724
B	10 <sup>Y</sup> -intercept	2.12 mg L <sup>-1</sup>	1.09 mg L <sup>-1</sup>
slope	Linear Regression Line	-0.0150	-0.00906
β	β = slope x 2.303	0.035 min <sup>-1</sup>	0.021 min <sup>-1</sup>
t <sub>1/2 el</sub>	t <sub>1/2 el</sub> = 0.693 / β	20.0 min	33.2 min
r <sup>2</sup>	Linear Regression Line	0.9987	0.9778
Distribution Phase			
Y-intercept	Linear Regression Line	0.7817	0.852
A	10 <sup>Y</sup> -intercept	6.05 mg L <sup>-1</sup>	7.11 mg L <sup>-1</sup>
slope	Linear Regression Line	-0.0202	-0.170
α	α = slope x 2.303	0.47 min <sup>-1</sup>	0.39 min <sup>-1</sup>
t <sub>1/2 dist</sub>	t <sub>1/2 dist</sub> = 0.693 / α	1.5 min	1.8 min
r <sup>2</sup>	Linear-Regression Line	0.9977	0.9939
k <sub>12</sub>	k <sub>12</sub> = ((A x B) x (β - α) <sup>2</sup> ) / ((A + B) x (Aβ+Bα))	0.24 min <sup>-1</sup>	0.23 min <sup>-1</sup>
k <sub>21</sub>	k <sub>21</sub> = (Aβ + Bα) / (A + B)	0.15 min <sup>-1</sup>	0.070 min <sup>-1</sup>
k <sub>10</sub>	k <sub>10</sub> = (αβ x (A + B)) / (Aβ + Bα)	0.11 min <sup>-1</sup>	0.12 min <sup>-1</sup>
Figure 3.10 C, D, G, and H			
Acute Oral Administration		PO (0.67 mg)	PO (0.67 mg)
PK Parameter	Equation/Method Used	▲	◆
AUC <sub>0-∞</sub>	AUC <sub>0-∞</sub> = AUC + C <sub>m</sub> / k	58.3 min · mg L <sup>-1</sup>	40.0 min · mg L <sup>-1</sup>
F	F = (AUC <sub>PO</sub> / AUC <sub>IV</sub> ) x 100%	78.6%	56.2%
Elimination Phase			
Y-intercept	Linear Regression Line	0.3101	0.1091
B	10 <sup>Y</sup> -intercept	2.04 mg L <sup>-1</sup>	0.78 mg L <sup>-1</sup>
slope	Linear Regression Line	-0.01663	-0.0113
β	β = slope x 2.303	0.038 min <sup>-1</sup>	0.026 min <sup>-1</sup>
t <sub>1/2 el</sub>	t <sub>1/2 el</sub> = 0.693 / β	18.5 min	26.6 min
r <sup>2</sup>	Linear Regression Line	0.9986	0.9939

Table 3.12 PK parameters calculated from IV and PO drug-plasma concentrations shown in Figure 3.10.

Pharmacokinetic parameters calculated from plasma samples collected from two-compartment IV and PO dosing experiments with varied tissue compartment volumes.

The corresponding urinary data for the plasma results in Figure 3.10 are shown in Figure 3.11. Overall, the parameters calculated from the sigma-minus method resulted in  $k_{el}$  values consistently lower than the values generated by the plasma data. As urinary data are generally prone to greater variability, the discrepancies were not unexpected. The IV and PO data for the TISSUE COMPARTMENT volume of 100 mL resulted in substantially higher plateau values than with volumes of 200 mL. As the TISSUE compartment volume was increased, there would be reduced concentrations of drug in the central compartment, thereby reducing the amount of drug available for elimination by the KIDNEY 1 pump. Thus, the reduced plateaus in the 200 mL conditions were in line with expectations.

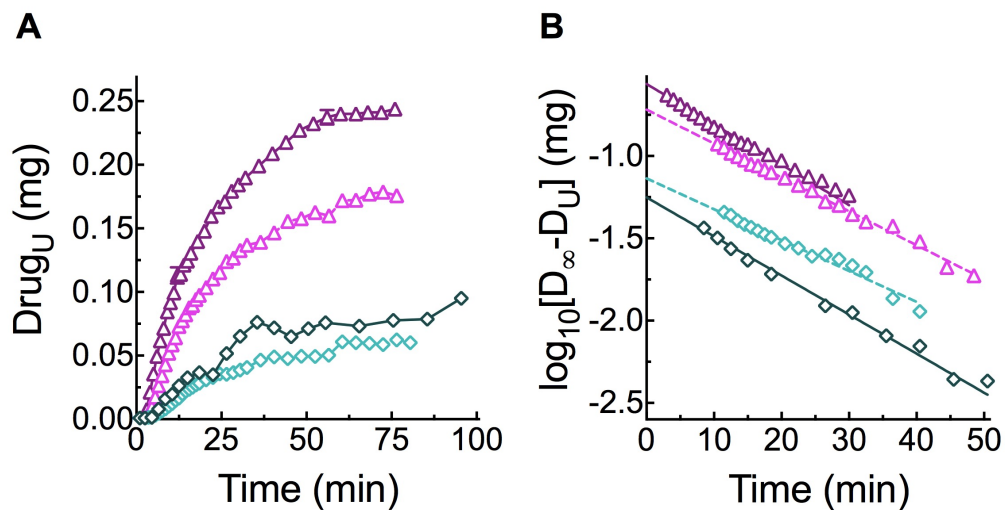


Figure 3.11. Complementary two-compartment IV and PO drug-urine concentrations for plasma data shown in Figure 3.10.

Calculated parameters are shown in Table 3.13. HEART pump setting:  $132 \text{ mL min}^{-1}$ , TISSUE pump setting:  $9 \text{ mL min}^{-1}$ , and LIVER pump setting:  $7 \text{ mL min}^{-1}$ . (A) urinary data connected with straight lines to show cumulative drug in urine. IV ( $\Delta$ ) and PO ( $\triangle$ ) data with TISSUE compartment volume of 100 mL, and IV ( $\diamond$ ) and PO ( $\diamond$ ) data with TISSUE compartment volume of 200 mL. (B) Analysis of the data in (A) by the sigma-minus method followed by nonlinear regression analysis.

Figure 3.11 Urine Analysis					
Figure 3.11 A and B					
Tissue Pump Setting		9 mL min <sup>-1</sup>			
Kidney 1 Pump Setting; Kidney 2 Pump Setting		3 mL min <sup>-1</sup> ; 4 mL min <sup>-1</sup>			
Liver Pump Setting		7 mL min <sup>-1</sup>			
Tissue Compartment Volume		100 mL		200 mL	
Drug Dose: 0.96		IV (0.96 mg)	PO (0.67 mg)	IV (0.96 mg)	PO (0.67 mg)
PK Parameter	Equation/Method Used	△	△	◇	◇
plateau (D <sub>∞</sub> )	Average of last three data points	0.242 mg	0.177 mg	0.0495 mg	0.0838 mg
slope	(D <sub>∞</sub> -D <sub>U</sub> ) non-linear regression fit	-0.0245	-0.0206	-0.0237	-0.0188
k	k = slope x 2.303	0.056 min <sup>-1</sup>	0.047 min <sup>-1</sup>	0.055 min <sup>-1</sup>	0.043 min <sup>-1</sup>
t <sub>1/2</sub>	t <sub>1/2</sub> = 0.693 / k	12.3 min	14.6 min	12.7 min	16.0 min
r <sup>2</sup>	(D <sub>∞</sub> -D <sub>U</sub> ) non-linear regression fit	0.9886	0.9858	0.9896	0.9653

Table 3.13 PK parameters calculated from two-compartment IV and PO drug-urine concentrations shown in Figure 3.11.

Pharmacokinetic parameters calculated from urine samples collected from two-compartment IV and PO dosing experiments with varied tissue compartment volumes.

PO drug administration allows for the determination of oral bioavailability, and as shown, altering the drug dose can reasonably provide a predicted F value in both one and two-compartment configurations. Further development of the modeller resulted in the addition of an ORAL BIOAVAILABILITY pump, which diverted a fraction of the orally administered drug from the stomach into the hepatic waste. This improvement negated the need to reduce the drug dose for PO administration, and required adjusting the ORAL BIOAVAILABILITY pump to achieve the desired F value. Figure 3.12A shows the linear plot data with alteration of the ORAL BIOAVAILABILITY pump rate while Figure 3.12B displays the semi-logarithmic plot of the data following absorption and distribution. Table 3.14 shows calculated PK parameters for these experiments. The ORAL BIOAVAILABILITY pump mimics first-pass metabolism; increasing or decreasing the pump rate decreases or increases the oral bioavailability, respectively. The use of the ORAL BIOAVAILABILITY pump demonstrated the robustness of the approach; the target values for this set of experiments were 70% and 30%, and the resulting values were 67% and 32%, respectively. Though the oral bioavailability between each of the experiments were altered, Figure 3.12B showed similarities in the slopes, resulting in similar  $\beta$  and t<sub>1/2</sub> values,

consistent with identical LIVER and KIDNEY 1 pump rate settings. In addition, increased ORAL BIOAVAILABILITY pump rates resulted in decreased calculated B-intercept values, which was consistent with the degree to which drug was lost to first-pass metabolism.

PO administration in the apparatus also allows for determination of parameters such as  $C_{max}$  (the highest drug concentration observed in plasma) and  $t_{max}$  (the time at which  $C_{max}$  is observed). The stomach in the apparatus is represented by an airtight 50 mL conical tube containing a volume that can be varied between 5 and 50 mL prior to beginning an experiment. Changes in stomach volume can mimic the gastric emptying effects, influencing the rate at which drug enters the systemic circulation. Figure 3.12C shows linear data profiles following a single PO dose of 0.96 mg with stomach volumes of 45 mL, 25 mL, and 5 mL. A higher stomach volume resulted in a lower  $C_{max}$  and a slightly longer  $t_{max}$ . Figure 3.12D demonstrates semi-logarithmic plots of the elimination phase of the data, with the slopes of the lines and calculated B-intercepts being almost identical. Table 3.14 further illustrates the calculated PK parameters for these experiments. Thus, changes in the stomach volume primarily affect the rate of absorption, with increased stomach volumes smoothing concentration-time profiles, and thus, mimicking a sustained-release oral preparation.

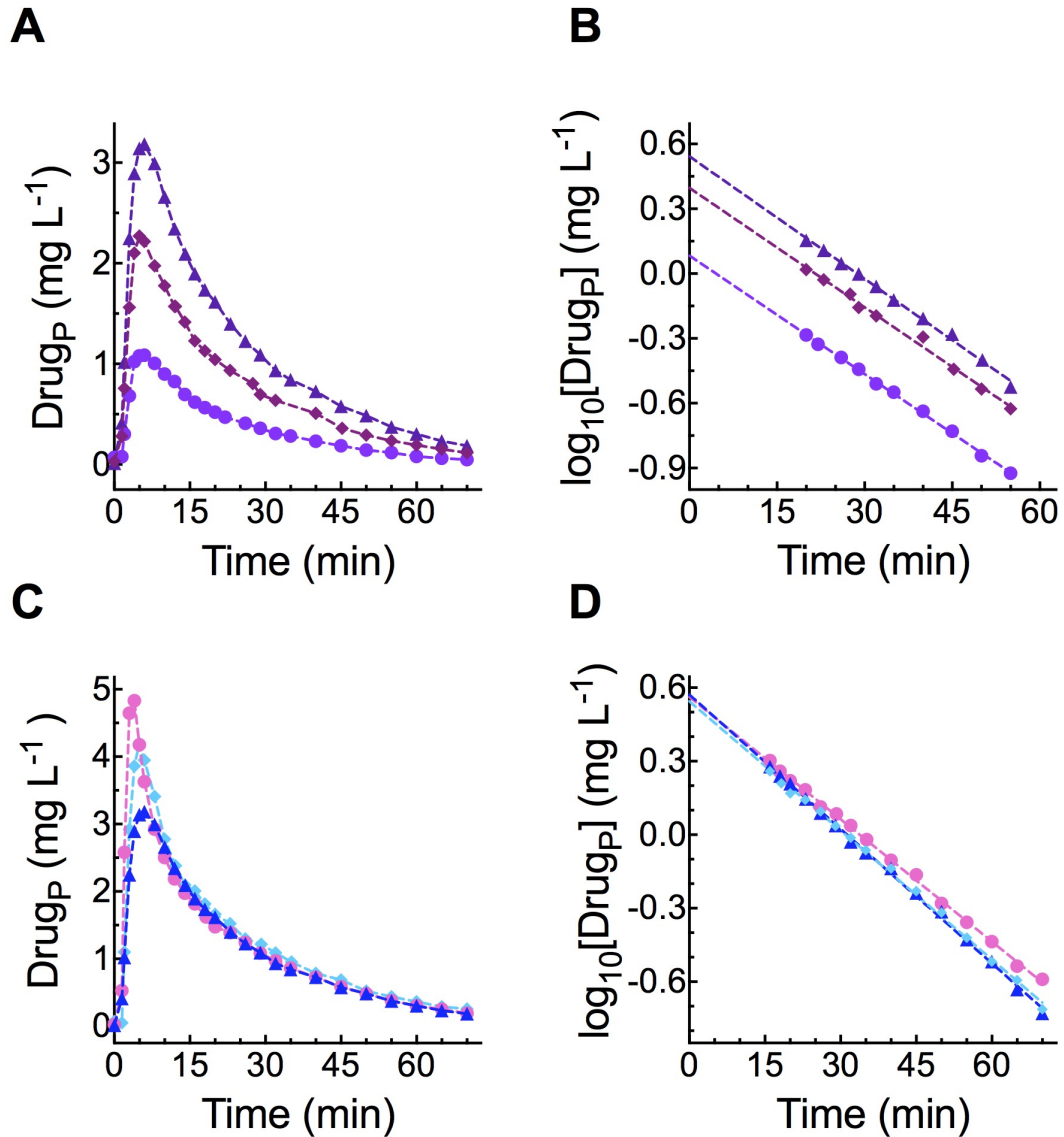


Figure 3.12. Modelling effects of varied ORAL BIOAVAILABILITY pump rates or stomach volumes on two-compartment PO drug-plasma concentrations.

Calculated PK parameters are shown in Table 3.14. HEART pump: 132 mL min<sup>-1</sup>, LIVER pump: 7 mL min<sup>-1</sup>, TISSUE pump: 12 mL min<sup>-1</sup>, KIDNEY 1 pump: 3 mL min<sup>-1</sup>, KIDNEY 2 pump: 4 mL min<sup>-1</sup>. (A) Effects of ORAL BIOAVAILABILITY pump rates on plasma concentration-time profiles. Rates of 0 (▲), 5 (◆), and 24 mL min<sup>-1</sup> (●) were chosen to model bioavailabilities of 100, 70, and 30%, respectively. (B) Semi-logarithmic plots of the elimination phase data, following absorption and distribution, shown in (A). (C) Effect of initial stomach volume on C<sub>max</sub> and t<sub>max</sub>. Water volumes initially present in the stomach were 45 mL (▲), 25 mL (◆), and 5 mL (●). (D) Semi-logarithmic plots of the elimination phase data, following absorption and distribution, shown in (C).

Figure 3.12				
Figure 3.12 A and B				
Liver Setting		7 mL min <sup>-1</sup>		
Kidney 1 Setting; Kidney 2 Setting		3 mL min <sup>-1</sup> ; 4 mL min <sup>-1</sup>		
Tissue Pump Setting; Tissue Compartment Volume		12 mL min <sup>-1</sup> ; 100 mL		
Drug Dose: 0.96 mg		Acute Oral Administration		
Oral Bioavailability Pump Setting		0 mL min <sup>-1</sup>	5 mL min <sup>-1</sup>	24 mL min <sup>-1</sup>
PK Parameter	Equation/Method Used	▲ 100%	◆ 70%	● 30%
AUC <sub>0-∞</sub>	AUC <sub>0-∞</sub> = AUC + C <sub>tn</sub> / k	81.45 min · mg L <sup>-1</sup>	54.5 min · mg L <sup>-1</sup>	26.4 min · mg L <sup>-1</sup>
F	F = (AUC <sub>PO</sub> / AUC <sub>IV</sub> ) × 100%	100%	66.9%	30.2%
CL <sub>Total</sub>	CL <sub>Total</sub> = Dose × F / AUC <sub>0-∞</sub>	11.8 mL min <sup>-1</sup>	11.8 mL min <sup>-1</sup>	11.0 mL min <sup>-1</sup>
Elimination Phase				
PK Parameter	Equation/Method Used	▲ 100%	◆ 70%	● 30%
Y-intercept	Linear-Regression Line	0.5425	0.3965	0.0832
B	10 <sup>Y-intercept</sup>	3.49 mg L <sup>-1</sup>	2.49 mg L <sup>-1</sup>	1.21 mg L <sup>-1</sup>
slope	Linear-Regression Line	-0.01889	-0.0184	-0.01827
β	β = -slope × 2.303	0.0435 min <sup>-1</sup>	0.0424 min <sup>-1</sup>	0.0421 min <sup>-1</sup>
t <sub>1/2 el</sub>	t <sub>1/2</sub> = 0.693 / β	15.9 min	16.3 min	16.5 min
r <sup>2</sup>	Linear-Regression Line	0.9960	0.9925	0.9986
Figure 3.12 C and D				
Liver Setting		7 mL min <sup>-1</sup>		
Kidney 1 Setting; Kidney 2 Setting		3 mL min <sup>-1</sup> ; 4 mL min <sup>-1</sup>		
Distribution Pump Setting; Tissue Compartment Volume		12 mL min <sup>-1</sup> ; 100 mL		
Drug Dose: 0.96 mg		Acute Oral Administration		
Oral Bioavailability Pump Setting		0 mL min <sup>-1</sup>		
Stomach Volume		45 mL	25 mL	5 mL
PK Parameter	Equation/Method Used	▲	◆	●
AUC <sub>0-∞</sub>	AUC <sub>0-∞</sub> = AUC + C <sub>tn</sub> / k	81.51 min · mg L <sup>-1</sup>	87.87 min · mg L <sup>-1</sup>	93.11 min · mg L <sup>-1</sup>
t <sub>max</sub>	Values estimated from graph	6 min	5 min	4 min
C <sub>max</sub>	Values estimated from graph	3.18 mg L <sup>-1</sup>	4.20 mg L <sup>-1</sup>	4.83 mg L <sup>-1</sup>
CL <sub>Total</sub>	CL <sub>Total</sub> = Dose / F / AUC	11.8 mL min <sup>-1</sup>	10.9 mL min <sup>-1</sup>	10.3 mL min <sup>-1</sup>
Elimination Phase				
PK Parameter	Equation/Method Used	▲	◆	●
Y-intercept	Linear-Regression Line	0.5718	0.5625	0.5444
B	10 <sup>Y-intercept</sup>	3.73 mg L <sup>-1</sup>	3.65 mg L <sup>-1</sup>	3.50 mg L <sup>-1</sup>
slope	Linear-Regression Line	-0.01828	-0.01664	-0.01756
β	β = -slope × 2.303	0.0421 min <sup>-1</sup>	0.0383 min <sup>-1</sup>	0.0404 min <sup>-1</sup>
t <sub>1/2 el</sub>	t <sub>1/2</sub> = 0.693 / β	16.5 min	18.1 min	17.1 min
r <sup>2</sup>	Linear-Regression Line	0.9982	0.9986	0.9980

Table 3.14 PK parameters calculated from PO drug-plasma concentrations shown in Figure 3.12.

Pharmacokinetic parameters calculated from plasma samples collected from two-compartment PO dosing experiments with varied ORAL BIOAVAILABILITY pump settings and stomach volumes.

Under a two-compartment configuration, the TISSUE pump was set to 3, 7, or 17 mL min<sup>-1</sup> with the dose of methylene blue, all other pump rate settings, and tissue compartment volume kept constant. Figure 3.13 includes semi-logarithmic plots of the data following curve stripping, and the inset graph shows the linear concentration-time profiles of each condition. The  $k_{12}$  and  $k_{21}$  were smaller at lower pump settings, and the  $k_{10}$  remained independent of the TISSUE pump rate, as shown in Table 3.15 calculations. The half-lives for both distribution and elimination were shorter with faster transfer of drug between compartments, as expected. The TISSUE pump rate of 3 mL min<sup>-1</sup> provided a distribution half-life of 4.7 min, which was the longest value recorded for this parameter, suggesting the strong impact of the TISSUE pump rate in combination with appropriate elimination pump rate settings (the LIVER pump rate was set to 7 mL min<sup>-1</sup> in this set of experiments).

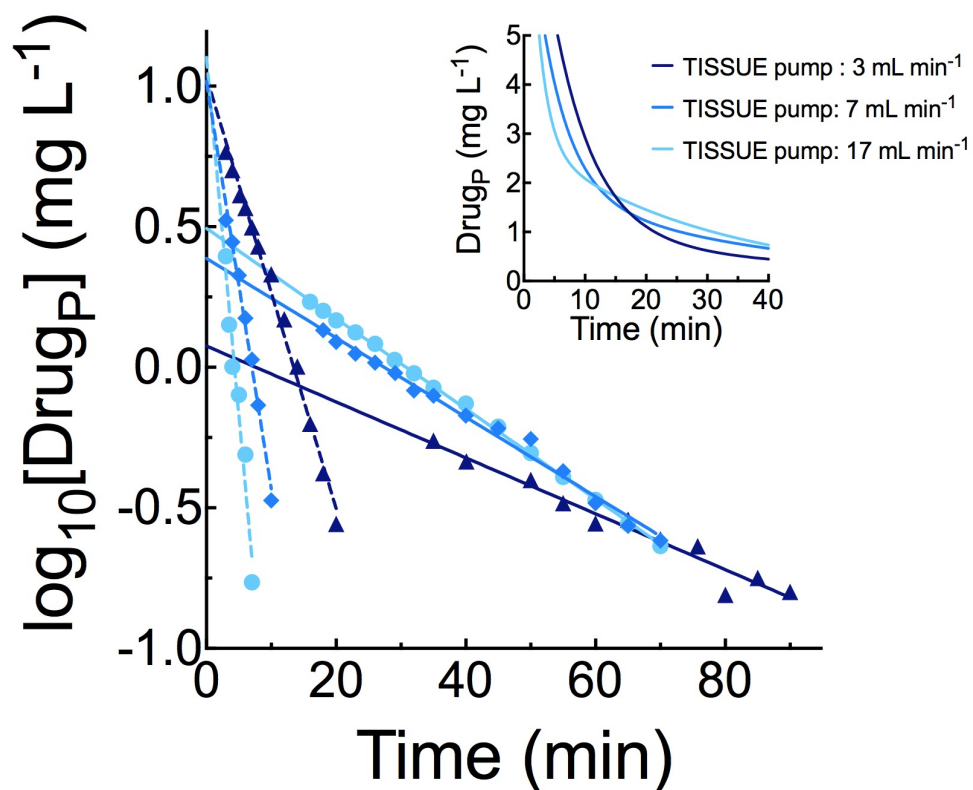


Figure 3.13. Modelling effects of varied TISSUE pump rates on two-compartment IV drug-plasma concentrations.

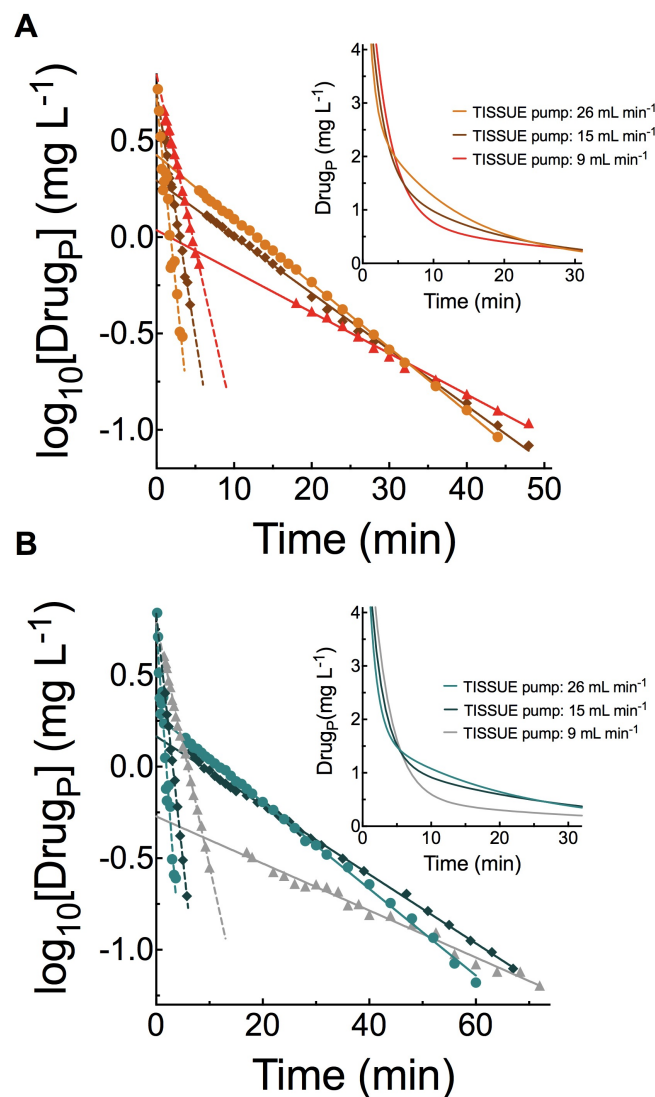
Calculated PK parameters are shown in Table 3.15. HEART pump: 132 mL min<sup>-1</sup>, LIVER pump: 7 mL min<sup>-1</sup>, KIDNEY 1 pump: 3 mL min<sup>-1</sup>, KIDNEY 2 pump: 5 mL min<sup>-1</sup> with TISSUE compartment volume at 100 mL. Comparison of data with TISSUE pump settings of 3 (▲), 7 (◆), and 17 mL min<sup>-1</sup> (●). Distribution and elimination phase of data plotted on semi-logarithmic graph using method of residuals with inset graph showing a close-up of the two-phase exponential decay equation fits for each condition.

Figure 3.13 Plasma Analysis				
Liver Pump Setting		7 mL min <sup>-1</sup>		
Kidney 1 Pump Setting; Kidney 2 Pump Setting		3 mL min <sup>-1</sup> ; 4 mL min <sup>-1</sup>		
Tissue Compartment Volume		100 mL		
Drug Dose: 0.96 mg		Acute Intravenous Administration		
Tissue Pump Setting		▲ 3 mL min <sup>-1</sup>	◆ 7 mL min <sup>-1</sup>	● 17 mL min <sup>-1</sup>
PK Parameter	Equation/Method Used			
<b>C<sub>t0</sub></b>	Two-Phase Exponential Decay Fit	10.38 mg L <sup>-1</sup>	10.24 mg L <sup>-1</sup>	13.68 mg L <sup>-1</sup>
<b>k<sub>dist</sub></b>	Two-Phase Exponential Decay Fit	0.15 min <sup>-1</sup>	0.26 min <sup>-1</sup>	0.61 min <sup>-1</sup>
<b>t<sub>1/2 dist</sub></b>	Two-Phase Exponential Decay Fit	4.7 min	2.7 min	1.1 min
<b>k<sub>el</sub></b>	Two-Phase Exponential Decay Fit	0.018 min <sup>-1</sup>	0.030 min <sup>-1</sup>	0.035 min <sup>-1</sup>
<b>t<sub>1/2 el</sub></b>	Two-Phase Exponential Decay Fit	38.8 min	23.5 min	19.7 min
<b>AUC<sub>0-∞</sub></b>	AUC <sub>0-∞</sub> = AUC + C <sub>tn</sub> / k	113.3 min · mg L <sup>-1</sup>	104.5 min · mg L <sup>-1</sup>	103.3 min · mg L <sup>-1</sup>
<b>V<sub>D SS</sub></b>	V <sub>D SS</sub> = (Dose x (A / α <sup>2</sup> + B / β <sup>2</sup> )) / AUC <sup>2</sup>	172 mL	208 mL	214 mL
<b>V<sub>D Area</sub></b>	V <sub>D Area</sub> = Dose / (AUC x β)	370 mL	283 mL	251 mL
<b>V<sub>D Extrap</sub></b>	V = Dose/ B	806 mL	393 mL	308 mL
<b>CL<sub>Total</sub></b>	CL <sub>Total</sub> = Dose / AUC <sub>0-∞</sub>	8.5 mL min <sup>-1</sup>	9.2 mL min <sup>-1</sup>	9.3 mL min <sup>-1</sup>
<b>r<sup>2</sup></b>	Two-Phase Exponential Decay Fit	0.9993	0.9979	0.9994
PK Parameter	Equation/Method Used			
<b>Y-intercept</b>	Linear-Regression Line	0.07584	0.3873	0.4944
<b>B</b>	10 <sup>Y-intercept</sup>	1.19 mg L <sup>-1</sup>	2.44 mg L <sup>-1</sup>	3.12 mg L <sup>-1</sup>
<b>slope</b>	Linear-Regression Line	-0.00994	-0.0141	-0.0160
<b>β</b>	β = -slope x 2.303	0.023 min <sup>-1</sup>	0.033 min <sup>-1</sup>	0.037 min <sup>-1</sup>
<b>t<sub>1/2 el</sub></b>	t <sub>1/2 el</sub> = 0.693 / β	30.3 min	21.3 min	18.7 min
<b>r<sup>2</sup></b>	Linear-Regression Line	0.96	0.9896	0.9992
PK Parameter	Equation/Method Used			
<b>Y-intercept</b>	Linear-Regression Line	1.193	1.01	0.992
<b>A</b>	10 <sup>Y-intercept</sup>	15.6 mg L <sup>-1</sup>	10.2 mg L <sup>-1</sup>	9.8 mg L <sup>-1</sup>
<b>slope</b>	Linear-Regression Line	-0.293	-0.177	-0.136
<b>α</b>	α = -slope x 2.303	0.68 min <sup>-1</sup>	0.41 min <sup>-1</sup>	0.31 min <sup>-1</sup>
<b>t<sub>1/2 dist</sub></b>	t <sub>1/2 dist</sub> = 0.693 / α	1.0 min	1.7 min	2.2 min
<b>r<sup>2</sup></b>	Linear-Regression Line	0.957	0.9948	0.9992
<b>k<sub>12</sub></b>	k <sub>12</sub> = ((A x B) x (β - α) <sup>2</sup> ) / ((A + B) x (Aβ + Bα))	0.34 min <sup>-1</sup>	0.21 min <sup>-1</sup>	0.16 min <sup>-1</sup>
<b>k<sub>21</sub></b>	k <sub>21</sub> = (Aβ + Bα) / (A + B)	0.14 min <sup>-1</sup>	0.076 min <sup>-1</sup>	0.035 min <sup>-1</sup>
<b>k<sub>10</sub></b>	k <sub>10</sub> = (αβ x (A + B)) / (Aβ + Bα)	0.24 min <sup>-1</sup>	0.15 min <sup>-1</sup>	0.14 min <sup>-1</sup>

Table 3.15 PK parameters calculated from IV drug-plasma concentrations under varied TISSUE pump rates shown in Figure 3.13.

Pharmacokinetic parameters calculated from plasma samples collected from two-compartment IV dosing experiments with varied TISSUE pump rates.

Experiments were also conducted to explore the effects of varied TISSUE pump rates with different TISSUE compartment volumes. Figure 3.14 shows results from experiments where the dose of methylene blue, elimination pump settings, and tissue compartment volume were kept constant, while the TISSUE pump rate was set to 9 (*slow*), 15 (*medium*), and 26 (*fast*) mL min<sup>-1</sup>. Figure 3.14A and B illustrate these comparisons when the TISSUE compartment volume was set at 100 mL, and 200 mL, respectively. The main graphs show semi-logarithmic plots following curve-stripping of the data, while the inset graphs show the concentration-time profiles on linear axes. As shown in Table 3.16, the calculated values for  $k_{12}$  and  $k_{21}$  were smaller at slower pump settings, and this trend was consistent regardless of TISSUE compartment volume. The  $k_{10}$  value was independent of the TISSUE pump rate or the TISSUE compartment volume, as it remained relatively stable between all six experiments, despite the varied TISSUE pump rates and TISSUE compartment volumes. The  $CL_{Total}$  and AUC values were also consistent between all the experiments, which continued to support the independence of clearance and volume of distribution parameters. As expected, the elimination and distribution half-lives decreased in response to increased TISSUE pump rate. As well, the half-life values increased appropriately when compared between the 100 mL and 200 mL experiments, with all other settings held constant.



**Figure 3.14. Modelling effects of varied TISSUE pump rates and TISSUE compartment volumes on two-compartment IV drug-plasma concentrations.**

Calculated PK parameters are shown in Table 3.16. HEART pump: 132 mL min<sup>-1</sup>, LIVER pump: 14 mL min<sup>-1</sup>, KIDNEY 1 pump: 3 mL min<sup>-1</sup>, KIDNEY 2 pump: 5 mL min<sup>-1</sup>. **(A)** Comparison of data with TISSUE pump settings of 9 (▲), 15 (◆), and 26 mL min<sup>-1</sup> (●) with TISSUE compartment volume of 100 mL. Distribution and elimination phase of data plotted on a semi-logarithmic graph using the method of residuals with inset graph showing a close-up of the two-phase exponential decay equation fits for each condition. **(B)** Comparison of data with TISSUE pump settings of 9 (▲), 15 (◆), and 26 mL min<sup>-1</sup> (●) with TISSUE compartment volume of 200 mL. Distribution and elimination phase of data plotted on a semi-logarithmic graph using the method of residuals with inset graph showing a close-up of the two-phase exponential decay equation fits for each condition.

Kidney 1 Pump Setting; Kidney 2 Pump Setting		Figure 3.14 Plasma Analysis					
		Liver Pump Setting		3 mL min <sup>-1</sup> ; 4 mL min <sup>-1</sup>		14 mL min <sup>-1</sup>	
Figure Panel		Figure 3.14 A		Figure 3.14 B		Figure 3.14 B	
Tissue Compartment Volume		100 mL		200 mL		26 mL min <sup>-1</sup>	
Tissue Pump Setting		9 mL min <sup>-1</sup>		15 mL min <sup>-1</sup>		9 mL min <sup>-1</sup>	
Drug Dose: 0.96 mg		Acute Intravenous Administration		26 mL min <sup>-1</sup>		15 mL min <sup>-1</sup>	
PK Parameter	Equation/Method Used	▲	◆	●	▲	◆	●
C <sub>0</sub>	Two-Phase Exponential Decay Fit	7.51 mg L <sup>-1</sup>	7.24 mg L <sup>-1</sup>	8.68 mg L <sup>-1</sup>	7.55 mg L <sup>-1</sup>	7.18 mg L <sup>-1</sup>	8.08 mg L <sup>-1</sup>
k <sub>dist</sub>	Two-Phase Exponential Decay Fit	0.37 min <sup>-1</sup>	0.53 min <sup>-1</sup>	1.16 min <sup>-1</sup>	0.37 min <sup>-1</sup>	0.51 min <sup>-1</sup>	0.84 min <sup>-1</sup>
t <sub>1/2 dist</sub>	Two-Phase Exponential Decay Fit	1.9 min	1.3 min	0.6 min	1.9 min	1.3 min	0.8 min
k <sub>el</sub>	Two-Phase Exponential Decay Fit	0.042 min <sup>-1</sup>	0.063 min <sup>-1</sup>	0.083 min <sup>-1</sup>	0.033 min <sup>-1</sup>	0.039 min <sup>-1</sup>	0.051 min <sup>-1</sup>
t <sub>1/2 el</sub>	Two-Phase Exponential Decay Fit	16.6 min	11.1 min	8.4 min	20.8 min	17.7 min	13.5 min
AUC <sub>0-∞</sub>	AUC <sub>0-∞</sub> = AUC + C <sub>tr</sub> /k	39.7 min · mg L <sup>-1</sup>	38.4 min · mg L <sup>-1</sup>	40.6 min · mg L <sup>-1</sup>	37.1 min · mg L <sup>-1</sup>	44.1 min · mg L <sup>-1</sup>	41.9 min · mg L <sup>-1</sup>
V <sub>D ss</sub>	V <sub>D ss</sub> = (Dose × (A / α <sup>2</sup> + B / β <sup>2</sup> )) / AUC <sup>2</sup>	299 mL	293 mL	267 mL	471 mL	393 mL	355 mL
V <sub>D Area</sub>	V <sub>D Area</sub> = Dose / (AUC × β)	492 mL	371 mL	308 mL	874 mL	502 mL	420 mL
V <sub>D Extrap</sub>	V <sub>D Extrap</sub> = Dose / B	883 mL	488 mL	360 mL	1794 mL	656 mL	503 mL
CL <sub>Total</sub>	CL <sub>Total</sub> = Dose / AUC <sub>0-∞</sub>	24.2 mL min <sup>-1</sup>	25 mL min <sup>-1</sup>	23.6 mL min <sup>-1</sup>	25.8 mL min <sup>-1</sup>	21.8 mL min <sup>-1</sup>	22.9 mL min <sup>-1</sup>
r <sup>2</sup>	Two-Phase Exponential Decay Fit	0.9987	0.9937	0.9913	0.9981	0.9958	0.9857
<b>Elimination Phase</b>							
Y-intercept	Linear Regression Line	0.0363	0.2939	0.4261	-0.2718	0.1654	0.2804
B	10 <sup>Y-intercept</sup>	1.09 mg L <sup>-1</sup>	1.97 mg L <sup>-1</sup>	2.67 mg L <sup>-1</sup>	0.53 mg L <sup>-1</sup>	1.46 mg L <sup>-1</sup>	1.91 mg L <sup>-1</sup>
slope	Linear Regression Line	-0.0213	-0.0292	-0.0333	-0.0128	-0.0188	-0.0237
β	β = slope × 2.303	0.049 min <sup>-1</sup>	0.067 min <sup>-1</sup>	0.077 min <sup>-1</sup>	0.030 min <sup>-1</sup>	0.043 min <sup>-1</sup>	0.055 min <sup>-1</sup>
t <sub>1/2 el</sub>	t <sub>1/2 el</sub> = 0.693 / β	14.1 min	10.3 min	9.0 min	23.4	16.0 min	12.7 min
r <sup>2</sup>	Linear Regression Line	0.9920	0.9977	0.9995	0.9760	0.9968	0.9977
<b>Distribution Phase</b>							
Y-intercept	Linear Regression Line	0.8424	0.7523	0.7185	0.7849	0.8357	0.766
A	10 <sup>Y-intercept</sup>	6.96 mg L <sup>-1</sup>	5.65 mg L <sup>-1</sup>	5.23 mg L <sup>-1</sup>	6.09 mg L <sup>-1</sup>	6.85 mg L <sup>-1</sup>	5.84 mg L <sup>-1</sup>
slope	Linear Regression Line	-0.181	-0.253	-0.392	-0.133	-0.268	-0.401
α	α = slope × 2.303	0.42 min <sup>-1</sup>	0.58 min <sup>-1</sup>	0.90 min <sup>-1</sup>	0.31 min <sup>-1</sup>	0.62 min <sup>-1</sup>	0.92 min <sup>-1</sup>
t <sub>1/2 dist</sub>	t <sub>1/2 dist</sub> = 0.693 / α	1.7 min	1.2 min	0.77 min	2.3 min	1.1 min	0.8 min
r <sup>2</sup>	Linear-Regression Line	0.9964	0.9933	0.9453	0.9977	0.9980	0.9423
k <sub>12</sub>	k <sub>12</sub> = ((A × B) × (β - α) <sup>2</sup> ) / ((A + B) × (Aβ + Bα))	0.16 min <sup>-1</sup>	0.25 min <sup>-1</sup>	0.43 min <sup>-1</sup>	0.11 min <sup>-1</sup>	0.33 min <sup>-1</sup>	0.52 min <sup>-1</sup>
k <sub>21</sub>	k <sub>21</sub> = (Aβ + Bα) / (A + B)	0.099 min <sup>-1</sup>	0.20 min <sup>-1</sup>	0.36 min <sup>-1</sup>	0.052 min <sup>-1</sup>	0.14 min <sup>-1</sup>	0.27 min <sup>-1</sup>
k <sub>10</sub>	k <sub>10</sub> = (αβ × (A + B)) / (Aβ + Bα)	0.21 min <sup>-1</sup>	0.20 min <sup>-1</sup>	0.19 min <sup>-1</sup>	0.17 min <sup>-1</sup>	0.19 min <sup>-1</sup>	0.19 min <sup>-1</sup>

Table 3.16 PK parameters calculated from IV drug-plasma concentrations under varied TISSUE pump rates and TISSUE compartment volumes shown in Figure 3.14.

Pharmacokinetic parameters calculated from plasma samples collected from two-compartment IV dosing experiments with varied tissue compartment volumes and TISSUE pump rates.

Varying the volume of water present in the tissue compartment bottle allows for the modelling of two-compartment drugs with different volumes of distribution. Consequently, it can also model individuals with varying levels of body fat and how these variations influence the PK of a drug that has low plasma protein binding. Figure 3.14 illustrates the effects of varying the TISSUE compartment volume between 100 and 200 mL, and Figure 3.15 further expands this comparison. Essentially, increasing the tissue compartment increases the  $V_D$ , which mimics more lipid-soluble compounds. The main graph depicts semi-logarithmic plots of distribution and elimination phases after intravenous administration of the same dose of drug when the TISSUE compartment volume was 100, 200, and 500 mL. The inset graph shows the two-phase exponential decay fits on linear axes, while Table 3.17 shows all calculated parameters. As discussed, and consistent with expectations, the  $t_{1/2\text{ dist}}$  and  $t_{1/2\text{ el}}$  values increased with increased TISSUE compartment volume, with decreases in the B-intercept value, consistent with increasing  $V_D$  values. The  $k_{12}$  and  $k_{21}$  values were altered accordingly, while the  $k_{10}$  value was consistent between the experiments.

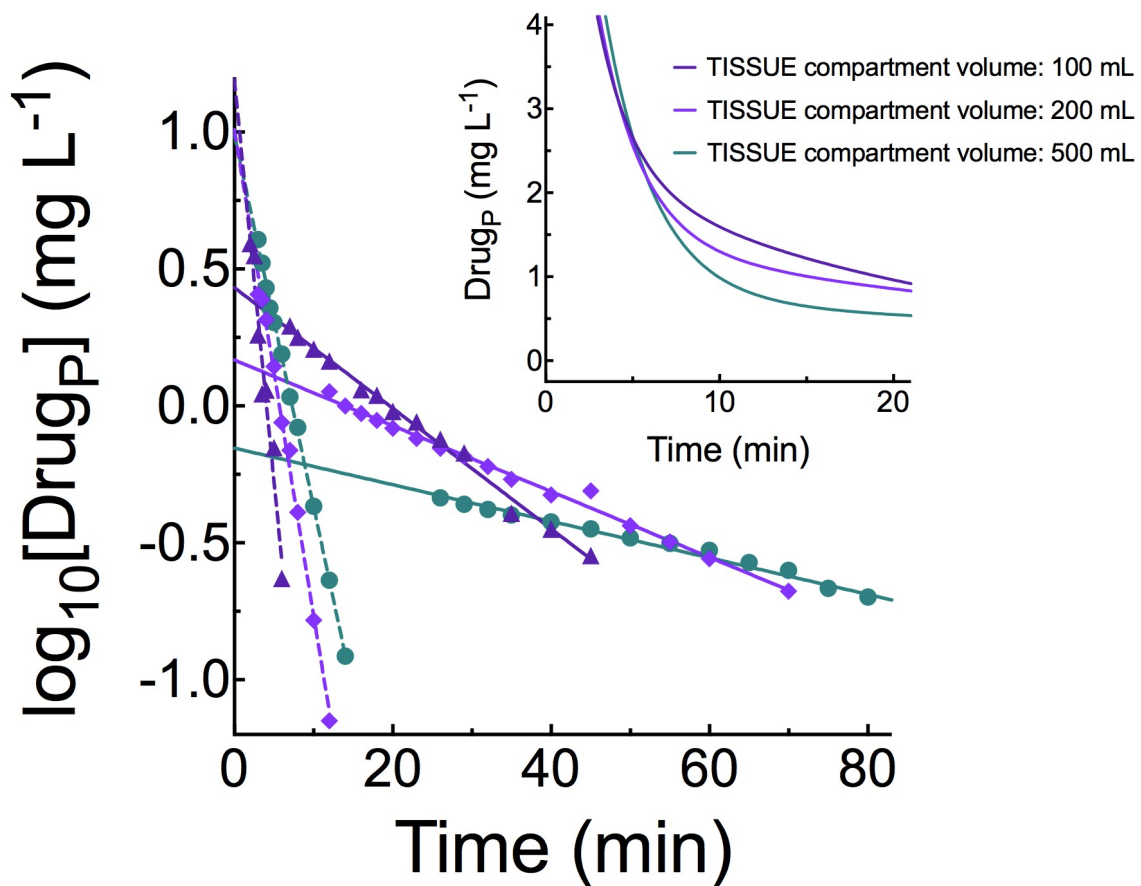


Figure 3.15. Modelling effects of varied TISSUE compartment volumes on two-compartment IV drug-plasma concentrations.

Calculated PK parameters are shown in Table 3.17. HEART pump:  $132 \text{ mL min}^{-1}$ , LIVER pump:  $7 \text{ mL min}^{-1}$ , TISSUE pump:  $10 \text{ mL min}^{-1}$ , KIDNEY 1 pump:  $3 \text{ mL min}^{-1}$ , KIDNEY 2 pump:  $5 \text{ mL min}^{-1}$  Comparison of data with TISSUE compartment volumes of 100 ( $\blacktriangle$ ), 200 ( $\blacklozenge$ ), and 500 mL ( $\bullet$ ). Distribution and elimination phase of data plotted on semi-logarithmic graph using the method of residuals with inset graph showing a close-up of the two-phase exponential decay equation fits for each condition.

Figure 3.15 Plasma Analysis				
Liver Pump Setting		7 mL min <sup>-1</sup>		
Kidney 1 Pump Setting; Kidney 2 Pump Setting		3 mL min <sup>-1</sup> ; 4 mL min <sup>-1</sup>		
Tissue Pump Setting		10 mL min <sup>-1</sup>		
Drug Dose: 0.96 mg		Acute Intravenous Administration		
Tissue Compartment Volume		▲ 100 mL	◆ 200 mL	● 500 mL
PK Parameter	Equation/Method Used	—	—	—
<b>C<sub>10</sub></b>	Two-Phase Exponential Decay Fit	11.02 mg L <sup>-1</sup>	11.04 mg L <sup>-1</sup>	11.87 mg L <sup>-1</sup>
<b>k<sub>dist</sub></b>	Two-Phase Exponential Decay Fit	0.49 min <sup>-1</sup>	0.40 min <sup>-1</sup>	0.34 min <sup>-1</sup>
<b>t<sub>1/2 dist</sub></b>	Two-Phase Exponential Decay Fit	1.4 min	1.7 min	2.0 min
<b>k<sub>el</sub></b>	Two-Phase Exponential Decay Fit	0.047 min <sup>-1</sup>	0.028 min <sup>-1</sup>	0.017 min <sup>-1</sup>
<b>t<sub>1/2 el</sub></b>	Two-Phase Exponential Decay Fit	14.8 min	24.3 min	41.2 min
<b>AUC<sub>0-∞</sub></b>	$AUC_{0-∞} = AUC + C_{in} / k$	72.2 min · mg L <sup>-1</sup>	77.2 min · mg L <sup>-1</sup>	78.4 min · mg L <sup>-1</sup>
<b>V<sub>D SS</sub></b>	$V_{D SS} = (Dose \times (A / \alpha^2 + B / \beta^2)) / AUC^2$	197 mL	312 mL	477 mL
<b>V<sub>D Area</sub></b>	$V_{D Area} = Dose / (AUC \times \beta)$	261 mL	444 mL	795 mL
<b>V<sub>D Extrap</sub></b>	$V = Dose / B$	355 mL	640 mL	1371 mL
<b>CL<sub>Total</sub></b>	$CL_{Total} = Dose / AUC_{0-∞}$	13.3 mL min <sup>-1</sup>	12.4 mL min <sup>-1</sup>	12.2 mL min <sup>-1</sup>
<b>r<sup>2</sup></b>	Two-Phase Exponential Decay Fit	0.9961	0.9923	0.9989
Elimination Phase				
PK Parameter	Equation/Method Used	—	—	—
<b>Y-intercept</b>	Linear-Regression Line	0.432	0.168	-0.154
<b>B</b>	$10^{Y-intercept}$	2.70 mg L <sup>-1</sup>	1.50 mg L <sup>-1</sup>	0.70 mg L <sup>-1</sup>
<b>slope</b>	Linear-Regression Line	-0.022	-0.12	-0.0067
<b>β</b>	$\beta = -slope \times 2.303$	0.051 min <sup>-1</sup>	0.028 min <sup>-1</sup>	0.015 min <sup>-1</sup>
<b>t<sub>1/2 el</sub></b>	$t_{1/2} = 0.693 / \beta$	13.6 min	24.8 min	46.2 min
<b>r<sup>2</sup></b>	Linear-Regression Line	0.9936	0.9919	0.9891
Distribution Phase				
PK Parameter	Equation/Method Used	.....	.....	.....
<b>Y-intercept</b>	Linear-Regression Line	1.193	1.01	0.992
<b>A</b>	$10^{Y-intercept}$	15.6 mg L <sup>-1</sup>	10.2 mg L <sup>-1</sup>	9.8 mg L <sup>-1</sup>
<b>slope</b>	Linear-Regression Line	-0.293	-0.177	-0.136
<b>α</b>	$\alpha = -slope \times 2.303$	0.68 min <sup>-1</sup>	0.41 min <sup>-1</sup>	0.31 min <sup>-1</sup>
<b>t<sub>1/2 dist</sub></b>	$t_{1/2 dist} = 0.693 / \alpha$	1.0 min	1.7 min	2.2 min
<b>r<sup>2</sup></b>	Linear-Regression Line	0.9570	0.9948	0.9992
<b>k<sub>12</sub></b>	$k_{12} = ((A \times B) \times (\beta - \alpha)) / ((A + B) \times (A\beta + B\alpha))$	0.34 min <sup>-1</sup>	0.21 min <sup>-1</sup>	0.16 min <sup>-1</sup>
<b>k<sub>21</sub></b>	$k_{21} = (A\beta + B\alpha) / (A + B)$	0.14 min <sup>-1</sup>	0.076 min <sup>-1</sup>	0.035 min <sup>-1</sup>
<b>k<sub>10</sub></b>	$k_{10} = (\alpha\beta \times (A + B)) / (A\beta + B\alpha)$	0.24 min <sup>-1</sup>	0.15 min <sup>-1</sup>	0.14 min <sup>-1</sup>

Table 3.17 PK parameters calculated from IV drug-plasma concentrations under varied TISSUE compartment volumes shown in Figure 3.15.

Pharmacokinetic parameters calculated from plasma samples collected from two-compartment IV dosing experiments with varied tissue compartment volumes.

The modeller simulates one- and two-compartment drug behaviour, but the system is scaled down to provide feasible timescales for teaching in a lab class. The rate constants, volume terms, and some of the other calculated PK parameters are smaller than would be expected if a real drug was administered into a real patient. While these values are not realistic, the approaches for calculating them are identical to the procedures used for calculating PK parameters in a real patient. However, it is possible to mimic more realistic values for at least some parameters by simply turning down the pump rate of the DISTRIBUTION pump, and increasing (perhaps significantly) the volume of the tissue compartment bottle. Depending on the settings employed, the modeller offers a range of values and parameters that can be used to mimic the outcomes of inter-individual variability as well as different properties of drugs that affect their ADME profile.

Figure 3.16 shows data fitted to a biphasic decay equation for 3 mg methylene blue administered intravenously into the modeller with 1 L in the TISSUE compartment. Figure 3.16B shows semi-logarithmic plots of distribution and elimination phases, obtained by curve stripping. Notably, as shown in Table 3.18, the elimination half-life for this experiment is determined to be ~100 minutes, with increased  $V_D$  terms in relation to other experiments. Figure 3.17 shows data fitted to a biphasic decay equation for 0.96 mg methylene blue administered intravenously into the modeller with 500 mL in the TISSUE compartment, with semi-logarithmic plots obtained by curve stripping in Figure 3.17B. The elimination half-life was 52.9 min *versus* the ~100 min obtained with 1 L in the TISSUE compartment. However, the distribution half-life between these two experiments were similar, as Figure 3.16 used a TISSUE pump rate of 15 mL min<sup>-1</sup> and a TISSUE compartment volume of 1 L, while Figure 3.17 had a reduced TISSUE pump rate of 9 mL min<sup>-1</sup> and 500 mL in the TISSUE compartment volume. In addition, the experiment in Figure 3.16 had a LIVER pump rate of 7 mL min<sup>-1</sup>, while the experiment in Figure 3.17 used a LIVER pump rate of 14 mL min<sup>-1</sup>.

These two experiments, though conducted under different settings, aim simply to show that the modeller can be adjusted to provide longer periods of sampling, but also that it is possible to alter the pump and tissue compartment parameters in such a way that there can be variability

for specific PK parameters to model pathophysiology, but still maintain consistency for other PK parameters that would not be affected by the deficiency in question.

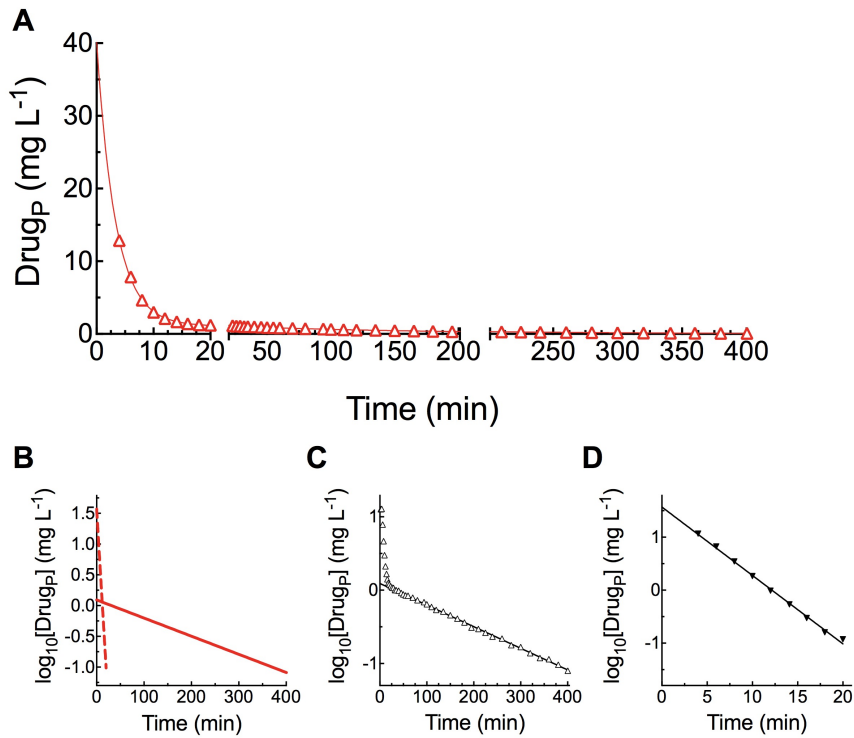


**Figure 3.16. Modelling effects of TISSUE compartment volume of 1000 mL on two-compartment IV drug-plasma concentrations.**

Calculated PK parameters are shown in Table 3.18. HEART pump:  $132 \text{ mL min}^{-1}$ , LIVER pump:  $14 \text{ mL min}^{-1}$ , TISSUE pump:  $15 \text{ mL min}^{-1}$ , KIDNEY 1 pump:  $3 \text{ mL min}^{-1}$ , KIDNEY 2 pump:  $5 \text{ mL min}^{-1}$ , TISSUE compartment volume: 1 L. **(A)** Plasma data fitted to a two-phase exponential decay equation on linear axis ( $\Delta$ ). **(B)** Distribution and elimination phase of data in (A) plotted on a semi-logarithmic graph using the method of residuals **(C)** Classic hockey-stick profile of data in (A) on a semi-logarithmic plot ( $\Delta$ ). **(D)** Distribution phase of data obtained through curve stripping showing a distribution phase extended to 20 minutes ( $\blacktriangledown$ ).

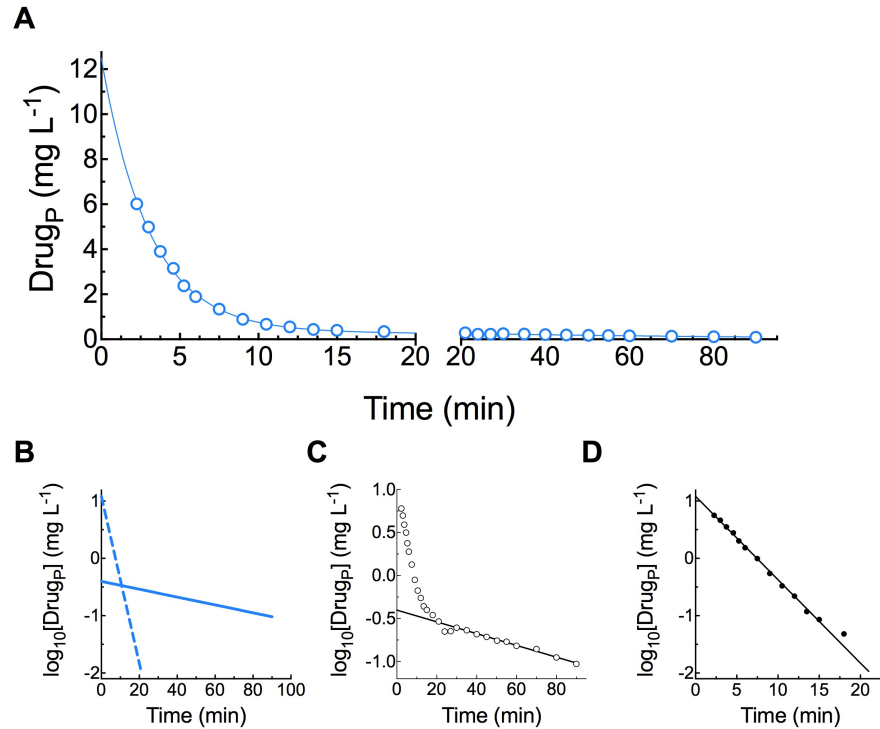


**Figure 3.17. Modelling effects of TISSUE compartment volume of 500 mL on two-compartment IV drug-plasma concentrations.**

Calculated PK parameters are shown in Table 3.18. HEART pump:  $132 \text{ mL min}^{-1}$ , LIVER pump:  $7 \text{ mL min}^{-1}$ , TISSUE pump:  $9 \text{ mL min}^{-1}$ , KIDNEY 1 pump:  $3 \text{ mL min}^{-1}$ , KIDNEY 2 pump:  $5 \text{ mL min}^{-1}$ , TISSUE compartment volume: 500 mL. **(A)** Plasma data fitted to a two-phase exponential decay equation on linear axes (○). **(B)** Distribution and elimination phases of data in (A) plotted on a semi-logarithmic graph using the method of residuals **(C)** Classic hockey-stick profile of data in (A) on a semi-logarithmic plot (○). **(D)** Distribution phases of data obtained through curve stripping showing a distribution phase extended to 20 minutes (●).

Figure 3.16 and 3.17			
Kidney 1 Pump Setting; Kidney 2 Pump Setting		3 mL min <sup>-1</sup> ; 4 mL min <sup>-1</sup>	
Figure and Panel		Figure 3.16 A	Figure 3.17 B
Liver Pump Setting		7 mL min <sup>-1</sup>	14 mL min <sup>-1</sup>
Drug Dose		3 mg	0.96 mg
Tissue Pump Setting; Tissue Compartment Volume		15 mL min <sup>-1</sup> ; 1000 mL	9 mL min <sup>-1</sup> ; 500 mL
PK Parameter	Equation/Method Used		
<b>C<sub>t0</sub></b>	Two-Phase Exponential Decay Fit	40.14 mg L <sup>-1</sup>	12.49 mg L <sup>-1</sup>
<b>k<sub>dist</sub></b>	Two-Phase Exponential Decay Fit	0.30 min <sup>-1</sup>	0.33 min <sup>-1</sup>
<b>t<sub>1/2 dist</sub></b>	Two-Phase Exponential Decay Fit	2.3 min	2.1 min
<b>k<sub>el</sub></b>	Two-Phase Exponential Decay Fit	0.0067 min <sup>-1</sup>	0.013 min <sup>-1</sup>
<b>t<sub>1/2 el</sub></b>	Two-Phase Exponential Decay Fit	103.4 min	52.9 min
<b>AUC<sub>0-∞</sub></b>	$AUC_{0-∞} = AUC + C_{tr}/k$	412.0 min · mg L <sup>-1</sup>	62.0 min · mg L <sup>-1</sup>
<b>V<sub>D SS</sub></b>	$V_{D SS} = (Dose \times (A/\alpha^2 + B/\beta^2)) / AUC^2$	481 mL	423 mL
<b>V<sub>D Area</sub></b>	$V_{D Area} = Dose / (AUC \times \beta)$	1071 mL	979 mL
<b>V<sub>D Extrap</sub></b>	$V_{D Extrap} = Dose / B$	2419 mL	2423 mL
<b>CL<sub>Total</sub></b>	$CL_{Total} = Dose / AUC_{0-∞}$	7.3 mL min <sup>-1</sup>	15.5 mL min <sup>-1</sup>
<b>r<sup>2</sup></b>	Two-Phase Exponential Decay Fit	0.9996	0.9988
Figure and Panel		Figure 3.16 C	Figure 3.17 C
Elimination Phase			
<b>Y-intercept</b>	Linear Regression Line	0.0921	-0.402
<b>B</b>	$10^{Y\text{-intercept}}$	1.24 mg L <sup>-1</sup>	0.396 mg L <sup>-1</sup>
<b>slope</b>	Linear Regression Line	-0.00295	-0.00684
<b>β</b>	$\beta = slope \times 2.303$	0.0068 min <sup>-1</sup>	0.016 min <sup>-1</sup>
<b>t<sub>1/2 el</sub></b>	$t_{1/2 el} = 0.693 / k$	102.0 min	44.0 min
<b>r<sup>2</sup></b>	Linear Regression Line	0.9974	0.9932
Figure and Panel		Figure 3.16 D	Figure 3.17 D
Distribution Phase			
<b>Y-intercept</b>	Linear Regression Line	1.569	1.083
<b>A</b>	$10^{Y\text{-intercept}}$	37.07 mg L <sup>-1</sup>	12.11 mg L <sup>-1</sup>
<b>slope</b>	Linear Regression Line	-0.129	-0.145
<b>α</b>	$\alpha = slope \times 2.303$	0.30 min <sup>-1</sup>	0.33 min <sup>-1</sup>
<b>t<sub>1/2 dist</sub></b>	$t_{1/2 dist} = 0.693 / k$	2.3 min	2.1 min
<b>r<sup>2</sup></b>	Linear-Regression Line	0.9969	0.9919
<b>k<sub>12</sub></b>	$k_{12} = (AB \times (\beta - \alpha)^2) / ((A+B) \times (A\beta + B\alpha))$	0.0092 min <sup>-1</sup>	0.0096 min <sup>-1</sup>
<b>k<sub>21</sub></b>	$k_{21} = (A\beta + B\alpha) / (A+B)$	0.29 min <sup>-1</sup>	0.32 min <sup>-1</sup>
<b>k<sub>10</sub></b>	$k_{10} = (\alpha\beta \times (A+B)) / (A\beta + B\alpha)$	0.007 min <sup>-1</sup>	0.016 min <sup>-1</sup>

Table 3.18 PK parameters calculated from IV drug-plasma concentrations under larger TISSUE compartment volumes shown in Figure 3.16 and 3.17.

Pharmacokinetic parameters calculated from plasma samples collected from two-compartment IV dosing experiments using 1000 mL and 500 mL tissue compartment volumes.

## TWO-COMPARTMENT CHRONIC DOSING

The modeller allows for the design and implementation of chronic (repeated or infusion) dosing regimens, as well as regimens requiring a loading dose. These experiments are designed by calculating PK parameters from acute IV (or if necessary, PO) dosing experiments; knowledge of the  $V_{D\text{ Extrap}}$  and  $k_{el}$  when the system is in a specific configuration are the most important with respect to designing these regimens (see Table 3.19). Figure 3.18 illustrates concentration-time profiles from an acute IV study, followed by subsequent chronic IV (injection and infusion), and chronic PO dosing experiments, all carried out under identical conditions. In the chronic PO dosing experiments, the ORAL BIOAVAILABILITY pump was not turned on, such that the  $F$  was 100%. Overall, the objective of these experiments was to achieve a desired mean steady state concentration ( $C_{SS}$ ) while maintaining plasma levels within a specified  $C_{min}$  and  $C_{max}$  range. Though the IV studies resulted in high peak:trough values, sometimes exceeding the  $C_{max}$ , the overall  $C_{SS}$  was maintained relatively well, and the transient peaks were considered as acceptable for the route of administration and dosing protocol. In comparison with the oral administration route, IV administration does not allow for smoothing of the peaks due to the absorption phase, which is often seen in the clinical setting.

Under a two-compartment configuration, a single IV dose of 0.96 mg drug was administered into the apparatus, and data were collected and analysed as shown in Figure 3.18A and Table 3.19. Figure 3.18B displays data from chronic PO dosing experiments (1.05 mg every 10 minutes) with an achieved  $C_{Av}$  of 6.28 mg L<sup>-1</sup> (the target was 6 mg L<sup>-1</sup>) where the stomach volume was 17 mL. The inset graph of Figure 3.18B demonstrates the peak:trough ratio at steady state from the data shown in Figure 3.18B and data from another experiment (not shown) where the stomach volume was 35 mL. Essentially, increasing the stomach volume reduced the peaks, mimicking slower absorption that might be observed with a sustained release oral preparation. Figure 3.18C demonstrates data from an experiment completed under similar conditions to those in Figure 3.18B, with an achieved  $C_{Av}$  of 6.53 mg L<sup>-1</sup>, but with drug administered by the IV route.

Figure 3.18D and E display data obtained following the administration of a loading dose by PO and IV routes. A loading dose allows drug to reach the target steady state concentration almost immediately, circumventing the time required to achieve the levels if administered under a normal repeated dosing regimen. The target  $C_{SS}$  for Figure 3.18D was  $7.4 \text{ mg L}^{-1}$ , and the loading dose of  $2.45 \text{ mg}$  followed by maintenance of  $0.78 \text{ mg}$  every 6 minutes allowed for immediate and consistent  $C_{Av}$  levels of  $7.58 \text{ mg L}^{-1}$ . Similarly, Figure 3.18E displays data obtained from an IV administration experiment, where a loading dose of  $2.02 \text{ mg}$  followed by maintenance doses of  $0.61 \text{ mg}$  every 6 minutes allowed the system to achieve a  $C_{Av}$  of  $5.87 \text{ mg L}^{-1}$  (the target  $C_{SS}$  was  $6 \text{ mg L}^{-1}$ ). The large spike observed with the loading dose is consistent with the rate of administration exceeding the rate of distribution, allowing for almost the entire dose initially to be present in the central compartment.

Figure 3.18F illustrates a concentration-time profile following the infusion of drug solution ( $106 \text{ } \mu\text{g mL}^{-1}$ ) at a constant rate of  $1 \text{ mL min}^{-1}$  using an IV infusion pump. The achieved  $C_{SS}$  was  $7.38 \text{ mg L}^{-1}$ , which was slightly higher than the target  $C_{SS}$  of  $6 \text{ mg L}^{-1}$ . Data points from the first and last 60 minutes (0-60 min and 120-180 min) were analysed using non-linear regression fits to a two-phase association equation, and to a two-phase exponential decay equation, respectively, and plotted as shown in the inset graph. The half-lives obtained (one for distribution, another for elimination) were similar between the two fits, showing the consistency between the exponential relationship of drug accumulation and elimination within the system. The two curves, as shown in the inset graph, were superimposed, and are mirror images of one another.

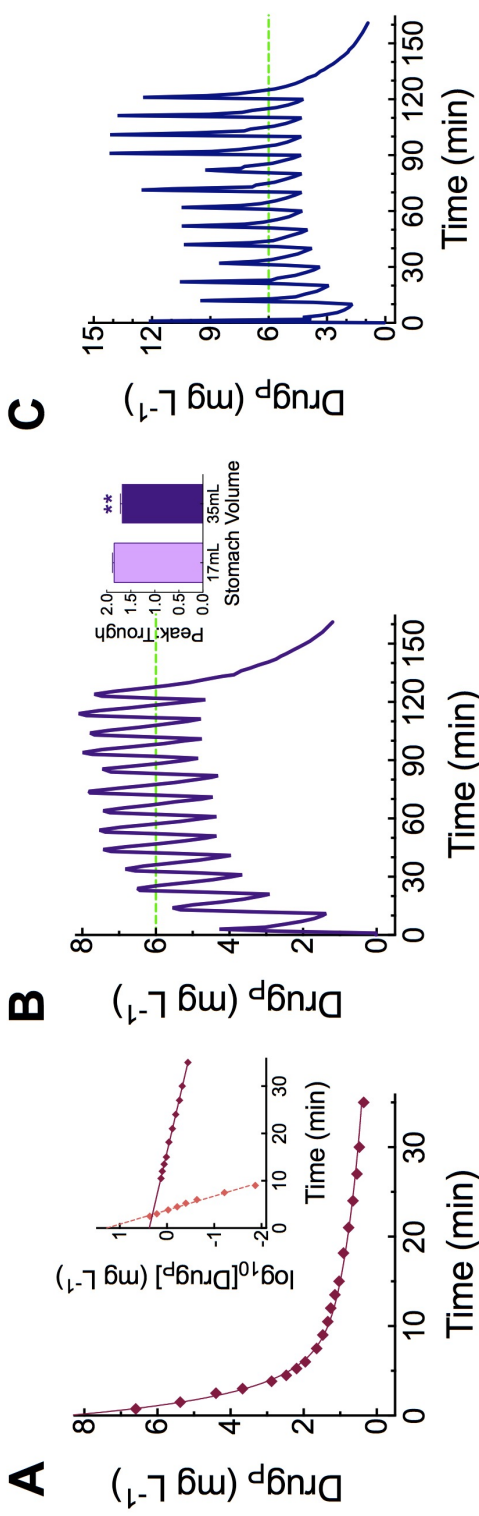


**Figure 3.18. Repeated or chronic drug administration, with or without loading dose, by IV and PO routes in a two-compartment configuration.**

Calculated PK parameters are shown in Table 3.19 and Table 3.20. HEART pump:  $132 \text{ mL min}^{-1}$ , LIVER pump rate:  $10 \text{ mL min}^{-1}$ , TISSUE pump rate:  $12 \text{ mL min}^{-1}$ , KIDNEY 1 pump rate:  $3 \text{ mL min}^{-1}$ , KIDNEY 2 pump rate:  $4 \text{ mL min}^{-1}$ , TISSUE compartment volume:  $100 \text{ mL}$ . **(A)** Plasma data fitted to a two-phase exponential decay equation plotted on a linear Y-axis following a single bolus IV injection ( $\blacklozenge$ ). Inset graph includes data plotted on a semi-logarithmic plot following curve stripping to obtain distribution ( $\blacklozenge$ ) and elimination ( $\blacklozenge$ ) phases. The PK parameters calculated from this experiment were used to calculate repeated dosing parameters for experiments in panels B-F. **(B)** Repeated PO dosing of  $1.05 \text{ mg}$  drug every 10 minutes, with achieved  $C_{SS}$  of  $6.28 \text{ mg L}^{-1}$  (target was  $6 \text{ mg L}^{-1}$  (---)). The inset graph shows peak:trough ratios at steady state from experiment shown in the main panel (stomach volume  $17 \text{ mL}$ ) and from a similar parallel experiment where the stomach volume was  $35 \text{ mL}$ . **(C)** Repeated IV dosing of  $1.05 \text{ mg}$  drug every 10 minutes with achieved  $C_{SS}$  of  $6.53 \text{ mg L}^{-1}$  (target was  $6 \text{ mg L}^{-1}$  (---)). **(D)** PO loading dose of  $2.45 \text{ mg}$  followed by repeated PO doses of  $0.78 \text{ mg}$  every 6 minutes, with stomach volume of  $35 \text{ mL}$  and an achieved  $C_{SS}$  of  $7.58 \text{ mg L}^{-1}$  (target was  $7.4 \text{ mg L}^{-1}$  (---)). **(E)** IV loading dose of  $2.02 \text{ mg}$  drug followed by repeated IV doses of  $0.61 \text{ mg}$  every 6 minutes with achieved  $C_{SS}$  of  $5.87 \text{ mg L}^{-1}$  (target was  $6 \text{ mg L}^{-1}$  (---)). **(F)** Continuous IV infusion ( $1 \text{ mL min}^{-1}$  and  $106 \mu\text{g min}^{-1}$ ) with achieved  $C_{SS}$  of  $7.38 \text{ mg L}^{-1}$  (target was  $6 \text{ mg L}^{-1}$  (---)). Inset graph shows superimposed data from the first ( $\blacktriangle$ ) and last ( $\blacktriangledown$ ) 60 minutes of the IV infusion shown in the main figure.

Figure 3.18 Plasma Analysis		
Liver Pump Setting		10 mL min <sup>-1</sup>
Kidney 1 Pump Setting; Kidney 2 Pump Setting		3 mL min <sup>-1</sup> ; 4 mL min <sup>-1</sup>
Tissue Pump Setting; Tissue Compartment Volume		12 mL min <sup>-1</sup> ; 100 mL
Figure 3.18A		
Drug Dose: 0.96 mg		Acute Intravenous Administration
PK Parameter	Equation/Method Used	
C <sub>to</sub>	Two-Phase Exponential Decay Fit	8.48 mg L <sup>-1</sup>
k <sub>dist</sub>	Two-Phase Exponential Decay Fit	0.40 min <sup>-1</sup>
t <sub>1/2 dist</sub>	Two-Phase Exponential Decay Fit	1.7 min
k <sub>el</sub>	Two-Phase Exponential Decay Fit	0.043 min <sup>-1</sup>
t <sub>1/2 el</sub>	Two-Phase Exponential Decay Fit	16.0 min
AUC <sub>0-∞</sub>	AUC <sub>0-∞</sub> = AUC + C <sub>tr</sub> /k	58.9 min · mg L <sup>-1</sup>
V <sub>D SS</sub>	V <sub>D SS</sub> = (Dose x (A/α <sup>2</sup> + B/β <sup>2</sup> )) / AUC <sup>2</sup>	236 mL
V <sub>D Area</sub>	V <sub>D Area</sub> = Dose / (AUC x β)	303 mL
V <sub>D Extrap</sub>	V <sub>D Extrap</sub> = Dose / B	405 mL
CL <sub>Total</sub>	CL <sub>Total</sub> = Dose / AUC <sub>0-∞</sub>	16.3 mL min <sup>-1</sup>
r <sup>2</sup>	Two-Phase Exponential Decay Fit	0.9988
PK Parameter	Equation/Method Used	
Y-intercept	Linear Regression Line	0.376
B	10 <sup>Y-intercept</sup>	2.38 mg L <sup>-1</sup>
slope	Linear Regression Line	-0.0234
β	β = slope x 2.303	0.054 min <sup>-1</sup>
t <sub>1/2 el</sub>	t <sub>1/2 el</sub> = 0.693 / β	12.9 min
r <sup>2</sup>	Linear Regression Line	0.9988
PK Parameter	Equation/Method Used	
Y-intercept	Linear Regression Line	1.28
A	10 <sup>Y-intercept</sup>	18.9 mg L <sup>-1</sup>
slope	Linear Regression Line	-0.336
α	α = slope x 2.303	0.77 min <sup>-1</sup>
t <sub>1/2 dist</sub>	t <sub>1/2 dist</sub> = 0.693 / α	0.90 min
r <sup>2</sup>	Linear-Regression Fit	0.9891
Figure 3.18B		Repeated Oral Dosing
PK Parameter	Equation/Method Used	
Maintenance Dose Rate	Maintenance Dose Rate = C <sub>SS</sub> x V <sub>D</sub> x k <sub>el</sub> ; C <sub>SS</sub> = 6 mg L <sup>-1</sup>	0.105 mg min <sup>-1</sup>
Oral Dose Rate	Oral Dose Rate = IV Dose Rate / F; F=100%	0.105 mg min <sup>-1</sup>
τ	C <sub>max</sub> / C <sub>min</sub> = 1 / e <sup>-kt</sup> ; 7.5 mg L <sup>-1</sup> , C <sub>min</sub> : 4.5 mg L <sup>-1</sup> = C <sub>max</sub> :C <sub>min</sub> = 1.7	9.5 min (10 min)
Total Dose every 10 min	Total Dose = Maintenance Dose Rate (mg min <sup>-1</sup> ) x 10 (min)	1.05 mg
Achieved C <sub>Av</sub>	Average of AUCs of Dosing Interval at C <sub>SS</sub> / Dosing Interval (10 min)	6.28 mg L <sup>-1</sup>
Figure 3.18C		Repeated Intravenous Dosing
PK Parameter	Equation/Method Used	
Maintenance Dose Rate	Maintenance Dose Rate = C <sub>SS</sub> x V <sub>D</sub> x k <sub>el</sub> ; C <sub>SS</sub> = 6 mg L <sup>-1</sup>	0.105 mg min <sup>-1</sup>
τ	C <sub>max</sub> / C <sub>min</sub> = 1 / e <sup>-kt</sup> ; 7.5 mg L <sup>-1</sup> , C <sub>min</sub> : 4.5 mg L <sup>-1</sup> = C <sub>max</sub> :C <sub>min</sub> = 1.7	9.5 min (10 min)
Total Dose every 10 min	Total Dose = Maintenance Dose Rate (mg min <sup>-1</sup> ) x 10 (min)	1.05 mg
Achieved C <sub>Av</sub>	Average of AUCs of Dosing Interval at C <sub>SS</sub> / Dosing Interval (10 min)	6.53 mg L <sup>-1</sup>

Table 3.19 PK parameters calculated from analyses of IV and PO drug-plasma concentrations from single, and repeated dosing shown in Figure 3.18A, B, and C.

Figure 3.18 Plasma Analysis		
Liver Pump Setting		10 mL min <sup>-1</sup>
Kidney 1 Pump Setting; Kidney 2 Pump Setting		3 mL min <sup>-1</sup> ; 4 mL min <sup>-1</sup>
Tissue Pump Setting; Tissue Compartment Volume		12 mL min <sup>-1</sup> ; 100 mL
Figure 3.18D		Repeated Oral Dosing with Loading Dose
PK Parameter	Equation/Method Used	
Loading Dose	Loading Dose = C <sub>SS</sub> x V <sub>D</sub> ; C <sub>SS</sub> = 7.4 mg L <sup>-1</sup>	3.04 mg
Maintenance Dose Rate	Maintenance Dose Rate = C <sub>SS</sub> x V <sub>D</sub> x k <sub>el</sub> ; C <sub>SS</sub> = 7.4 mg L <sup>-1</sup>	0.130 mg min <sup>-1</sup>
Oral Dose Rate	Oral Dose Rate = IV Dose Rate / F; F=100%	0.130 mg min <sup>-1</sup>
τ	C <sub>max</sub> / C <sub>min</sub> = 1 / e <sup>-kt</sup> ; 9 mg L <sup>-1</sup> , C <sub>min</sub> : 6 mg L <sup>-1</sup> = C <sub>max</sub> :C <sub>min</sub> = 1.5	9.4 min (6 min)
Total Dose every 6 min	Total Dose = Maintenance Dose Rate (mg min <sup>-1</sup> ) x 6 (min)	0.782 mg
Achieved C <sub>Av</sub>	Average of AUCs of Dosing Interval at C <sub>SS</sub> / Dosing Interval (6 min)	7.58 mg L <sup>-1</sup>
Figure 3.18E		Repeated Intravenous Dosing with Loading Dose
PK Parameter	Equation/Method Used	
Loading Dose	Loading Dose = C <sub>SS</sub> x V <sub>D</sub> ; C <sub>SS</sub> = 6 mg L <sup>-1</sup>	2.05 mg
Maintenance Dose Rate	Maintenance Dose Rate = C <sub>SS</sub> x V <sub>D</sub> x k <sub>el</sub> ; C <sub>SS</sub> = 6 mg L <sup>-1</sup>	0.102 mg min <sup>-1</sup>
τ	C <sub>max</sub> / C <sub>min</sub> = 1 / e <sup>-kt</sup> ; 7.5 mg L <sup>-1</sup> , C <sub>min</sub> : 4.5 mg L <sup>-1</sup> = C <sub>max</sub> :C <sub>min</sub> = 1.7	9.5 min (6 min)
Total Dose every 6 min	Total Dose = Maintenance Dose Rate (mg min <sup>-1</sup> ) x 6 (min)	0.612 mg
Achieved C <sub>Av</sub>	Average of AUCs of Dosing Interval at C <sub>SS</sub> / Dosing Interval (6 min)	5.87 mg L <sup>-1</sup>
Figure 3.18F		Intravenous Infusion
PK Parameter	Equation/Method Used	
Maintenance Dose Rate	Maintenance Dose Rate = C <sub>SS</sub> x V <sub>D</sub> x k <sub>el</sub> ; C <sub>SS</sub> = 6 mg L <sup>-1</sup>	0.105 mg min <sup>-1</sup>
Total Dose/Hour	Maintenance Dose Rate (mg min <sup>-1</sup> ) x 60 (mins hour <sup>-1</sup> )	6.31 mg hour <sup>-1</sup>
Achieved C <sub>SS</sub>	Average plasma concentration achieved at C <sub>SS</sub>	7.38 mg L <sup>-1</sup>
t <sub>1/2</sub> ▲	Two-Phase Association Fit	1.30 and 11.7 min
t <sub>1/2</sub> ▼	Two-Phase Exponential Decay Fit	1.84 and 15.2 min

Table 3.20 PK parameters calculated from analyses of IV and PO drug-plasma concentrations from repeated dosing with loading dose, and continuous IV infusion experiments shown in Figure 3.18D, E, and F.

Figure 3.19 shows results from a repeated PO dosing experiment based on the conditions and PK parameters displayed in Figure 3.18A. Figure 3.19A illustrates the successful achievement of a C<sub>Av</sub> of 6.0 mg L<sup>-1</sup> following PO administration of 1.60 mg every 15 minutes, while Figure 3.19B displays a more frequent dosing regimen (1.05 mg every 10 minutes) and achievement of a C<sub>Av</sub> of 6.28 mg L<sup>-1</sup>. The inset graph displays the peak:trough ratio between the two conditions, clearly showing that the more frequent administration dosing results in a reduced ratio, which follows conventional understanding of the effects of dosing frequency on drug

accumulation and plasma concentrations. The chronic and repeated dosing data shown in Figure 3.18 and Figure 3.19 demonstrate the apparatus' capability of mimicking real-life clinical outcomes.

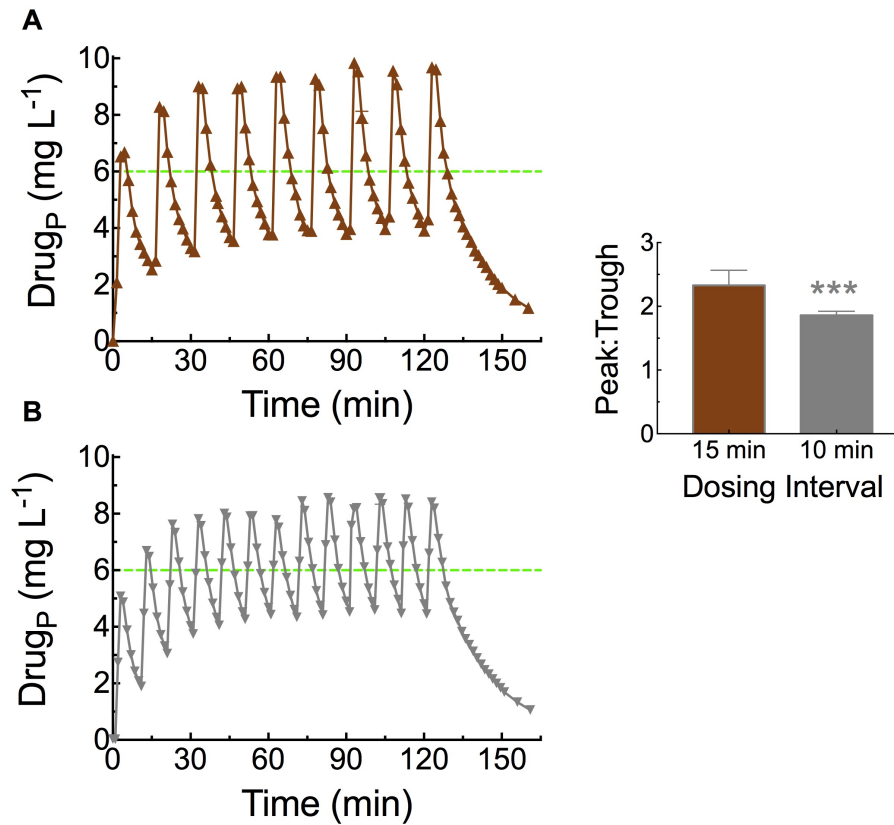


Figure 3.19. Drug-plasma concentration time profiles following repeated PO drug administration in a two-compartment configuration using two different dosing intervals: 15 min and 10 min.

The dosing regimens were designed based on the single IV dose values calculated from Figure 3.18A. The calculated PK parameters from the above experiments are shown in Table 3.21. HEART pump: 132 mL min<sup>-1</sup>, LIVER pump rate: 10 mL min<sup>-1</sup>, TISSUE pump rate: 12 mL min<sup>-1</sup>, KIDNEY 1 pump rate: 3 mL min<sup>-1</sup>, KIDNEY 2 pump rate: 4 mL min<sup>-1</sup>, TISSUE compartment volume: 100 mL, STOMACH volume: 20 mL. (A) Repeated PO dosing (▲) of 1.60 mg drug every 15 minutes, with achieved C<sub>SS</sub> of 6.0 mg L<sup>-1</sup> (target was 6 mg L<sup>-1</sup> (---)). (B) Repeated PO dosing (▼) of 1.06 mg drug every 10 minutes, with achieved C<sub>SS</sub> of 6.28 mg L<sup>-1</sup> (target was 6 mg L<sup>-1</sup> (---)). The inset graph shows peak:trough ratios at steady state from experiments in (A) and (B) to display the impact of dosing interval.

Figure 3.19 Plasma Analysis		
Liver Pump Setting		10 mL min <sup>-1</sup>
Kidney 1 Pump Setting; Kidney 2 Pump Setting		3 mL min <sup>-1</sup> ; 4 mL min <sup>-1</sup>
Tissue Pump Setting; Tissue Compartment Volume		12 mL min <sup>-1</sup> ; 100 mL
Figure 3.19A		Repeated Oral Dosing
PK Parameter	Equation/Method Used	 —
Maintenance Dose Rate	Maintenance Dose Rate = $C_{SS} \times V_D \times k_{el}$ ; $C_{SS} = 6 \text{ mg L}^{-1}$	0.105 mg min <sup>-1</sup>
Oral Dose Rate	Oral Dose Rate = IV Dose Rate / F; F=100%	0.105 mg min <sup>-1</sup>
$\tau$	$C_{max} / C_{min} = 1 / e^{-k\tau}$ ; 8 mg L <sup>-1</sup> , $C_{min}: 4 \text{ mg L}^{-1} = C_{max}:C_{min} = 2$	16.1 min ( <b>15 min</b> )
Total Dose every 10 min	Total Dose = Maintenance Dose Rate (mg min <sup>-1</sup> ) x 10 (min)	1.60 mg
Achieved $C_{Av}$	Average of AUCs of Dosing Interval at $C_{SS}$ / Dosing Interval (10 min)	6.0 mg L <sup>-1</sup>
Figure 3.19B		Repeated Oral Dosing
PK Parameter	Equation/Method Used	 —
Maintenance Dose Rate	Maintenance Dose Rate = $C_{SS} \times V_D \times k_{el}$ ; $C_{SS} = 6 \text{ mg L}^{-1}$	0.105 mg min <sup>-1</sup>
Oral Dose Rate	Oral Dose Rate = IV Dose Rate / F; F=100%	0.105 mg min <sup>-1</sup>
$\tau$	$C_{max} / C_{min} = 1 / e^{-k\tau}$ ; 8 mg L <sup>-1</sup> , $C_{min}: 4 \text{ mg L}^{-1} = C_{max}:C_{min} = 2$	16.1 min ( <b>10 min</b> )
Total Dose every 10 min	Total Dose = Maintenance Dose Rate (mg min <sup>-1</sup> ) x 10 (min)	1.05 mg
Achieved $C_{Av}$	Average of AUCs of Dosing Interval at $C_{SS}$ / Dosing Interval (10 min)	6.28 mg L <sup>-1</sup>

Table 3.21 PK parameters calculated from PO drug-plasma concentrations under varied repeated PO dosing regimens shown in Figure 3.19.

Pharmacokinetic parameters calculated from plasma samples collected from two-compartment repeated PO dosing experiments.

### 3.3 STUDENT RESULTS

Students who previously completed undergraduate work in a course covering PK principles and calculations significantly improved in their ability to answer short PK calculation quiz questions after attending two laboratory classes using the apparatus (Figure 3.20A). As well, students were asked to self-assess their competence in PK calculations and understanding of PK concepts prior to and after the laboratory class; in both cases, students reported improvement following the laboratory class (see Figure 3.20B and C). Students also reported their opinions on a scale of 1 to 5 (with 1 representing *strongly disagree* and 5 corresponding to *strongly agree*) regarding the effectiveness of the laboratory protocols in improving their competence and understanding, whether they felt the lab protocols were easy and enjoyable, and whether they felt the simulator was an effective educational tool (see Figure 3.21). In terms of the educational effectiveness of the ADAM, the students returned a score of  $4.5 \pm 0.2$  (mean  $\pm$  SEM, n=13).

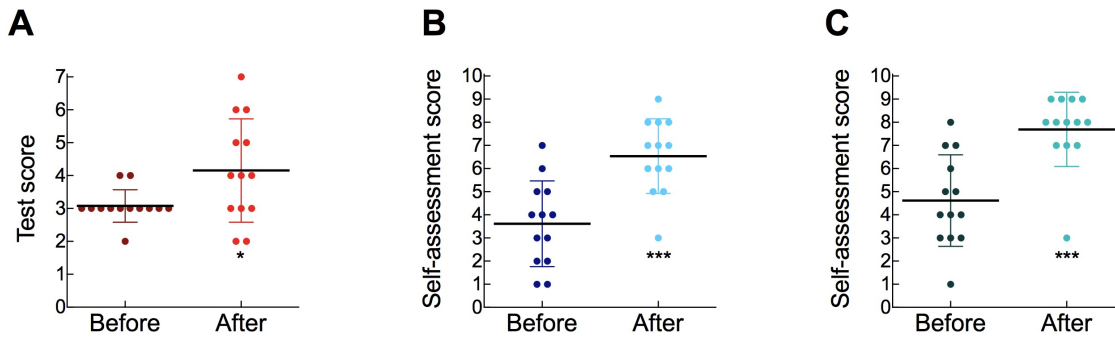


Figure 3.20. Scatter plots showing undergraduate student performance and self-assessment scores before and after completing two laboratory classes with the PK simulator.

Statistical comparisons were made with Wilcoxon’s matched pairs tests; bars show mean  $\pm$  SD (n=13) (A) Scores obtained in a short test of ability to carry out PK calculations (\*  $p = 0.0313$ ). (B) Student self-reporting of perception of their own competence in dealing with the mathematical and graphing aspects of PK, before and after completing the laboratory class (\*\*\*)  $p = 0.0002$ ). (C) Student self-reporting of perception of their understanding of the mathematical aspects of PK, before and after completing the laboratory class (\*\*\*)  $p = 0.002$ .

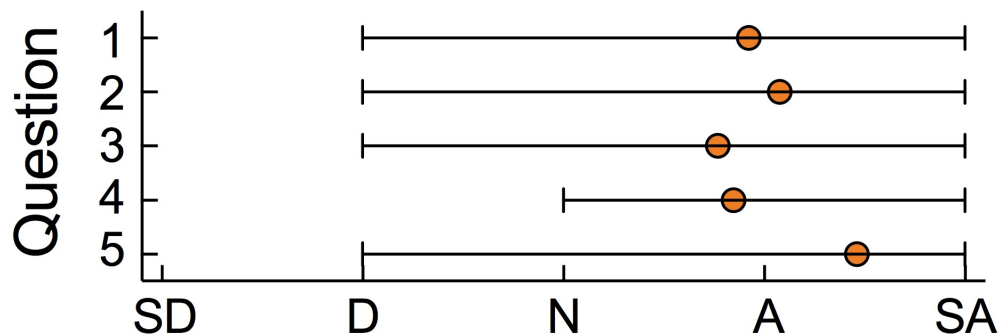


Figure 3.21. Survey results showing undergraduate student responses to questions concerning the undergraduate laboratory and modeller rated on a scale of 1 to 5 (where 1 corresponds to *strongly disagree* and 5 corresponds to *strongly agree*).

The graph shows a range of responses, with the reported mean (●) (n=13). (Question 1) The lab protocols and workbooks improved my competence in using pharmacokinetic calculations. (mean score: 3.9) (Question 2) The lab protocols and workbooks improved my understanding of the concepts underlying pharmacokinetics. (mean score: 4.1) (Question 3) The lab protocols were easily understood and simple to perform. (mean score: 3.8) (Question 4) I enjoyed these lab modules. (mean score: 3.9) (Question 5) I believe these modellers and the lab modules were an effective educational tool in regards to my overall understanding and application of pharmacokinetics. (mean score: 4.5)

### 3.4 REAL TIME MONITORING

An additional modification to the apparatus allows for continuous spectrophotometric measurement of absorbance in a flow-through cuvette (see Figure 2.1Q), with the output projected onto a screen. This would allow for live demonstrations of PK behaviour to larger audiences, or for tutorial purposes. Figure 3.22 shows real-time outputs from a spectrophotometer following single and repeated IV and PO doses of methylene blue. Figure 3.22A displays single IV and PO doses under one-compartment configurations with oral bioavailability set at 100% and 60%. Under identical conditions to Figure 3.22A, repeated IV injections, and repeated oral doses at 60% bioavailability were administered to achieve a  $C_{SS}$  of  $6 \text{ mg L}^{-1}$ , respectively (Figure 3.22B). An intermittent IV infusion protocol was also designed and successfully implemented as shown in Figure 3.22C. In addition, a single IV injection was administered with the apparatus in a two-compartment configuration, and the output was recorded in Figure 3.22D. The same data are shown on a linear axis and logarithmic axis, revealing the classic “hockey-stick” curve associated with two-compartment distribution behaviour.

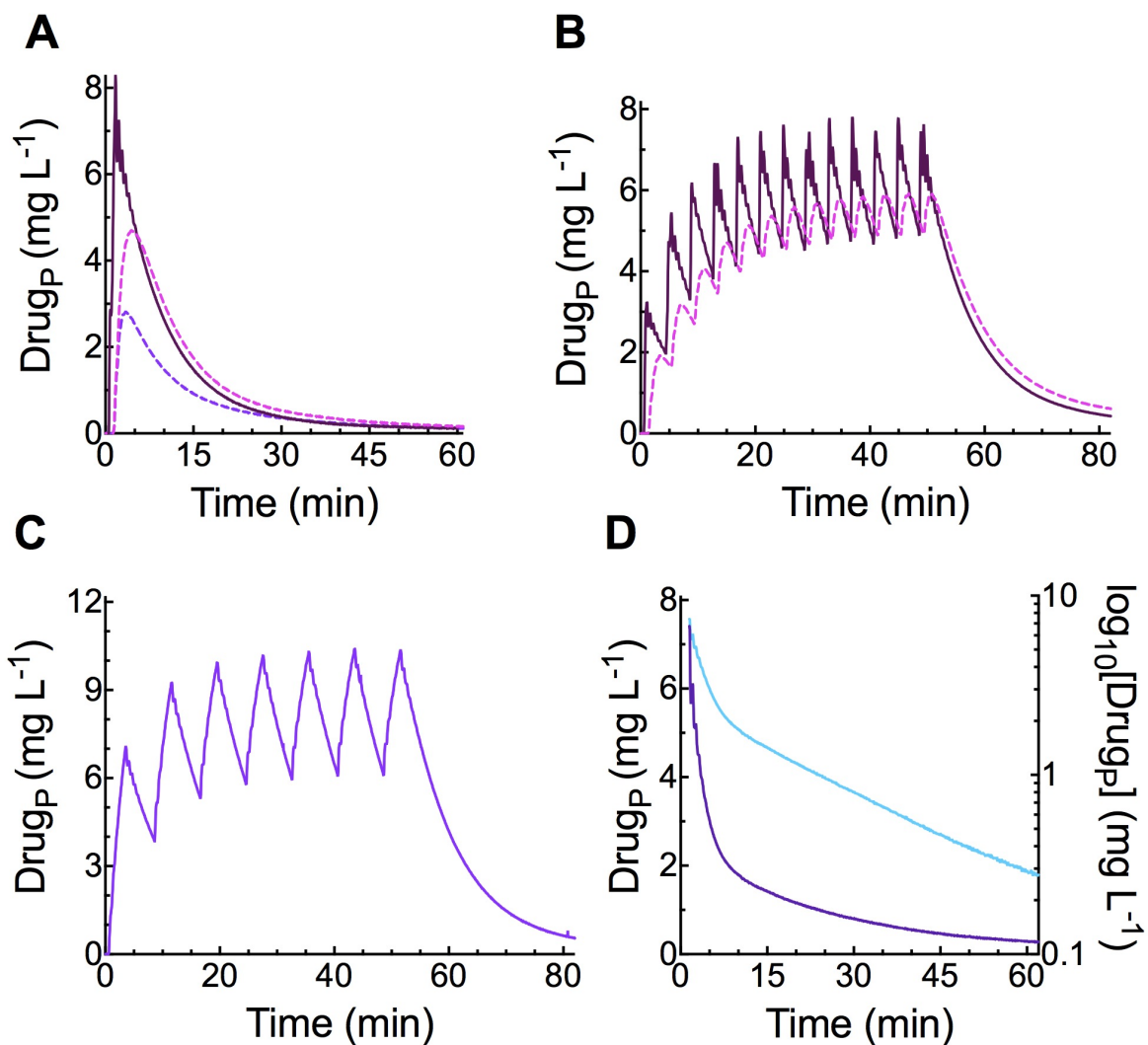


Figure 3.22. Examples of real-time spectrophotometer output, obtained by diverting a small portion of systemic circulation through a flow-through cuvette.

(A) Single IV and PO doses of 1mg, with oral bioavailability set to 100% or 60% in a one-compartment configuration. (B) Repeated IV injections of 0.34 mg every 4 minutes and repeated PO doses of 0.57 mg every 4 minutes with oral bioavailability set to 60%, calculated to achieve a C<sub>SS</sub> of 6 mg L<sup>-1</sup>. (C) Intermittent IV infusions (0.68 mg infused over 3 minutes, every 8 minutes) in a one-compartment configuration, calculated to achieve a C<sub>SS</sub> of 6 mg L<sup>-1</sup>. (D) Single IV injection of 1 mg with the simulator in a two-compartment configuration plotted on a linear or logarithmic Y-axis.

## CHAPTER 4: DISCUSSION AND CONCLUSION

Mastering PK principles is difficult, because the subject is highly quantitative, yet abstract in nature (Gumtow, Proudfoot & Talada, 1988). Thus, observing theoretical principles through hands-on experience allows for students to consolidate and apply the abstract concepts in a practical way (Gumtow, Proudfoot & Talada, 1988). The Alberta Drug Administration Modeller has been proven to be mathematically robust, efficient, and effective in explaining and mimicking drug behaviour. The data generated from the ADAM were validated through analysis using PKSolver, which showed that the outputs are physiologically sound; the values calculated by the classic methods, in some of the figures in Chapter 3, were similar to the values generated by PKSolver (see Appendix I). Through observation and experimentation, students can comprehend how pump rate or tissue volume changes impact PK parameters. Thus, they can engage with the equations and analysis techniques learned in lectures, and formulate drug-dosing regimens in a zero-risk environment. When the ADAM was introduced into the classroom, students reported increased confidence in analysing and interpreting PK data, while improvements in their ability to handle PK graphing and calculation problems were also observed. As a teaching and learning tool, the ADAM is a unique and effective addition to the toolbox of those tasked with teaching PK, and complements didactic and *in silico* learning currently used in the health professional curriculum.

### 4.1 SUMMARY OF RESULTS

The ADAM and its design offer extensive opportunities to mimic inter-individual variations or to explore a variety of drug behaviours, including one- and two-compartment distribution kinetics. As shown in Chapter 3, the data obtained from sampling and fitted to either single- or two-phase exponential decay equations resulted in fits that typically exceeded an  $r^2$  of 0.99. When the data were plotted on semi-logarithmic graphs, the results were visually consistent with one-compartment distribution kinetics, or with two compartment distribution kinetics, where data exhibited the classic hockey-stick profile. Additional chronic dosing and repeated

dosing experiments under various configurations were successful in achieving target steady state values, revealing the complex capabilities of the modeller. Overall, the relationships between the PK parameters were consistent, mirroring expected physiological outcomes.

Circulating the drug within only the main tubing circuit resulted in one-compartment kinetics which allowed for exploration of different elimination pump settings. For instance, with slight alteration of the LIVER pump, KIDNEY 1 pump, and KIDNEY 2 pump, it was possible to show inter-individual variability and how this would affect a drug's PK parameters (see Figure 3.1 and Figure 3.3). More pronounced changes in the LIVER pump rate allowed for modelling of physiological outcomes resulting from reduced or increased hepatic enzyme function (achieved by setting the modeller to a *slow* or *fast* elimination setting) (see Figure 3.5). Changing the oral dose (or altering the ORAL BIOAVAILABILITY pump rate as later shown), in addition to alternating the LIVER pump settings between *fast* or *slow* (see Figure 3.6), provided expected PK outputs from a high extraction ratio drug (30% bioavailability) vs a low extraction ratio drug (70% bioavailability). In addition, the apparatus allowed for chronic dosing regimens based on results from an acute dosing experiment (Figure 3.7), as shown for multiple IV dosing with an achieved desired  $C_{SS}$  and maintenance within a therapeutic window. An additional experiment using an intermittent IV infusion protocol also successfully maintained a desired  $C_{SS}$  within an even narrower therapeutic window. Complementary urine data were also analysed with these experiments (see Figure 3.2, 3.4, 3.5, 3.6), and the sigma-minus method was successfully employed; resulting PK parameters from urine data closely mirrored the PK parameters calculated from the plasma.

Opening the diversion taps (K and L) allowed drug to circulate through a TISSUE compartment (M) in parallel with the main circulation, mimicking two-compartment drug behaviour. Figure 3.8 and 3.9 show data from a set of experiments where elimination pump settings and TISSUE compartment volumes were altered, and plasma and urine analyses were compared. The analysis provided insight into two-compartment distribution behaviour, and revealed the mathematical robustness of the modeller. The use of the method of residuals successfully allowed for the calculation of many PK parameters, including the micro-rate constants  $k_{12}$ ,  $k_{21}$ ,

and  $k_{10}$ . The modeller also depicted the importance of understanding physiological relationships between clearance, half-life, and volume of distribution, which are conceptually abstract. Subsequent experiments included comparisons between IV and oral administration in the two-compartment model (see Figure 3.10 and 3.11), reiterating the modeller's capability in providing bioavailability analysis in a more complex configuration. The introduction of the ORAL BIOAVAILABILITY pump and subsequent analyses displayed a successful addition in mimicking changed oral bioavailability, while manipulation of the stomach volume influenced the  $C_{max}$  and  $t_{max}$ , showing the modeller's capability in mimicking sustained release preparations (see Figure 3.12). Figure 3.13, 3.14, and 3.15 largely focused on the manipulation of distribution settings, including TISSUE pump rate changes, and TISSUE compartment volumes, which provided greater insight into the effects of volume of distribution on factors such as half-life or the micro-rate constants. In addition, the modeller provided an ability to mimic differences in lipid solubility, or adipose profiles of individuals. While the calculated PK parameters were generally numerically smaller than physiological values, adjustments to the modeller can result in more life-like dosing situations, as depicted by Figure 3.16 and 3.17. Though some values, such as the volume of distribution, were much lower than would be expected in a human patient, the ability to manipulate the parameters through pump settings or compartment volumes provides strong evidence of the modeller design's adaptability in potential future applications.

Chronic dosing, and repeated dosing regimens with and without a loading dose were also tested in the two-compartment configuration (as shown in Figure 3.18 and 3.19), and the resulting  $C_{ss}$  and plasma peak and trough values showed successful implementation of these regimens, further reinforcing the apparatus' complex modelling capabilities. The implementation of the modeller into an undergraduate pharmacology tutorial course (PMCOL 337) was successful in enhancing student understanding of PK concepts and calculations, as their performance on a skills-based test improved after the intervention (see Figure 3.20). In addition, student attitudes concerning the modeller and the subject of PK were generally positive, strongly suggesting that the ADAM is an effective learning tool for the subject of PK

(see Figure 3.21). Finally, the optional modification of connecting a flow-through cuvette in parallel to the systemic circulation, allowing for the observation of drug behaviour in real time, demonstrates enhanced versatility of the modeller as it has the potential to be used as an in-class teaching tool (see Figure 3.22).

## 4.2 STRENGTHS, LIMITATIONS AND DESIGN ALTERATIONS

The apparatus design allows for mimicking the *outcome* of physiological or pathophysiological processes affecting drug behaviour, rather than the processes which cause them. This allows students to visualise the effects of various parameters on certain outcomes, as observed through analysis of plasma-concentration time data. Further questioning of the students *via* worksheets and in-class discussion can prompt critical thinking about the modeller's design and *how* one might change certain aspects to elicit various drug behaviour scenarios. The simplicity and ease of operating the modeller is a great strength, as the processes of ADME are represented in such a way that it provides a visual for the abstract aspects, and an opportunity for application.

One- and two-compartment drug behaviour is mimicked through simple manipulation of the diversion taps, and the resulting semi-logarithmic plots have shown accurate and realistic outcomes from these configurations. Altered absorption due to differences in formulations is easily modelled through increasing or decreasing the stomach volume, where an increased volume would result in larger smoothing and longer absorption times. Changes in liver or renal function is achieved through increasing or decreasing the LIVER, ORAL BIOAVAILABILITY, and KIDNEY 1, and KIDNEY 2 pump, respectively. Other outcomes, such as mimicking high or low extraction ratio drugs, requires careful consideration to the physiological relationships and equations relating the drug's bioavailability and  $CL_{int}$  prior to appropriately adjusting the pumps. Nevertheless, mimicking the PK parameters expected of these drugs is possible – a high extraction ratio drug, for instance, would likely experience a low oral bioavailability, which could be easily adjusted by simply increasing the ORAL BIOAVAILABILITY pump. In addition, mimicking the outcome of changed plasma protein binding can be achieved through altering the volume of distribution, clearance, and elimination rate constants of the modeller through

changed TISSUE COMPARTMENT volumes, and elimination pump rates, respectively. For instance, a drug highly bound to plasma proteins will have low volume of distribution; adjusting the TISSUE compartment volume would thus require lower volumes for drug to distribute into. However, a highly protein bound drug may still exhibit a longer elimination half-life, and as such, LIVER pump rates and KIDNEY 1 pump rates can be decreased to compensate for the lower TISSUE compartment volume to facilitate a longer half-life. Hypoalbuminemia, as discussed, reduces the potential for plasma protein binding – for a drug with an  $f_{b,p}$  of 0.99, the easiest way to mimic the effects of this pathology on its PK parameters would be to increase slightly the volume of distribution by increasing the TISSUE COMPARTMENT volume. If renal failure caused the hypoalbuminemia, then increasing KIDNEY 1 pump rates would result in more drug being lost in this manner, resulting in altered PK parameters as would be expected in such circumstances.

Of the scenarios that are modelled, each depend on manual adjustment of pump rate settings and compartment volumes, which is a simple alteration. Though the modeller does not (and in some cases, cannot) model physiological processes, the outcomes that it generates *via* plasma-concentration and urine time profiles is reliable, mathematically robust, and appropriate for the undergraduate student. Another great strength of the design of the modeller and its applications is that it is easily modified and adjusted for simplicity or complexity, depending on the needs of the students, time constraints, and even cost efficiency.

The current design of the modeller allows for plasma and urine sample collection over a period of several half-lives to abide by time constraints of a laboratory class. If more realistic PK values are required, it was shown that increasing the TISSUE COMPARTMENT volume significantly (up to 1 L) and decreasing the TISSUE PUMP rate could generate drug half-lives of around 2 hours, with all other aspects of the design kept as-is. In addition to an increased TISSUE COMPARTMENT reservoir to model more realistic PK values, the modeller could also be modified by incorporating a large stirred reservoir in series with the systemic circulation.

Other modifications that would allow modelling of more complex drug behaviour would include the introduction of a second "DEEP" TISSUE COMPARTMENT and TISSUE PUMP connected in parallel with the systemic circulation to generate a three-compartment open model. One parallel set of TISSUE could represent medium to highly perfused organs, with a low/medium TISSUE COMPARTMENT volume and faster/medium TISSUE PUMP rate, while another could represent less accessible organs, such as the adipose and bone – through a large TISSUE COMPARTMENT volume and slow TISSUE pump rate.

Currently, only IV and PO administration are the routes of administration modelled in the apparatus. Drug administration *via* SC, IM, SL, topical, buccal, dermal, and inhalation would be more difficult to model, though not all would be impossible. Sublingual and buccal administration allows for bypassing of the GI tract so that drug reaches the circulation rapidly. The addition of a small compartment located on the tubing between the stomach and the central circulation could allow for "sublingual" or "buccal" administration and mimic the more rapidly attained levels of these routes without going through the "stomach" and being subjected to the ORAL BIOAVAILABILITY pump. Consequently, modelling a drug administered through these routes could include administering drug into the stomach with the ORAL BIOAVAILABILITY pump turned off to demonstrate complete absorption. However, as shown in Figure 3.12, even 100% bioavailability displays an appreciable absorption phase, and as such, it would be difficult to differentiate the sublingual or buccal plasma concentration time profile from that following PO administration. Intramuscular or subcutaneous administration could be modelled in a similar way by adding a small administration compartment to the IV injection port in which drug is slowly administered, and mixed into a small volume, resulting in plasma concentration values that peak less rapidly than with IV administration. Because the plasma concentration outputs are determined by the route of administration, modelling these different administration routes should be relatively straightforward.

In Chapter 3, PO administration and oral bioavailability observations were modelled by reducing the administered oral dose by a specific factor in relation to the comparative IV dose. Later introduction of the ORAL BIOAVAILABILITY pump replaced this practice, but the results

of the earlier experiments were included as they are valid and offer an alternative approach in mimicking the process of oral bioavailability. The successful use of multiple strategies to model specific PK behaviour in the modeller is a strength, in that the design provides accessibility to departments and faculties with limited funds; the pumps are the most expensive component of the apparatus, and having the flexibility of modelling a concept without each piece of equipment is ideal. However, the apparatus is generally easy and cost-effective to construct.

Some student populations, such as licensed practical nurses do not need to understand every complexity surrounding PK relationships, but they would benefit from a practical session in drug administration and modelling. A simple one-compartment IV and PO dose comparison would allow them to understand concepts such as half-life and clearance, visualise drug elimination, and develop a more intuitive understanding of a drug's journey in the body. In this case, the construction of the modeller could be more simplistic, perhaps consisting only of a central compartment with the stomach, and elimination pumps.

If classes focused on teaching PK concepts are limited by lack of allocated laboratory or practical time, then the addition of the flow-through cuvette in parallel with the systemic circulation can provide real-time demonstrations in a lecture hall through VGA output to a projector. Instructors could conduct an experiment during a one-hour lecture, wherein students could "dose" their patient through single or repeated administrations. The output could then be used as a case study, encouraging students to calculate different PK parameters and, if the output in question is a single administration, to design proper dosing regimens to achieve a  $C_{SS}$  for the following lecture. The versatility of the apparatus therefore allows it also to deliver an active learning environment, which is important for maintaining student attention and interest.

The limitation of the apparatus mimicking the outcomes of drug behaviour rather than the processes is that students may draw erroneous conclusions about the general set up of the system. For instance, blood flow to the liver is the main determinant of  $CL_{int}$  for high extraction ratio drugs, but it is a physiological process that is not modelled in the apparatus. When the LIVER pump rate is increased, it is simply increasing the amount of drug it removes from the

system; the blood flow through the organ ( $Q$ ) is not altered, though the drug's clearance changes. Yet, if students focus on processes rather than expected outcomes, they may gravitate towards assumptions that  $Q$  changes, and will consider the modeller's mechanisms as physiologically relevant to a human patient.

As has been demonstrated, the modeller can relate physiological processes and relationships in an accurate and mathematically robust manner, but the observations are indirectly communicated through plasma concentration time profiles. As mentioned, the modeller cannot directly model plasma protein binding, and depends on alterations to pump rates and/or compartment volumes to mimic the outcomes that the binding would influence. In terms of enzyme induction or inhibition, the outcomes, once again, would be dependent on the changes in the LIVER pump or ORAL BIOAVAILABILITY pump settings, rather than the observation of the process of enzyme induction. When the premise of an experiment is to model a highly lipid soluble drug, or to model individuals of varying levels of obesity, the TISSUE COMPARTMENT volume is increased, resulting in a drug concentration time profile that communicates the expected PK parameters. The only process that has proven to be impossible to simulate is zero-order elimination, where drug concentration decreases in a linear, rather than exponential fashion. Generating this outcome in the urine would be more straightforward, but the complexity involved in generating a plasma-concentration time profile that mimics this outcome would likely require manipulation of the sample points or precise and constant alterations to elimination pump rate settings throughout data collection.

The mobility of the apparatus is also a current limitation. Each apparatus is affixed to a laboratory cart, which facilitates transport, but the set-up is bulky and rigid, and the apparatus requires space for storage and for use. A more compact version of the apparatus could be created, with less emphasis on resembling a patient, which would still model accurate relationships between PK parameters and potentially provide more ease of transport between classrooms, and for workshop facilitation. In addition, achieving optimal drug-plasma and -urine concentration curves requires consideration to some of the specific conditions outlined in

Chapter 2; bypassing these small adjustments may result in less accurate data for analysis, which can be problematic when there are time constraints in the laboratory classes.

The overall positive results from the laboratory class illustrated that the modeller is an effective learning tool. However, the sample size is small as only 13 students provided consent for their responses, and ideally, more quantitative data would bolster the results of the effectiveness of this tool. However, the survey and quiz results, overall, do not capture the informal learning observed in each 6-hour laboratory session. Though students generally began the first laboratory session with trepidation, the ease of use of the modeller and experimental set ups developed a sense of confidence within each cohort by the 2<sup>nd</sup> session. Having observed student attitudes concerning the subject of PK during and after the lab classes over the last three years, it is extraordinary how quickly they accustom to discussing the PK concepts and developing insight into the general mechanism of the modeller and how it relates to human physiology. It is not uncommon to hear students say things like “this makes so much more sense now” or “I wish I had used this to study for the PMCOL 201 final. I would have done so much better on it.” Students will discuss concepts of half-life or volume of distribution between one another; the breadth of learning occurring within each lab session is tangible. Though these anecdotes are not quantifiable, they provide important insights about student attitudes and confidence. Providing students with the opportunity to apply their knowledge, to work in a cohesive team environment, to learn from their mistakes, and to evaluate information critically in a positive environment, are the keys to enhancing their understanding of even the most difficult subjects.

### **4.3 SIMILAR INNOVATIONS**

The concept and model design of the ADAM was inspired by a report in *Pharmacology Matters* by Steven Tucker of the University of Aberdeen, where he used an open model system and methylene blue drug. A beaker containing water represented the volume of distribution with two pumps mimicking the removal of methylene blue (Tucker, 2014). The ADAM was adapted extensively from this system to incorporate more complex modelling and applications.

Historical accounts show that other instructors have also presented similar models for mimicking drug pharmacokinetics. In 1977, a PK simulator which uses dyes to represent drugs was presented by Jansen at the Meeting of the Scandinavian Pharmacological Society. The abstract describes a simulator with one small and two large glass vessels with water, two reservoirs, magnetic stirrers, and a peristaltic pump (Jansen, 1977). The larger vessel represented the central compartment with the other vessel representing the peripheral compartment, with the two connected *via* tubing and a pump providing equal and constant flow in both directions. Elimination was facilitated through outflow driven by gravity, and a reservoir maintaining the water level used the same mechanism to keep water levels constant. Plasma concentration was recorded using a spectrophotometer and flow cell connected to the central compartment (Jansen, 1977). Unfortunately, additional details or data concerning student performance was not available for further inquiry.

In 1988, Gumtow and colleagues published a paper describing an *in vitro* pharmacokinetic system for one- and two-compartment modelling used as early as 1974; it was referred to as the Glassman Patient. The model was comprised of beakers, magnetic stirrers, plastic and glass tubing, and a peristaltic pump (Gumtow, Proudfoot & Talada, 1988). There were two main compartments within the system – a stirred beaker representing the gut, and another stirred beaker representing the central compartment. Elongated spouts with a piece of cotton string draped over each were affixed to each of these beakers to provide steady quantitative transfer of excess liquid by gravity overflow (Gumtow, Proudfoot & Talada, 1988). Much like the ADAM and the Jansen's description, a separate compartment was positioned to run in parallel to the central compartment using a peristaltic pump to deliver drug to the peripheral compartments at a constant rate, and drug was circulated back from the peripheral compartment to the central compartment using an elongated spout *via* gravity overflow at the same rate (Gumtow, Proudfoot & Talada, 1988). Elimination of drug occurred from the central compartment beaker through another elongated spout into a collection beaker, which represented the total clearance of the system. The magnitudes of the transfer rates and elimination rates were tailored by varying the flow rates in the system and/or the sizes of the beaker volumes (Gumtow,

Proudfoot & Talada, 1988). Essentially, the system allowed for one- and two-compartment modelling by either turning on or off the peristaltic pump, and permitted intravenous or oral dosing by administering the drug into the beaker representing the gut, or the central compartment beaker, respectively (Gumtow, Proudfoot & Talada, 1988). Rather than using a dye to represent drug, the authors used a dose sodium salicylate (NASA) as a stock solution of 160 mg/mL, and samples were diluted with 0.1 N HCl prior to being analysed spectrophotometrically. The modelling system allowed for students to compare concentration-time profiles resulting from various routes and modes of drug administration, and to conduct multiple dosing and continuous infusions with or without loading doses with great success (Gumtow, Proudfoot & Talada, 1988). The authors incorporated computer modelling simulations into these workshops to save time, but they noted that students comprehended the scope of their work on the computer more effectively if they initially worked with the Glassman Patient. Gumtow *et al.* recommended that students use the simulator *in addition* to the current technology of the time, rather than limit their experience to only a computer program (Gumtow, Proudfoot & Talada, 1988).

The similarity of modelling described by Jansen and Gumtow reveal the synchronous thought process of people with PK expertise and experience with teaching the subject to various student populations. As compartmental modelling often describes one-compartment drugs as distributing into a “homogenous” container of fluid, it is logical that many people would extrapolate such a concept into more complex modelling systems. The use of pumps and beakers to model compartments and transfer processes shows that the concept of ADAM, while perhaps not entirely novel, is valid in teaching the difficult concepts of drug PK. Interestingly, the modelling of zero-order processes was not mentioned for either case, suggesting that this type of drug behaviour is not straightforward to depict in this type of simulator. Jansen described the use of dyes for the process, but as shown by Gumtow, if a suitable quantitative assay method is available, then any drug may be administered into the simulator to enhance the realism of students’ experiences. Each of the authors use a single peristaltic pump to mimic the transfer of drug between compartments. Though the initial design of the ADAM used a

dialysis membrane to mimic drug diffusion, it was later changed also to use a pump to facilitate distribution between the compartments.

Interestingly, other than the 2-compartment modelling, Guntow and Jansen rely heavily on gravity outflow to facilitate movement of fluid through and out of the modeller. The design that they describe is linear in terms of the drug's trajectory through the system, with the exception of when it travels to and from the peripheral compartment. The design of the ADAM provides more realism in terms of how a drug distributes and travels within the body, as the central compartment is not represented by a static volume of water stirred in a beaker, but rather by a fixed volume of tubing within which water is circulated by the HEART pump. This representation is more physiological in that it shows a drug's movement through a "body's circulation" rather than the textbook description of one-compartment drugs.

The ADAM apparatuses are constructed in such a way that there is realism and a "patient presence." The pumps and tubing are mounted on a series of shelves, which are bolted to a laboratory cart and concealed behind a full-size human outline printed on a rigid board. Students administer drug through a cannula in the mouth, or an injection port on a "vein" exposed on a patient's forearm, collect "plasma" samples from the sampling port on the forearm, or "urine" samples from a cannula representing the urethra. The methylene blue is distributed within the system and its distribution and elimination is clearly visualised so that students can observe the initial drug peak and drug elimination over the course of an experiment. The use of a dye clearly shows the slow increase of drug concentration in the TISSUE COMPARTMENT and subsequent fading of the colour as drug moves back to the central compartment for elimination. If a dye was used in the Glassman Patient, this phenomenon would also be observed.

The ADAM incorporates the use of many pumps that mimic the contribution of specific organs to drug PK – the HEART pump distributes "blood" throughout the body, while the LIVER and KIDNEY 1 pump eliminate the drug through their own respective methods. Even the ORAL BIOAVAILABILITY pump describes an aspect of PK which occurs when drugs are administered

orally. Such a set up allows for students to understand, first hand, the impact of how changes in specific pump settings can mimic pathologies or drug interactions.

Though it is possible to change rates of drug flow by changing beaker volumes in the Glassman Patient, changing pump rates in the ADAM is straightforward; the effects are easily observed and rationalised (see any Figure in Chapter 3). Further, the range of the pump rates involved in each of the processes allows for a large variation in drug PK parameters and the ability to model many different situations. By altering the TISSUE pump rate settings, or the TISSUE COMPARTMENT volume, for instance, it is extremely simple to observe altered drug distribution behaviours, or variability in individual adipose profiles.

By including only one collection beaker for eliminated drug, the Glassman Patient does not allow for students to evaluate separately the  $CL_R$  and  $CL_H$  of their patient, or to carry out urine analysis. While urine analysis, in general, lacks adaptability and quantitiveness as compared with plasma analysis, it is still a worthwhile procedure to learn to understand better the different procedures available for pharmacokinetic analysis. Though the Glassman model is more simple and cost-effective as a simulator, especially for classrooms that are limited by funding, the modelling is not as intuitive as the ADAM. However, the caveat with ADAM is that sampling using the current design is limited to the plasma and the urine, rather than sampling tissues or even the gut, as was shown with the Glassman Patient. However, our modeller could be adapted to allow for sampling from the tissue compartment simply by including a rubber septum in the lid of the compartment bottle for sampling via a needle and syringe. In essence, if the Glassman Patient can model it, then the ADAM can also model the same type of regimen or drug behaviour.

Additional applications of the Glassman Patient included establishing effective plasma drug levels in an emergency; students were required to design a dosing regimen to achieve rapid  $C_{SS}$  and maintenance of a drug within an extremely narrow therapeutic window: between 2.0 and 2.5 mg/mL (Gumtow, Phillips & Cox, 1989). The caveat was that the drug was associated with multi-compartment PK, a narrow therapeutic index, a short distribution half-life, and a long

plasma half-life; a single intravenous bolus with continuous IV infusion would therefore not be effective for this situation (Gumtow, Phillips & Cox, 1989). Instructors prepared a patient with specific PK parameters including  $k_{10}$ ,  $k_{12}$ ,  $k_{21}$ ,  $\alpha$ ,  $\beta$  and  $V_C$ , communicated these parameters to students, and then challenged the students to propose and test multiple dosing regimens to achieve the proposed steady state for this complicated drug without harming the Glassman Patient (Gumtow, Phillips & Cox, 1989). Students conducted multiple experiments to verify the best approach to this emergency situation, including a single intravenous bolus of 564 mg, the 564 mg bolus simultaneously administered with a constant infusion, and finally, a 1277 mg loading dose of short infusions *via* syringe (over 45 minutes) administered in parallel with a continuous IV infusion protocol (Gumtow, Phillips & Cox, 1989). The third attempt proved to be successful, and the intricacy of the relationships and equations allowed for students to develop a more robust understanding of drug administration concerning compounds which exhibit more complicated pharmacokinetics. Such a protocol may not be within the necessary level of experience of the undergraduate students in our undergraduate laboratory course, but developing protocols for such situations would provide greater insight for clinicians and pharmacists determining such regimens. Creating a workbook centred on achieving rapid levels of a drug with a narrow therapeutic index using continuous IV infusions could be further explored using the ADAM in the future.

#### 4.4 FUTURE APPLICATIONS OF ADAM

While aspects of the simulators created separately by Jansen and Gumtow over 40 years ago resemble the design and application of the ADAM, it is curious that these types of simulators were largely ignored, especially when the ensuing decades were plagued with alerts over inadequate pharmacology training in medical curricula. Potentially, the introduction of computer simulations and various technologies steered the teaching of PK into *in silico* programs rather than *in vitro*. Likely, the novelty of the use of computers created a higher demand for ease, as it allowed convenient modelling of many PK situations. Yet, the current evidence of the sheer number of instructors and institutions developing active learning

techniques and innovative ways to teach this subject matter shows that students need clinical context and simplicity to understand the complex aspects of PK. Though active learning techniques have included think-pair-share discussions, case studies, and even games, the use of technology has also become prevalent in the form of iClickers, online assessments, and online dosing programs. These are all valid activities if used appropriately, but with the ever-growing trend in incorporating technology into the classroom, or the use of medical apps, it is becoming problematic as students are not learning the basics to apply their knowledge. Rather, some of these active learning techniques are used for entertainment, rather than facilitating understanding. Thus, the introduction of the ADAM into the current framework of PK teaching is perfectly timed to address the potential issues arising from disconnect of knowledge and application. There is a huge opportunity to implement this teaching tool into health care curricula, as well as undergraduate pharmacology education for various levels. The versatility and adaptability of the modeller provides ample opportunity for modifications to suit the needs of various student learners, and the hands-on aspect provides a clinical context without harming a patient or animal. Though a practical laboratory session provides students with the greatest opportunity to understand PK concepts, implementing the modeller into a classroom would still be beneficial. A previously-mentioned application of ADAM includes the use of a flow-through cell in classroom settings to provide an active learning technique for PK instruction, and the ease of use would facilitate real-time data collection, and encourage students to plan, discuss, and observe a dosing regimen in the classroom. This type of learning is paramount to student success as it allows for the chance to develop a deeper insight into drug PK. In addition, the creation of videos using the apparatus to describe the processes of drug PK could help to disseminate the work and provide a visual learning piece for students across the world.

Many reports have consistently stated that inadequate training and lack of knowledge is one of the main contributing factors leading to prescribing and medication errors. Though each student population is trained for the responsibilities of their profession, there are deficiencies in their knowledge base and understanding of drug pharmacokinetics. Unfortunately, this affects patient care and contributes to the increasingly growing cost of healthcare. These

deficiencies have been pinpointed by various institutions and groups, with many calling for an increase in the content concerning drugs and drug administration. As the topic of PK is complex and abstract, there needs not only to be increased content in the curricula, but more holistic learning opportunities. The ADAM is a cost-effective and simple to use apparatus that will transform and improve current teaching practices, and improve the competence in PK in our future health care professionals.

## BIBLIOGRAPHY

Abernethy DR, Greenblatt DJ, Divoll M, & Shader RI (1983). Prolonged accumulation of diazepam in obesity. *J Clin Pharmacol* 23: 369-376.

Abuhelwa AY, Foster DJ, & Upton RN (2016). A quantitative review and meta-models of the variability and factors affecting oral drug absorption-part I: gastrointestinal pH. *AAPS J* 18: 1309-1321.

Alanazi MA, Tully MP, & Lewis PJ (2016). A systematic review of the prevalence and incidence of prescribing errors with high-risk medicines in hospitals. *J Clin Pharm Ther* 41: 239-245.

Aldridge A, Aranda JV, & Neims AH (1979). Caffeine metabolism in the newborn. *Clin Pharmacol Ther* 25: 447-453.

Amidon GL, Lennernas H, Shah VP, & Crison JR (1995). A theoretical basis for a biopharmaceutic drug classification - the correlation of in-vitro drug product dissolution and in-vivo bioavailability. *Pharmaceut Res* 12: 413-420.

Anderson GD (2010). Developmental pharmacokinetics. *Semin Pediatr Neurol* 17: 208-213.

Armstrong LE (2005). Hydration assessment techniques. *Nutr Rev* 63: S40-54.

Aronson JK (2006). A prescription for better prescribing. *Br J Clin Pharmacol* 61: 487-491.

Aronson JK, Henderson G, Webb DJ, & Rawlins MD (2006). A prescription for better prescribing. *BMJ* 333: 459-460.

Aronsson P, Booth S, Hagg S, Kjellgren K, Zetterqvist A, Tobin G, *et al.* (2015). The understanding of core pharmacological concepts among health care students in their final semester. *BMC Med Educ* 15: 235.

Ashcroft DM, Lewis PJ, Tully MP, Farragher TM, Taylor D, Wass V, et al. (2015). Prevalence, nature, severity and risk factors for prescribing errors in hospital inpatients: prospective study in 20 UK hospitals. *Drug Saf* 38: 833-843.

Bates DW, Spell N, Cullen DJ, Burdick E, Laird N, Petersen LA, et al. (1997). The costs of adverse drug events in hospitalized patients. Adverse Drug Events Prevention Study Group. *JAMA* 277: 307-311.

Bauer LA (2006). *Clinical Pharmacokinetic and Pharmacodynamic Concepts In Clinical Pharmacokinetics Handbook*. ed Brown M., Edmonson, K. McGraw-Hill United States of America.

Benet LZ, & Ronfeld RA (1969). Volume terms in pharmacokinetics. *J Pharm Sci* 58: 639-641.

Benet LZ, & Zech K (1994). Pharmacokinetics--a relevant factor for the choice of a drug? *Aliment Pharmacol Ther* 8 Suppl 1: 25-32.

Benet LZ, & Zia-Amirhosseini P (1995). Basic principles of pharmacokinetics. *Toxicol Pathol* 23: 115-123.

Blouin RA, & Warren GW (1999). Pharmacokinetic considerations in obesity. *J Pharm Sci* 88: 1-7.

Bolger MB (1995). Cyber Patient(TM): A multimedia pharmacokinetic simulation program for case study generation in a problem-solving curriculum. *Am J Pharm Educ* 59: 409-416.

Boyes RN, Adams HJ, & Duce BR (1970). Oral absorption and disposition kinetics of lidocaine hydrochloride in dogs. *J Pharmacol Exp Ther* 174: 1-8.

Brackett CC, & Reuning RH (1999). Teaching Pharmacokinetics Using a Student-Centered, Modified Mastery-Based Approach. *Am J Pharm Educ* 63: 272-277.

Brater DC, & Nierenberg DW (1988). Medical student education in clinical pharmacology and therapeutics. *Ann Intern Med* 108: 136-137.

Brocks DR (2015). uSIMPk. An Excel for Windows-based simulation program for instruction of basic pharmacokinetics principles to pharmacy students. *Comput Methods Programs Biomed* 120: 154-163.

Buxton ILO, Benet LZ, Brunton LL, Chabner BA, & Knollmann BC (2011). *Pharmacokinetics: The Dynamics of Drug Absorption, Distribution, Metabolism* In Goodman & Gilman's: *The Pharmacological Basis of Therapeutics* McGraw Hill Education New York, NY.

Campbell RL, Bellolio MF, Knutson BD, Bellamkonda VR, Fedko MG, Nestler DM, *et al.* (2015). Epinephrine in anaphylaxis: higher risk of cardiovascular complications and overdose after administration of intravenous bolus epinephrine compared with intramuscular epinephrine. *J Allergy Clin Immunol Pract* 3: 76-80.

Carver PL, Fleisher D, Zhou SY, Kaul D, Kazanjian P, & Li C (1999). Meal composition effects on the oral bioavailability of indinavir in HIV-infected patients. *Pharm Res* 16: 718-724.

Clarke W (2016). Chapter 1: Overview of Therapeutic Drug Monitoring. *Clinical Challenges in Therapeutic Drug Monitoring*. 1-15. Doi: 10.1016/b978-0-12-802025-8.00001-5.

Classen DC, Pestotnik SL, Evans RS, Lloyd JF, & Burke JP (1997). Adverse drug events in hospitalized patients. Excess length of stay, extra costs, and attributable mortality. *JAMA* 277: 301-306.

Collins J (2008). Audience response systems: technology to engage learners. *J Am Coll Radiol* 5: 993-1000.

Collins LJ (2007). Livening up the classroom: using audience response systems to promote active learning. *Med Ref Serv Q* 26: 81-88.

Conney AH (1982). Induction of microsomal enzymes by foreign chemicals and carcinogenesis by polycyclic aromatic hydrocarbons: G. H. A. Clowes Memorial Lecture. *Cancer Res* 42: 4875-4917.

Davies DF, & Shock NW (1950). Age changes in glomerular filtration rate, effective renal plasma flow, and tubular excretory capacity in adult males. *J Clin Invest* 29: 496-507.

Dean B, Schachter M, Vincent C, & Barber N (2002a). Causes of prescribing errors in hospital inpatients: a prospective study. *Lancet* 359: 1373-1378.

Dean B, Schachter M, Vincent C, & Barber N (2002b). Prescribing errors in hospital inpatients: their incidence and clinical significance. *Qual Saf Health Care* 11: 340-344.

Dhillon S, & Kostrzewski A (2006) *Clinical Pharmacokinetics*. Pharmaceutical Press: London, U.K.

Difazio MH, & Shargel L (1989). A mathematical utility program to facilitate student comprehension of the pharmacokinetics of the one compartment model. *Am J Pharm Educ* 53: 50-53.

Dupuis RE, & Persky AM (2008). Use of case-based learning in a clinical pharmacokinetics course. *Am J Pharm Educ* 72: 29.

Edginton A, & Holbrook J (2010). A blended learning approach to teaching basic pharmacokinetics and the significance of face-to-face interaction. *Am J Pharm Educ* 74.

Ewy GA, Kapadia GG, Yao L, Lullin M, & Marcus FI (1969). Digoxin metabolism in the elderly. *Circulation* 39: 449-453.

Fan J, & de Lannoy IA (2014). Pharmacokinetics. *Biochem Pharmacol* 87: 93-120.

Flannigan C, & McAloon J (2011). Students prescribing emergency drug infusions utilising smartphones outperform consultants using BNFCs. *Resuscitation* 82: 1424-1427.

Fleisher D, Li C, Zhou Y, Pao LH, & Karim A (1999). Drug, meal and formulation interactions influencing drug absorption after oral administration. Clinical implications. *Clin Pharmacokinet* 36: 233-254.

Flockhart DA, Usdin Yasuda S, Pezzullo JC, & Knollmann BC (2002). Teaching rational prescribing: a new clinical pharmacology curriculum for medical schools. *Naunyn Schmiedebergs Arch Pharmacol* 366: 33-43.

Franko OI, & Tirrell TF (2012). Smartphone app use among medical providers in ACGME training programs. *J Med Syst* 36: 3135-3139.

Freeman S, Eddy SL, McDonough M, Smith MK, Okoroafor N, Jordt H, et al. (2014). Active learning increases student performance in science, engineering, and mathematics. *Proc Natl Acad Sci U S A* 111: 8410-8415.

Gabrielsson J, & Weiner D (2012). Non-compartmental analysis. *Methods Mol Biol* 929: 377-389.

Gauci SA, Dantas AM, Williams DA, & Kemm RE (2009). Promoting student-centered active learning in lectures with a personal response system. *Adv Physiol Educ* 33: 60-71.

Giacomini KM, & Sugiyama Y (2011). Membrane Transporters and Drug Response In Goodman & Gilman's: The Pharmacological Basis of Therapeutics McGraw-Hill New York, NY

Gibaldi M (1984) *Biopharmaceutics and Clinical Pharmacokinetics* 3rd. edn. Lea & Febiger: United States of America

Gibaldi M, Boyes RN, & Feldman S (1971). Influence of first-pass effect on availability of drugs on oral administration. *J Pharm Sci* 60: 1338-1340.

Gibson GG, Skett P. (2001) *Introduction to Drug Metabolism*. 3rd edn. Nelson Thornes Publisher. United Kingdom.

Gillespie WR (1991). Noncompartmental versus compartmental modelling in clinical pharmacokinetics. *Clin Pharmacokinet* 20: 253-262.

Gonzalez FJ, Coughtrie M, & Turkey RH (2011). Drug Metabolism In Goodman & Gilman's: The Pharmacological Basis of Therapeutics. McGraw-Hill New York, NY.

Greenblatt DJ (1979). Reduced serum albumin concentration in the elderly: a report from the Boston Collaborative Drug Surveillance Program. *J Am Geriatr Soc* 27: 20-22.

Greenblatt DJ (2014). Volume of distribution - Again. *Clin Pharmacol Drug Dev* 3: 419-420.

Greenblatt DJ, Abernethy DR, & Divoll M (1983). Is volume of distribution at steady state a meaningful kinetic variable? *J Clin Pharmacol* 23: 391-400.

Greenblatt DJ, & Shader RI (1985) *Pharmacokinetics in Clinical Practice*. W.B. Saunders Company Philadelphia, PA

Gumtow RH, Phillips LM, & Cox WL (1989). Establishment of safe and effective plasma drug levels in simulated emergency situations using a 2-compartment Glassman Patient. *Am J Pharm Educ* 53: 244-246.

Gumtow RH, Proudfoot J, & Talada A (1988). An invitro pharmacokinetic system for use in the undergraduate pharmaceuticals laboratory - a one-compartment and 2-compartment pharmacokinetic bench model - the Glassman Patient. *Am J Pharm Educ* 52: 117-121.

Haffey F, Brady RR, & Maxwell S (2013). A comparison of the reliability of smartphone apps for opioid conversion. *Drug Saf* 36: 111-117.

Haffey F, Brady RR, & Maxwell S (2014). Smartphone apps to support hospital prescribing and pharmacology education: a review of current provision. *Br J Clin Pharmacol* 77: 31-38.

Hanley MJ, Abernethy DR, & Greenblatt DJ (2010). Effect of obesity on the pharmacokinetics of drugs in humans. *Clin Pharmacokinet* 49: 71-87.

Harris PA, & Riegelman S (1969). Influence of the route of administration on the area under the plasma concentration-time curve. *J Pharm Sci* 58: 71-75.

Hebert MF, Roberts JP, Prueksaritanont T, & Benet LZ (1992). Bioavailability of cyclosporine with concomitant rifampin administration is markedly less than predicted by hepatic enzyme induction. *Clin Pharmacol Ther* 52: 453-457.

Hedaya MA (1998). Development and evaluation of an interactive Internet-based pharmacokinetic teaching module. *Am J Pharm Educ* 62: 12-16.

Hedaya MA, & Collins P (1999). Pharmacokinetic teaching utilizing the world wide web: A Flashlight (TM) assessment. *Am J Pharm Educ* 63: 415-421.

Institute of Medicine (US) CoQoHCiA (2000) *To Err is Human: Building a Safer Health System*. Washington (DC): National Academies Press (US). Available from <https://www.ncbi.nlm.nih.gov/books/NBK225182/>.

Jambhekar SS, & Breen PJ (2009) *Basic Pharmacokinetics*. Pharmaceutical Press London, U.K. .

Jansen JA (1977) A simple simulator as an aid to teaching of pharmacokinetics. Meeting of the Scandinavian Pharmacological Society. Scandinavian Pharmacological Societies. 41.

Jin JF, Zhu LL, Chen M, Xu HM, Wang HF, Feng XQ, *et al.* (2015). The optimal choice of medication administration route regarding intravenous, intramuscular, and subcutaneous injection. *Patient Prefer Adherence* 9: 923-942.

Joy MS (2012). Impact of glomerular kidney diseases on the clearance of drugs. *J Clin Pharmacol* 52: 23S-34S.

Joy MS, Gipson DS, Dike M, Powell L, Thompson A, Vento S, *et al.* (2009). Phase I trial of rosiglitazone in FSGS: I. Report of the FONT Study Group. *Clin J Am Soc Nephrol* 4: 39-47.

Kamel A, & Harriman S (2013). Inhibition of cytochrome P450 enzymes and biochemical aspects of mechanism-based inactivation (MBI). *Drug Discov Today Technol* 10: e177-189.

Keijsers CJ, Brouwers JR, de Wildt DJ, Custers EJ, Ten Cate OT, Hazen AC, *et al.* (2014). A comparison of medical and pharmacy students' knowledge and skills of pharmacology and pharmacotherapy. *Br J Clin Pharmacol* 78: 781-788.

Keijsers CJ, Leendertse AJ, Faber A, Brouwers JR, de Wildt DJ, & Jansen PA (2015). Pharmacists' and general practitioners' pharmacology knowledge and pharmacotherapy skills. *J Clin Pharmacol* 55: 936-943.

Keijsers CJ, Segers WS, de Wildt DJ, Brouwers JR, Keijsers L, & Jansen PA (2015). Implementation of the WHO-6-step method in the medical curriculum to improve pharmacology knowledge and pharmacotherapy skills. *Br J Clin Pharmacol* 79: 896-906.

Kitis G, Lucas ML, Bishop H, Sargent A, Schneider RE, Blair JA, *et al.* (1982). Altered jejunal surface pH in coeliac disease: its effect on propranolol and folic acid absorption. *Clin Sci (Lond)* 63: 373-380.

Klammt S, Wojak HJ, Mitzner A, Koball S, Rychly J, Reisinger EC, et al. (2012). Albumin-binding capacity (ABiC) is reduced in patients with chronic kidney disease along with an accumulation of protein-bound uraemic toxins. *Nephrol Dial Transplant* 27: 2377-2383.

Lang CC, Brown RM, Kinirons MT, Deathridge MA, Guengerich FP, Kelleher D, et al. (1996). Decreased intestinal CYP3A in celiac disease: reversal after successful gluten-free diet: a potential source of interindividual variability in first-pass drug metabolism. *Clin Pharmacol Ther* 59: 41-46.

Leblanc PP, & Aiache JM (1994). Problem-based and computer-assisted-learning of pharmacokinetics. *Am J Pharm Educ* 58: 94-95.

Lehmann DF (2011). Teaching from catastrophe: using therapeutic misadventures from hydromorphone to teach key principles in clinical pharmacology. *J Clin Pharmacol* 51: 1596-1602.

Lesar TS (2002). Prescribing errors involving medication dosage forms. *J Gen Intern Med* 17: 579-587.

Lesar TS, Briceland LL, Delcoure K, Parmalee JC, Masta-Gornic V, & Pohl H (1990). Medication prescribing errors in a teaching hospital. *JAMA* 263: 2329-2334.

Lesar TS, Lomaestro BM, & Pohl H (1997). Medication-prescribing errors in a teaching hospital. A 9-year experience. *Arch Intern Med* 157: 1569-1576.

Lewis LD, & Nierenberg DW (2007). American Board of Clinical Pharmacology fellowship training and certification in clinical pharmacology: educational value and future needs for the discipline. *Clin Pharmacol Ther* 81: 134-137.

Lewis PJ, Dornan T, Taylor D, Tully MP, Wass V, & Ashcroft DM (2009). Prevalence, incidence and nature of prescribing errors in hospital inpatients: a systematic review. *Drug Saf* 32: 379-389.

Li HK, Agweyu A, English M, & Bejon P (2015). An unsupported preference for intravenous antibiotics. *PLoS Med* 12: e1001825.

Li RC, Wong SL, & Chan KKH (1995). Microcomputer-based programs for pharmacokinetic simulations. *Am J Pharm Educ* 59: 143-147.

Lipinski CA, Lombardo F, Dominy BW, & Feeney PJ (2001). Experimental and computational approaches to estimate solubility and permeability in drug discovery and development settings. *Adv Drug Deliv Rev* 46: 3-26.

Lubawy W, & Brandt B (2002). A variable structure, less resource intensive modification of problem-based learning for pharmacology instruction to health science students. *Naunyn Schmiedebergs Arch Pharmacol* 366: 48-57.

Lucas KH, Testman JA, Hoyland MN, Kimble AM, & Euler ML (2013). Correlation between active-learning coursework and student retention of core content during advanced pharmacy practice experiences. *Am J Pharm Educ* 77: 171.

Macheras P, Karalis V, & Valsami G (2013). Keeping a critical eye on the science and the regulation of oral drug absorption: a review. *J Pharm Sci* 102: 3018-3036.

Mahmood I (1998). Simple method for the estimation of absorption rate constant( $k_a$ ) after oral administration. *Am J Ther* 5: 377-381.

Martinez MN, & Amidon GL (2002). A mechanistic approach to understanding the factors affecting drug absorption: a review of fundamentals. *J Clin Pharmacol* 42: 620-643.

Maxwell S, Walley T, & Ferner RE (2002). Using drugs safely. *BMJ* 324: 930-931.

Maxwell SR, McQueen DS, & Ellaway R (2006). eDrug: a dynamic interactive electronic drug formulary for medical students. *Br J Clin Pharmacol* 62: 673-681.

Mayer PR, & Brazzell RK (1988). Application of statistical moment theory to pharmacokinetics. *J Clin Pharmacol* 28: 481-483.

Mayersohn M (1994). Pharmacokinetics in the elderly. *Environ Health Perspect* 102 Suppl 11: 119-124.

McQueen DS, Begg MJ, & Maxwell SR (2010). eDrugCalc: an online self-assessment package to enhance medical students' drug dose calculation skills. *Br J Clin Pharmacol* 70: 492-499.

Mehvar R (1999). On-line, individualized, and interactive pharmacokinetic scenarios with immediate grading and feedback and potential for use by multiple instructors. *Am J Pharm Educ* 63: 348-353.

Mehvar R (2001). Principles of nonlinear pharmacokinetics. *Am J Pharm Educ* 65: 178-184.

Mehvar R (2004). The relationship among pharmacokinetic parameters: effects of altered kinetics on the drug plasma concentration-time profiles. *Am J Pharm Educ* 68.

Mehvar R (2006). Interdependency of pharmacokinetic parameters: a chicken-and-egg problem? *Not! J Pharm Pharm Sci* 9: 113-118.

Mehvar R (2008). Dependence of time to reach steady-state on the length of dosage interval. *Ann Pharmacother* 42: 1518-1519.

Mehvar R (2012). Effects of simulations on the learning of pharmacokinetic concepts. *Currents in Pharmacy Teaching and Learning* 4: 278-284.e271.

Michel MC, Bischoff A, Zu Heringdorf M, Neumann D, & Jakobs KH (2002). Problem- vs. lecture-based pharmacology teaching in a German medical school. *Naunyn Schmiedebergs Arch Pharmacol* 366: 64-68.

Miller AD, Krauss GL, & Hamzeh FM (2004). Improved CNS tolerability following conversion from immediate- to extended-release carbamazepine. *Acta Neurol Scand* 109: 374-377.

Miller CJ, McNear J, & Metz MJ (2013). A comparison of traditional and engaging lecture methods in a large, professional-level course. *Adv Physiol Educ* 37: 347-355.

Moore RA, Derry S, Wiffen PJ, & Straube S (2015). Effects of food on pharmacokinetics of immediate release oral formulations of aspirin, dipyron, paracetamol and NSAIDs - a systematic review. *Br J Clin Pharmacol* 80: 381-388.

Munar MY, Singh H, Belle D, Brackett CC, & Earle SB (2006). The use of wireless laptop computers for computer-assisted learning in pharmacokinetics. *Am J Pharm Educ* 70: 4.

Noyes AA, & Whitney WR (1897). The rate of solution of solid substances in their own solutions. *J Am Chem Soc* 19: 930-934.

Orr ST, Ripp SL, Ballard TE, Henderson JL, Scott DO, Obach RS, *et al.* (2012). Mechanism-based inactivation (MBI) of cytochrome P450 enzymes: structure-activity relationships and discovery strategies to mitigate drug-drug interaction risks. *J Med Chem* 55: 4896-4933.

Pantuck EJ, Pantuck CB, Garland WA, Min BH, Wattenberg LW, Anderson KE, *et al.* (1979). Stimulatory effect of brussels sprouts and cabbage on human drug metabolism. *Clin Pharmacol Ther* 25: 88-95.

Parsons RL, Kaye CM, Raymond K, Trounce JR, & Turner P (1976). Absorption of propranolol and practolol in Coeliac disease. *Gut* 17: 139-143.

Pellock JM, Smith MC, Cloyd JC, Uthman B, & Wilder BJ (2004). Extended-release formulations: simplifying strategies in the management of antiepileptic drug therapy. *Epilepsy Behav* 5: 301-307.

Persky AM (2012). The impact of team-based learning on a foundational pharmacokinetics course. *Am J Pharm Educ* 76: 31.

Persky AM, & Dupuis RE (2014). An eight-year retrospective study in "flipped" pharmacokinetics courses. *Am J Pharm Educ* 78: 190.

Persky AM, & Pollack GM (2009). A hybrid jigsaw approach to teaching renal clearance concepts. *Am J Pharm Educ* 73: 49.

Persky AM, Stegall-Zanation J, & Dupuis RE (2007). Students' perceptions of the incorporation of games into classroom instruction for basic and clinical pharmacokinetics. *Am J Pharm Educ* 71: 21.

Piafsky KM, Borga O, Odar-Cederlof I, Johansson C, & Sjoqvist F (1978). Increased plasma protein binding of propranolol and chlorpromazine mediated by disease-induced elevations of plasma alpha1 acid glycoprotein. *N Engl J Med* 299: 1435-1439.

Pilgrim JL, Gerostamoulos D, & Drummer OH (2011). Review: pharmacogenetic aspects of the effect of cytochrome P450 polymorphisms on serotonergic drug metabolism, response, interactions, and adverse effects. *Forensic Sci Med Pathol* 7: 162-184.

Robbins DK, Wedlund P, & Williams JT (1989). Simbas - a user-friendly computer-program which simulates drug concentration-time profiles. *Am J Pharm Educ* 53: 138-140.

Ross S, & Maxwell S (2012). Prescribing and the core curriculum for tomorrow's doctors: BPS curriculum in clinical pharmacology and prescribing for medical students. *Br J Clin Pharmacol* 74: 644-661.

Ross S, Ryan C, Duncan EM, Francis JJ, Johnston M, Ker JS, et al. (2013). Perceived causes of prescribing errors by junior doctors in hospital inpatients: a study from the PROTECT programme. *BMJ Qual Saf* 22: 97-102.

Rotermann M, Sanmartin C, Hennessy D, & Arthur M (2014). Prescription medication use by Canadians aged 6 to 79. In *Health Reports*. ed. Canada S., pp 3-9.

Rowland M, Benet LZ, & Graham GG (1973). Clearance concepts in pharmacokinetics. *J Pharmacokinet Biopharm* 1: 123-136.

Rowland M, & Tozer TN (1986) *Clinical Pharmacokinetics Concepts and Applications* 2nd edn. Lea & Febiger Philadelphia, PA

Schein JR (1997). Cruciferous vegetables and drug metabolism. *Eur J Drug Metab Pharmacokinet* 22: 85-86.

Schneider J, Munro I, & Krishnan S (2014). Flipping the Classroom for Pharmacokinetics. *Am J Pharm Educ Res* 2: 1225-1229.

Shah VP, & Amidon GL (2014). GL Amidon, H. Lennernas, VP Shah, and JR Crison. A theoretical basis for a biopharmaceutic drug classification: the correlation of in vitro drug product dissolution and in vivo bioavailability, *Pharm Res* 12, 413-420, 1995-Backstory of BCS. *Aaps Journal* 16: 894-898.

Shargel L, & Yu ABC (1999) *Applied Biopharmaceutics and Pharmacokinetics* 4e edn. McGraw-Hill: United States of America

Shou M, Dai R, Cui D, Korzekwa KR, Baillie TA, & Rushmore TH (2001). A kinetic model for the metabolic interaction of two substrates at the active site of cytochrome P450 3A4. *J Biol Chem* 276: 2256-2262.

Singer SJ (2004). Some early history of membrane molecular biology. *Annu Rev Physiol* 66: 1-27.

Skrabal MZ, Stading JA, & Monaghan MS (2003). Rhabdomyolysis associated with simvastatin-nefazodone therapy. *South Med J* 96: 1034-1035.

Steinert Y, & Snell LS (1999). Interactive lecturing: strategies for increasing participation in large group presentations. *Medical Teacher* 21: 37-42.

Stipp D (2000). A DNA tragedy. *Fortune* 142: 170-174, 178, 180 passim.

Sullivan TJ (1988). Computer-assisted-instruction in pharmacokinetics - the Simu Series. *Am J Pharm Educ* 52: 256-258.

Sullivan TJ (1992). Use of Mathcad in a pharmacokinetics course for Pharmd students. *Am J Pharm Educ* 56: 144-147.

Swanson, Piscik M, & Swanson H (2014). A pilot study on the use of lecture tools to enhance the teaching of pharmacokinetics and pharmacodynamics. *J Med Educ Curric Devt*: 23.

Sweeney BP, & Bromilow J (2006). Liver enzyme induction and inhibition: implications for anaesthesia. *Anaesthesia* 61: 159-177.

Tobaiqy M, McLay J, & Ross S (2007). Foundation year 1 doctors and clinical pharmacology and therapeutics teaching. A retrospective view in light of experience. *Br J Clin Pharmacol* 64: 363-372.

Tucker S (2014). Open your Is and you won't fall off the bicycle. *Pharmacology Matters* 10-12

Urien S (1995). Micropharm-K, a microcomputer interactive program for the analysis and simulation of pharmacokinetic processes. *Pharmaceut Res* 12: 1225-1230.

Vestal RE, McGuire EA, Tobin JD, Andres R, Norris AH, & Mezey E (1977). Aging and ethanol metabolism. *Clin Pharmacol Ther* 21: 343-354.

Vogelman B, Gudmundsson S, Leggett J, Turnidge J, Ebert S, & Craig WA (1988). Correlation of antimicrobial pharmacokinetic parameters with therapeutic efficacy in an animal model. *J Infect Dis* 158: 831-847.

Wagner JG (1961). Biopharmaceutics: absorption aspects. *J Pharm Sci* 50: 359-387.

Wagner JG (2006). Biopharmaceutics: influence of formulation on therapeutic activity 1. Definitions, scope and relationship to gastrointestinal physiology. *Ann Pharmacother* 40: 537-541.

Waite C, Waite P, & Pirmohamed M (2004). Intravenous therapy. *Postgrad Med J* 80: 1-6.

Wang I, & Hopper I (2014). Celiac disease and drug absorption: implications for cardiovascular therapeutics. *Cardiovasc Ther* 32: 253-256.

Wiernik PH (2015). A dangerous lack of pharmacology education in medical and nursing schools: A policy statement from the American College of Clinical Pharmacology. *J Clin Pharmacol* 55: 953-954.

Winter ME (2010) *Basic Clinical Pharmacokinetics* 5th edn. Lippincott Williams & Wilkins. Philadelphia, PA.

Winterstein AG, Johns TE, Rosenberg EI, Hatton RC, Gonzalez-Rothi R, & Kanjanarat P (2004). Nature and causes of clinically significant medication errors in a tertiary care hospital. *Am J Health Syst Pharm* 61: 1908-1916.

Woodman OL, Dodds AE, Frauman AG, & Mosepele M (2004). Teaching pharmacology to medical students in an integrated problem-based learning curriculum: an Australian perspective. *Acta Pharmacol Sin* 25: 1195-1203.

Wurster DE, & Shrewsbury RP (1981). Simulation package for multiple intravenous infusions of two compartment pharmacokinetic drugs. *Int J Biomed Comput* 12: 455-470.

Yamaoka K, Nakagawa T, & Uno T (1978). Statistical moments in pharmacokinetics. *J Pharmacokinet Biopharm* 6: 547-558.

Zhang Y, Huo M, Zhou J, & Xie S (2010). PKSolver: An add-in program for pharmacokinetic and pharmacodynamic data analysis in Microsoft Excel. *Comput Methods Programs Biomed* 99: 306-314.

# APPENDIX I

PKSolver Analysis of selected data in Chapter 3: Results. The values generated by PKSolver analysis demonstrate accuracy of the classic methods used for data analysis. In addition, PKSolver validates the data generated by the ADAM as physiologically sound.

Figure 3.6 PKSolver Analysis			
Figure 3.6 A and B			
Liver Pump Setting		3 mL min <sup>-1</sup>	14 mL min <sup>-1</sup>
Kidney 2 Pump Setting		5 mL min <sup>-1</sup>	4 mL min <sup>-1</sup>
Kidney 1 Pump Setting		3 mL min <sup>-1</sup>	4 mL min <sup>-1</sup>
Drug Dose: 0.32 mg		Acute Intravenous Administration	
PK Parameter	Equation/Method Used	▲	◆
<b>C<sub>10</sub></b>	PKSolver Compartmental Analysis	3.64 mg L <sup>-1</sup>	3.72 mg L <sup>-1</sup>
<b>k</b>	PKSolver Compartmental Analysis	0.073 min <sup>-1</sup>	0.19 min <sup>-1</sup>
<b>t<sub>1/2</sub></b>	PKSolver Compartmental Analysis	9.5 min	3.6 min
<b>AUC<sub>0-∞</sub></b>	PKSolver Compartmental Analysis	50.0 min · mg L <sup>-1</sup>	19.4 min · mg L <sup>-1</sup>
<b>V<sub>D</sub></b>	PKSolver Compartmental Analysis	88 mL	85.8 mL
<b>CL<sub>Total</sub></b>	PKSolver Compartmental Analysis	6.4 mL min <sup>-1</sup>	16.5 mL min <sup>-1</sup>
<b>r<sup>2</sup></b>	PKSolver Compartmental Analysis	0.9994	0.9981

Table I.I PKSolver Analysis of one-compartment IV data shown in Figure 3.6.

The PK values generated by PKSolver Analysis are similar to those calculated using classic methods as shown in Figure 3.6.

Figure 3.8 PKSolver Analysis					
Tissue Pump Setting		26 mL min <sup>-1</sup>			
Kidney 1 Setting; Kidney 2 Setting		3 mL min <sup>-1</sup> ; 4 mL min <sup>-1</sup>			
Liver Pump Setting		7 mL min <sup>-1</sup>		14 mL min <sup>-1</sup>	
Tissue Compartment Volume		100 mL	200 mL	100 mL	200 mL
Drug Dose: 0.96		Acute Intravenous Administration			
PK Parameter	Equation/Method Used	▲	▲	▲	▲
<b>A</b>	PKSolver Compartmental Analysis	5.46 mg L <sup>-1</sup>	6.47 mg L <sup>-1</sup>	5.95 mg L <sup>-1</sup>	6.32 mg L <sup>-1</sup>
<b>B</b>	PKSolver Compartmental Analysis	3.17 mg L <sup>-1</sup>	1.69 mg L <sup>-1</sup>	2.92 mg L <sup>-1</sup>	1.78 mg L <sup>-1</sup>
<b>α</b>	PKSolver Compartmental Analysis	1.22 min <sup>-1</sup>	0.76 min <sup>-1</sup>	1.23 min <sup>-1</sup>	0.83 min <sup>-1</sup>
<b>β</b>	PKSolver Compartmental Analysis	0.045 min <sup>-1</sup>	0.035 min <sup>-1</sup>	0.084 min <sup>-1</sup>	0.051 min <sup>-1</sup>
<b>t<sub>1/2 dist</sub></b>	PKSolver Compartmental Analysis	0.6 min	0.9 min	0.6 min	0.8 min
<b>t<sub>1/2 el</sub></b>	PKSolver Compartmental Analysis	15.5 min	20.0 min	8.2 min	13.6 min
<b>AUC<sub>0-∞</sub></b>	PKSolver Compartmental Analysis	75.3 min · mg L <sup>-1</sup>	57.2 min · mg L <sup>-1</sup>	39.5 min · mg L <sup>-1</sup>	42.7 min · mg L <sup>-1</sup>
<b>V<sub>D SS</sub></b>	PKSolver Compartmental Analysis	268 mL	415 mL	255 mL	368 mL
<b>CL<sub>Total</sub></b>	PKSolver Compartmental Analysis	12.8 mL min <sup>-1</sup>	16.8 mL min <sup>-1</sup>	24.3 mL min <sup>-1</sup>	22.5 mL min <sup>-1</sup>
<b>k<sub>12</sub></b>	PKSolver Compartmental Analysis	0.68 min <sup>-1</sup>	0.47 min <sup>-1</sup>	0.63 min <sup>-1</sup>	0.47 min <sup>-1</sup>
<b>k<sub>21</sub></b>	PKSolver Compartmental Analysis	0.48 min <sup>-1</sup>	0.18 min <sup>-1</sup>	0.46 min <sup>-1</sup>	0.22 min <sup>-1</sup>
<b>k<sub>10</sub></b>	PKSolver Compartmental Analysis	0.11 min <sup>-1</sup>	0.14 min <sup>-1</sup>	0.22 min <sup>-1</sup>	0.19 min <sup>-1</sup>
<b>r<sup>2</sup></b>	PKSolver Compartmental Analysis	0.9930	0.9973	0.9958	0.9926

Table I.II PKSolver Analysis of two-compartment IV data shown in Figure 3.8.

PK values generated by PKSolver Analysis are similar to those calculated using classic methods as shown in Figure 3.8. The compartmental analysis allowed for generation of micro-constant values, and other parameters associated with two-compartment distribution.

Figure 3.13 PKSolver Analysis				
Liver Pump Setting		7 mL min <sup>-1</sup>		
Kidney 1 Pump Setting; Kidney 2 Pump Setting		3 mL min <sup>-1</sup> ; 4 mL min <sup>-1</sup>		
Tissue Compartment Volume		100 mL		
Drug Dose: 0.96 mg		Acute Intravenous Administration		
Tissue Compartment		3 mL min <sup>-1</sup>	7 mL min <sup>-1</sup>	17 mL min <sup>-1</sup>
PK Parameter	Equation/Method Used	▲	◆	●
A	PKSolver Compartmental Analysis	9.52 mg L <sup>-1</sup>	6.83 mg L <sup>-1</sup>	10.7 mg L <sup>-1</sup>
B	PKSolver Compartmental Analysis	0.86 mg L <sup>-1</sup>	1.81 mg L <sup>-1</sup>	2.96 mg L <sup>-1</sup>
α	PKSolver Compartmental Analysis	0.15 min <sup>-1</sup>	0.21 min <sup>-1</sup>	0.60 min <sup>-1</sup>
β	PKSolver Compartmental Analysis	0.018 min <sup>-1</sup>	0.025 min <sup>-1</sup>	0.035 min <sup>-1</sup>
t <sub>1/2 dist</sub>	PKSolver Compartmental Analysis	4.7 min	3.4 min	1.1 min
t <sub>1/2 el</sub>	PKSolver Compartmental Analysis	38.7 min	28.3 min	19.8 min
AUC <sub>0-∞</sub>	PKSolver Compartmental Analysis	113.0 min · mg L <sup>-1</sup>	107.0 min · mg L <sup>-1</sup>	102.1 min · mg L <sup>-1</sup>
V <sub>D SS</sub>	PKSolver Compartmental Analysis	235 mL	266 mL	224 mL
CL <sub>Total</sub>	PKSolver Compartmental Analysis	8.5 mL min <sup>-1</sup>	9.0 mL min <sup>-1</sup>	9.4 mL min <sup>-1</sup>
k <sub>12</sub>	PKSolver Compartmental Analysis	0.044 min <sup>-1</sup>	0.087 min <sup>-1</sup>	0.35 min <sup>-1</sup>
k <sub>21</sub>	PKSolver Compartmental Analysis	0.029 min <sup>-1</sup>	0.062 min <sup>-1</sup>	0.16 min <sup>-1</sup>
k <sub>10</sub>	PKSolver Compartmental Analysis	0.091 min <sup>-1</sup>	0.081 min <sup>-1</sup>	0.13 min <sup>-1</sup>
r <sup>2</sup>	PKSolver Compartmental Analysis	0.9996	0.9973	0.9996

Table I.III PKSolver Analysis of two-compartment IV data shown in Figure 3.13 with varied TISSUE PUMP rates.

The PK values generated by PKSolver Analysis are similar to those calculated using classic methods as shown in Figure 3.13. The compartmental analysis allowed for generation of micro-constant values, and other parameters associated with two-compartment distribution. The values reflected the changes expected with the alteration.

Figure 3.15 PKSolver Analysis				
Liver Pump Setting		7 mL min <sup>-1</sup>		
Kidney 1 Pump Setting; Kidney 2 Pump Setting		3 mL min <sup>-1</sup> ; 4 mL min <sup>-1</sup>		
Tissue Pump Setting		10 mL min <sup>-1</sup>		
Drug Dose: 0.96 mg		Acute Intravenous Administration		
Tissue Compartment		100 mL	200 mL	500 mL
PK Parameter	Equation/Method Used	▲	◆	●
A	PKSolver Compartmental Analysis	15.5 mg L <sup>-1</sup>	9.53 mg L <sup>-1</sup>	8.17 mg L <sup>-1</sup>
B	PKSolver Compartmental Analysis	2.57 mg L <sup>-1</sup>	1.51 mg L <sup>-1</sup>	0.56 mg L <sup>-1</sup>
α	PKSolver Compartmental Analysis	0.65 min <sup>-1</sup>	0.40 min <sup>-1</sup>	0.26 min <sup>-1</sup>
β	PKSolver Compartmental Analysis	0.051 min <sup>-1</sup>	0.028 min <sup>-1</sup>	0.012 min <sup>-1</sup>
t <sub>1/2 dist</sub>	PKSolver Compartmental Analysis	1.1 min	1.7 min	2.7 min
t <sub>1/2 el</sub>	PKSolver Compartmental Analysis	13.7 min	24.3 min	56.8 min
AUC <sub>0-∞</sub>	PKSolver Compartmental Analysis	74.5 min · mg L <sup>-1</sup>	76.5 min · mg L <sup>-1</sup>	77.7 min · mg L <sup>-1</sup>
V <sub>D SS</sub>	PKSolver Compartmental Analysis	179 mL	315 mL	619 mL
CL <sub>Total</sub>	PKSolver Compartmental Analysis	12.9 mL min <sup>-1</sup>	12.5 mL min <sup>-1</sup>	12.4 mL min <sup>-1</sup>
k <sub>12</sub>	PKSolver Compartmental Analysis	0.32 min <sup>-1</sup>	0.21 min <sup>-1</sup>	0.13 min <sup>-1</sup>
k <sub>21</sub>	PKSolver Compartmental Analysis	0.14 min <sup>-1</sup>	0.080 min <sup>-1</sup>	0.028 min <sup>-1</sup>
k <sub>10</sub>	PKSolver Compartmental Analysis	0.24 min <sup>-1</sup>	0.14 min <sup>-1</sup>	0.11 min <sup>-1</sup>
r <sup>2</sup>	PKSolver Compartmental Analysis	0.9945	0.9961	0.9955

Table I.IV PKSolver Analysis of two-compartment IV data shown in Figure 3.15 with varied TISSUE COMPARTMENT volumes.

The PK values generated by PKSolver Analysis are similar to those calculated using classic methods as shown in Figure 3.15. The compartmental analysis allowed for generation of micro-constant values, and other parameters associated with two-compartment distribution. The values reflected the changes expected with the alteration.